A Novel Phenotyping Pipeline for Root System Architecture

Evaluation with Diversity Panels of Bread and Durum Wheat

Clothilde Collet

Thèse présentée en vue de l'obtention du grade de Docteur en sciences agronomiques et ingénierie biologique

Supervisor:
Xavier Draye (UCLouvain)

Composition of the jury	
President	Frédéric Gaspart (UCLouvain)
Members	Karine Chenu (The University of Queensland)
	Guillaume Lobet (Forschungszentrum Juelich & UCLouvain)
	Bertrand Muller (INRAE)
	Loïc Pagès (INRAE)







Fundings

This thesis was funded by the European Union Horizon 2020 research and innovation programme under the grant agreement No 727247 (SolACE).

This work that took part in the SolACE European project was carried out at the Université catholique de Louvain in the ELI institute.

ACKNOWLEDGEMENTS

On dit d'une thèse que c'est un projet personnel, mais en réalité, je le vois comme étant bien plus que cela. C'est un travail qui émane des nombreuses collaborations et rencontres que j'ai eu la chance de faire, et qui, sans toutes ces personnes qui m'ont accompagnée, n'aurait pas été le même.

Je me dois de débuter ces remerciements par la personne que j'ai le plus sollicitée durant toutes ces années, mon promoteur Xavier Draye. Xavier, tu es avant tout un grand scientifique mais j'ai pour habitude de penser que tu es plutôt un génie. J'ai eu la chance d'en apprendre des tonnes à tes côtés et autant dire qu'avec quelqu'un d'aussi passionné que toi, passer des heures, à coder en Java, à réparer un bug mécanique ou électronique sur RootPhAir, ou à imaginer les améliorations pour le pipeline d'analyse, n'a maintenant plus rien d'anormal ! J'ai adoré la manière dont tu te dédies corps et âme à la recherche mais surtout à aider les autres, c'est une de tes plus grandes qualités mais qui peut parfois te faire défaut, surtout en termes de ponctualité (ce qui m'a néanmoins été bénéfique car j'ai pu gagner en flexibilité !). Je ne pourrais jamais assez te remercier pour tous ces partages de savoir, ta disponibilité et ton soutien. Mais surtout un grand merci pour toutes les d'opportunités que tu m'as offertes. Sans toi, je n'aurais jamais pu aller récolter des racines et visiter des plateformes de phénotypage à travers toute l'Europe, je n'aurais jamais pu apprécier autant regarder des racines pousser, je n'aurais probablement jamais mis les pieds en Israël, où l'on a pu visiter la plus grande station aéroponique du monde et où j'ai présenté mon premier poster à l'international, je n'aurais pas non plus pu vivre toutes ces rencontres et collaborations enrichissantes avec les partenaires de SolACE, mais surtout, je n'aurais pas pu travailler au sein de ce merveilleux labo qu'est PEPA. Je t'en suis très reconnaissante ! Je repars donc avec toutes ces belles expériences, et bien plus encore, mais aussi avec pour seul souhait, de trouver un jour, dans mon travail quotidien, la même passion que celle que tu partages.

Je voudrais aussi remercier l'ensemble des membres de mon jury, Karine Chenu, Guillaume Lobet, Bertrand Muller et Loïc Pagès pour avoir accepté ce rôle et pour leurs lectures et suggestions constructives sur mon travail, ainsi que Frédéric Gaspart pour avoir accepté de présider ce jury. En particulier, j'aimerais, remercier Guillaume et Loïc pour avoir été présents depuis le début

de ma thèse en tant que membres de mon comité d'accompagnement. Guillaume, tu as toujours su écouter et me donner de précieux conseils lorsque j'en avais besoin. Ta sérénité, mais surtout ta créativité et ta manière innovante de voir les choses, me surprennent à chaque fois. Je me considère chanceuse d'avoir été l'une de tes collègues et d'avoir pu écouter tes idées inspirantes ! Loïc, malgré les quelques rencontres que nous avons eues, j'ai beaucoup apprécié votre intérêt pour mon travail ainsi que vos précieux conseils en tant que qu'expert racinaire. Je tiens également à remercier grandement Bertrand qui, lui aussi, a suivi mon parcours de thèse depuis le début. J'ai énormément apprécié ton engagement dans mes recherches et tous les échanges enrichissants que l'on a pu partager. Tu es l'une figures les plus bienveillantes que j'ai pu rencontrer au sein du projet SolACE.

When it comes to SolACE partners, I realise how many wonderful people I have had the chance to meet and work with! I couldn't name everyone personally, but I'll mention a few anyway.

I would like first to thank Renaud Rincent for having passed on and taught me how to handle the codes to carry out the genetic analyses when I was starting, almost, from scratch. Your availability and kindness were very precious. Special thanks to Gabriella Dono (as well as Guiseppe Petruzzino and the entire CREA team) for her knowledge sharing and dynamic support in the statistical analysis of the phenotyping data and in the genetic analysis process. Your motivation was very inspiring! Thank you also to Jacques Legouis, Pierre Roumet, Pasquale De Vita, Giovanni Laido and Yann Mannes for their help and answers to all my questions about the bread and durum wheat panels and many other information I needed. Thanks also to the master student Blaise Mottoulle for carrying out the preliminary experiments on pouches.

Thank you to all partners who welcomed me and showed me their field trials in 2018 or their facilities, among others, Magali Camous, Olivier Moulin and Stéphane Jezequel at the Arvalis field trial in Gréoux-les-Bains, Pierre Roumet and colleagues at the INRAE-AGAP field trials in Mauguio, Yohann Hyvernaud, David Guiard and colleagues at the Syngenta field trial in Levroux, where I collected root samples with Marco Cosme, and finally, Sergio Saia, Nicola Pecchioni and their colleagues for the warm hospitality at CREA in Foggia, where I also spent a great time collecting roots with Sarah Symanczik. I also

would like to thank Christophe Salon, Christian Jeudy, Mickaël Lamboeuf and their team for their friendly welcome at the 4PMI platform in Dijon. Equally, I am grateful for the time spent with Katia Beauchêne at the University of Copenhagen, where Kristian Thorup-Kristensen, Olga Popovic and Abraham George Smith welcomed us with open arms and let us discover the great RadiMax platform and RootPainter software. I also would like to thank in particular my two thesis colleagues at SolACE, Marcé Doubell and Hong Anh Nguyen for their kindness and support during all these years. To all, thank you again for sharing your time, your expertise, your valuable data and analyses with me. Finally, I would like to thank all the other amazing people I have interacted with within SolACE. This project was an incredible first professional experience, and I really enjoyed meeting you all!

Durant ces 4 années et quelques, j'ai eu la chance incroyable d'avoir des collègues que je n'échangerais pour rien au monde ! Un énorme merci à PEPA pour tout ce que l'on a pu partager. Une mention un peu spéciale à mon acolyte de manip, Thomas. Merci à toi pour avoir rendu les expériences en aéroponie moins monotone, d'être venu à la rescousse quand j'en avais besoin et d'avoir toujours été là pour me faire sortir de mon bureau à la pause-café ou à midi. Ta bonne humeur et ton dynamisme font que tu es indispensable au labo ! Aussi, j'aimerais remercier grandement mon fidèle collègue de bureau, Valentin. Merci pour tout, pour les échanges, les conseils et ta bienveillance constante. J'ai adoré être ta voisine de bureau, tu as été un de mes plus grands soutien au labo, un bel exemple à suivre et je ne te remercierai jamais assez pour ça. Merci aussi à toi Lola, pour ton oreille attentive et pour la belle personne que tu es. Et puis, bien sûr, merci à Céline, Adrien, Sixtine, Charlotte, Nicolas, Clément, Marc, Oni, Nhung, Angel et tous les autres, merci pour ces partages quotidiens et de m'avoir fait découvrir vos passions. Je peux maintenant dire que je m'y connais un peu en bandes dessinées, beaucoup en jeux de société et passionnément en plantes ! Merci aussi à celles sans qui le labo ne tournerait pas, nos deux « mamans » de labo, Isabelle et Anne. Merci d'avoir toujours été là et à l'écoute si besoin.

La vie serait nettement moins belle sans amis. Je voudrais également remercier mes copines de thèse, Céline, Elisabeth, Noemi, Ophélie et Laura. Vivre cette expérience ensemble m'a énormément aidé. Une petite mention spéciale à Céline et Noemi, avec qui je partage le même parcours depuis le

premier jour de travaux pratiques en bioingénieur et qui ont été aussi folles que moi pour s'aventurer dans une thèse. Un énorme merci à Céline pour avoir emménagé dans les nouveaux bureaux avec moi. J'ai adoré partager nos histoires de vie quotidiennes et j'admire toujours autant ta persévérance et ta détermination. Également, un immense merci à Noemi. Merci d'avoir été là, surtout en cette fin de thèse. Je n'aurais pas survécu, si ce n'est grâce à ton soutien et à nos petites astuces pour se motiver ensemble. Je rajouterai aussi un merci particulier à mes amies Clémence D., Charlotte D. et Valentine qui ont été présentes durant toutes ces années et dont le soutien a été aussi très important. Je remercie le destin de toutes vous avoir rencontrées, il y a maintenant 10 ans. J'aimerais bien évidemment dire aussi un grand merci à toutes mes autres amies d'agro (Alison, Aurore, Maëlle, Océane et Stéphanie) et d'enfance (Alice, Clara, Hélène, Pauline et Wivinne). Et un grand merci à mes amis bruxellois pour tous ces moments partagés à la capitale (Cécile & Adrien, Charlotte & Hugo, Pauline & Joseph).

Pour finir, j'aimerais remercier ma famille, ma sœur et mon frère, leurs belles « pièces rapportées », mes parents et beaux-parents, mes trois merveilleuses grand-mères et mon neveu adoré. Merci de m'avoir épaulé lors de ce long parcours, mais aussi merci, de m'avoir transmis toutes ces belles valeurs qui m'ont permis d'être celle que je suis aujourd'hui !

Enfin, parce que c'est une évidence, merci à toi, Antoine, mon amoureux, mon compagnon et mon pilier. Merci de m'avoir supporté dans les belles et moins belles journées. Tu as l'art de savoir m'apaiser avec une simple étreinte et de m'encourager avec une simple phrase. Je pense sincèrement que sans toi, je n'y serais pas arrivé. Je réalise la chance que j'ai de t'avoir dans ma vie et je me réjouis de partager avec toi toutes ces nouvelles aventures qui nous attendent.

Merci à tous et toutes, vous qui m'avez accompagnée de près ou de loin !

Clothilde,

Louvain-la-Neuve,

22 août 2022.

TABLE OF CONTENTS

CONTRIBUTION OF THE THESIS TO SOLACE 1

OUTLINE 3

CHAPTER 1. GENERAL INTRODUCTION 5

1.1. CONTEXT 5

1.2. ROOT SYSTEM ARCHITECTURE REPRESENTATIONS 6

1.2.1. INTEGRATIVE VARIABLES 7

1.2.2. PROCESS VARIABLES 7

1.2.3. ARE THERE BEST ROOT SYSTEM ARCHITECTURE DESCRIPTORS? 8

1.2.4. ROOT SYSTEM ARCHITECTURE THROUGH GROWTH AND DEVELOPMENT PROCESSES 8

1.2.4.1. EMISSION 9

1.2.4.2. ELONGATION 10

1.2.4.3. TROPISM 11

1.2.4.4. BRANCHING 12

1.2.4.5. SENESCENCE 12

1.3. MODELLING & ROOT SYSTEM ARCHITECTURE 13

1.3.1. BACKGROUND 13

1.3.2. IDEOTYPES 17

1.4. PHENOTYPING 19

1.4.1. POUCHES 19

1.4.2. RHIZOTRONS & MINI-RHIZOTRONS 19

1.4.3. RHIZOTUBES 20

1.4.4. AEROPONICS 21

1.4.5. POT EXPERIMENTS 21

1.4.6. ROOT VARIABLES TARGETED IN PHENOTYPING PLATFORMS 22

1.4.7. CONSISTENCY BETWEEN PLATFORMS AND FIELD TRIALS 23

1.5. WHEAT ROOT ARCHITECTURE 24

1.6. GENETICS 25

1.6.1. ROOT TRAITS IN BREEDING 25

1.6.2. ROOT GENETICS IN WHEAT 26

1.6.3. ROOT QTLS REVIEW FOR BREAD WHEAT 27

1.7. OBJECTIVES OF THE THESIS 29

INTERCHAPTER 1-2 31

CHAPTER 2. A SIMPLE METHOD TO CONVERT TIME SERIES OF ROOT TIP COORDINATES INTO DYNAMIC REPRESENTATIONS OF PLANT ROOT SYSTEMS.. 33
2.1. INTRODUCTION 33
2.2. RESULTS AND DISCUSSION 35
2.2.1. ROOT TIPS OVER TIME ARE INCREMENTAL SNAPSHOTS OF ROOT SYSTEM ARCHITECTURE 35
2.2.2. TRACKING ROOT TIPS DISPLACEMENT LEADS TO INSTANTANEOUS ELONGATION RATE ESTIMATION 36
2.2.3. ROOT TIP COORDINATES ARE THE RAW DATA FOR ROOT DENSITY ANALYSIS 38
2.2.4. A NEW PATH FROM ROOT TIPS TO DYNAMIC GROWTH AND BRANCHING PARAMETERS 39
2.2.5. PLATFORM DESCRIPTION 43
2.2.6. PIPELINE EVALUATION 43
2.2.6.1. ROOT TIP DETECTION 43
2.2.6.2. EMBRYONIC ROOT NUMBER 46
2.2.6.3. PRIMARY ROOT ELONGATION RATE 46
2.2.6.4. DURATION OF PRIMORDIUM DEVELOPMENT 47
2.2.6.5. LATERAL ROOT DENSITY 47
2.2.7. A REAL-LIFE EXPERIMENT 49
2.3. CONCLUSIONS 52
2.4. MATERIAL AND METHODS 53
2.4.1. PLANT MATERIAL 53
2.4.2. PHENOTYPING IN ROOTPHAIR 54
2.4.3. IMAGE ACQUISITION SYSTEM 55
2.4.4. IMAGE ANALYSIS SYSTEM 56
2.4.5. DATA ANALYSIS PIPELINE 58
2.4.5.1. OUTLIER PLANTS AND FALSE-POSITIVE ROOT TIPS 58
2.4.5.2. EMBRYONIC ROOT NUMBER AND SEMINAL ROOT ANGLE MEASUREMENTS 59
2.5. STATISTICAL MODEL AND VARIANCE COMPONENTS 60
2.5.1. HERITABILITY FORMULA 61
2.5.2. COEFFICIENT OF VARIATION FORMULA 61
2.6. PERSPECTIVES BEYOND THE THESIS 62
INTERCHAPTER 2-3 63
CHAPTER 3. CROSS-PLATFORM ANALYSIS OF ROOT ARCHITECTURE PHENOTYPE 65
3.1. INTRODUCTION 65

3.2. Material and methods 67
3.2.1. Plant material 67
3.2.2. High throughput phenotyping experiments 68
3.2.2.1. RootPhAir 68
3.2.2.2. Pouch – a well-known method 70
3.2.2.3. 4PMI 71
3.2.2.4. Field trials and sensitivity index 72
3.2.3. Classification of the platform traits 73
3.2.4. Statistical models and variance components 74
3.2.4.1. RootPhAir 74
3.2.4.2. Pouch 76
3.2.4.3. 4PMI 77
3.2.5. Heritability formula 77
3.2.6. Coefficient of variation formula 77
3.2.7. Correlations between platform and field trials 77
3.2.8. Comparison between wheat species 78
3.2.9. Clustering of the genotypes based on metadata 78
3.2.10. Potential heterosis effects 78
3.3. Results 79
3.3.1. Phenotyping 79
3.3.1.1. Diversity of platform traits 79
3.3.1.2. Impact of continent of origin and known collections on phenotyping traits 83
3.3.1.3. Characteristics of clusters 85
3.3.1.4. Impact of breeding 90
3.3.2. Genetics 91
3.3.2.1. Broad-sense heritability 91
3.3.2.2. Potential heterosis effects 92
3.3.2.3. Genetic correlations within platforms 94
3.3.3. Environmental impacts 98
3.3.3.1. Consistency between platforms (correlations and heritabilities) 98
3.3.3.2. Correlations between platform traits and yield-related traits 101
3.4. Discussion 103
3.4.1. Main messages 103
3.4.2. New process variables VS integrative variables 104
3.4.3. Discussion on platforms heritabilities 106

3.4.4. Cross-platform experiments outperform single-platform experiments to account for yield performance 108
3.5. Perspectives beyond the thesis 110

INTERCHAPTER 3-4 111

CHAPTER 4. ROOT PHENOTYPE DESCRIPTORS CLOSE TO GROWTH AND DEVELOPMENT DO NOT HAVE SIMPLER GENETIC ARCHITECTURE THAN SHAPE DESCRIPTORS 113
4.1. Introduction 113
4.2. Material and methods 114
4.2.1. Plant material and genetic maps 114
4.2.2. Platform experiments 114
4.2.3. Genetic analysis: QTLs detection via GWAS analysis 116
4.2.4. QTLs classification 117
4.3. Results 118
4.3.1. QTLs detected for platform and field traits 118
4.3.2. Correlations and QTL co-locations for traits showing at least one QTL 121
4.3.3. Co-locations of QTLs for platform traits with QTLs of yield-related traits 123
4.3.4. Comparison of the QTLs locations found with predominant locations in the literature for similar traits 124
4.4. Discussion 127
4.4.1. Consequences of missing consensus on terms and descriptors 127
4.4.2. QTL co-localisation - a promising tool to link root features and crop performance? 128
4.4.3. Genetic architecture of root traits 128
4.4.4. Traits close to development processes do not necessarily warrant simple genetic architecture 129
4.5. Perspectives beyond the thesis 130

INTERCHAPTER 4-5 131

CHAPTER 5. GENERAL DISCUSSION 133
5.1. Main findings 133
5.2. Discussion 133
5.2.1. Achievement of the objectives 134
5.2.1.1. From tips to input parameters of root architectural models 134
5.2.1.2. What are the benefits of cross-platform analysis? 134

5.2.1.3. What is the added value of variables related to root development processes?..... 135
5.2.2. Outstanding results 136
5.2.2.1. Unexpected elongation stability 136
5.2.2.2. From seedling root traits to field performance 137
5.2.3. A brief conclusion on the objectives 138
5.3. Avenues of exploration 139
5.3.1. One step further to modelling 139
5.3.2. Make platforms homogeneous 139
5.3.3. Repositioning the root system architecture 140
REFERENCES 143
ANNEXES 159

List of figures

Figure 1. Scheme of SolACE work packages.....1

Figure 2. Simulation of root architecture ideotypes for maize plants and common bean plants with OpenSimRoot software.....18

Figure 3. Selection of several phenotyping technics and high throughput platforms.....22

Figure 4. Nomenclature used in this work for the first roots of a wheat seedling.....25

Figure 5. Organisation of the different chapters of the thesis.....29

Figure 6. Images of root tips detected at different temporal resolutions for a 14-day old plant of Arabidopsis thaliana grown on a Petri dish (2D) and for a 4-day old plant of Triticum turgidum durum grown in aeroponics (3D).....36

Figure 7. Illustrations of different exploitation routes of tips data.....39

Figure 8. Analysis pipeline to estimate root traits from a population of root tips.....42

Figure 9. Comparison between computed and manual measurements of the number of tips detected (A), the embryonic root number (B), the lateral root density (C), followed by a graph of the relationship between the slope of the envelope curve made on all lateral root tips over the slope made on the tips with the highest tip-collar distance (tips of rank 1) (D), a graph of the distribution of r-square densities (E), an example of regression used to calculate the lateral root density of one plant (F), an example of regression used to calculate the primary root elongation rate of one plant (G) and a last example of root tip categorisation with one plant (H).....45

Figure 10. Schematic views of the RootPhAir platform.....54

Figure 11. Typical image taken in the RootPhAir platform.....57

Figure 12. Illustrations of the flooding method used by AeroScan to detect the root tips and assess the root diameter (A) and viewer window of the in-house software MosaicViewer (B).....58

Figure 13. The three devices used for phenotyping.....69

Figure 14. Heatmaps of the hierarchical clustering performed for the bread wheat panel (A) followed by plant schemes to illustrate each cluster (B)..... 87

Figure 15. Heatmaps of the hierarchical clustering performed for the durum wheat panel (A) followed by plant schemes to illustrate each cluster (B).....87

Figure 16. Genetic correlation matrices between phenotyping traits (platform and field traits).....97

Figure 17. Principal component analysis carried out for the bread wheat panel for the traits measured in the three platforms (RootPhAir, Pouch and 4PMI) and the field trials.....98

Figure 18. Principal component analysis carried out for the bread wheat panel for the traits measured in the three platforms (RootPhAir, Pouch and 4PMI) and the field trials.....99

Figure 19. Manhattan plot viewed from top with the set of all significant SNPs detected.....119

Figure 20. Matrix illustrating the genetic correlations and the number of QTL co-localisations found between pairs of root platform traits.....122

Figure 21. Tables reviewing: A) the number of studies detecting QTLs on each chromosome per root trait category; B) the number of QTLs reported on each chromosome and category divided by the number of studies where at least one QTL was reported 126

Figure 22. Manhattan plot viewed from top with the set of all significant SNPs detected with colour to visualise all co-localising SNPs.....173

Figure 23. Manhattan plot viewed from top with the set of all significant SNPs detected with the FDR method.....175

List of tables

Table 1. Strategies for representing the different root development processes in the four well-known following architectural models.....15

Table 2. Root categories in which the QTLs for root traits of bread wheat species have been classified.....28

Table 3. Simplified list of the common parameters of four dynamic popular architectural models.....35

Table 4. List of root traits extracted by the pipeline.....40

Table 5. Heritabilities of the bread wheat and durum wheat panel phenotyped in RootPhAir.....50

Table 6. List of the traits determined from the data of all platform experiments.....74

Table 7. Range of variability and broad sense heritabilities of the traits estimated across the platform experiments (RootPhAir, Pouch and 4PMI) for both wheat species.....81

Table 8. Results of the ANOVA analyses between platform traits and the collections, continent of origin and the cluster groups for both bread wheat and durum wheat panels separately.....83

Table 9. Contrasts between the hybrids and their mean parent values to see if there is a heterosis effect.....93

Table 10. Categories created to classify the QTLs found in this study and be able to compare them with equivalent QTLs from the same categories found in the literature. 117

Table 11. List of the QTLs found with a SNP significance threshold set at a p-value < 10^{-5} or $-\log_{10}(pval) > 5$.....121

Table 12. Composition of the bread wheat panel, names of the genotypes, their category of origin, their country and continent of origin, as well as their year of release.....159

Table 13. Composition of the durum wheat panel, names of the genotypes, their category of origin, their country and continent of origin, as well as their year of release.....163

Table 14. RootPhAir nutritive solution (½ Hoagland).....167

Table 15. 4PMI nutritive solution.....167

Table 16. Articles selected for the review of studies aimed at finding QTLs for bread wheat root traits (from 2005 to 2020).....168

Table 17. List of all significant SNPs detected within the bread wheat panel.....170

List of annexes

Annexe 1. Panel composition.....159

Annexe 2. RootPhAir nutritive solution.....167

Annexe 3. 4PMI nutritive solution.....167

Annexe 4. List of articles used for the root QTLs review 168

Annexe 5. List of significant SNPs detected with GWAS 170

Annexe 6. Co-localisations visualisation 172

Annexe 7. Significant SNPs detected with FDR method.....174

List of abbreviations

Abbreviation	Name
1LR	First lateral root
AI	Artificial intelligence
AMF	Arbuscular mycorrhizae fungi
ARL	Average root length
BW	Bread wheat
BZ	Branched zone
CH	Convex hull
CV_g	Genotypic coefficient of variation
DAS	Days after sowing
Diam	Diameter
DPD	Duration of primordium development
DW	Durum wheat
Emer	Emergence
ER	Embryonic root
ERate	Elongation rate
GWAS	Genome wide association study
GYC	Grain yield under controlled conditions
GYS	Grain yield under stressed conditions
GYSI	Grain yield sensitivity index
H^2	Broad-sense heritability
QTL(s)	Quantitative trait locus (loci)
LR	Lateral root
LRD	Lateral root density
MRL	Maximum root length
N	Nitrogen
Nb	Number
NbT	Number of tips
NR	Nodal root
P	Phosphorus
PR	Primary root
R/S	Root to shoot ratio
R^2	R-square
RMass	Root biomass
RPA	RootPhAir
SMass	Shoot biomass
SR	Seminal root
SRA	Seminal root angle
Surf	Surface
TC	Tip-collar
TRL	Total root length
URI	Uniform resource identifier
W	Water
WRANK	Weighted rank
$\boldsymbol{\sigma}_g$	Genotypic standard deviation
$\boldsymbol{\sigma}_r$	Residual standard deviation

Contribution of the thesis to SolACE

This work was part of the SolACE project (www.solace-eu.net), funded by the European Union Horizon 2020 research and innovation programme under the grant agreement No 727247 (SolACE) and coordinated by Philippe Hinsinger (INRAE).

The global aim of the project was to develop "Solutions for improving Agroecosystem and Crop Efficiency for water and nutrient use". The project was organised in five experimental work packages shown in Figure 1.

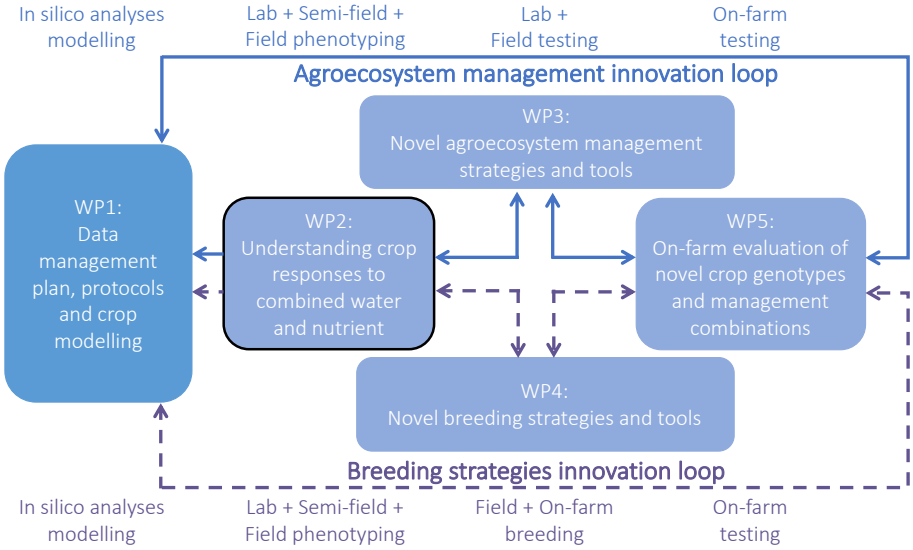


Figure 1. Scheme of SolACE work packages. The techniques used to achieve the objectives of each of these work packages are indicated at the top and bottom of the schema (Source: SolACE Management guidelines, Lise Vedel).

This thesis took place in work package 2 whose objective was to understand the responses of wheat and potato to combinations of water and nitrogen deficits based on analyses of diversity of genotypes. In that context, the thesis focuses on the below-ground responses of bread and durum wheat.

As a multi-actor project, SolACE comprised 25 partner organisations (research institutes, universities, and industries) from 14 different EU countries (SolACE, 2022). The following paragraphs indicate my own contribution to this ensemble and highlight the partners and disciplines I have been interacting with.

As mentioned in Figure 1, experiments with complementary approaches were performed, from real field conditions to highly controlled laboratory conditions. Four field trials have been carried out by SolACE partners (SYNGENTA, ARVALIS, INRAE and CREA) to characterise the response of 500 wheat genotypes to combined low water and nitrogen. I have visited these trials to collect root samples that were used for mycorrhizae analysis (thesis of Marcé Doubell, UCLouvain). I was also in charge of developing the common protocols and data templates for the four partners and to assemble the resulting datasets.

Next to these field trials, the same genotypes were characterized in three greenhouse and lab experiments. I performed the experiment in the RootPhAir phenotyping platform and the Pouch experiment (the latter with the help of the master student Blaise Mottoulle). I also contributed to the harvest of the bread wheat experiment conducted in the 4PMI platform at INRAE Dijon. close guidance of these partners.

Outline

Scientists have been innovative in developing many representation and phenotyping methods to investigate the root system architecture. From field experiments to controlled conditions, each methods brings its advantages and disadvantages. Often coupled with image analysis, root phenotyping requires multiple scientific skills, from growing plants to developing and analysing huge databases (Wasaya *et al.*, 2018). Additionally, root traits, that are used to describe root system, its architecture, morphology and anatomy, are often under a complex polygenic and quantitative control which makes the root system architecture study even more challenging (Wasaya *et al.*, 2018). However, the way in which the root system is represented remains unsatisfactory, resulting in a lack of estimation of root traits close to the development functions of the root system and in the determination of their genetic determinism.

Furthermore, process variables are needed as input parameters for many root architectural models and it was pointed out that modelling is and will remain a major tool to be used in synergy with phenotyping to improve our understanding of ecophysiology, especially in the context of combined stresses.

In this thesis, the eco-physiology and genetics of root system architecture of both bread and durum wheat species will be investigated with the aim of determining novel root traits related to the development processes of root system architecture, and used as input parameters for root architecture models, and which could bring new insights in the analysis of crop responses to combined water and nutrient limitations

First of all, in Chapter 1, the overall context of this thesis is described in a little more detail.

Then, in Chapter 2, we will develop a unique analysis pipeline to represent the root system architecture from root tips coordinates, features that are relatively simple to extract from dense image time series of root systems, in order to assess dynamic characteristics of root systems. The pipeline will be illustrated with phenotyping experiments performed in aeroponics with two large panels of bread and durum wheat.

Afterwards, in Chapter 3, we will perform a multi-platform analysis by cross-analysing the root traits obtained from aeroponics (analysis pipeline) with two distinct phenotyping facilities (a pouch-like device and rhizotubes of the 4PMI platform). We will study the correlations between these three platforms, but also between the platforms and the field behaviour through some yield-related variables added to the dataset.

Furthermore, in Chapter 4, the genetic architecture of the traits estimated in the three phenotyping platforms will be investigated via genome-wide association studies to determine whether root traits related to processes, and which are generally considered to be closer to development functions, would have a different determinism than simple morphological root traits. The quantitative traits loci (QTLs) candidates found will be placed in the context of the literature through a review carried out from 2005 to 2020 that brings together all the QTLs found for root traits for the bread wheat species.

Finally, in Chapter 5, the main findings will be brought together, some discussion points will be addressed, and finally, some points of perspective will be presented.

Chapter 1.

General Introduction

1.1. CONTEXT

The fact that the world is facing a global climate change is not anymore to prove (Masson-Delmotte *et al.*, 2018). Extreme climatic events such as long episodes of droughts or heavy rainfalls and the variability of occurrence for such events will increase. Additionally, it is also now agreed that there is a need to reduce our dependence on fertilizers, such as nitrogen (N) and phosphorus (P), for both ecological (N and P flows exceeding the "planet boundaries" and being at the origin of e.g. eutrophication and greenhouse gases emission in regions of intense agriculture (Steffen *et al.*, 2015)) and economical purposes (future socio-economic projections of rising fertilizers prices (Brunelle *et al.*, 2015)).

Based on these statements, it is expected that the constraints will become increasingly complex and that plants will be confronted with not one but more likely several stresses during the same season (Zhang and Sonnewald, 2017; Anwar *et al.*, 2021). Many studies have looked at various stresses individually, such as water stress (e.g., drought or flooding), nutrient stress (nitrogen, phosphorus, etc.), or even biotic stress (e.g., pests and diseases). Despite the strong interest in investigating these major stresses individually, they are actually still poorly managed (Passioura, 2010, 2020), except for some rare major advancements (e.g., *Bt* genes introgression for pest resistance, dwarfing genes *Rht1* and *Rht2* for semi-dwarf varieties). Nowadays, the focus is moving towards the study of combined stresses (van der Bom, Williams and Bell, 2020). It is likely that plants will not react in the same way to one or multiple stresses since their combinations may not be the simple addition of the impacts of individual stresses (Humbert *et al.*, 2013; Suzuki *et al.*, 2014; Zhang and Sonnewald, 2017; Anwar *et al.*, 2021). Multiple stresses are expected to lead to complex plant responses due to the diverse interactions that might occur between the stresses, for example, negative interactions (such as water and nitrogen stresses that together affect gene expressions to a much larger extent than when separated (Humbert *et al.*, 2013) or drought

and heat waves that together cause worse effects than the two separate stresses (Suzuki et al., 2014)) or positive interactions (such as salt and heat stresses that, together, provide protection to tomato plants compared to the effects of a single salt stress (Suzuki et al., 2014)). Thus, maintaining the amount of food currently produced under more complex scenarios while reducing the agricultural impact of agriculture is a new challenge that will require a combination of new germplasms with adequate management practices (Rivington *et al.*, 2015; Mbow *et al.*, 2019).

There is a general agreement that roots might play a major role in maintaining crop yields when facing stresses, especially if these concern soil resources such as nutrients (N, P) or water (W) (Lynch, 2007). Roots are an integral part of the functioning of the ecosystem. They play multiple essential roles in ensuring plant fitness via resource uptake, but also through the maintenance and stability of the soil, as well as the interaction with the microorganisms in the rhizosphere. However, root systems are especially difficult to investigate because they are highly sensitive to their environment and its heterogeneity (a phenomenon named “plasticity”) and, simultaneously, contribute to shape their environment and its heterogeneity (Freschet *et al.*, 2020).

Root system architecture is defined by Jonathan Lynch (1995) as “the spatial distribution of the root system in the soil”. Since resources are heterogeneously distributed in the soil and their availability changes over time, the ability of plants to adapt their root architecture is thought to be an important component of growth even more when growing in sub-optimal soil conditions (Lynch, 1995; Manschadi, Manske and Vlek, 2013) – even if this idea remains debated. Investigating the processes underlying the root system architecture and its plasticity is therefore a logical step to improve resource absorption efficiency, plant anchorage and resources transport from root to shoot parts (Lynch, 1995). In particular, a thorough understanding of root system architecture should help improving plant tolerance to abiotic and biotic stresses via plant breeding and innovative crop management (Wasaya *et al.*, 2018).

1.2. ROOT SYSTEM ARCHITECTURE REPRESENTATIONS

Any avenue to improve our understanding of plant functions starts with observation. However, roots growing underground and being highly influenced by the environment, it is challenging to acquire a complete and

accurate view of their distribution and architecture. In addition, the links between root architecture and root functions can be so complex that there is a need to observe a wide array of root features to build a clear view of how root systems really work (Atkinson, 2000). As a result, there are probably as many root observation methods, techniques and phenotypic descriptors as there are research questions (Atkinson, 2000). This has led to several ways to represent root system architecture, which are often aligned with specific observation methods.

1.2.1. INTEGRATIVE VARIABLES

The most common way of quantifying the architecture of the root system is through the assessment of easily accessible morphological traits, e.g., convex hull area of the root system, total lengths, biomasses, number of roots (Freschet *et al.*, 2020). These variables are generally quite easy to acquire, and most phenotyping methods allow their evaluation. These root traits will be mentioned in this work as "integrative variables" describing the root system at a certain time point, usually at the end of an experiment.

1.2.2. PROCESS VARIABLES

Root system architecture can also be described by the growth and development processes that operate continuously during the plant life. A root system is a branched and growing set of type- and age-structured roots. These roots are produced after emission and branching processes, elongate under the action of certain tropism and enter senescence after poorly known processes. While elongation and tropism are growth processes, which do not alter the root biological program, emission, branching, type-acquisition and senescence are development processes and do alter the biological program. Unlike integrative variables, these "process variables" do not describe the root system at a time point. Instead, they show how a root system changes between successive time points. Process-based representations of root system architecture are therefore well suited to understand the construction of architecture as a succession of decision rules (de Dorlodot *et al.*, 2007). However, they can be data intensive as they require the observation of the root system at many time points.

1.2.3. ARE THERE BEST ROOT SYSTEM ARCHITECTURE DESCRIPTORS?

The recourse to a certain type of root system architecture representation is often linked with the decision of what to measure and, therefore, depends on various contextual elements (Atkinson, 2000):

- the availability of methods at the experimental site,
- the focus of the investigation on specific traits or processes,
- the temporal and spatial granularity of these traits or processes that is required by the investigation,
- the scientific goals of the investigation.

Because the different types of variables characterise complementary aspects of the root system, it is common for researchers to combine different formalisms or for others to use different formalisms for the same question. As a result, the re-use of existing datasets is often complicated by compatibility issues.

A parallel observation is that, for practical reasons, most root phenotyping studies fail to use the complete set of descriptors that make up representations. For example, most reports in the literature that use the keywords "root system architecture" in fact report only a handful of integrative variables, with real consequences on our ability to interpret results. There is, therefore, an important challenge to define “minimum sets of variables” that avoid redundancy (or correlations) between variables and provide as complete as possible information to build correct interpretations of root system data (de Dorlodot *et al.*, 2007).

The following sections provide background information on the growth and development processes (section 1.2.4) and introduces modelling as a promising avenue towards defining such minimum sets of variables (section 1.3).

1.2.4. ROOT SYSTEM ARCHITECTURE THROUGH GROWTH AND DEVELOPMENT PROCESSES

A root system develops from various generating organs (embryo, stem, rhizome, etc.). Once a new root is formed, it will engage in elongation, tropism, branching and senescence under the influence of its local surrounding conditions (Pagès *et al.*, 2004).

1.2.4.1. EMISSION

From a biologic point of view each root appears from an emission zone. The first root to emerge from the seed is the radicle which will become the primary root, generally the longest and most vertical root in wheat species, then comes the seminal and the nodal roots (cf. section 1.5), each of which may give rise to lateral roots. The number of roots initiated will depend largely on the carbon resources of the plant, its fitness and its local environment.

In the literature, various integrative variables are used to evaluate the root emission processes, e.g., the root biomass, the root system dimensions (length, width, convex hull) and the total number of roots (per root type or not). Often these parameters are estimated at the end of an experiment. In a field trial, shovelomics methods are used to access these variables, which is time consuming, but the root systems are often damaged during excavation, resulting in a significant bias. In a controlled experiment, accessing these variables can also be time consuming, especially if the roots have to be cleaned from the substrate.

Process variables to assess root emission can also be estimated during the course of controlled experiments using non-destructive methods. For example, image-based technologies that track changes in root system emission over time or automatically count the number of roots at successive time points via AI or other software such as SmartRoot (Lobet, Pagès and Draye, 2011).

Emission processes can be seen through many different conceptual ideas. Often roots are associated to a root type or class, either simply according to their root branching order (first order being primary and seminal roots, second order being laterals as in OpenSimRoot (Postma *et al.,* 2017), Table 1), or to different kinds of classification based on processes characteristics (maximal length, elongation rates and/or growth arrest as with the A-B-C model explained by Passot *et al.*, (2018)). Moreover, following numerous observations, preconceived ideas may exist, such as the emission strategy followed by plants depending on whether they are dicots or monocots (as explained in Pagès *et al.* (2004), dicots will tend to have root systems that consist in a unique primary root axis from which secondary branch emerged, and monocots plants will tend to develop fasciculated root system with

several main roots continuously growing from the central base of the root system).

1.2.4.2. ELONGATION

Biologically, elongation starts from cell division, the creation of new cell walls and then cell expansion. It is therefore dependant on the photosynthesis, the cell hydric potential and other local soil constraints such as the soil moisture (Sharp *et al.*, 2004), mechanical impedance or temperature (Kronenberg *et al.*, 2020). The water component is very important since it is the hydric status that guides this very energy consuming process.

Elongation is often measure at specific times during an experiment. Either the elongation is estimated at harvest according to the time elapsed and the root lengths measured or the dispositive allows a constant visualisation of the root system (through transparent basket, rhizotubes, pouches, etc.) during the experiment and elongation can be assessed at specific time points.

However, it is known that elongation is very plastic and varies according to soil conditions, for example soil moisture, impedance or depth (it has been observed that root growth tends to decrease in the uppermost layers as the conditions become drier (Pagès *et al.*, 2004)). Finer monitoring can therefore also be achieved using the image-based technologies as just explained for the emission.

Elongation can also be perceived and represented with various concepts. Elongation can be defined as varying according to the diameter – elongation rate relationship (e.g., in the Root Typ model (Pagès *et al.*, 2004), Table 1). Indeed, it is well-known that elongation is correlated to root diameter (Pagès, 1995; Thaler and Pagès, 1996; Pagès *et al.*, 2010) and therefore it is generally more appropriate to estimate it separately per root type. Root elongation can also be seen as varying in time and/or space either by assessing the impact of the external conditions (e.g., correction factor by soil layers) or by correcting its value with an intrinsic parameter set to influence root elongation independently of external conditions (Table 1). Also, elongation might be considered as arising from the influence of an intrinsic random diversity occurring for similar roots under similar conditions, as suggested by Muller *et al.*, (2019) for root branching.

1.2.4.3. TROPISM

Plants growth orientation is subject to several types of tropisms such as gravitropism, hydrotropism, phototropism, thermotropism, etc. (Izzo and Aronne, 2021). The mechanisms involved in root sensitivity to tropisms are however still poorly understood, except for the molecular mechanisms behind root gravitropism have been largely investigated in *Arabidopsis thaliana* and which have been approved to results from differences in auxin distribution (Su *et al.*, 2017; Sáenz Rodríguez and Cassab, 2021). Moreover, the impact of the other types of tropisms are still hard to distinguish from this gravitropism effect (Izzo and Aronne, 2021). These are some of the reasons why tropism has received little attention and is only studied by a small number of people.

Integrative variables to assess the tropism of root systems are often root orientation angles or the amplitude between some pairs of seminal roots (several studies have shown a link between more performant genotypes under dry conditions because of a steeper root angle between their seminal roots allowing to reach faster deep soil layers where water was accessible (Manschadi *et al.*, 2010)). To characterize this seminal root angle, several technics have been developed to allow the visualisation of root seedlings orientation such as pouches, rhizotrons or transparent pots. However, this trait is generally measured on young seedling stages and thus at an early specific time of growth.

Because of the diversity of tropisms to which roots are exposed and which are clearly dependent on soil conditions, root tropisms have a dynamic impact on the root orientation, which constantly changes during growth. However, it is still rather difficult to assess the evolution that tropism can have on a root over time.

Tropism impact is often conceptualized as a coefficient influencing root orientation which can be set at various intensities depending on the soil layer and conditions in which the roots are located. However, the number of tropisms included in this parameter may vary from one study to another and often only gravitropism will be taken into account (Table 1). In addition, tropism changes often depend on the previous direction of the root, ensuring a plausible sequence of direction.

1.2.4.4. BRANCHING

Most roots branch to increase the root surface area in soil regions where resources are abundant, as well as to ensure plant anchorage. The branched roots emerge at a specific pre-branching site determined by a response to an auxin signal from the root tip. The hormonal response is an asymmetric division of one of the pericycle cells and from this, a lateral primordium may emerge to make way for the new branched root (Atkinson *et al.*, 2014; Muller *et al.*, 2019). This usually happens first to the roots that have emerged from the embryo (embryonic roots) because they quickly become the longest. This process again depends on the carbon stock available by the plant, as the creation of new tissue is very energy intensive but also of the soil conditions.

Root branching processes is often estimated with a lateral root density or an inter-branched distance. However, this parameter is known to be highly variable along roots. Manual techniques are therefore, for obvious reasons, very time-consuming and automation of the estimation of this parameter is still limited because of this large plasticity.

Root branching is generally conceptualised as following an acropetal sequence from the root tip which means that the initiation of a lateral root occurs close to the root extremity (Dubrovsky and Rost, 2003). Once the root primordium is initiated, there is a lag time before the root emergence (called in this work the duration of primordium development). Then, either, the root branching density or the inter-branched distance is set as a fixed parameter that does not vary (despite the high local plasticity observed), or the root branching values will be considered as dependent on the carbon stock available by the plant or influenced by the local soil conditions (Table 1). Similarly, as mentioned for elongation, a new suggestion has been raised that branching could also largely result from significant intrinsic variability (Muller *et al.*, 2019).

1.2.4.5. SENESCENCE

Biologically, root senescence occurs once the root has no more activity (Deacon and Mitchell, 1985), either in terms of resource extraction or growth.

Senescence is very poorly measured because many studies of root architecture under controlled conditions are limited to very young stages and the exact mechanisms underlying it are therefore still poorly understood.

Root senescence is often represented and mainly related to the elongation state of the root, i.e., when the rate is too low, senescence is expected to occur. Other ways of looking at senescence is that it occurs when an exact life span has elapsed or when the root reaches a too thin diameter (Table 1). Once these situations are encountered, the senescent root will usually self- pruned, or it will remain attached to the root system if it still bears living roots.

1.3. MODELLING & ROOT SYSTEM ARCHITECTURE

1.3.1. BACKGROUND

Modelling came out quite late in plant sciences (in the 1950s) mainly due to the complexity to simulate plants and plant processes that are constantly evolving according to fluctuant environments (Tardieu, 2010). It developed as a synergy between mathematics and (eco-)physiology and, more recently, plant phenotyping. Several root system models have been developed, with the aim to propose hypotheses on how different biological processes or regulatory mechanisms could interact to drive root system growth and development (Dunbabin *et al.*, 2013; Fiorani and Schurr, 2013; Tracy *et al.*, 2020).

For example, Lobet, Pagès and Draye (2014) have addressed the interactions between plant hydraulics and architecture while Draye *et al.* (2010) investigated the interactions between root system architecture and soil water uptake. More recently, Pagès, Bernert and Pagès (2020) developed a model interpreting the plasticity of the root elongation patterns under different scenarios. These are examples under among many others and the growing collection of articles on modelling indicates an interest of the root community towards these tools (Saint Cast *et al.*, 2022).

Models simulating root system architecture in 3D were introduced in the late 1980s. These models allowed to simulate the evolution of spatial root distribution over the plant life, typically to investigate the benefits of matching root and resources distributions (Dunbabin *et al.*, 2013). Root architecture models therefore simulate avatars of root system architecture according to a short list of input parameters. By visualising the root system spatially and temporally, they can help in better understanding the plant functions and development, sometimes in relation to soil properties (Pagès *et al.*, 2004, 2012; Postma *et al.*, 2017; Schnepf *et al.*, 2018).

A list of root architecture models is available at www.quantitative-plant.org (Lobet, Draye and Périlleux, 2013; Saint Cast *et al.*, 2022), but five architectural models are widely used today: ArchiSimple (Pagès *et al.*, 2012), CRootBox (Schnepf *et al.*, 2018), DigR (Barczi *et al.*, 2018), Root Typ (Pagès *et al.*, 2004), OpenSimRoot (Lynch *et al.*, 1996; Postma *et al.*, 2017). These are based on a limited number of parameters which, for each model, constitute a set of variables that are sufficient to being able to reproduce a root system architecture. They are therefore useful variables to synthesize plant architecture and its dynamic behaviour (de Dorlodot *et al.*, 2007).

In each model, root processes are represented differently, usually influenced by the background of the developers (e.g., mathematician, agronomist, etc.). As processes are conceptualised in different ways in the models, the minimum set of variables used to represent the architecture of the root system may vary (Table 1). These are therefore valuable examples of synthesis that can guide us in our choice of representation.

Table 1. Strategies for representing the different root development processes in the four well-known following architectural models: ArchiSimple (Pagès et al., 2012), CRootBox (Schnepf et al., 2018), OpenSimRoot (Postma et al., 2017) and Root Typ (Pagès et al., 2004).

Processes	ArchiSimple	CRootBox
Emission	The number of root axes produced depends on the thermal time cumulated.	Each root is associated to a root type (tap root, lateral roots, basal roots and /or shoot borne roots) whose growth characteristics are described in the input parameters of the model (occurrence, time delay between two root emergences, maximal number of root axes).
Elongation	Elongation is expressed as a "growth potential" depending on root diameter since it has been proven that diameter and elongation are highly correlated.	The elongation rate is defined according to the age of the root and is limited to a root life parameter duration. The initial elongation rate and the maximal root length are chosen by the user.
Tropism	Tropism is calculated based on three components: the root direction, a random term representing the mechanical constraint of the soil and a gravitropism coefficient.	The orientation of the root tip is randomly changed after each "distance" (i.e., a set parameter) reached. Then, the tropism is adapted to represent changing soil conditions according to a "random optimisation process" (that minimises an objective function and respect the flexibility of the root).
Branching	Branching follows an acropetal sequence (new roots initiated close to the root tip), with a fixed inter-branch distance and a fixed lag-time before emergence (both defined by the user). The diameter of a lateral root will depend on the diameter of its mother root. The lateral root density will be impacted according to the soil layer conditions.	In the designed branching zone, the lateral roots emerged at a fixed branching angle and a fixed branching distance.
Senescence	Each root has a life duration defined according to a threshold diameter from which it is considered that no elongation is longer possible. Once dead, the root self-pruned or remains attached to the root system if it bears living roots.	Root stop growing after a "root lifetime" parameter (set by the user).

Processes	OpenSimRoot	Root Typ
Emission	The root system is represented by vertices and edges and thus each root tip has its own dynamic coordinates.	Each root is considered individually and associated with a root type having its own associated parameters allowing the development processes (elongation, branching, tropism, etc.) to be root-type specific.
Elongation	Root elongation rates are predefined in the parameters but are scaled according to a root vigor factor (which can be root specific since it can be based on the initial root diameter that is defined in the parameters per root type). A local soil variable can impact elongation (as a function of local soil compaction). Elongation is limited by a carbon pool available and as soon as the stored carbon is depleted, growth rates decline.	Elongation is calculated based on time, an initial growth rate and a maximal root length decided by the user. This elongation is corrected by a coefficient representing the reductions that might occurred due to soil characteristics (layer-dependent).
Tropism	Root tropism can change through the impact of a vector which is the sum of several vectors representing gravitropism, random impedance, and nutrient tropisms. The new root orientation is then the impact of these tropisms on the previous normalized growth direction. A local soil variable can impact gravitropism (e.g., scaled based on local nutrient concentration).	The orientation of the roots is the resultant of three parameters, the previous direction, the impact of the tropism and the soil directional constraints. This orientation changes at each time step (defined by the user, as well as the overall simulation).
Branching	Each root branches along with the following properties: branching time and branching space. New roots can be of different types (classed according to the order) and the whole process is repeated. A local soil variable can impact branching.	Branching follows an acropetal sequence (new roots initiated close to the root tip), with a fixed inter-branch distance and a fixed lag-time before emergence (both defined by the user). The newly formed roots might be associated to several root types (based on a proportion root type parameter defined by the user).
Senescence	/	Root elongation stops when it becomes insignificant i.e., when it falls below a certain threshold (e.g., 0.01 mm). After a necrosis duration parameter, the root self-pruned or remains attached to the root system if it bears living roots.

Roots and root architecture are known to be extremely plastic and therefore depend greatly on the soil substrate, the rhizosphere status, the environmental conditions, and the plant status (Muller *et al.*, 2019). Thus, an accurate prediction of root traits would require many more mathematical equations parameters than are present in current root architecture models. It is believed that incorporating more plant, soil and rhizosphere processes and properties in root architecture models would contribute to improve their predictive power, yet our understanding of these processes and how they interact with root growth and development remains largely limited.

1.3.2. IDEOTYPES

Model are mostly useful to simulate root system architecture and investigate how the dynamic development and physiological functions of roots under various conditions may contribute to improved performance under non-optimal resources conditions (Tracy *et al.*, 2020). In particular, these models have often been used to determine the characteristics of "root ideotypes", i.e., under given environmental and soil conditions, an ideal root system that shows the expected performances under such conditions. Several root ideotypes have been proposed in literature (White *et al.*, 2013), yet two of them have received more support by the community.

(i) Under low P conditions, the "Topsoil foraging" ideotype maximizes the absorption of the non-mobile phosphorus located in the most upper soil layers (Lynch, 2019). The main architectural characteristics of this ideotype are a high number of axial roots, a shallow development of axial roots and thus wide root angles from vertical, a high lateral root density, a reduced metabolic cost and a high root hair density (Figure 2) (Lynch, 2019).

(ii) Under low water or nitrogen conditions and when the soil is deep, the "Steep-cheap-deep" ideotype develops long roots with a minimal carbon cost which is able to reach mobile resources, such as water or nitrogen, that have percolated in the deeper soil layers (Lynch, 2013, 2019). The main characteristics of this ideotype are steep root angles, a small number of nodal roots, a small lateral root density and a relatively low architectural plasticity in response to variation of resources availability (Figure 2) (Lynch, 2019).

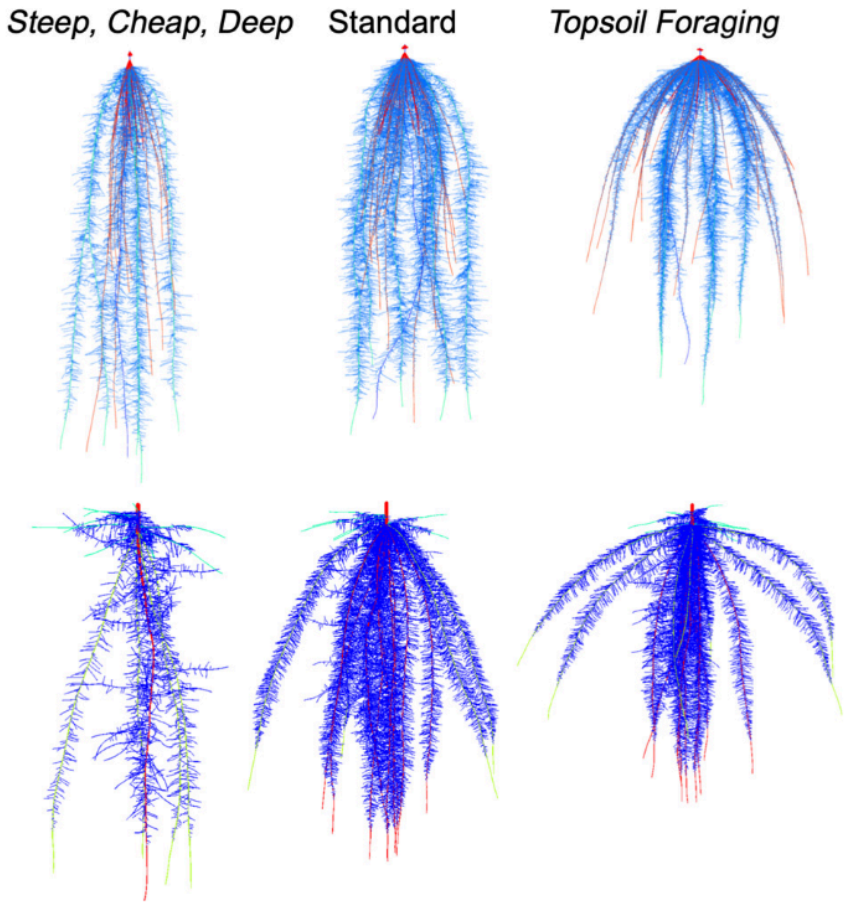


Figure 2 from (Lynch, 2019). Simulation of root architecture ideotypes for maize plants (upper panel) and common bean plants (lower panel) with OpenSimRoot software. Succession of "Steep, cheap, deep" phenotypes, standard phenotypes, and "Topsoil foraging" phenotypes.

These ideotypes have mainly been determined for single stresses but attempts to propose multiple stress ideotypes have been made recently and raise a need for root exploration trade-offs to access fluctuating soil resources (Lynch, 2019; van der Bom, Williams and Bell, 2020). For example, in specific condition, such as dryland soil managed under no-till, spatial separation of water and nutrient resources appears with the drying of the profile and thus a spatio-temporal trade-off would be a key to efficiently accessing the two resources located in opposite places (van der Bom, Williams and Bell, 2020).

1.4. PHENOTYPING

Root phenotyping platforms have been developed to estimate root features and investigate root properties or processes that were not possible to observe in the field. They exist also in a high throughput version that have been developed for studies involving large numbers of plants, as panels used in genetic investigations (Kuijken *et al.*, 2015).

Several installations have been created (Emphasis, 2022; IPPN, 2022), relying on advanced technologies and allowing considerable time savings through automation. Phenotyping platforms differ in many ways, involving carrying capacity, growing substrate, data acquisition methods, dimensionality (number of variables) and possibilities for manipulating the environment (e.g., stress application). We introduce here some of the most widespread root phenotyping techniques as well as singular high throughput root phenotyping platforms that are operational today.

1.4.1. POUCHES

Pouches are the most widely used root phenotyping technique (Bonser, Lynch and Snapp, 1996; Hund, Trachsel and Stamp, 2009; Atkinson *et al.*, 2015). In pouches, roots are developing along a vertical sheet of germination paper that is moistened by capillarity with water or nutritive solution (Figure 3 – A). Seeds are attached at the top part of the pouch, so that the root system unfolds in 2D along the surface of the plate. Pouches are often used to phenotype relatively young plants and mainly focus on the estimation of root traits related to plant emergence (e.g., angle, number and length of seminal roots) (Xie *et al.*, 2017; Khokhar *et al.*, 2019; Rich *et al.*, 2020).

1.4.2. RHIZOTRONS & MINI-RHIZOTRONS

The rhizotron technology relies on the monitoring of root growth at a transparent interface (Thaler and Pagès, 1996; Price *et al.*, 2002). Seeds are sown in a solid substrate (e.g., soil, sand, perlite, or a mix) contained in an inclined (ca. 15° to the vertical), thin (up to a few centimetres) and rectangular box whose downward-facing side is transparent. In this device, roots tend to grow along the transparent face and can be monitored regularly (Figure 3 – B). Images of the root system are usually taken, either manually (Shrestha *et al.*, 2014; Martins *et al.*, 2020) or automatically (Nagel *et al.*, 2012; Rellán-Álvarez *et al.*, 2015) depending on the platform. The age to which plants can

be grown in rhizotrons depends on the size of the bounding box which is usually less than one meter deep.

Mini-rhizotrons are a special kind of rhizotrons that can be deployed in the field. They are long (up to 10 meters) and inclined transparent tubes inserted in the soil in order to assess root distribution as a function of depth (Bragg, Govi and Cannell, 1983; Johnson *et al.*, 2001). A camera or a scanner is inserted inside the tube to capture a root profile. The tube installation, image acquisition and image analysis make this technology very time consuming (Johnson *et al.*, 2001; Rajurkar *et al.*, 2022). In particular, the segmentation of roots from their complex background (including dead roots or worms) requires expert visual evaluation. Fortunately, several software have been developed to facilitate the annotation of the roots (Möller *et al.*, 2019) and deep learning methods pave the way for an acceleration of mini-rhizotron image processing (Smith *et al.*, 2020). Mini-rhizotrons do not allow to analyse the root system architecture as it only reveals small and isolated portions of root systems. However, this is the only technology that allows the observation of plant roots during a whole season in field or near-field conditions (Wacker *et al.*, 2022).

1.4.3. RHIZOTUBES

Rhizotubes are a new technology developed by INRAE. Rhizotubes combine the principles of rhizotrons and pouches in a cylindrical setup. They consist of Plexiglas cylinders containing a cloth bag filled with a substrate containing the nutrient solution, which can be re-watered automatically (Figure 3 – D) (Jeudy *et al.*, 2016). Seedlings grow between the cloth (acting as a pouch) and the Plexiglas (acting as a rhizotron), leaving the possibility to monitor the root system evolution using rotating scanners. Tubes are covered between successive image acquisition to maintain roots in the dark. In the 4PMI platforms, which comprises more than 1000 rhizotubes, AI and machine learning programs (Salon, Jeudy and Lamboeuf, unpublished), are used to reconstruct root systems from images and estimate morphological variables such as bounding box, specific root length, etc. In the 4PMI platform, plants can grow up to 6–8 weeks old (depending on the conditions applied and the plant species, (Jeudy *et al.*, 2016)).

1.4.4. AEROPONICS

Aeroponics studies have started a long time ago (> 80 years) with the main objectives to investigate root growth, mineral nutrition or even root exudations (Waisel *et al.*, 2002). Aeroponics consists in growing plants in the air and feed them with nutritive solutions in the form of spray or mist. The lack of substrate makes it possible to access the whole root system or individual roots very easily for imaging or sampling. The RootPhAir platform has been created in UCLouvain (IPPN Aeroponics, 2022) to allow the monitoring of root growth and root system architecture of up to 990 plants with 2-hour and 24 µm temporal and spatial resolutions, respectively (Figure 3 – E). The image processing is based on the analysis of dense time series and is therefore dedicated to root growth dynamics. In this platform, plants are also limited to young stages, generally up to 2-3 weeks old, since the root length is limited by the size of the platform.

1.4.5. POT EXPERIMENTS

In some studies, plants are grown in soil-filled pots or columns, in order to approximate field conditions as closely as possible (Colombi and Walter, 2016; Rich *et al.*, 2020). Experiments in these containers can last longer than the young stages mentioned above and are only limited by the size of the container. Roots are mostly collected at the end of the experiments and access to more precise characteristics than biomass or a few morphological variables is therefore limited. Harvested root systems can be washed, photographed and traced with specific software (e.g., SmartRoot (Lobet, Pagès and Draye, 2011)), yet this is a time-consuming operation which is therefore limited to a small number of plants and dependent on the stage of the plant (Rich *et al.*, 2020). Soil columns are the preferred containers in platforms equipped with X-ray or MRI instruments (Figure 3 – C) which can be used to scan the whole volume (Colombi and Walter, 2017; Hounsfield Facility, 2022).

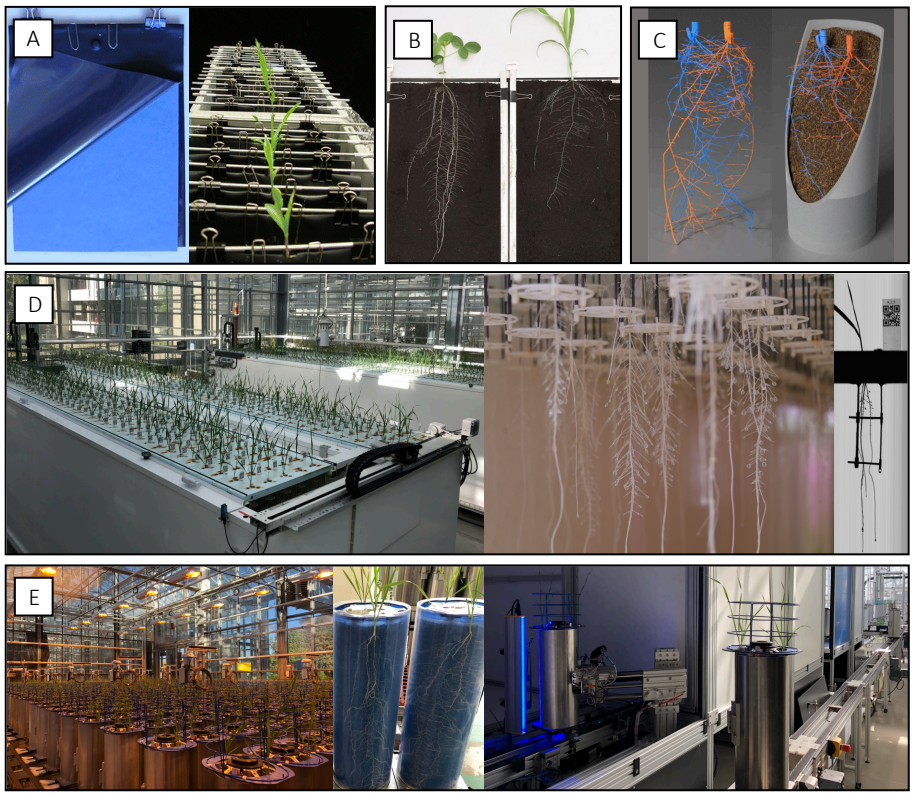


Figure 3. Selection of several phenotyping technics and high throughput platforms. ***A)*** *Pouch device (Source: Figure 1 in Hund, Trachsel and Stamp (2009)),* ***B)*** *Rhizotrons filled with soil (Source: Figure 2 in Martins et al. (2020)),* ***C)*** *X-Ray computed tomography of two plants of Triticum aestivum (Source: Figure 2 in Morris et al., 2017),* ***D)*** *The RootPhAir aeroponic platform, some root systems growing and an example of images taken (Source: Pictures by Clothilde Collet),* ***E)*** *The 4PMI platform with its rhizotubes and the automated imaging system (Jeudy et al. (2016), Source: Pictures by Clothilde Collet).*

1.4.6. ROOT VARIABLES TARGETED IN PHENOTYPING PLATFORMS

To date, high throughput root phenotyping platforms have been able to observe various aspects of root systems, their architecture and growth dynamic in one or several controlled conditions. However, most of the variables that are estimated consist of integrative variables such as root system width, height, number of roots, root lengths, etc. (de Dorlodot *et al.*, 2007; Freschet *et al.*, 2020; Tracy *et al.*, 2020). One of the reasons why dynamics-related features, or more process variables, are not so often estimated is the complexity of handling massive numbers of images contained in time series from high throughput phenotyping platforms. Advances in artificial intelligence and machine learning programs, such as convolutional

neural networks, is expected to streamline time series analysis in the future (Yasrab *et al.*, 2019; Smith *et al.*, 2020).

The interest in process variables is supported by the fact that most parameters of root architecture models (cf. section 1.3) are describing aspects of root dynamics. Therefore, if we want to leverage on the combination of modelling, ecophysiology, phenotyping, we should attempt to target root dynamics via these development processes (section 1.2.4). With the right variables, modelling studies should allow to investigate more plant-environment scenarios than what will be possible to test in high throughput phenotyping platforms. Model-assisted phenotyping can be seen as a possible reinforcement to accelerate knowledge discovery in various areas of root research (Muller and Martre, 2019).

Another question in the actuality is the adequation of simple phenotypic variables to investigate the contribution of root systems to abiotic stress tolerance. Traits that are close proxies of the dynamics of growth and development processes may seem, a priori, better suited to address stress-related problems.

1.4.7. CONSISTENCY BETWEEN PLATFORMS AND FIELD TRIALS

The ecosystem of high throughput root phenotyping platforms is generating a considerable volume of data points. However, since different platforms investigate different aspects of root systems in contrasting environments, it is difficult – and rarely attempted – to co-analyse features from various platforms on the same genetic resources. Likewise, the link between phenotyping in controlled conditions and in field conditions is controversial (Khokhar *et al.*, 2019; Colombo *et al.*, 2022).

Several studies report good correlations between phenotyping root traits with several indicators of plant performance in the field. For example Xie *et al.*, (2017) suggests that the root system architecture of young seedling of wheat grown in pouches is useful to predict field performance as they found correlations between the traits of the root system architecture and yield related traits. Similarly, Colombi and Walter (2016), taking the opposite approach, showed that it was possible to mimic the root responses to compaction as those observed in the field using soil columns in controlled conditions.

Inversely, several examples showed that these correlations were very weak or inexistant, which suggests that the complexity of field environment can hardly be reproduced under controlled conditions. For example, Atkinson *et al.* (2015) reported no consistent correlations between seedling root traits of wheat estimated in pouches with plant heigh, nitrogen uptake nor grain yield estimated in the field. Similar observations have been made by Rich *et al.*, (2020) who reported that wheat seedling root traits estimated with different screening methods (soil tubes, pouches, agar chamber, soil baskets) were inconsistent with deep root characteristics of mature plants grown in the field.

Given that platforms have been largely motivated by (i) the need to measure variables that can hardly be measured in field conditions, especially at such high throughputs, (ii) the advantage to generate reusable data and allow between-platform comparison, and (iii) the intention to better predict field crop responses, the combined analysis of platforms and field datasets is one of the challenges that must be addressed by the phenotyping community.

1.5. WHEAT ROOT ARCHITECTURE

Bread and durum wheat are both monocot plants (cf. section 1.6.2). Accordingly, the backbone of their root system is composed of several main root axes that are connected to the base of the plant (Pagès *et al.*, 2004). At germination, several "seminal root" axes appear from the embryo. The "primary root" is the first seminal root to emerge from the seed. It is also the one that grows the most vertical. The other seminal roots generally appear as pairs (up to 6 seminal roots are generally observed) (Gregory *et al.*, 1978; O'Brien, 1979; Manske and Vlek, 2002; Manschadi *et al.*, 2008). Primary and seminal roots are named "embryonic roots" in this work as they all emerge from the scutellum and epiblast nodes of the embryo (Figure 4). The other root axes are post-embryonic and are named "nodal roots" because they are formed on the coleoptile and on the basal nodes of the stem (Klepper, Belford and Rickman, 1984; Manske and Vlek, 2002).

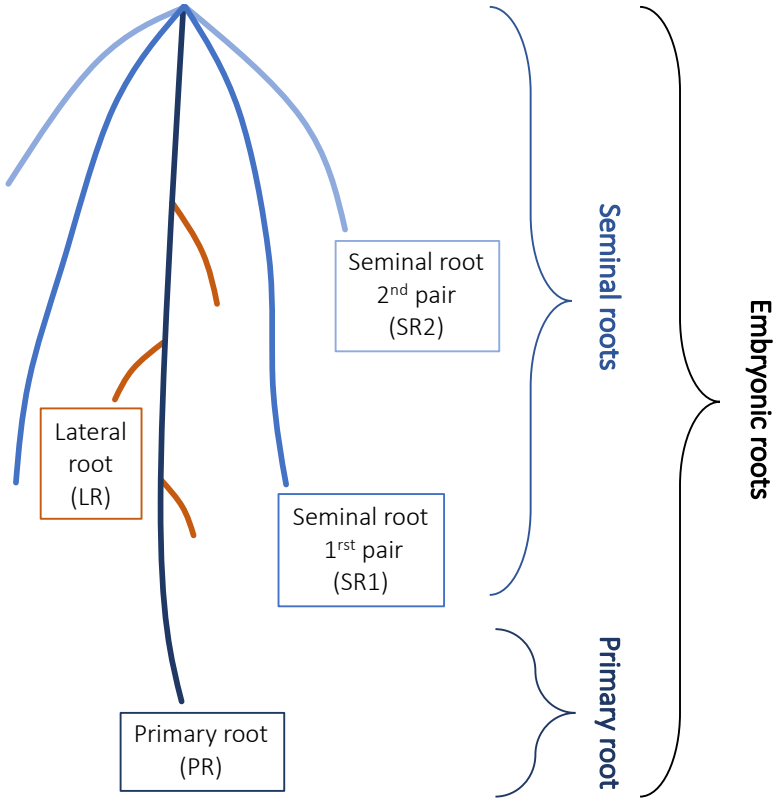


Figure 4. Nomenclature used in this work for the first roots of a wheat seedling. The primary root (PR) is generally the longest and most vertical root, followed by the apparition of seminal roots often coming in pairs (SR1, SR2, etc.). Together they will represent what will be call the embryonic roots. The nodal roots are not represented in this scheme but develop afterwards from coleoptile and following stem nodes. Lateral roots (LR) might appear from any of these root types (Klepper, Belford and Rickman, 1984).

1.6. GENETICS

1.6.1. ROOT TRAITS IN BREEDING

Before we are able to reshape the root architecture of breeding lines towards given root ideotypes, an understanding of the genetic architecture of the relevant root traits is needed. Understanding the genetic architecture of a trait starts with the estimation of broad- and narrow-sense heritabilities and continues with the discovery of polymorphic loci which influence the trait and the estimation of their effects, by means of genome wide association studies (GWAS). Such information is critical in driving the selection process. High throughput root phenotyping platforms have been largely developed in order

to provide detailed phenotypic information that is not accessible in the field, with the throughput required for genetic analysis.

GWAS has been performed for root traits in many species. Root traits are quantitative traits, determined by several gene regions and interacting greatly with the environment (Wasaya *et al.*, 2018). Many quantitative traits loci (QTLs) have already been detected for integrative root variables. However, breeding examples where root QTLs have been brought to commercial varieties are scarce (one example with AQUAmax maize hybrids developed by Pioneer that "included key native traits that improve crop root system (…) to manage drought stress", (Pioneer, 2022)). Among the reasons for such low adoption is the fact that novel traits or QTLs will only be considered in breeding activities if they have predictable effects on performance under stress, are easy to observe at high throughput and have a high heritability or, at least, a clear determinism with few QTLs having large effects – though the recent development of genomic selection may help in the selection for traits with complex genetic architecture.

1.6.2. ROOT GENETICS IN WHEAT

Since the 1950s, selection of wheat phenotypic characteristics has been at the origin of major yield improvements. As mentioned by Monneveux, Jing and Misra (2012), the replacement of the traditional cultivars with varieties carrying dwarfing genes and better adapted to fertilizers-fed environments allowed major yield ameliorations. In particular, the reduction of plant height has allowed a larger share of carbon to the grains, an increased harvest index and a reduction of lodging risks (Flintham *et al.*, 1997; Brancourt-Hulmel *et al.*, 2003). This has been achieved through the selection of yield-productive genotypes (Jiang *et al.*, 2003) having higher grain number per square meter without reduction of grain weight (Donmez *et al.*, 2001). The growing interest for productive varieties in stressed environments has emerged in the last decades and, even if breeding remains largely focused on grain yield, root traits have been advocated in the root community as the basis for a new green revolution (Lynch, 2007).

It is expected that the genetic diversity for root traits in wheat has been largely under-exploited. Bread wheat accounts for about 95% of the wheat production, followed by the durum wheat (5%) (Shewry, 2009; Monneveux, Jing and Misra, 2012). Bread wheat or *Triticum aestivum* L., a monocotyl of

the Poaceae family, is the result of the natural hybridisation of *Triticum dicoccoides* (AABB) with *Triticum tauschii* (DD). Twenty-one chromosomes compose its genome (AABBDD, 6n=42) with a length of 16 thousand Mb (five times larger than the human genome) (O'Brien and DePauw, 2004). Durum wheat or *Triticum turgidum* subsp. *durum* comes from the hybridisation of two diploid grasses (2n=7), *Triticum monococcum* (AA) and *Aegilops speltoides* (BB) (O'Brien and DePauw, 2004). It is therefore tetraploid (AABB 4n=28) and is composed of 14 chromosomes. Durum wheat is known to have a higher tolerance to drought conditions than bread wheat, in line with its extensive cultivation in rainfed Mediterranean environments (Monneveux, Jing and Misra, 2012).

In wheat, GWAS studies on the architecture of the root system have only started in the last 15 years. This late onset might be explained by recent increased of interest in root parts on the one hand, but also by the complexity of the polyploid genomes of wheat species on the other. Indeed, many root studies had been performed in other species like rice, maize many years before (Tuberosa *et al.*, 2003), Arabidopsis, etc. (Tuberosa and Salvi, 2005).

The first genetic studies mentioning wheat QTLs for root traits were performed with the aim of identifying traits related with specific plant abilities or stress conditions (e.g., lodging resistance (Verma *et al.*, 2005), aluminium resistance (Ma *et al.*, 2005), nitrogen uptake (An *et al.*, 2006), soil-penetration (Kubo *et al.*, 2007)). The traits investigated in these studies were quite diverse and mainly focused on the above-ground parts, leaving the roots traits investigated in the background and being often very simple morphological traits such as root weights, root lengths or root depths. The first study that we identified whose focus was the investigation of root architecture was reported by Sanguineti *et al.* in 2007 in durum wheat and by Sharma *et al.* in 2011 in bread wheat.

1.6.3. ROOT QTLS REVIEW FOR BREAD WHEAT

We have performed a systematic literature search for root QTLs in bread wheat. From 2005 to 2020, 59 articles reported at least one QTLs for root traits. From these articles, a list of 1700 QTLs has been assembled, with the QTL name, its position (base pair and chromosome number) and their pic or flanking markers (if available) and uploaded on Zenodo (Annexe 4, Collet, 2022). The combination of these studies covers an important fraction of the

root phenotypic space. Because root descriptors from these studies were largely study-specific, we attempted a classification of traits in 17 arbitrary-built categories in order to ease meta-analysis (Table 2).

Table 2. Root categories in which the QTLs for root traits of bread wheat species have been classified. The last column represents the number studies that found at least one QTL in the corresponding category.

Root categories	Definition	Number of studies
Angle	Traits related to the root orientation angles (e.g., angles from the vertical or angle between pair of seminal roots)	9
Area	Traits related to the surface area occupied by the root system (e.g., total root surface area)	13
Branching	Traits related to root branching (e.g., forks number)	2
Depth	Traits related to root system depth (e.g., maximum root length or root plate depth	22
Diameter	Traits related to root diameters (e.g., root diameter, average root diameter)	11
Distribution	Traits related to distribution of the root system within the soil (e.g., convex hull or root length density per cm^3 of soil)	2
Elongation	Traits related to root elongation (e.g., elongation or growth rate)	3
Length	Traits related to root length (e.g., total, primary, seminal root lengths)	31
NbRoot	Traits related to root number (e.g., seminal, total, or average root number)	29
NbTillers	Tiller number	8
R/S	Root to shoot ratios (fresh or dry)	13
RHair	Traits related to root hairs (e.g., root hair density)	2
RMass	Root biomass (fresh or dry)	32
SMass	Shoot biomass (fresh or dry)	25
TMass	Total plant biomass (fresh or dry)	10
Volume	Traits related to root volume (e.g., total root volume)	11
Yield	Traits related to yield (e.g., grain yield)	8

A clear trend is confirmed from Table 2: most of the traits addressed in the QTL studies are simple, easily measurable morphological traits such as root biomass (e.g., RMass with 32 studies), root lengths (e.g., Length with 31 studies) or root number (e.g., NbRoot with 29 studies). In contrasts, very few QTLs are recorded for traits more closely linked to root dynamics such as root growth (e.g., Elongation with 3 studies), root diameters (e.g., Diameter with 11 studies) or root branching (e.g., Branching with 2 studies). This means that studies investigating the genetic determinism of such traits are still scarce and their genetic architecture remains unexplored.

1.7. OBJECTIVES OF THE THESIS

Our review indicated that different and complementary representations of root system architecture have been proposed and that these are supported by root architecture models that can be used to enrich the exploitation of expensive root phenotyping data. Nevertheless, these have not received much attention in the root phenotyping community which results in a dissatisfaction between what is delivered by high throughput root phenotyping platforms, and the possibilities offered by model-assisted phenotyping.

Therefore, the aim of this thesis was to propose new methods that exploit dense time series of root system images to estimate phenotypic variables derived from the modelling literature and evaluate these variables in the context of multi-platform and genetic investigations.

Accordingly, the objectives of these thesis were to:

(i) Develop an analysis pipeline to estimate root growth and development variables and be able to process dense time series of images from high throughput root phenotyping platforms (Chapter 2).

(ii) Assess the benefits of these phenotypic variables in relation with other platforms in the context of large diversity collections (Chapter 3).

(iii) Evaluate whether the genetic architecture of these phenotypic variables differ from that of the most commonly measured traits (Chapter 4).

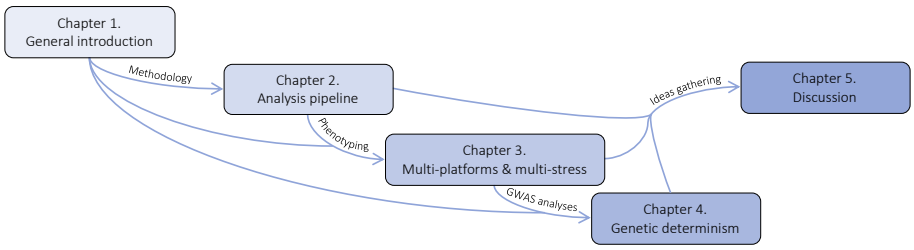


Figure 5. Organisation of the different chapters of the thesis.

Interchapter 1-2

After introducing the overall context of this thesis and the main objectives pursued, we will present, in the next Chapter 2, a unique analysis pipeline. This pipeline was designed in response to the lack of success of current phenotyping methods in assessing root traits close to growth dynamics.

From the exploitation of very simple features, such as root tips extracted from dense image time series, we will show that root architectures and their growth can be sensibly approximated.

The set of estimated features related to the morphology and growth dynamics of the root system will be presented and the pipeline illustrated with two wheat species (bread and durum wheat) phenotyped in the aeroponic high-throughput root phenotyping platform, RootPhAir.

Their genetic variability and heritability will already start to be discussed but will be developed in more detail in Chapter 3.

Chapter 2.

A Simple Method to Convert Time Series of Root Tip Coordinates into Dynamic Representations of Plant Root Systems

2.1. INTRODUCTION

Plant phenotyping platforms have been developed to assess plant characteristics and improve our understanding of plant-environment interactions. These facilities often use image-based technologies to capture plant phenotypes, generating a massive number of images for analysis (Li, Zhang and Huang, 2014; Pieruschka and Schurr, 2019; Bekkering, Huang and Tian, 2020). The information content of these resources is frequently underexploited as data extraction from multiscale image time series remains a complex task for which tools are not always available (Lobet, 2017a).

Which characteristics are extracted from images and how the treatment of the temporal dynamics is handled can be restricted by many factors. Firstly, the complexity of the analysis impacts the recurrence at which some variables are considered. Accordingly, most of the traits reported tend to be the most accessible and measurable ones, generally integrative variables (morphologic traits as bounding box, length, etc.) (Freschet *et al.*, 2020) and process variables representing the dynamic of plant growth are usually poorly represented (de Dorlodot *et al.*, 2007; Tracy *et al.*, 2020). Unfortunately, architectural features are often not well captured by highly integrative traits but require multiple elementary traits that interact with each other as well as with the environment and with time. This makes it more difficult to infer traits describing elementary architectural characteristics. Secondly, the choice of a trait differs depending on the discipline in which the study is performed. The target trait in genetics is generally one with a high heritability, whereas in eco-physiology the target trait is the one that predicts a good performance or a function (as described in Freschet et al. 2020). Finally, the choice of a trait also depends on the scale studied (e.g., canopy scale, root system scale, root type scale) as well as the research scope (e.g., water uptake, carbon capture).

The exploitation of growth dynamics using image time series increases the burden as it involves the processing of large number of images. Not surprisingly, most of the analyses reported are restricted to descriptive statistical approaches (non-parametric or spline) which simplify the approach. When it comes to detailed architectural characteristics, only few time points are selected among the entire time series, leaving much data untapped.

Defining a parsimonious set of variables is at the heart of the practice of modelling. Close to the scales and focus of plant phenotyping, functional structural plant models summarise the state of knowledge about the interactions between plant processes with soil and environmental properties, and simulate the structure and spatial distribution of plant organs over time, sometimes taking resource availability into consideration (Pagès *et al.*, 2004, 2012; Dupuy, Gregory and Bengough, 2010; Barczi *et al.*, 2018; Schnepf *et al.*, 2018). Looking at the root parameter sets of functional structural plant models is therefore a sound strategy to identify key variables that have a simple biological significance and are sufficient to capture essential aspects of root systems architecture processes and functions.

The models ArchiSimple (Pagès *et al.*, 2012), CRootBox (Schnepf *et al.*, 2018), OpenSimRoot (Lynch *et al.*, 1996; Postma *et al.*, 2017) and Root Typ (Pagès *et al.*, 2004) use about ten features as input parameters, which are sufficient to simulate root growth and development over time for many species and genotypes. These key parameters mainly describe dynamic processes such as growth, elongation, emission, branching and decay (Table 3).

One can hope that artificial intelligence software developed to analyse image time series and assess plant characteristics and development (Ubbens and Stavness, 2017; Jiang and Li, 2020; Smith *et al.*, 2020) will streamline the estimation of model parameters from large collections of images, also taking advantage of the capability of models to generate training sets of images and parameters. However, they also come with their own restrictions as to the nature of the variables that can be reliably estimated (Lobet, 2017b; Lobet *et al.*, 2017).

In this Chapter 2, we propose a simple analysis pipeline to address the above-mentioned challenges. Written in R (R Core Team, 2021, version R 4.1.2.), the pipeline performs a succession of data manipulations on the outputs of a tip detection algorithm applied to time sequences of root system images. It

estimates several root phenotypic variables, inspired from model parameters, that have straightforward dynamic processes and biological interpretations. We choose to focus on the determination of process variables because they are closely connected to root development processes, and this could help to better understand the genesis of the root system architecture through growth and development processes. In a first step, we illustrate how tip detection, when applied to time lapse images, comes down to a temporal sampling which can be reversed to estimate root trajectories over time. In a second step, we provide different proof of concepts cases of exploiting root tip information. In a third step, we present the pipeline and assess the accuracy of results compared to manual tracing. Finally, we summarise some results of the analysis of a wheat diversity panel using the proposed pipeline.

Table 3. Simplified list of the common parameters of four popular architectural root models: ArchiSimple (Pagès et al., 2012), CRootBox (Schnepf et al., 2018), OpenSimRoot (Lynch et al., 1996; Postma et al., 2017) and Root Typ (Pagès et al., 2004).

Process	Parameter	ArchiSimple	CRootBox	OpenSimRoot	Root Typ
Growth	Duration before emergence	✓	✓		✓
	Elongation rate	✓	✓	✓	✓
	Apical diameter	✓	✓	✓	✓
	Diameter & radial growth	✓	✓	✓	✓
	Maximal root length		✓	✓	✓
	Sensitivity to mechanical constraints		✓	✓	✓
Shape or direction	Gravitropism	✓	✓	✓	✓
	Insertion angle	✓	✓	✓	✓
Branching	Proportions of root types	✓	✓		✓
	Inter-branch distance	✓	✓	✓	✓
Decay	Senescence	✓	✓		✓

2.2. RESULTS AND DISCUSSION

2.2.1. ROOT TIPS OVER TIME ARE INCREMENTAL SNAPSHOTS OF ROOT SYSTEM ARCHITECTURE

The recognition of root tips on images constitutes a basic operation that can be performed very quickly and is therefore compatible with large numbers of images such as dense image time series. Tips are generally used to count the number of roots. Nevertheless, it escapes our mind that a reasonably correct

representation of a root system can be obtained from the location of all of its root tips over time. As shown on Figure 6 – A, the shape of the root system architecture of *Arabidopsis thaliana* grown in 2D can be sampled by the application of tip detection algorithm at regular time intervals. The overlapping of the tips detected at different time intervals reveals the importance of the temporal resolution of the imaging process. With smaller time intervals between successive images, finer details of the root system architecture will be captured and, therefore the reconstruction of root trajectories should be eased. The same process has been performed with durum wheat grown in 3D (Figure 6 – B) and also highlights the importance of the temporal resolution. In this second case, however, the spatial projection from 3D to a plane image makes it more challenging to distinguish roots, a problem that becomes acute when lateral roots start to appear (not yet visible on Figure 6 – B).

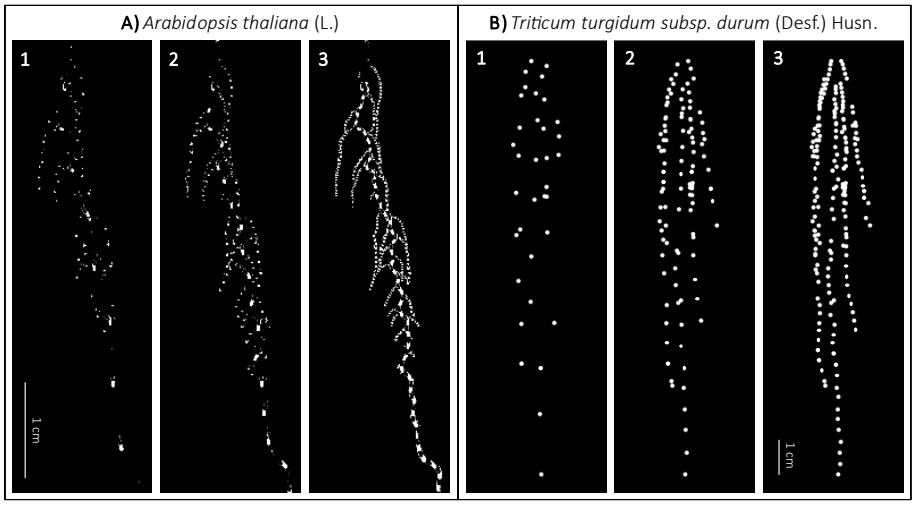


*Figure 6. Images of root tips detected at different temporal resolutions for a 14-day old plant of Arabidopsis thaliana grown on a Petri dish (2D) (**A**) and for a 4-day old plant of Triticum turgidum durum grown in aeroponics (3D) (**B**). The importance of time resolution is illustrated through three different image acquisition frequencies: **A)** tips recorded every 50 minutes (1), every 25 minutes (2) and every 10 minutes (3); **B)** tips recorded every 10 hours (1), every 4 hours (2) and every 2 hours (3).*

2.2.2. TRACKING ROOT TIPS DISPLACEMENT LEADS TO INSTANTANEOUS ELONGATION RATE ESTIMATION

Along the sampling process explained in the previous section individual root tips lose their identity. Fortunately, this loss of information can be reversed.

Indeed, root trajectories can be regenerated in the form segmented lines, as long as the tips can be assigned to the root to which they belong. Under these conditions, growth directions and instantaneous elongation rates can be inferred along the reconstructed trajectories.

In the *Arabidopsis* example (Figure 6 – A), the root trajectories are easily found using an iterative search: for a given root trajectory reconstructed until time t, the tip at t+1 that is the closest to the end of the trajectory is selected and appended to the trajectory. This process is repeated until no suitable follower tip can be found, i.e., when the distance to the nearest tip is larger than a reasonable displacement. From the root tracing and the temporal information, the root elongation rate can be estimated as $ERate_{(t)} = \frac{dL}{dt}$ by taking the derivative of the length along the root path ($L = f(t)$). This gives access to the temporal evolution of individual root elongation rates. This simple method is applicable a long as the displacement of tips across successive image acquisitions is smaller than the distance between neighbour roots, so that the assignment can be done unambiguously.

For denser root systems as for the wheat example (Figure 6 – B), the same iteration method is not easily applicable, because the probability of finding a closest tip that does not belong to the same root can be considerably larger (cf. inset image in Figure 7 – A). Alabart and Devleeschouwer (Alabart, 2017) have developed a dedicated algorithm based on multi-object tracking, which combines a forward and backward traversals of the whole tips collection. In the forward traversal, the trajectory established during the previous iterations (ending at time t) is used to predict the (expected) spatial distribution of the follower tip at t + 1. The observed tip for which the density of probability is the largest is then appended to the trajectory. The backward traversal is used to remove incorrect connections that were established during the forward travel. Starting from a tip at time t, the tip with the shortest path at time t-1 is selected and considered for reconnection or removal (Alabart, 2017). As a proof of concept, from images of experiments carried out with wheat growing in a 3D substrate-free environment (section 2.4.2), they were able to reconstruct the trajectories of most seminals but also of several lateral roots (Figure 7 – A). This algorithm is currently being evaluated for automated operation.

The main limitation of these two methods is that the temporal resolution must be matched to the root elongation rate and root tip density to allow the reconstruction process. In the *Arabidopsis* example, a resolution of 15 minutes allowed a nearly perfect reconstruction of the whole root system. In the wheat example, a resolution of two hours was a minimum to allow the reconstruction of the fast-growing seminal roots. This range of resolution, however, is only achievable by dedicated high throughput conveyor systems.

2.2.3. ROOT TIP COORDINATES ARE THE RAW DATA FOR ROOT DENSITY ANALYSIS

Root tip coordinates have also been used in simpler models based on spatial root tip distribution. Indeed, the tip distribution can be seen as a proxy of the root length density which is often used as an indicator of resource capture capacity. Using the coordinates of the whole set of tips detected along a 3-week long experiment (section 2.4.2), Kelly and colleagues were able to provide a description of the entire root system with only three parameters (Figure 7 – B) (unpublished, Kelly *et al.*, 2020). The formula of the model is the following one:

$$\lambda(u) = \exp\left(\beta_0 + \beta_1|x| + \beta_2 y\right)$$

Where u is a tip point with spatial coordinates (x,y) and λ is the local density. This model is largely inspired by the exponential function commonly used in the soil hydrological models community to represent the distribution of root length density in the soil (Gerwitz and Page, 1974; Raats, 1974; Zang, Elliott and Ketring, 1993; Li, Boisvert and Jong, 1999). It can be extrapolated to other experiments since it is built on a rather simple hypothesis that the highest tip density is close to the seed and decreases exponentially from there (horizontally and vertically).

Tips are also the raw material for more elaborated density models such as those proposed by Kalogiros *et al.* (2016) and providing continuous probabilistic representations of root system architecture. In their model, the hypothesis of the exponential decrease from the seed is relaxed and the evolution of the density is allowed to vary in time and space. Density maps can then be given for root lengths, root tips, growth directions or branching points densities (Figure 7 – C). Proof of concept studies of estimating density

maps from tips datasets have been provided by Dupuy, Gregory and Bengough (2010), Dupuy (2011) and Kalogiros *et al.* (2016).

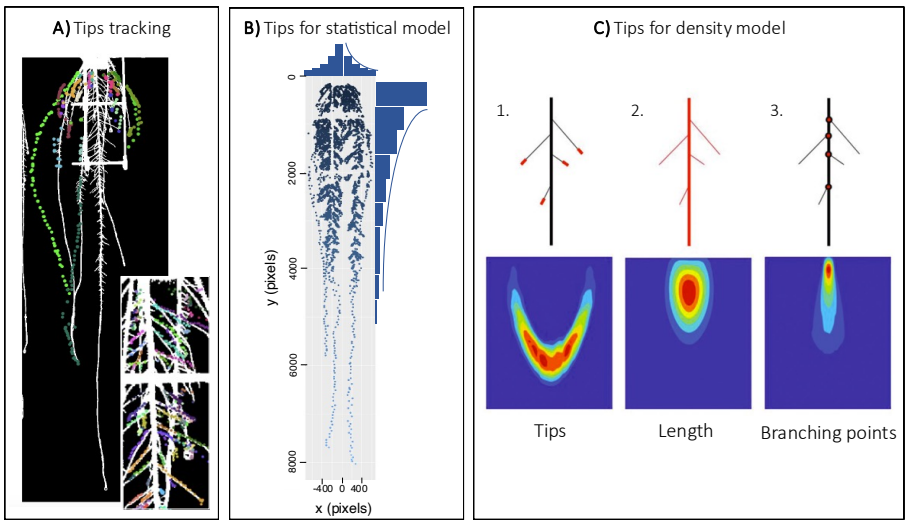


Figure 7. Illustrations of different exploitation routes of tips data. ***A)*** *Spatial reconstruction of root trajectories: tips of the same seminal roots or lateral roots (inset image, below right) are assigned with the same colour (Alabart, 2017).* ***B)*** *Tips data for statistical analysis: root phenotypes can be described with a statistical model (with only three parameters) based on the hypothesis that the highest tip density is close to the seed and decreases exponentially from there, in both directions (Kelly et al., 2020). C) Root data as information for density models: maps of the tips, root lengths or branching points densities. Only the first two are estimable from tips data (Kalogiros et al., 2016).*

2.2.4. A NEW PATH FROM ROOT TIPS TO DYNAMIC GROWTH AND BRANCHING PARAMETERS

The raw output of tip detection algorithms usually comprises the set of (x,y) coordinates of all tips present in an image. When applied to a succession of images of the same root system, the coordinates of tips change from one image to the next, as roots continue growing, and the size of the set increases with the production of new roots. In a time series dataset, the coordinates of a tip can therefore be extended with a time stamp and formulated as (x,y,t).

Different variables can be computed from these coordinates. One of them is the euclidian distance between tips and the plant collar. In “fasciculated” root systems with several axial roots growing relatively straight from the shoot base, this variable can be used to identify the tips with the largest tip-collar distance, which should belong to those axial roots. For these roots, the tip-collar distance increases over time at a rate that approximates their

elongation rate. The tip-collar distance is therefore useful for classifying tips in groups, which will be the basis for counting, assignment to roots and estimation of growth dynamics.

Using similar reasoning, we assembled an analysis pipeline which is graphically represented in Figure 8 and explained in the legend. The pipeline processes the (x,y,t) coordinates of root tips throughout an experiment to get most of the variables listed in Table 4.

Table 4. List of root traits extracted by the pipeline, their description, their extraction method (from which entity and unit used), and whether or not they are used as input parameters of root architectural models (DAS = days after sowing, ER = embryonic root, PR = primary root, 1LR = first lateral root).

Trait	Description	Method	Entity	Unit	Inputs in models
$Diam_{ER}$	Median diameter of the embryonic roots	Computed	Tips population	cm	✓
$Diam_{LR}$	Median diameter of the lateral roots	Computed	Tips population	cm	✓
DPD	Duration of primordium development	Computed	Tips population	DAS	✓
$ERate_{PR}$	Elongation rate of the primary root	Computed	Tips population	cm/day	✓
$Emer_{PR}$	Emergence of the primary root	Computed	Tips population	DAS	
$Emer_{1LR}$	Emergence of the first lateral root	Computed	Tips population	DAS	
LRD	Lateral root density corresponding to the number of lateral roots per centimeter of branching root	Computed	Tips population	number of lateral roots/cm	✓
MRL	Maximum root length at mid-experiment	Computed	Tips population	cm	✓
Nb_{ER}	Number of embryonic roots	Manual validation	Subset of images (4)	number	
R/S_{Dry}	Root to shoot ratio (dry weights)	Precision scale	Entire plant	-	
R/S_{Fresh}	Root to shoot ratio (fresh weights)	Scale	Entire plant	-	
$RMass_{Dry}$	Root dry weight	Precision scale	Root parts	g	
$RMass_{Fresh}$	Root fresh weight	Scale	Root parts	g	
$SMass_{Dry}$	Shoot dry weight	Precision scale	Shoot parts	g	
$SMass_{Fresh}$	Shoot fresh weight	Scale	Shoot parts	g	
SRA	Root angle between the first pair of seminal roots	Manual validation	Subset of images (4)	radian	✓

The version of the pipeline described here has been designed from different case studies with 2- to 3-week-old cereals plants (wheat, rice, sorghum, maize, millet) and is illustrated in this case with a wheat experiment. During the pipeline design, typical wheat descriptions were taken into consideration, which led to the following principles or simplifications:

- Roots were classified in two categories. The first category named "embryonic root" comprises the primary root and the seminal roots (up to 6). Because they emerge first and elongate fast, their tips will be easy to identify based on the tip-collar distance. The other roots comprise the nodal and lateral roots. The number of nodal roots (0 to 4 were observed in the experiment) being negligible compared to the number of lateral roots (hundreds observed), the second category will be named "lateral root".
- Because embryonic roots usually grow relatively straight in the conditions of the experiment, their length was approximated by the tip-collar distance.
- The ***DPD*** is the time elapsed between the initiation of a lateral root primordium and the emergence of this lateral root (Lecompte, Ozier-Lafontaine and Pagès, 2001; Pagès *et al.*, 2010). By assuming that the ***DPD*** is constant over time and is the same for all embryonic roots, it could be easily estimated as the time elapsed between the emergence of the primary root and that of the first lateral root (Figure 8 – F).
- The ***LRD*** is defined as the number of tips detected per unit length of the branching section of the parent root. Assuming the ***LRD*** to be constant along the embryonic roots allowed us to estimate it as the ratio of the number of lateral roots to the length of the embryonic root branching section.
- To estimate the length of the branching section, we took advantage of the fact that lateral roots formation in cereals (i) is acropetal, (ii) takes place very close to the tip of the parent root and (iii) precedes by ***DPD*** the time of a lateral root emergence. As a consequence, the length of an embryonic root at time *t* is equal to the length of its branching zone at time *t* + ***DPD*** (Figure 8 – G).

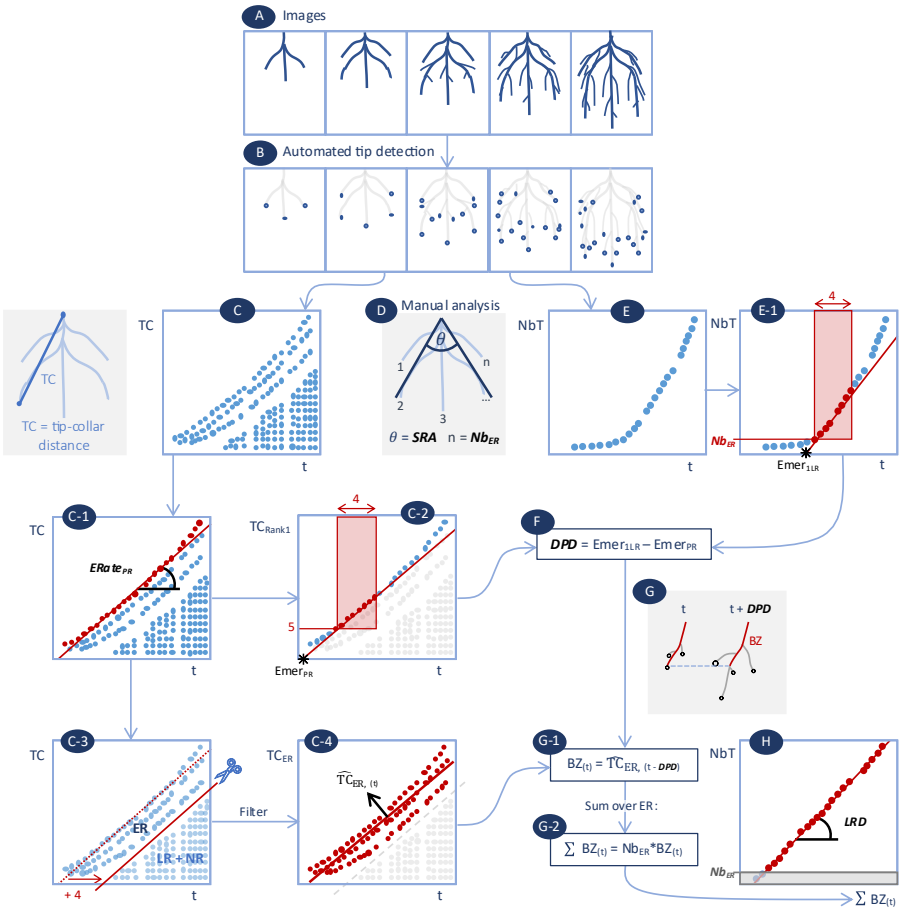


*Figure 8. Analysis pipeline to estimate root traits from a population of root tips (section 2.2.4 for implicit simplifications). All graphs relate to a single plant, so the pipeline must be run for each plant in the experiment. Points used for regressions are in red; root traits are in black and bold; dots filtered are in light grey. Time is expressed in days after sowing (**DAS**); distances in cm. **A)** Dense image time-series capturing the root system growth of one plant are generated in the aeroponics root phenotyping platform RootPhAir (section 2.4.2). **B)** Automated detection of root tips with an in-house software. **C)** Scatterplot of the tip-collar distance (TC = euclidian distance from root tip to collar) over time. **C-1)** The elongation rate of the primary root (**$ERate_{PR}$**) is estimated as the slope of regression on the tips with the highest tip-collar distance value at each time (= tips of rank 1). **C-2)** The emergence of the primary root (**$Emer_{PR}$**) is the abscissa intercept of the regression made on a subset of tips of rank 1 (TC_{Rank1} > 5 cm, window of 4 days). **C-3)** A categorisation of the tips is made by shifting the regression on the tips of rank 1 (**C-1**) by 4 days to the right (the shift was determined empirically for all plants). The tips of embryonic roots (ER) are on the left of the shifted regression line and the ones of lateral and nodal roots (LR+NR) are on the right. **C-4)** The predicted tip-collar distance of any embryonic root at each time ($\widehat{TC}_{ER}$) is estimated with a regression made on all embryonic root tips. **D)** Manual analysis of the number of embryonic roots (**Nb_{ER}**) and the seminal root angle between the first pair of seminal roots (**SRA**) when the number of seminal roots is stabilized (based on a set of images at 3, 5, 7 and 9 DAS). **E)** Plot of the total number of tips (NbT) over time. **E-1)** The emergence time of the first lateral root (**$Emer_{1LR}$**) is estimated as the abscissa intercept of the regression of the*

*total number of tips over time, using a subset of points (NbT > **Nb_{ER}**, window of 4 days). **F)** The average duration of lateral root primordium development (**DPD**) is calculated as the difference between **$Emer_{1LR}$** and **$Emer_{PR}$**. **G)** Principle of estimation of the length of the branching zone (BZ) of an embryonic root: since lateral roots are initiated in the vicinity of the embryonic root tip, the length of the embryonic root at time t corresponds to the length of the branching zone of the same embryonic root at time t+**DPD** (Lecompte, Ozier-Lafontaine and Pagès, 2001). **G-1)** Accordingly, the length of the branching zone of any embryonic root at time t is approximated as the predicted tip-collar distance of any embryonic root at time t-**DPD** ($\widehat{TC}_{ER,(t-DPD)}$). **G-2)** The cumulated length of the branching zone of all embryonic roots ($\sum BZ_{(t)}$) is obtained by multiplying $BZ_{(t)}$ by **Nb_{ER}**. **H)** The average number of lateral roots per cm of branched embryonic root (**LRD**) is estimated as the slope of the regression of the total number of tips over $\sum$ BZ (after filtering data points where NbT < **Nb_{ER}**).*

2.2.5. PLATFORM DESCRIPTION

We illustrate the pipeline with a wheat experiment conducted in the RootPhAir platform (IPPN Aeroponics, 2022). RootPhAir is an aeroponic facility where plant roots develop in a substrate-free environment, i.e., in the absence of mechanical constraints. The platform can hold up to 990 plants organised in two separate boxes. Conveyors operate continuously to bring plants in front of a high resolution backlight imaging station. About 130 images are taken per root system (one every two hours) for an experiment lasting two weeks. For more details about the facility cf. section 2.4.2.

2.2.6. PIPELINE EVALUATION

2.2.6.1. ROOT TIP DETECTION

The analysis pipeline relies on the quality of tip detection. We used an in-house software called AeroScan (Draye, unpublished) and validated its output against a manual counting performed with the ImageJ software (Rasband W.S., 2011). A manual tip counting (ca. 10 hours) was performed on twenty-four images from the entire collection, selected randomly, and taking care to include a wide range of root densities. As observed on Figure 9 – A, all points are located above the 1:1 line, indicating that AeroScan underestimates the number of tips compared to the validated data. Not surprisingly, the error is size dependent as the gap between the regression and the 1:1 line increases. Indeed, as the root density grows, so does the number of tips and the underestimation accumulates. The adequation of a unique linear regression for these contrasted images indicates that the underestimation is a constant factor and can be considered as a bias which can be corrected for and not as a random error.

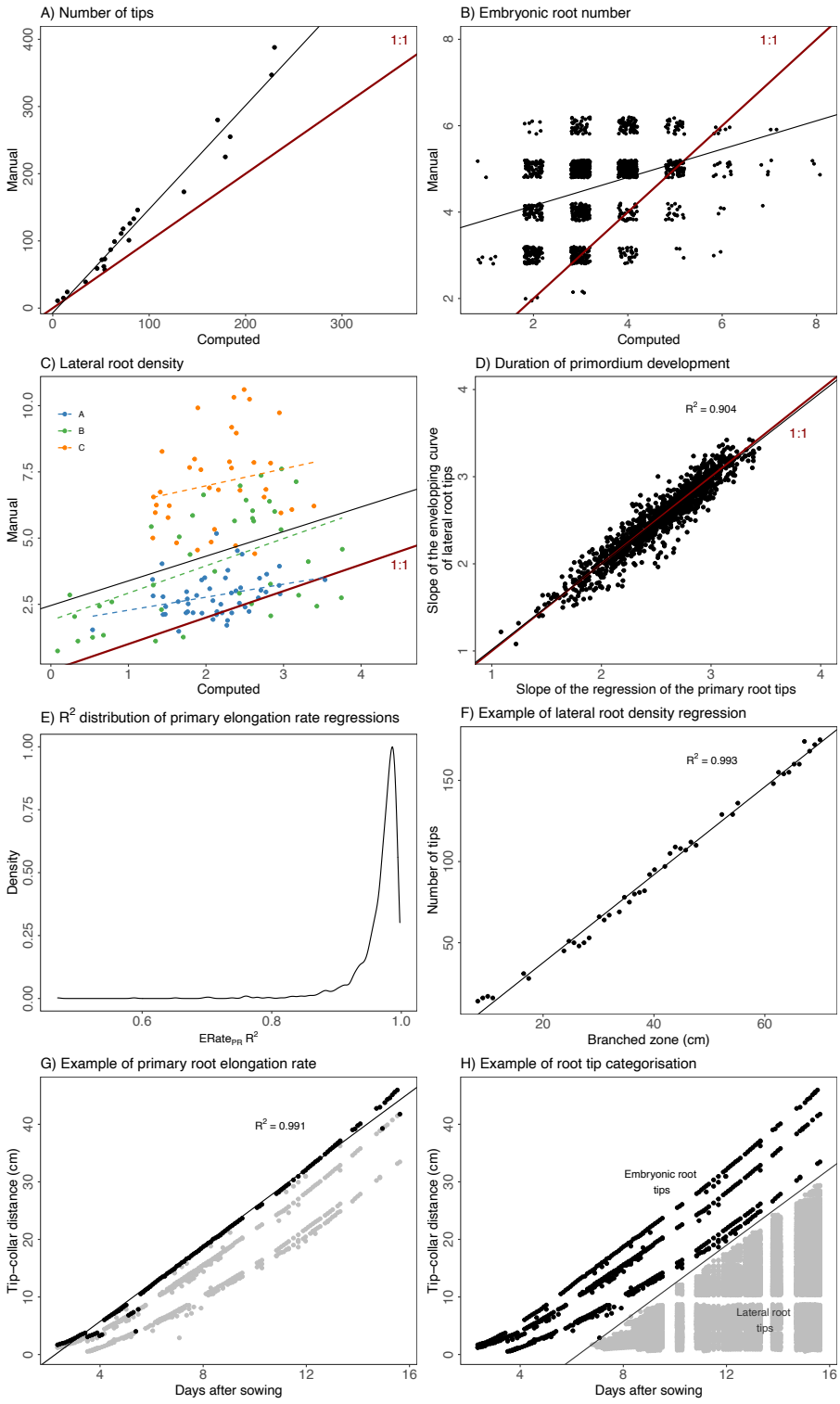

A) Number of tips
1:1
Manual
Computed
B) Embryonic root number
1:1
Manual
Computed
C) Lateral root density
A
B
C
1:1
Manual
Computed
D) Duration of primordium development
R² = 0.904
1:1
Slope of the envelopping curve of lateral root tips
Slope of the regression of the primary root tips
E) R² distribution of primary elongation rate regressions
Density
ERate_PR R²
F) Example of lateral root density regression
R² = 0.993
Number of tips
Branched zone (cm)
G) Example of primary root elongation rate
R² = 0.991
Tip–collar distance (cm)
Days after sowing
H) Example of root tip categorisation
Embryonic root tips
Lateral root tips
Tip–collar distance (cm)
Days after sowing

*Figure 9 (previous page). Comparison between computed and manual measurements of the number of tips detected (**A**), the embryonic root number (**B**), the lateral root density (**C**), a graph of the relationship between the slope of the envelope curve made on all lateral root tips over the slope made on the tips with the highest tip-collar distance (tips of rank 1) (**D**), a graph of the distribution of r-square densities for the regressions of the primary root elongation rate (**E**), an example of regression used to calculate the lateral root density of one plant (**F**), an example of regression used to calculate the primary root elongation rate of one plant (**G**) and a last example of root tip categorisation with one plant (**H**). Black regressions correspond to linear regressions made on the black points, and burgundy red regressions are the 1:1 lines. **A)** Relationship between the number of tips manually counted in ImageJ over the number of tips automatically detected by AeroScan. Each dot represents an image of one plant. All images are from different plants and genotypes. **B)** Relationship between the embryonic root number manually counted with the in-house program MosaicViewer over the mean embryonic root number present in the categorisation made with the R pipeline. Each dot represents one plant (jitter applied), all genotypes of the panels are present. **C)** Relationship between the lateral root density manually validated in SmartRoot or ImageJ over the **LRD** computed with the R analysis pipeline. Each dot represents one plant. Most of the plants are from different genotypes. The three validation types correspond to different methods of validation carried out by two different teams (A: method of the team n°1 in SmartRoot by drawing long roots (in its entirety) and their lateral roots to assess the **LRD**; B: method of the team n°1 in SmartRoot by using a mark tool on several small root segments to assess the **LRD**; C: method of the team n°2 in ImageJ by drawing several intervals between two lateral roots to assess the **LRD**; more details about the methods cf. section 2.2.6.5). The regression in black is the overall regression for all types of validation and each dotted line regressions corresponds to the regressions per validation type. Six points have been previously filtered based on their Cooks distance (threshold set to 4/n, where n is the number of observations). **D)** Relationship between the slope of the envelope curve made on all lateral root tips over the slope made on the tips having the highest tip-collar distance (tips of rank 1) to see if the **DPD** is constant over time. **E)** Distribution of the R^2 obtained for the regression made to calculate the $\mathbf{ERate_{PR}}$. **F)** Relationship between the number of tips and the root branched zone of one plant. The regression is used to calculate the lateral root density. **G)** Illustration of the linearity of the primary root elongation rate regression with one plant. The regression is made between the tip-collar distance of the tips belonging to the primary root (in black the tips of rank 1 used to calculate the slope, in grey all tips belonging to embryonic roots) and **H)** Illustration for one plant of the root tips categorisation made. The regression corresponds to the same regression as in **G)** but shifted by 4 days (empirically) allowing to edge the beginning of the lateral root tips apparition.*

The causes of the underestimation by AeroScan are multiple. The most likely is the occlusion that occurs with the projection of 3D root systems to 2D images. As a result, tips masked by other parts of the root system cannot be detected. Also, as roots systems expand, some roots may intertwine and stick together, decreasing the number of tips that can be detected. Finally, since the resolution of AeroScan is about 57 µm per pixel, it might be possible that the very first millimetres of lateral roots were not recognised at the first moments following their emergence. With the manual validation, even the smallest and the joined roots could be counted.

2.2.6.2. EMBRYONIC ROOT NUMBER

To validate the root categorization made in the analysis pipeline (Figure 8 – C3 and illustrated in Figure 9 – H), the number of root tips classified as embryonic roots in the embryonic root category was compared with the Nb_{ER} measured manually using an interactive graphical interface developed on purpose (MosaicViewer, section 2.4.5.2) (Figure 9 – B). The analysis pipeline seems to underestimate the number of embryonic roots per plant. Because embryonic root tips are located far from most other root tips, occlusion is unlikely to occur. In this case, interwinding of roots, or other situations where the root tip is not detected (underestimations) or where false positive tip detections occurs (overestimations) are the main causes for the large discrepancies between the automated and manual methods. Given these, we decided to use the manual estimation of Nb_{ER} in all calculations of the pipeline.

2.2.6.3. PRIMARY ROOT ELONGATION RATE

The elongation rate of the primary root, $ERate_{PR}$ was estimated from the time course of the tip-collar distance of the primary root tips. The evolution over time was easy to analyse and could be simplified into a linear relationship for most plants (despite the slight parabolic trend at the beginning and end of the points, the overall trend has been simplified as linear) (Figure 9 – G). Indeed, for more than 90% of the primary root, the R^2 of a linear regression of tip-collar distance against time was higher than 0.9 (Figure 9 – E). The situation was similar for the seminal roots. Furthermore, in view of the parallelism between the evolution of the other seminal roots, a simplification was made to establish that all embryonic roots of a plant elongate at the same rate (Figure 9 – G). This result seems to validate the use of the tip-collar distance to estimate root length and indicates that the embryonic root elongation rate was a constant value for all genotypes.

Root elongation rates are largely influenced by environmental conditions. They are driven by the availabilities of resources (Klepper, Belford and Rickman, 1984; Fitter, 1994; Rich and Watt, 2013) but also by the mechanical impedance of the substrate (Atwell, 1990; Bengough *et al.*, 2011; Sjulgård *et al.*, 2021). The substrate-free and resource-uniform aeroponics environment may therefore have contributed to the similarity of the elongation rate of the embryonic roots of a plant.

Even under these conditions, the stability of the elongation rate of embryonic roots during the three weeks of growth remains surprising. Indeed, several new organs, leaf and roots, appeared and expanded during the period and, accordingly, the offer and demand of assimilates was far from being stable. Surprisingly, there is no sign of any impact of day and night on the elongation rate. This indicates that the source-sink coordination was such that the root growth demand, which is set at the embryonic root emergence time and which was constant thereafter, could be satisfied during the following three weeks (and was able to be maintained constant even during the night). This may suggest that the embryonic root sink is supplied with a higher priority than other sinks (lateral root formation and elongation and leaf expansion). Given the importance of leaf area for assimilation, lateral root formation and elongation remain the two sinks that can accommodate to rapid variations of assimilate availability.

2.2.6.4. DURATION OF PRIMORDIUM DEVELOPMENT

In the pipeline design, we assumed that the ***DPD*** was constant over time and equal for all embryonic roots. If this is the case, the time between the initiation of a lateral root and its emergence should not change during the entire experiment. The time course of appearance of lateral roots along the primary root should therefore follow that of the length of the primary root with a constant lag, corresponding to the ***DPD***. To assess this assumption, we computed, for each plant, the linear regression of tip-collar distance against time across the primary root tips (as in Figure 8 – C1 and illustrated in Figure 9 – G) and the linear regression across the lateral root tips having the highest tip-collar distance, which corresponds to the envelope regression of all tips classified in the lateral root group (Figure 8 – C3 and categorisation illustrated in Figure 9 – H). The strong similarity between the slopes of these two regressions (Figure 9 – D), indicates that our assumption was correct for the primary root. The linearity of the evolution of the number of lateral roots against the cumulated length of the branched zones of all embryonic roots further suggests that the assumption was valid for all embryonic roots (Figure 8 – H and illustrated in Figure 9 – F, cf. next section 2.2.6.5).

2.2.6.5. LATERAL ROOT DENSITY

For the sake of simplicity, the lateral root density was estimated from a linear regression of the number of lateral root tips detected against the cumulated

branched zones of the embryonic roots, over the whole period. This simplification has been made based on a few exemplary plants such as the one illustration example on Figure 9 – F. Nevertheless, we were surprised by the systematic observation in all plants of a linear relationship. Indeed, the ***LRD*** is known to be highly variable, both spatially and temporally. By embracing the entire tip population, it is likely that the pipeline filtered out the "high frequency" portion of this variability, revealing the "low frequency" portion that turned out to be a constant value for a given plant. This value could be considered as an "apparent lateral root density", which is quite independent of the number of growing organs (embryonic roots, lateral roots and leaves) and of environmental conditions (e.g., light, temperature). Also, the linear trend did not seem to be influenced by the emergence of nodal roots at the end of the experiment (data not shown).

The lateral root density (***LRD***) estimated by the pipeline was validated against manual measurements with SmartRoot (Lobet, Pagès and Draye, 2011) and ImageJ on a subset of 125 images randomly taken for different genotypes (Figure 9 – C). Three independent validations, corresponding to methods found in the literature have been carried out by two different teams.

The first method (A) uses SmartRoot on long root segments. For this method, the first team has traced the entire parent root with its child roots. The data table exported from SmartRoot gave the ***LRD*** for each parent root. Thus, the intra-plant variability reflects differences of whole-root branching density between embryonic roots (Figure 9 – C: blue points corresponding to method (A) are strongly clustered).

In the second method (B), short embryonic root segments were traced and annotated manually with SmartRoot. A first mark was set along the traced segment at the position of the first lateral root encountered and a second mark at the fifth lateral root along the segment. ***LRD*** was calculated as the inverse of the inter-lateral distance, obtained by dividing the distance between the two marks by 4. Intra-plant variability with method (B) includes therefore the variability between embryonic roots and the variability of lateral roots density along a given embryonic root (Figure 9 – C: green points corresponding to type (B) show higher variability than the type (A), blue points). Method B was applied by the same team as method A.

In the third method (C), embryonic root segments between two successive branching points were picked randomly and their length was recorded with ImageJ. The ***LRD*** was obtained as the inverse of the average length of these inter-lateral segments. Method (C) was applied by the second team (Muller and Hong, unpublished).

The discrepancies between method C on the one side, and methods A and B on the other side, suggests a strong team bias in the selection of the root segments used for manual validation (Figure 9 – C: orange points).

The analysis pipeline seems to underestimate the ***LRD*** compared to the manual validation because most of the points are located above the 1:1 line of the graph (Figure 9 – C). This underestimation is mostly attributable to the underestimation of the number of tips (section 2.2.6.1, effect of occlusion). It is, however, not proportional to ***LRD***. Indeed, occlusion increases with the number of tips, but the number of tips does not necessarily increase with ***LRD***. For example, images with a large number of tips (and large errors on the total number of tips and ***LRD***) may have a small ***LRD*** value (with long and numerous embryonic roots) or a large ***LRD*** value (with short and few embryonic roots). Accordingly, Figure 9 – C suggests that, in the analysis pipeline, ***LRD*** is systematically under-estimated by a constant factor that could be corrected for, and that non-systematic errors of estimations can be considered as random and should smooth out among replicate plants.

2.2.7. A REAL-LIFE EXPERIMENT

The pipeline is illustrated here with the evaluation of the heritability of the output variables from two high throughput phenotyping experiments involving diversity panels of bread wheat (bread wheat, 234 genotypes) and durum wheat (durum wheat, 250 genotypes). These experiments were performed in the RootPhAir aeroponics root phenotyping platform (section 2.4.2) with a total of 1980 plants phenotyped with a temporal resolution of two hours for a duration of 17 or 19 days after germination (first and second experiment, respectively).

Broad sense heritabilities (H^2) of the root traits estimated with the pipeline suggest that the traits have in general slightly higher heritabilities in bread wheat than in durum wheat (Table 5). However, the observed H^2 remain quite low and moderate as the largest does not exceed 60%. It is quite common

that root traits show generally low heritabilities due to their large environmental variance and their multigenic nature (Tsegaye *et al.*, 2012; Mathew *et al.*, 2018; Guo *et al.*, 2020). For example, deep-root traits had lower heritabilities compared to grain-related traits and this was attributed to their environmental sensitivity (Guo *et al.*, 2020).

Table 5. Heritabilities of the bread wheat and durum wheat panel phenotyped in RootPhAir (All = all types of roots confounded, CV_g = genotypic coefficient of variation (%); ER = embryonic root; H^2 = broad-sense heritability (%); PR = primary root; 1LR = first lateral root; σ_g = genotypic standard deviation; σ_r = residual standard deviation).

	Bread Wheat					Durum Wheat				
Root trait	Mean	σ_g	σ_r	CV_g	H^2	Mean	σ_g	σ_r	CV_g	H^2
$Diam_{All}$	0.0223	1.16E-03	1.85E-03	5.18	56.00	0.0207	8.69E-04	1.84E-03	4.19	36.85
$Diam_{ER}$	0.0433	3.18E-03	6.75E-03	7.34	41.96	0.0451	3.18E-03	6.40E-03	7.07	39.20
$Diam_{LR}$	0.0218	1.13E-03	1.76E-03	5.18	57.19	0.0202	7.93E-04	1.64E-03	3.93	37.73
DPD	4.849	2.26E-01	1.00E+00	4.67	14.24	5.245	0.00	1.08E+00	0.00	0.00
$Emer_{1LR}$	7.527	0.00	1.08E+00	0.00	0.00	7.708	2.82E-01	1.21E+00	3.66	12.35
$Emer_{PR}$	2.638	2.96E-01	8.45E-01	11.23	28.61	2.411	4.69E-01	7.74E-01	19.44	48.84
$ERate_{PR}$	2.470	1.88E-01	3.08E-01	7.61	54.86	2.642	1.89E-01	3.51E-01	7.14	42.94
LRD	2.171	1.97E-01	6.22E-01	9.08	24.59	2.230	3.37E-01	6.86E-01	15.10	38.55
MRL	14.203	1.38E+00	3.21E+00	9.70	37.41	15.574	1.62E+00	4.28E+00	10.37	27.09
Nb_{ER}	4.417	4.12E-01	8.43E-01	9.33	43.71	4.823	3.64E-01	7.10E-01	7.55	40.64
R/S_{Dry}	0.498	3.67E-02	5.48E-02	7.38	59.45	0.506	4.18E-02	5.65E-02	8.26	58.76
R/S_{Fresh}	0.949	9.51E-02	1.70E-01	10.01	50.50	0.928	9.23E-02	1.64E-01	9.94	45.04
$RMass_{Dry}$	0.0437	5.72E-03	1.80E-02	13.08	24.70	0.045	7.75E-03	1.92E-02	17.27	29.71
$RMass_{Fresh}$	0.690	1.05E-01	3.10E-01	15.23	27.26	0.682	1.30E-01	3.16E-01	19.07	30.67
$SMass_{Dry}$	0.086	1.21E-02	3.24E-02	14.08	31.31	0.0884	1.48E-02	3.60E-02	16.75	30.51
$SMass_{Fresh}$	0.718	1.11E-01	2.66E-01	15.45	36.07	0.742	1.35E-01	3.04E-01	18.25	34.06
SRA	0.513	1.13E-01	2.20E-01	22.13	46.46	0.516	1.12E-01	2.47E-01	21.74	35.00

R/S_{Dry} heritabilities almost reach 60% which is in between of the values of heritability usually found in previous studies (47% (Mathew *et al.*, 2018), 55% (Ahmad *et al.*, 2014), 84.5% (Dhanda, Sethi and Behl, 2004)). On the contrary, both root ($RMass_{Dry}$) and shoot dry weight ($SMass_{Dry}$) seem relatively low (about 30% and 25% respectively) compared to the values generally recorded ($RMass_{Dry}$: 79% (Mathew *et al.*, 2018), ~50-60% (Colombi and Walter, 2017); $SMass_{Dry}$: 97% (Ahmad *et al.*, 2014), 73% (Mathew *et al.*, 2018), ~50-60% (Colombi and Walter, 2017)).

These low values may be explained by the mechanically unconstrained but well-nourished environment provided by aeroponics. It has been observed in the past that genotypic differences for root system size observed in stress conditions tend to vanish in optimal growth conditions (B. Forster, unpublished data), although the reasons for such behaviour remain unclear. It is further intriguing that this would not be the case of the ***R/S*** ratio.

The Nb_{ER} and ***SRA*** heritabilities (around 40% for both) are in the lower range of what has already been found in the literature (Nb_{ER}: ~30% (Christopher *et al.*, 2013), ~70% (Colombi and Walter, 2017), ~50% (Hohn and Bektas, 2020), ~40% (Richard *et al.*, 2015); ***SRA***: ~50% (Christopher *et al.*, 2013), ~50% (Richard *et al.*, 2015), ~60% (Hohn and Bektas, 2020)).

The lack of mechanical impedance of the aeroponics platform may contribute to the low heritabilities of both Nb_{ER} and ***SRA***. Indeed, Colombi and Walter (2017) have observed that impedance increased the genotypic coefficient of variation (CV_g) of the number of seminal roots. In our experiments, the coefficient of variation CV_g of the ***SRA*** was the highest of all variables. The heritability did not reflect this CV_g, however, probably because ***SRA*** is estimated on 2D projections and that it depends on the relative orientation of the seed and camera plane.

Among the new variables estimated by the pipeline, The $Diam_{ER}$ and $Diam_{LR}$ as well the $ERate_{PR}$ show some of the highest H^2 observed in these experiments for both species (all > 40%). According to their relationship with the size of the dividing cell population in the root apical meristem, root tip diameters are considered as predictors of the potential root elongation rate (Pagès, 1995; Thaler and Pagès, 1996; Pagès *et al.*, 2010). The moderately high heritabilities observed for the median diameter of embryonic roots ($Diam_{ER}$) support and confirm the H^2 observed for the elongation rate of the primary root ($ERate_{PR}$), which is also a good indication of the elongation rate of other embryonic roots (section 2.2.6.3). In the same perspective, the fact that similarly large H^2 were estimated for the median lateral root diameter ($Diam_{LR}$) may suggest that the same would be true for the H^2 of lateral root elongation rate, which has not been estimated with the pipeline.

The H^2 of the ***LRD*** were in the low range in our experiments. For the durum wheat panel, the H^2 reaches 40% and only 25% for the bread wheat panel. This trend is also confirmed by the CV_g (~15% for the durum wheat panel and

only ~9% for the bread wheat panel) indicating that the durum wheat species seems to have more genetic variability concerning the ***LRD***. The values of H^2 are equivalent to the one (25%) found for young seedling of wheat grown for ten days in hydroponics in Guo *et al.* (2021), but are also way lower compared to other (rare) ones found as in the paper of Colombi and Walter (2017), where the ***LRD*** heritability under the lowest soil compaction reached 86%. This large value is surprising in view of our validation experiments which tended to indicate that ***LRD*** is a "noisy" variable. Finally, the duration of primordium development (***DPD***) and the emergence of the first lateral root (***Emer$_{1LR}$***) (from which ***DPD*** is computed) show low heritability for both species (H^2 < 10%). These low values are not surprising if we consider that ***DPD*** was shown to be similar in a broad range of species (Lecompte, Ozier-Lafontaine and Pagès, 2001; Pagès *et al.*, 2010).

2.3. CONCLUSIONS

- In this Chapter 2, a new pipeline to analyse root system architecture has been described. The method is inspired from root architecture models, which are often used downstream of phenotyping (Passot *et al.*, 2019). The pipeline focuses on finding root traits related to root development processes and is therefore unique in providing many of the parameters required by these models and paves the way for *in silico* genetic analysis of root system functions (Rangarajan *et al.*, 2022).
- The pipeline is largely based on dense time series of root tips coordinates. Tips are simple morphological features that are easily detected from images of whole root systems. Our study illustrates how a careful pipeline design allows complex properties to be derived from simple features. We also connect to other approaches that are still under development.
- The analysis indicates that the spatio-temporal variability of lateral root density may have low- and high frequency components and that the latter may reduce to a constant "apparent ***LRD***", which leads to straightforward phenotypic description. Validation experiments further indicate that conventional and time-consuming ***LRD*** estimation methods can be prone to important operator biases and sampling errors.

- The application of the pipeline to the wheat cases in aeroponics indicated that variables that are known to be time-dependent, such as ***ERate*** and ***LRD***, can be summarized by single values derived from their time-courses.
- The new set of variables that are produced by the pipeline display relatively low heritabilities. Since many of the process variables are parameters of root development models that are, in principle, close to the genesis of root system architecture, this may mean that the genetic variability of this root system architecture arises in the interaction between these parameters or between these parameters and the environment, more than in these parameters themselves. However, the particular environment in which the experiments have been conducted may have contributed to lowering several of the heritabilities so that it is premature to conclude on these low values.

2.4. MATERIAL AND METHODS

2.4.1. PLANT MATERIAL

Two large diversity panels comprising 234 bread wheat genotypes (*Triticum aestivum* L.) and 250 durum wheat genotypes (*Triticum durum* L.) were used in this study (exact composition of the panels cf. Annexe 1). The two panels have been assembled within the EU project SolACE (SolACE, 2022) and are composed of genotypes from different origins covering a wide genetic diversity.

In wheat, several categories of roots can be defined. The seminal roots regroup roots coming from the scutellum and epiblast nodes of the plant embryo (Klepper, Belford and Rickman, 1984; Manske and Vlek, 2002). Even if the primary root coming from the radicle is also considered as a seminal root, in this work, the primary root will be referred to as such to distinguish it from other seminal roots. When the primary root and seminal roots set will be mentioned together, they will be called embryonic roots. The nodal roots constitute another root category. They come from the coleoptile and following stem nodes. The number of embryonic roots ranges generally from 3 to 7 (max. 10), primary root included (Gregory *et al.*, 1978; O'Brien, 1979; Manske and Vlek, 2002; Manschadi *et al.*, 2008).

2.4.2. PHENOTYPING IN ROOTPHAIR

Two experiments were carried out in the RootPhAir high throughput root phenotyping platform. RootPhAir is a platform enabling the observation of the root system growth in aeroponics. Root system images are captured by an automated imaging station. To allow a continuous shooting, plants are continuously moving inside the boxes (Figure 10 – A). This enables the throughput that allows dense time series to be recorded. The complete automation of the platform is controlled by in-house software programs (Draye, unpublished).

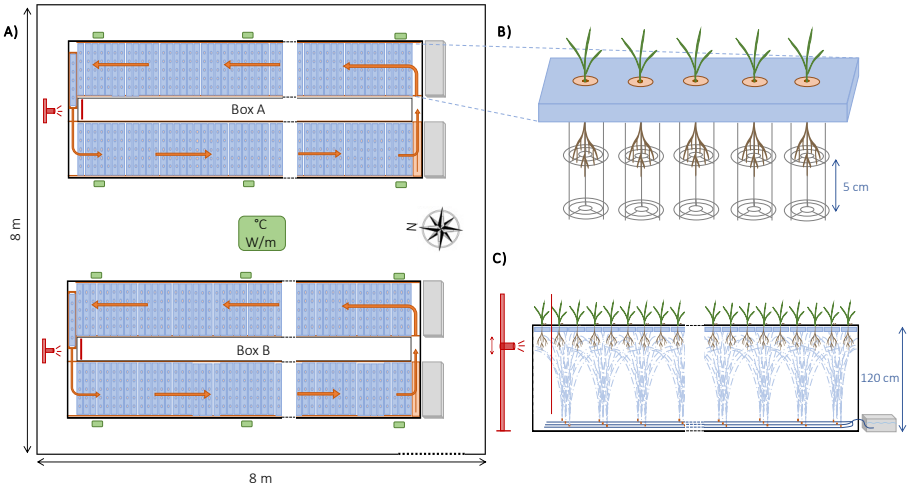


Figure 10. Schematic views of the RootPhAir platform: ***A)*** *An aerial view of the layout of the greenhouse room disposition that houses the two aeroponic boxes. The direction of rotation of the 99 strips is represented in orange, as well as the position of the camera in red, the environmental captors in green and the four tanks containing the nutritive solution in grey;* ***B)*** *Focus on one strip that can hold five plants. Seeds are stuck with plugs (in orange) within the holes of the strip and the roots develop below the strip. Below the plants, example of a structure design that can be placed below the strip to avoid the roots to intertwine;* ***C)*** *A cross section of one aeroponic box. Sprays are located below the roots, and the tanks with the nutritive solution connected to them are installed on one side of the box (in grey). The image capture system with its backlight located behind the plants (in red) is set on the opposite side of the box, allowing to take pictures of the root system of each plant.*

The facility is located in a compartment (length: 8 m, width: 8 m, height: 4 m) of the greenhouses at Université catholique de Louvain (UCLouvain), in Belgium (Latitude 50.665707; Longitude 4.619475; Elevation 116m). It is composed of two identical aeroponics units (Box A and Box B) (length: 5 m, width: 1.2 m, height: 1.2 m) having a capacity of 495 plants each (Figure 10 – A). A randomized complete block design was used for both experiments, where each box was considered as a full replicate (block) (more details of the

design construction cf. Chapter 3). The first experiment was carried out from the 15th to the 31st of January 2019 and the second from the 29th of April to the 17th of May 2019. Plants were thus growing for 17 or 19 days, which corresponds to most plants reaching the 3-leaf stage. This relatively young plant stage may also coincide with the beginning of nodal root formation and the emergence of the first tiller (Klepper, Belford and Rickman, 1984).

Seeds are introduced in Peat Foam plugs (inert material) inside the holes of polystyrene rectangles that are called "strips". Each strip is a holder of five plants (there are 99 strips per box) (Figure 10 – B). Each plant received a unique URI (Figure 11).

In RootPhAir, plants are growing in a substrate-free environment. They receive nutrients and water through a nutritive solution sprayed from the bottom of the boxes (Figure 10 – C). The seeds germinating within the platform were sprayed, first with demineralized water and, as soon as the first centimetres of roots were visible, with Hoagland nutritive solution (½ concentrated and pH adjusted to 5, cf. Annexe 2). The recurrence of the sprays was set initially at 5 seconds every 5 minutes but increased to 10 seconds every 3 minutes for both experiments to make sure roots remained hydrated.

As root systems become more and more heavy when plants grow, light plastic structures were also installed below each plant to maintain the roots in place and avoid roots to intertwine due to gravity and platform movements (Figure 10 – B). The structures were designed to be as minimally invasive as possible in the growth of root systems and to have a minimal imprint on the images.

2.4.3. IMAGE ACQUISITION SYSTEM

The imaging station is a back-light scanning system with a monochrome high resolution horizontal linescan camera (4K, Teledyne Dalsa, Spider) moving vertically in front of a red backlight (Figure 10 – C). The resulting images are highly contrasted with dark root pixels and clear background pixels (Figure 11). The time required for scanning 495 plants leads to a revolution period (and temporal phenotyping resolution) of ca. 2 hours.

2.4.4. IMAGE ANALYSIS SYSTEM

The root tips were detected with a flooding method used by the software AeroScan (Figure 12 – A). This method consists in a stepwise construction of a topological tree from top to bottom of the image. A first horizontal line is processed by the software, with all neighbour black pixels being recorded as a root portion. Another line, located five pixels further down, is then processed in the same way and the root portions of the two lines are compared. (Figure 12 – A1). If two different zones of the second line overlap the same zone of the first line, the software attributes it to a root intersection. If only one zone is detected, then the root simply continues. If no zone is detected, then a root tip is defined, and its coordinates recorded (x and y) (Figure 12 – A2). Additionally, the diameter of the roots is estimated at 1 cm from the apex using an algorithm similar to SmartRoot (Lobet, Pagès and Draye, 2011) (Figure 12 – A3).

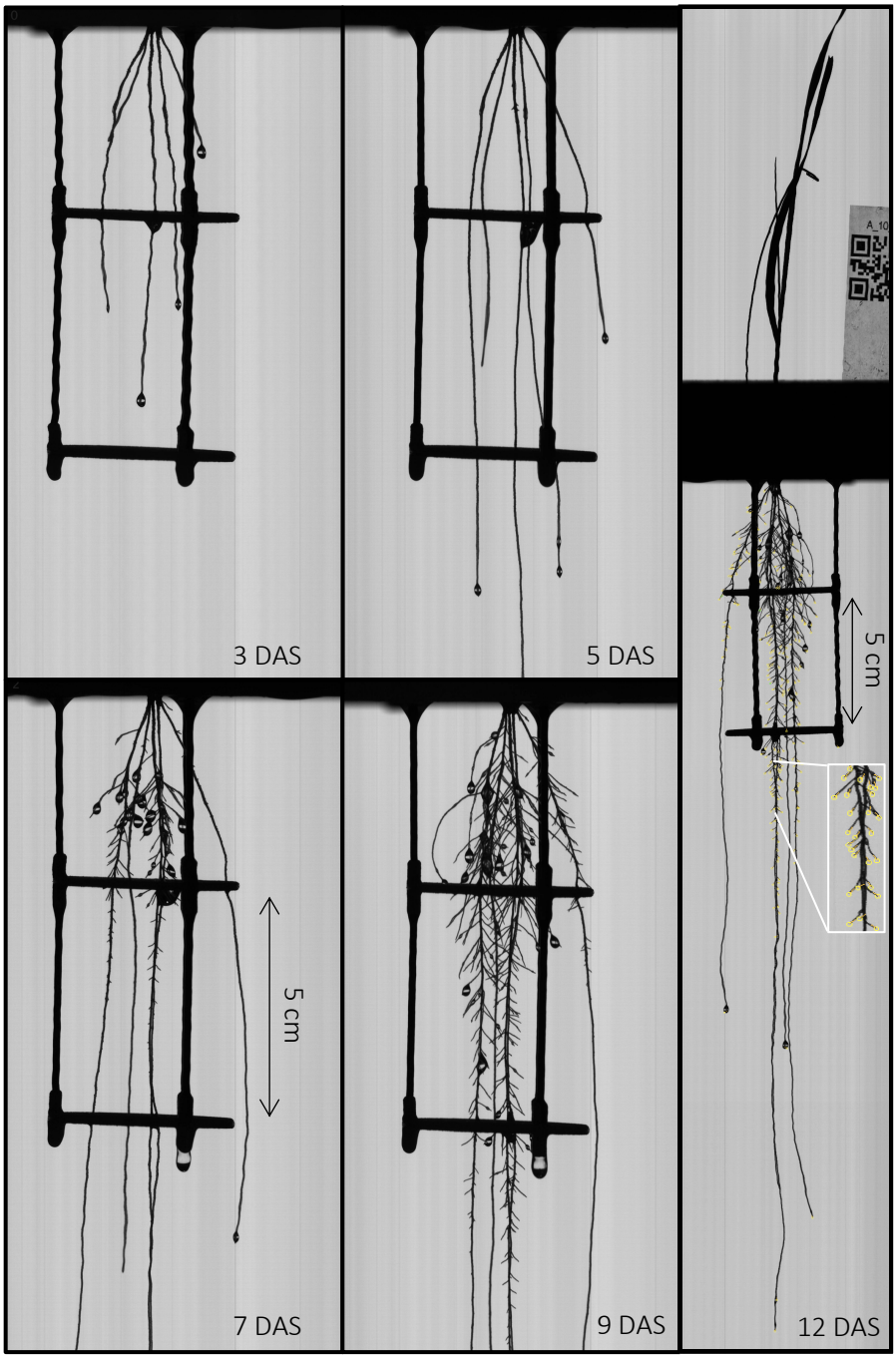


Figure 11. Typical images taken in the RootPhAir platform. A time-lapse of the same plant at 3, 5, 7, 9 and 12 days after sowing (DAS). The whole plant is in black and white, the URI of the plant is under a QR-code form, the structure underneath the plant is visible and the black rectangle corresponds to the longitudinal side of the strip. The tips detected by AeroScan are indicated by small yellow dots around them (only on the 12 DAS image, cf. white inset image).

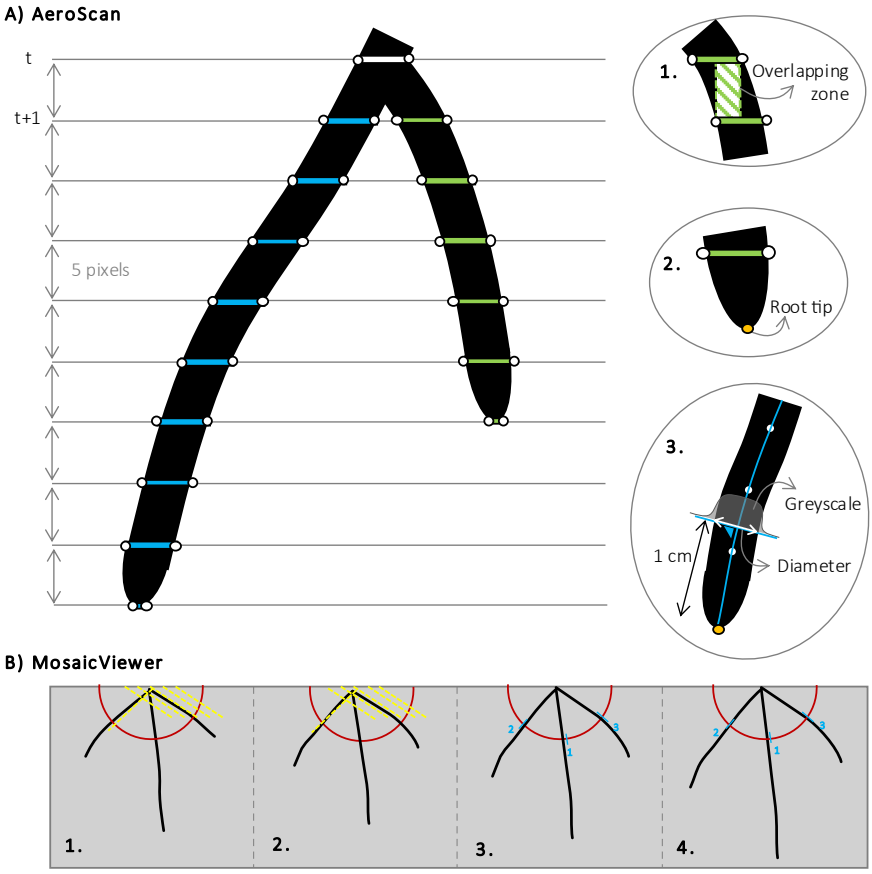


Figure 12. ***A)*** *Illustration of the flooding method used by AeroScan to detect the root tips and assess the root diameter (section 2.4.4).* ***B)*** *Viewer window of the in-house software MosaicViewer. Four images of one plant (subset at 3 (B1.), 5 (B2.), 7 (B3.) and 9 DAS (B4.)) are used to validate the seminal root angle between the first pair of seminal roots (**SRA_{SR1}**) and the embryonic root number (**Nb_{ER}**). On the two images on the left, the yellow lines represented helped in selecting the orientation of the leftmost and rightmost root of the first pair of seminal roots. On the two images on the right, the blue numbers indicate the root counting.*

2.4.5. DATA ANALYSIS PIPELINE

About 130 images per plant were recorded during the experiment of 17 or 19 days. The raw data table reached 3 to 5 million lines, each line containing the coordinates and additional information (e.g., diameter, orientation) for one root tip.

2.4.5.1. OUTLIER PLANTS AND FALSE-POSITIVE ROOT TIPS

In the first instance, outlier plants were discarded from the dataset. The outlier plants detection was done manually by looking at the last images taken

per plant. A plant was set as an outlier and removed from the dataset if: (i) its shoot was undeveloped (i.e., when the aerial parts of the plant did not develop above the strip); (ii) if the plant was falling (i.e., when the plant fell down on the first plateau of the structure); (iii) if it was abnormally small (i.e., when the plant was smaller than the structure (~10 cm), which was generally associated to a visible stunted growth or a (a)biotic stress).

In a second stage, outlier tips were removed from the dataset. Indeed, during the process of tips recognition on the images by AeroScan, some false-positive tips appeared. One of the main causes was the presence of the structure, on which drops of water usually formed at the bottom of the last plateau or at the ends of the vertical bars (Figure 10 – B and Figure 11) and were detected as tips. Other false-positive tips were also detected at the inferior edge of the strip or at the point where two intertwining roots meet. Most false-positive tips were easily visualized on the graph of the tip-collar distance over time (Figure 8 – C). Indeed, a tip detected on a droplet of water has a constant tip-collar distance over time. On the graph, it formed a constant horizontal line of root tips or abnormal tip-collar values. Hence, the filtering zones were set manually per plant by looking at the tip-collar distance graph over time.

Once the large datasets were cleaned, the analysis pipeline, entirely designed in RStudio (an integrated development environment for R) could be implemented (RStudio Team, 2019; R Core Team, 2021). The main steps to compute the different root traits are described in the Figure 8.

2.4.5.2. EMBRYONIC ROOT NUMBER AND SEMINAL ROOT ANGLE MEASUREMENTS

The pipeline comprised some visual and manual measurements for the root traits that were hard to estimate accurately, Nb_{ER} and ***SRA***.

The manual measurements of the Nb_{ER} and the ***SRA*** have been facilitated by an interactive in-house software MosaicViewer (Draye, unpublished). This program allows to draw, on a selection of 4 images per plant (at 3, 5, 7 and 9 DAS), the angle between the first pair of seminal roots by clicking on the leftmost and on the rightmost root (Figure 11 & Figure 12 – B1). Once the ***SRA*** is drawn, the Nb_{ER} can be validated by clicking on each individual root where a number will appear on the viewer next to each root (Figure 12 – B3).

These semi-manual measurements took less than 4 hours to complete 990 plants, which can be considered as a time-efficient method and certifies the accuracy of the measurement.

2.5. STATISTICAL MODEL AND VARIANCE COMPONENTS

Statistical analyses have been achieved separately for each species (bread wheat and durum wheat). In order to choose the appropriate model to apply, we performed a backward approach from the most complete model to increasingly simpler models by removing one factor at a time. The selected model was the one with the number of factors that maximized the percentage of variance explained for all root traits.

We considered the two aeroponics experiments and the two boxes as four full replicates, with one plant per genotype in each replicate. This replicate factor with four levels is therefore equivalent to separate experiment and the box factors with their interaction. The "lmer" function of the package "lme4" in the R software were used and the following mixed model was applied:

$$Trait_{ijklm} = \mu + Geno_i + Rep_j + Position(Rep)_{jk} + Block(Rep)_{jl} + \varepsilon_{ijklm}$$

$$\text{with } Block(Rep)_{jl} \sim N(0, {\sigma^2}_b) \text{ and } \varepsilon_{ijklm} \sim N(0, \sigma^2)$$

where $Trait_{ijklm}$ is the value of the root trait for a plant of the ith genotype (i=1…234 for bread wheat; 1…250 for durum wheat) in the jth replicate (j=1…4) at the kth position (k = 1, 2; 1 = the 2 external positions on a strip, defined as "edge position"; 2 = the three inner positions on a strip defined as "middle position") in the lth incomplete block (l = 1…11; each block being a set of 9 successive strips within box). The parameter μ is the mean value of the population, $Geno_i$ represents the effect of the ith genotype, Rep_j accounts for the effect of the replicate and is set as a fixed variable since the boxes were exposed to different environmental conditions in the greenhouse and across the two experiments. $Position(Rep)_{jk}$ represents the nested effect of the kth position within the jth box and is set fixed too as it accounts for reproducible effects. The nested effects of the lth blocks within the jth replicate, $Block(Rep)_{jl}$, are considered as random and are assumed to be independent with common normal distribution $Block(Rep)_{jl} \sim N(0, {\sigma^2}_b)$. The choice to set $Block(Rep)_{jl}$ as random was taken because of some unpredictable local environmental conditions that may have been different

from one block to another during an experiment (e.g., in case of platform breakdown, some strips may have been exposed to a higher risk a dehydration depending on their location inside the box). The deviations, ε_{ijklm}, are also assumed to be independent with normal distribution $\varepsilon_{ijklm} \sim N(0, \sigma^2)$.

The BLUES or adjusted means have been calculated for each genotype with the "emmeans" function of the R software, after filtering all observations having standardized residuals above a threshold of three. To estimate the variances needed for heritability formula, we used the same mixed model, except that the genotype term, $Geno_i$, was set as a random term.

2.5.1. HERITABILITY FORMULA

The formula of the broad-sense heritability used for the RootPhAir experiments is the following (Kuijken *et al.*, 2015):

$$H^2 = \frac{\sigma_G^2}{\sigma_P^2} = \frac{\sigma_G^2}{\sigma_G^2 + (\sigma_e^2 / n)}$$

where σ_G^2 is the genotypic variance, σ_P^2 is the phenotypic variance, σ_e^2 is the error variance and n is the number of independent measurements or replicates per genotype within an experiment.

2.5.2. COEFFICIENT OF VARIATION FORMULA

The coefficient of variation expresses the genotypic variability with respect to the mean value. The following formula was used (Albert and Zhang, 2010):

$$CV_g = \frac{\sigma_G}{\mu} * 100$$

where CV_g is the genotypic coefficient of variation, σ_G is the genotypic standard variation, μ is the mean value of the data population. The CV_g is then multiplied by 100 to express it as a percentage.

2.6. PERSPECTIVES BEYOND THE THESIS

- Among the process variables determined, some variable as the ***ERate***, ***Theta*** or ***Length*** have been determined per root category (e.g., for the embryonic roots, pairs of seminal roots, etc.). One category was however missing, the lateral root category and this category is very much present in the model inputs. The development of technic to estimate the growth rate as well as the length of these roots is far more complex than for other root types since lateral roots grow more horizontally and therefore their length cannot be estimated from the tip-collar distance (initial step in our pipeline).
- Interpellant results emerged as the linearity of the primary root elongation rate. Indeed, even with the apparition of new organs or day-night alternation, the growth of the primary root remained quite linear. Further exploration of this trend should be pursued at latter stages as the last tips recorded suggested that the trajectory is likely to change (pointing to an acceleration).
- Additionally, from a locally highly fluctuating variable as the lateral root density, which is largely dependent on external conditions, a global density factor could have been determined (low frequency of the variability). This factor seems to well-characterised the overall strategy adopted by the plant in terms of ramifications. Moreover, this constant factor seems to not be influences by the creation of new organs, neither the environmental conditions, which is surprising. It would therefore be very interesting to confirms this global density factor with other panels or species.
- From the values obtained for our process variables, we could be tempted to try some simulations using architectural models to see if the avatars of the root systems reproduced *in silico* resemble our images or not, and also investigate how they would perform with different environmental or soil conditions.

Interchapter 2-3

In the previous Chapter 2, a unique analysis pipeline illustrating root architecture, based on the relatively simple extraction of the root tips from images, has been presented. A first phenotyping study in aeroponics derived from this pipeline was presented with two large diversity panels of bread and durum wheat species.

In the next Chapter 3, knowing that root traits are highly plastic, these two panels will also be cross-analysed in two other distinct environments, in the well-known pouch-like device and in the 4PMI platform (INRAE-Dijon) composed of rhizotubes.

Additionally, three yield-related traits, estimated from a series of field trials (under controlled and combined water and nitrogen stressed conditions) will be added to the dataset to allow the revelation of correlations between root traits measured on relatively young plants in platforms and performance of mature plants evaluated in the field.

Genetic variability and heritability of the broad set of traits will be interpreted per root categories (e.g., Biomass, Elongation, Production, etc.). The impact of selection, the correlations inter- and intra-platforms, the correlations between platforms and field trials, as well as a clustering method based on root platform characteristics will be presented.

Chapter 3.

Cross-Platform Analysis of Root Architecture Phenotype

3.1. INTRODUCTION

With the advent of high throughput phenotyping platforms, access to root architectural data has been facilitated and many studies have been carried out with the advantages and limitations given by the controlled conditions and the platforms themselves (Kuijken *et al.*, 2015; Watt *et al.*, 2020). In particular, throughput, which is difficult to reach in the field or with manual phenotyping, has allowed the study of large panels but also the access to integrative root traits as the ones related to root development processes (Fiorani and Schurr, 2013; Arsova *et al.*, 2020; Chapter 2). However, the new dynamic information is not fully exploited at present, mainly because of the complexity of the resulting analysis of dense image time series (Fahlgren, Gehan and Baxter, 2015; Lobet, 2017a; Atkinson *et al.*, 2019). Moreover, most root experiments carried out in high throughput phenotyping platforms are limited to early growth stages (Watt *et al.*, 2013; Richard *et al.*, 2015).

Many studies have intended to find correlations between root traits obtained in platform experiments on young plants with root characteristics or yield-related traits estimated in the field at more mature plant stages. For wheat, the conclusions are not always consistent (Colombo *et al.*, 2022). Some positive correlations were found between root traits estimated at early stages and more mature plant stage in the field. For instance, the seminal root number, total root length and maximum width of the root system showed positive correlations with some yield related traits in the field (Xie *et al.*, 2017). On the other side, negative correlations were observed between the root angle of the first pair of seminal roots and grain yield (Khokhar *et al.*, 2019) or the extraction of water from the deep soil profiles (Manschadi *et al.*, 2010). However, some studies reported small or no correlations between root traits estimated in platforms conditions with traits related to field performance (Atkinson *et al.*, 2015; Bai *et al.*, 2019) or with roots characteristics in the field (Rich *et al.*, 2020).

It has been established that the link between platform and field depends on the selection of traits and, more fundamentally, on how the root phenotype is dissected into its components (phenes) (Lynch, 2015). In the context of water and nutrient limitation and thanks to modelling approaches, key-variables needed for an improved resource acquisition have been identified and proposed as pieces of root "ideotypes". Root ideotypes can be defined as phenotypes with specific root features which, when present and under given environmental conditions, allow the plant to better perform. These ideotypes have been elaborated with the aim to provide plant breeders with clear selection targets. Several experimental validations exist for the root ideotypes that have been designed through modelling studies. A well-known "steep-cheap-deep" root ideotype has been described by Lynch (2013, 2019) to help plants cope with water (W) or nitrogen (N) deficits in the field. The main features of this ideotype are a steep root system comprised of few nodal roots with a moderate density of lateral roots. This ideotype could more effectively reach mobile resources such as water and nitrates that have percolated into the deep soil layers. Another common root ideotype, called the "topsoil foraging", develops a shallow root system, with great lateral root density and long root hairs. This one is known to better acquire the phosphorus that is mainly present in the shallow layers of the soil because of the low mobility of phosphorus (Lynch and Brown, 2001; Lynch, 2013, 2019). In a few cases, the characteristics of these root ideotypes can be easily evaluated in high throughput phenotyping platforms. However, several of the ideotype features can only be assessed via insights into the dynamics of root growth and development, for which the potential of high throughput phenotyping platforms is not fully realised yet.

In Chapter 2, a method to estimate several parameters of root models has been described. The exploration of root growth and development was made possible by the specific conditions of the RootPhAir aeroponic platform. In this study, two large diversity panels of bread and durum wheat, covering different geographical regions and release dates, have been phenotyped in the platform RootPhAir (section 2.2.7). Knowing the large plasticity of root traits, this experiment was repeated in two other environments: (i) in the known reference setup called "pouch" (section 3.2.2.2), and (ii) in another unique setup based on Rhizotubes of the 4PMI platform, where a combined W and N stress was applied (section 3.2.2.3). Moreover, basic field

performance data have also been retrieved and have been analysed with the platform data (section 3.2.2.4). The combination of all these aspects, viz. root dynamics, large diversity panels, two species, multiple platforms and field trials is a unique feature of this study and set the scene for evaluating or revisit questions related to cross-platform evaluation, platform-field performance, and dissection of root phenotype into components.

3.2. MATERIAL AND METHODS

3.2.1. PLANT MATERIAL

This study is based on two diversity panels of wheat, comprised of 234 genotypes of bread wheat and 250 genotypes of durum wheat, that were assembled during the EU project SolACE (SolACE, 2022) to analyse wheat responses to combined water and nitrogen deficits using field trials, platform experiments and participatory trials across Europe. The inclusion of genotypes in the panels was largely based on agronomic performance and genotypic information to maximise the genetic diversity, minimise the population structure and maintain relevance in breeding programmes. The seeds used came from the same lots in each of the phenotyping experiments described in this work (kindly provided by SolACE partners).

The genotypes of the bread wheat panel can be grouped into the following collections (Annexe 1.1): (i) “BreedWheat”, 200 genotypes coming from the panel of the BreedWheat project, initially formed by 450 genotypes selected with the aim of representing global diversity while being adapted to European growing conditions (Rincent *et al.*, 2019); (ii) “Checks”, five commonly used genotypes; (iii) “Hybrids”, 10 genotypes developed by Syngenta; (iv) “Parents”, 14 genotypes used to form the hybrids and also developed by Syngenta; (v) “Local varieties”, five genotypes with a good performance that can be considered as representative of different regions of Europe corresponding. A second classification was done according to their continent of origin: (i) Africa; (ii) America; (iii) Asia; (iv) Europe; or (v) Oceania (information collected from partners of the SolACE project and online resources (‘GRIS’, 2017; ‘EU Plant variety database (v.3.4)’, 2022)).

For the durum wheat panel, the same two classifications were done. Durum wheat genotypes were classified according to the following collections (Annexe 1.2): (i) “CREA”, 69 genotypes composed of Italian cultivars,

worldwide cultivars and breeding lines selected based on field observations by CREA (M. Maccaferri, personal communication); (ii) "EPO", 58 genotypes selected among the elite panel EPO (David *et al.*, 2014); (iii) "GPDUR", 48 genotypes, old and modern cultivars selected from various origins (South and North America, Western and Eastern Europe, Africa, Australia) (D. Hourcade, personal communication); (iv) "UNIBO", subset of 75 genotypes from the "elite lines" durum wheat panel complemented with some founders genotypes of the pre-breeding era and some representative genotypes of several breeding programs worldwide from 1974 to about 2000s (M. Maccaferri; personal communication, Maccaferri *et al.*, 2005, 2006, 2011).

3.2.2. HIGH THROUGHPUT PHENOTYPING EXPERIMENTS

3.2.2.1. ROOTPHAIR

The two panels have been phenotyped in the root phenotyping platform RootPhAir. In RootPhAir, plants evolve in 3D, in a contact-free aeroponics environment. The platform is composed of two boxes (A and B) with a capacity of 495 plants each. Roots are constantly moistened with sprays of nutritive solution coming from the bottom of the boxes and root systems images are captured by a backlight scanning system located at one extremity of each box (Figure 13 – A, more details about this platform, cf. Chapter 2). The 495 plants are arranged over 99 strips, holding five plants each, that perform a continuous revolution so that each plant comes in front of the imaging station every two hours. Non-germinated seeds were sowed directly in the platform. They were sprayed with demineralized water and, as soon as the first centimetres of roots were visible, with Hoagland nutritive solution (½ concentrated and pH adjusted to 5, Annexe 2). Plants were grown for a minimum of 17 days under a temperature set at 20°C during the day and 18°C at night, a relative humidity of 60% and a photoperiod 16:8.

Two replicate experiments with a complete randomized block design were performed, in January 2019 and in May 2019, for 17 and 19 days respectively (about the 3-leaf stage). The 484 genotypes were grown in, with one plant per genotype and box and replicate experiment, leaving eleven vacant positions in each box. Eleven incomplete blocks of 45 plants (or 9 consecutive strips) were formed and additional plants of the Bermude genotype were assigned to the vacant position in each block. The design was generated on Excel by randomizing the position of the repeated genotype within the eleven blocks

first, and then, by randomizing all other genotypes on the remaining spots. Over the two experiments, there were therefore four replicate plants per genotype.

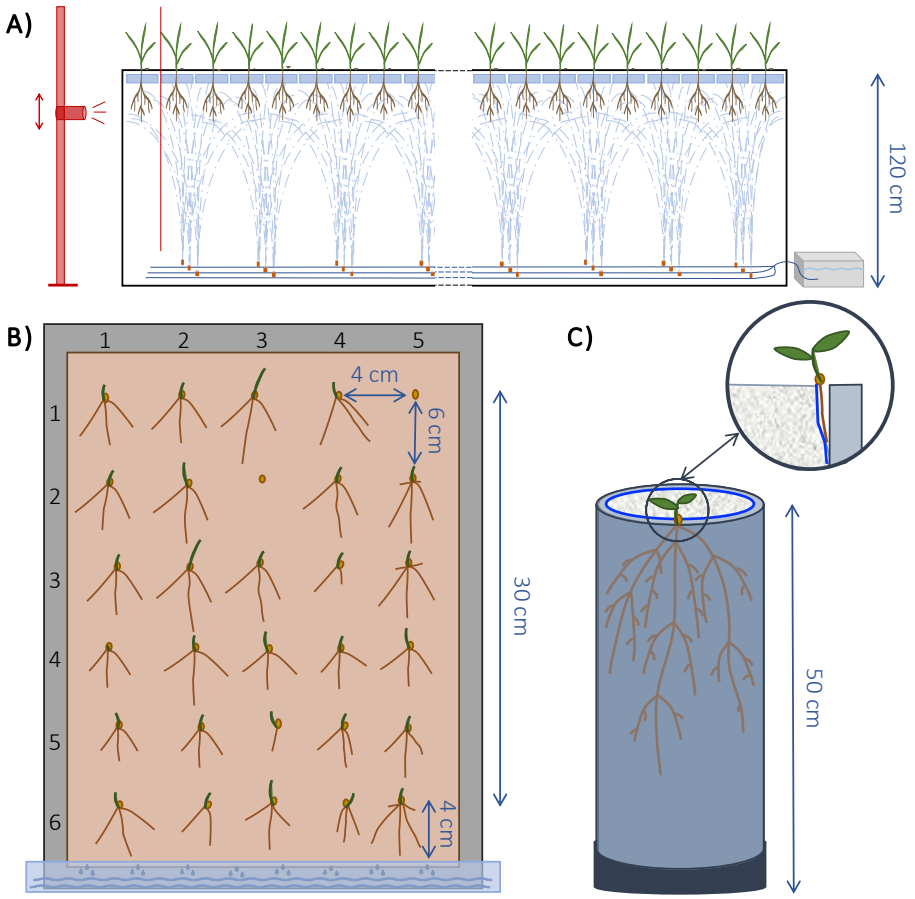


Figure 13. The three devices used for phenotyping. ***A)*** *A cross section of one aeroponic box. Sprays are located below the roots growing on 3D in a substrate-free environment. The tanks with the nutritive solution connected to the boxes are installed on one side (in grey). The image-capture station with its backlight scanning system (in red) is set on the opposite side of the box, allowing to take pictures of the root systems (cf. Chapter 2, section 2.4.2).* ***B)*** *A pouch on which a sheet of filter paper is adhered with demineralized water. Plants are arranged in rows (6) and columns (5). Each column corresponds to plants of a unique genotype. Water rises by capillarity. Plant located on row 1 are the ones the further away from the water table (34 cm away) and plants on row 6 the closest ones (4 cm from the water table).* ***C)*** *Schema of one Rhizotube® of the 4PMI platform (inspired from Figure 1 in the article of Jeudy et al., 2016). The roots of the plants grow in 2D between a transparent Plexiglas (covert during the experiment) and a thin cloth membrane (in flash blue) that separate the roots from the substrate located in the centre of the tube (in grey). All tubes are photographed daily (cf. Jeudy et al., 2016).*

The resulting time series of root system images comprised up to 140 images per plant per experiment (which represents a collection of more than 200

thousand images for the two experiments), from which 17 root traits were extracted using an image analyse pipeline described in the Figure 8 of the Chapter 2: 6 traits in the biomass category, 8 traits in the elongation category, two traits in the production category, and one trait in the tropism category (Table 6).

3.2.2.2. POUCH – A WELL-KNOWN METHOD

The two panels were phenotyped at a young seedling stage (4 days old) to determine the genetic variability of the root angle between the seminal roots using a pouch protocol widely used in previous studies (Atkinson *et al.*, 2015; Richard *et al.*, 2015; Xie *et al.*, 2017; Khokhar *et al.*, 2019; Rich *et al.*, 2020). The seeds of the two panels were fixed with a 1% agar solution on moist filter paper sheets maintained on flat PVC plates (Figure 13 – B) that were arranged in a vertical position in a box containing some demineralized water, such that water was able to rise by capillarity along the filter paper. Each pouch held 30 seeds arranged in five columns (4 cm apart) and 6 rows (6 cm apart). The number of pouches allowed for 6 replicate plants of each genotype in an experiment. The pouches were maintained in a room at 20°C in the obscurity during the experiments. Images of the seedlings were captured daily during two or three days.

Two fully replicated experiments were carried out, one in June 2018 (4-days experiment – one image capture daily on the last three days) and the other in July 2018 (4-days experiment – two image captures daily on the last two days). Due to the potential effect of the row position (height of the seed above the water level), each column of the pouch was randomly assigned to one genotype to enable crossing the row and genotype effects (thus the 6 plants per genotype in each experiment were arranged along a single column).

From these Pouch experiments, 19 root traits were determined based on the images of the seedlings: 9 in the elongation category, three in the production category and 7 in the tropism category (Table 6).The image analysis was performed with the SmartRoot software (Lobet, Pagès and Draye, 2011) and the variables of Table 6 were computed from the SmartRoot output tables. The average root length (***ARL***) and the total root length (***TRL***) were respectively assessed as the mean and the sum of all roots traced (***Length***, in cm). The total number of embryonic roots (Nb_{ER}) was counted from the output table and the convex hull (***CH***), which represents the surrounding area of the root system (in cm^2), was calculated based on the most extreme points of the

root system. To estimate the root growth (***ERate***), the mean length differences per plant between images captured at two different time intervals were calculated and divided by this time interval (in cm per day).

Finally, the categorisation of the roots in different root types was carried out based on the root angle from the vertical (***Theta***). Each root has been assigned to a type: either the primary root, or a seminal root of the ith pair (SRi, i=1…3; 3 being the maximum number of seminal root pairs observed). The most vertical root was automatically attributed to rank 1 as it was assumed that the primary root had the most vertical growth. With an uneven number of roots, the first roots met on the left and on the right of the primary root were assigned to rank 2 (first pair of seminal roots), the second pair met to rank 3 (second pair of seminal roots), and finally the third pair, if met, to rank 4. With an even number of roots, the same method was applied and then, the smallest root, which was assumed to be to the last to appear, was attributed to a rank higher than the last rank used. From the attributed rank numbers, root lengths (***Length***), elongation rates (***ERate***), root number (***Nb***), root angles from vertical (***Theta***) and seminal root angles (***SRA***) were computed per root type. The absolute values of $Theta_{PR}$ were taken to interpret $Theta_{PR}$ as an indicator of gravitropism sensitivity.

3.2.2.3. 4PMI

The two panels were also phenotyped in the 4PMI platform (INRAE-Dijon) under low W and N conditions. The 4PMI platform uses the Rhizotube® technology (Jeudy et al. 2016) where roots develop in 2D between a transparent Plexiglas (protected from light) and a thin cloth membrane separating the roots from the substrate (mix of sand and perlite, located in the centre of the Rhizotube) (Figure 13 – C). Nutritive solution is given individually to each Rhizotube following a precise control.

Two experiments of 25 days were performed, one in October 2018 with the bread wheat panel and another one in January 2019 with the durum wheat panel. Two Rhizotubes were assigned per genotype for a total of four plants per genotype (one Rhizotube containing two plants). All genotypes have been randomized across rows and columns and 6 highly replicated check genotypes were inserted in the design (with 10 rhizotubes per check genotype (Colombo *et al.*, 2022)). A combined deficit of W and N was applied for both experiments by stopping the irrigation and fertilisation at three days after sowing (DAS).

Plants were grown under the following conditions: 10mM Nitrogen Nutritive solution (Annexe 3), temperatures of about 22°C during the day, 18°C at night and an average PAR of 355 µmol.m^2.s. High resolution images of the root systems were acquired daily (RGB camera).

From images and harvests, 9 traits were estimated: three in the biomass category, two in the elongation category, two in the production category and two in the tropism category (Table 6). Traits of the biomass category and traits of the production category were measured or counted at harvest (around 4-leaf stage, each harvest lasted four days). The other traits were assessed from the skeletons of the root systems at 11 days after sowing, using a pipeline developed by INRAE and involving AI-based segmentation methods (Salon, Jeudy and Lamboeuf, unpublished).

3.2.2.4. FIELD TRIALS AND SENSITIVITY INDEX

The dataset generated in the three previous platforms has been augmented with yield data in controlled and stressed conditions (low W and/or N) from 7 (bread wheat) and 6 (durum wheat) field evaluation trials, as well as with arbuscular mycorrhizal fungi (***AMF***) colonisation data from one evaluation trial (durum wheat). The datasets were kindly provided by partners of the BreedWheat consortium (Colombo *et al.*, 2022) and by SolACE partners (unpublished data).

From the yield data, the average grain yield per genotype under controlled (***GYC***, 7 bread wheat trials and 6 durum wheat trials) and stressed conditions (***GYS***, 7 bread wheat trials and 6 durum wheat trials) have been estimated. In addition, a non-parametric index expressing the grain yield sensitivity to stress (***GYSI***) over the 7 (bread wheat) or 6 (durum wheat) environments has been estimated, as follows. The residuals of a linear regression between grain yield in controlled versus stressed conditions in each trial have been used to rank the genotypes according to their specific response to stress. The ranks of each genotype in each trial have then been weighted by the average response to stress of the whole panel in each trial:

$$WRANK_{ij} = RANK_{ij} * \frac{(\overline{GYC_j} - \overline{GYS_j})}{\overline{GYC_j}}$$

where $WRANK_{ij}$ is the weighted rank of the ith genotype (i=1…196 for bread wheat; 1…254 for durum wheat) in the jth trial (j=1…7 for bread wheat; 1…6

for durum wheat), $RANK_{ij}$ is the rank of the ith genotype in the jth trial, $\overline{GYC_j}$ and $\overline{GYS_j}$ are the genotype mean grain value for the jth trials under controlled and stressed conditions respectively. Finally, ***GYSI*** has been computed for each genotype as the sum of the weighted ranks ($WRANK_{ij}$) over the trials. Therefore, a large ***GYSI*** value was attributed to genotypes that were generally more tolerant (i.e., above the stress yield vs control yield regression line) in trials where stress response was more pronounced.

The percentage of root colonization by ***AMF*** was measured on root samples collected from a field trial (controlled conditions) carried out by CREA in Foggia (Italy) with the durum wheat panel only (Declerck and Doubell, unpublished data).

3.2.3. CLASSIFICATION OF THE PLATFORM TRAITS

In total, 45 variables were determined from all experiments (in bold and italics in the text). To ease the interpretation of results, the variables have been classified manually into four categories according to the underlying biological processes (de Dorlodot, 2007): biomass (integrative processes), elongation (cell division and expansion, source/sink), production (development, source/sink), or tropism (asymmetric cell expansion) (Table 6).

Some root traits have been determined per root types. In this study, we considered all roots emerged from the scutellum and epiblast nodes of the plant embryo as embryonic roots. These included both primary root and seminal roots. The primary was assumed to be the longest and most vertical root per plant. The other embryonic roots were considered as seminal roots. The nodal roots constitute another root category that come from the coleoptile nodes.

Table 6. List of the traits determined from the data of all platform experiments: RootPhAir, Pouch and 4PMI experiments (All = all root types confounded, DAS = days after sowing, ER = embryonic roots, PR = primary root, SR1 = first pair of seminal roots, SR2 = second pair of seminal roots, 1LR = first lateral root). For more details about root type classification cf. section 3.2.3.

Category	Trait	Description	Method	Entity	Unit	RootPhAir	Pouch	4PMI
Biomass	***R/S***	Root to shoot ratio	Scale	Entire plant	-	Dry, Fresh		Dry
	RMass	Root mass	Scale	Root system	g	Dry, Fresh		Dry
	SMass	Shoot mass	Scale	Shoot system	g	Dry, Fresh		Dry
Elongation	***Diam***	Median diameter	Computed	Root class	cm	All, ER, LR		
	DPD	Duration of lateral root primordium development	Computed	Root class	DAS	✓		
	Emer	Emergence	Computed	Root class	DAS	1LR, PR		
	ERate	Elongation rate	Computed	Root class	cm/day	PR	ER, PR, SR1, SR2	
	Length	Root length	Manual	Root class	cm		PR, SR1, SR2	
	ARL	Average root length	Manual	Root system	cm		✓	
	MRL	Maximum root length	Computed	Root system	cm	@8 DAS		@11 DAS
	TRL	Total root length	Manual	Root system	cm		✓	
	Surf	Projected surface of the root system	Computed	Root system	cm^2			@11 DAS
Production	***LRD***	Lateral root density corresponding to the number of lateral roots per centimeter of branched root	Computed	Root class	count/cm	✓		
	Nb	Number of roots	Manual	Root class	count	ER	ER, SR1, SR2	
	NbLeaves	Number of leaves	Manual	Shoot system	count			✓
	NbTillers	Number of tillers	Manual	Shoot system	count			✓
Tropism	***SRA***	Angle between seminal roots	Manual	Root class	radian	SR1	ER, SR1, SR2	
	Theta	Root direction (from vertical or primary root)	Manual	Root class	radian		PR, SR1, SR2	
	CH	Convex hull area	Computed	Root system	cm^2		✓	@11 DAS
	Width	Width of the root system	Computed	Root system	cm			@11 DAS

3.2.4. STATISTICAL MODELS AND VARIANCE COMPONENTS

All statistical analyses have been achieved separately for each species (bread wheat and durum wheat) (R Core Team, 2021, version R 4.1.2.).

3.2.4.1. ROOTPHAIR

Statistical analyses have been achieved separately for each species (bread wheat and durum wheat). In order to choose the appropriate model to apply, we performed a backward approach from the most complete model to increasingly simpler models by removing one factor at a time. The selected

model was the one with the number of factors that maximized the percentage of variance explained for all root traits.

We considered the two aeroponics experiments and the two boxes as four full replicates, with one plant per genotype in each replicate. This replicate factor with four levels is therefore equivalent to separate experiment and the box factors with their interaction. The "lmer" function of the package "lme4" in the R software were used and the following mixed model was applied:

$$Trait_{ijklm} = \mu + Geno_i + Rep_j + Position(Rep)_{jk} + Block(Rep)_{jl} + \varepsilon_{ijklm}$$

$$\text{with } Block(Rep)_{jl} \sim N(0, {\sigma^2}_b) \text{ and } \varepsilon_{ijklm} \sim N(0, \sigma^2)$$

where $Trait_{ijklm}$ is the value of the root trait for a plant of the ith genotype (i=1…234 for bread wheat; 1…250 for durum wheat) in the jth replicate (j=1…4) at the kth position (k = 1, 2; 1 = the two external positions on a strip, defined as "edge position"; 2 = the three inner positions on a strip defined as "middle position") in the lth incomplete block (l = 1…11; each block being a set of 9 successive strips within box). The parameter μ is the mean value of the population, $Geno_i$ represents the effect of the ith genotype, Rep_j accounts for the effect of the replicate and is set as a fixed variable since the boxes were exposed to different environmental conditions in the greenhouse and across the two experiments. $Position(Rep)_{jk}$ represents the nested effect of the kth position within the jth box and is set fixed too as it accounts for reproducible effects. The nested effects of the lth blocks within the jth replicate, $Block(Rep)_{jl}$, are considered as random and are assumed to be independent with common normal distribution $Block(Rep)_{jl} \sim N(0, {\sigma^2}_b)$. The choice to set $Block(Rep)_{jl}$ as random was taken because of some unpredictable local environmental conditions that may have been different from one block to another during an experiment (e.g., in case of platform breakdown, some strips may have been exposed to a higher risk a dehydration depending on their location inside the box). The deviations, ε_{ijklm}, are also assumed to be independent with normal distribution $\varepsilon_{ijklm} \sim N(0, \sigma^2)$.

The BLUES or adjusted means have been calculated for each genotype with the "emmeans" function of the R software, after filtering all observations having standardized residuals above a threshold of three. To estimate the variances needed for heritability formula, we used the same mixed model, except that the genotype term, $Geno_i$, was set as a random term.

3.2.4.2. POUCH

In the Pouch experiment, each genotype was replicated 6 times. In a preliminary analysis, we observed that the six plants were affected in a systematic way by their heights above the water table, presumably due to a difference of water supply according to the height (row number). To smooth out this effect, the 6 replicate plants were used to estimate a single adjusted value per genotype (and experiment), computed as the prediction from a linear regression of the 6 observed values against height, at the mid-row location. The following regression model was adjusted separately on each column of 6 replicate plants for each genotype:

$$Trait_i = Intercept + Row_i * Slope + \varepsilon_i$$

with $\varepsilon_i \sim N(0, \sigma^2)$ and i=1…6

where $Trait_i$ is the trait value measured on the plant at the ith row and Row_i is the row of the corresponding plant, and the adjusted mean at mid-row was computed as:

$$Adjusted_i = \widehat{Intercept} + 3.5 * \widehat{Slope}$$

This adjusted value was therefore free from the impact of the height to the water table but was obtained at the cost of the within column replication that could not be exploited in the main analysis.

The "lmer" function of package "lme4" in R was used and the following mixed model, which corresponds to a complete randomized block design, was applied:

$$Adjusted_{ij} = \mu + Geno_i + Exp_j$$

with $Exp_j \sim N(0, \sigma^2)$

where $Adjusted_{ij}$ is the adjusted value of the trait for the ith genotype (i=1…234 for bread wheat; 1…250 for durum wheat) for the jth experiment (j=1,2; there were two experiments). The parameter μ is the mean value of the population, $Geno_i$ represents the fixed effect of the ith genotype and Exp_j accounts for the effect of the jth experiment and is set as a random variable. The Exp_j is a block effect assumed to be independent with normal distribution $Exp_j \sim N(0, \sigma^2)$.

The BLUES or adjusted means were calculated with the "emmeans" function from R, after filtering all observations having standardized residuals above a threshold of three. To calculate the BLUPs and variances needed for heritability, we used the same mixed model, but the genotype term, $Geno_i$ was treated as random.

3.2.4.3. 4PMI

For the 4PMI experiment with the Rhizotubes, the R-package SpATS (Spatial Analysis of Field Trials with Splines) has been used to estimate the genotypic means by considering spatial effects in the greenhouse (similar to Colombo *et al.*, 2022).

3.2.5. HERITABILITY FORMULA

The formula of the broad-sense heritability used for the RootPhAir and Pouch experiments is the following (Kuijken *et al.*, 2015):

$$H^2 = \frac{\sigma_G^2}{\sigma_P^2} = \frac{\sigma_G^2}{\sigma_G^2 + (\sigma_e^2 / n)}$$

where σ_G^2 is the genotypic variance, σ_P^2 is the phenotypic variance, σ_e^2 is the error variance and n is the number of independent measurements or replicates per genotype within an experiment.

For the 4PMI experiments, the broad-sense heritability was calculated through the "getHeritability" function of the SpATS R-package according to Oakey *et al.* (2006).

3.2.6. COEFFICIENT OF VARIATION FORMULA

The coefficient of variation expresses the genotypic variability with respect to the mean value. The following formula was used (Albert and Zhang, 2010):

$$CV_g = \frac{\sigma_G}{\mu} * 100$$

where CV_g is the genotypic coefficient of variation, σ_G is the genotypic standard variation, μ is the mean value of the data population. The CV_g is then multiplied by 100 to express it as a percentage.

3.2.7. CORRELATIONS BETWEEN PLATFORM AND FIELD TRIALS

Linear correlations between the traits obtained from the three platforms and the field trials have been performed with the "cor" function of the R software

(R Core Team, 2021), using the pairwise complete observation method. Principal component analyses have also been computed with all traits through the "PCA" function in R. All these analyses have been performed separately for each species.

3.2.8. COMPARISON BETWEEN WHEAT SPECIES

The BLUEs obtained for the 484 genotypes were analysed with a one-way ANOVA, with species set as unique (fixed) factor, using the "aov" function, to test for differences between the mean of the two wheat species.

3.2.9. CLUSTERING OF THE GENOTYPES BASED ON METADATA

Linear regressions, using the "lm" function in R, were done between the traits and the year of release of each genotype (where available, Annexe 1) to test for potential effects of the selection across years of breeding (bread wheat: from 1920 to 2016; durum wheat: from 1970 to 2016).

In addition, other variance analyses were performed (with the "aov" function in R) to test for group effect, considering the collection of the genotypes and the continent of origin (section 3.2.1).

Finally, a hierarchical clustering has been performed across the platform traits, with the "agnes" function in R using the Ward's method, to reveal groups of genotypes having phenotyping similarities.

Traits that were mostly constant over all plants or had low genetic variances were not considered in these analyses. This was the case for $Emer_{1LR}$, $Emer_{PR}$, $Theta_{PR}$ and the Nb_{SR1} of the Pouch experiment. Also, the traits related to the second pair of seminal roots have not been considered for most analyses because of the low number of observations compared to the other traits (> 25% of the genotypes had only one pair of seminals).

3.2.10. POTENTIAL HETEROSIS EFFECTS

In the main mixed models of the platform trait data, the value of the hybrid genotypes and the mean trait values of their parent were compared with the "contrast" function in R, in order to test for heterosis effects (bread wheat panel).

3.3. RESULTS

The results are presented in three main sections. The first one analyses the diversity of the platform phenotypes and considers the impacts of the geographical and collection origin as well as the impact of selection breeding on root features (section 3.3.1).

The second section presents the results of the genetic part of the analysis, with the broad-sense heritabilities, genetic correlations and heterosis (section 3.3.2).

Finally, the last section analyses the environmental impact and considers the consistency between the platforms as well as between the platform traits and the yield-related traits (section 3.3.3).

3.3.1. PHENOTYPING

3.3.1.1. DIVERSITY OF PLATFORM TRAITS

The diversity of the traits estimated in the three platforms will be discussed per trait category (section 3.2.3) based on the data summarized in Table 7.

The traits of the biomass category estimated in the RootPhAir experiment showed moderate variability since the coefficient of variation (CV_g) ranged from 7.4% to 15.5% (Table 7). For both species, the R/S_{Dry} means were about 0.5 indicating that the general trend of the genotypes grown in RootPhAir was to invest twice as much in the shoots parts as in the roots, as it was confirmed by the mean $SMass_{Dry}$ (~0.09 g) and the mean $RMass_{Dry}$ (~0.04 g) values. For the biomass category traits of the 4PMI experiment, where the plants were about few days older (3 to 6 days) than in the RootPhAir but also exposed to W and N stress, the R/S_{Dry} mean values were higher (0.9 for bread wheat and 0.7 for durum wheat). This corroborates the general agreement that plants when exposed to W and N stress tend to invest relatively more in their roots than in their shoots (Shi *et al.*, 2014; Eziz *et al.*, 2017), although it may also reflect a platform effect.

Concerning the traits in the elongation category, the elongation rate $ERate_{PR}$ was estimated in both Pouches and RootPhAir. In Pouch, all roots were growing at a speed of about 1 cm/day for bread wheat and about 1.3 cm/day for durum wheat (all root types confounded, except the second pair of seminal roots) which is similar but in lower range values already found in

literature (e.g., range of 1.2 to 4.4 cm/day found for bread wheat grown in pouches by Chen *et al.* (2020)). In RootPhAir, the ***ERate$_{PR}$*** was faster than in Pouch, reaching about 2.5 cm/day for both species. This value is closer but still higher than the 1.78 cm/day recorded for bread wheat grown in loosened soil by Atwell (1990). However, in his study, Atwell (1990) showed than more compacted soil conditions decreased the seminal root elongation rate (to 0.6 cm/day), suggesting that the mechanically unconstrained environment of RootPhAir may contribute to these faster root elongation rates. The difference between Pouch and RootPhAir values may also result from the drier environment provided by the Pouch device (Salim, Todd and Schlehuber, 1965; Bengough *et al.*, 2011; Rich and Watt, 2013) but also to the younger age of the plant in the Pouch setup. The CV_g were relatively high, from ~7% to ~20% for both species. The high values for the traits related to the second pair of seminal roots (> 60% for bread wheat panel, > 30% for durum wheat panel) should be considered cautiously since only 40% of the genotypes owned a second pair of seminal roots.

The ***MRL*** was estimated in RootPhAir and 4PMI. In the former, it reached ~14.2 cm for bread wheat and ~15.6 cm for durum wheat at 8 DAS, with CV_g values of ~10%. In the 4PMI experiment (at 11 DAS), the mean values for the bread wheat and durum wheat were almost doubled compared to RootPhAir (27.4 cm and 29 cm for bread wheat and durum wheat respectively). This large increase is partly due to the age difference of the plants but may also reflect the nutrient stress conditions applied in 4PMI which may have favoured root elongation at depth (Wasson *et al.*, 2012; Lynch, 2013).

Another set of traits in the elongation category were estimated in RootPhAir only. The mean ***Diam$_{ER}$*** was ~0.04 cm and the mean ***Diam$_{LR}$*** was ~0.02 cm (which are values equivalent to those found in the literature (Guo *et al.*, 2012; R. Liu *et al.*, 2020)), so the lateral roots were twice as thin as their embryonic parent roots (for both species). These variables had low CV_g, from 4.0% to 7.4%. The primary root emerged (***Emer$_{PR}$***) at about 2.5 DAS and the first lateral (***Emer$_{1LR}$***) at 7.5 DAS (for both species). Emergence times showed also very low CV_g values (that were not exceeding 10%). The duration of primordium development, ***DPD***, was about 4.8 days for bread wheat and 5.2 days for durum wheat.

The variables related to the production of roots, namely ***LRD*** and ***Nb_{ER}***, showed quite high CV_g. Again, the same extreme high values of CV_g were seen for the traits linked to the second pair of seminal roots. For the ***Nb_{Leaves}*** estimated in the 4PMI conditions, the mean values were equivalent between both species (~4 leaves), but the ***$Nb_{Tillers}$*** was slightly larger for bread wheat compared to durum wheat (1.41 tillers for bread wheat compared to 0.9 tillers for durum wheat).

Finally, the traits of tropism category in all three platforms displayed the largest CV_g, all categories combined, with values ranging from ~10-15% for ***SRA*** to more than 40% for the ***CH***. The mean values of ***SRA_{SR1}*** were three times smaller in RootPhAir (~0.5 radians) than in Pouch (~1.5 or ~1.8 radians, bread wheat and durum wheat respectively). This could be mainly due to the absence of support which is specific to the aeroponic conditions of RootPhAir. However, within RootPhAir, the ***SRA_{SR1}*** shows the highest CV_g with more than 20%, all trait categories confounded. The ***CH*** mean values in Pouch reached 4.1 cm^2 for bread wheat and 8.0 cm^2 for the durum wheat, suggesting than the durum wheat seedlings occupied two times more space than bread wheat at the end of the four days of the Pouch experiments, which is confirmed by the higher mean values of all traits of the elongation category, that were always higher for the durum wheat panel in Pouch (e.g., ***TRL*** ~6.8 cm for bread wheat and ~10.3 cm for durum wheat). However, under the stressed conditions of 4PMI, no differences are seen for the ***CH*** values between the species (~210 cm^2 for both species). The gap in ***CH*** values between the Pouch and 4PMI is probably due to a difference in the age of the seedlings and possibly to the abiotic stress applied in 4PMI which could have trigger plants to increase their root expansion.

Table 7 (next page). Range of variability and broad sense heritabilities of the traits estimated across the platform experiments (RootPhAir, Pouch and 4PMI) for both wheat species (All = all root types confounded, CV_g = genetic coefficient of variation (%); DAS = days after sowing; H^2 = broad-sense heritability (%), ER = embryonic roots, PR = primary root, sd = standard deviation, SR1 = first pair of seminal roots, SR2 = second pair of seminal roots, 1LR = first lateral root).

		RootPhAir			RootPhAir									Pouch									4PMI					
					Bread wheat					Durum wheat				Bread wheat					Durum wheat				Bread wheat			Durum wheat		
Category	Trait	RootPhAir	Pouch	4PMI	Mean	σ_g	σ_r	CV_g	H^2 (%)	Mean	σ_g	σ_r	CV_g	H^2 (%)	Mean	σ_g	σ_r	CV_g	H^2 (%)	Mean	σ_g	σ_r	CV_g	H^2 (%)	Mean	sd	H^2 (%)	Mean	sd	H^2 (%)
Biomass	*R/S*	Dry		Dry	0.50	0.037	0.055	7.38	59.45	0.51	0.042	0.057	8.26	58.76												0.90	0.13	/	0.73	0.09	/
		Fresh			0.95	0.095	0.170	10.01	50.50	0.93	0.092	0.164	9.94	45.04																
	RMass	Dry		Dry	0.04	0.006	0.018	13.08	24.70	0.04	0.008	0.019	17.27	29.71										0.18	0.04	66.00	0.12	0.03	66.00
		Fresh			0.69	0.105	0.310	15.23	27.26	0.68	0.130	0.316	19.07	30.67																
	SMass	Dry		Dry	0.09	0.012	0.032	14.08	31.31	0.09	0.015	0.036	16.75	30.51										0.20	0.05	69.00	0.16	0.04	68.00
		Fresh			0.72	0.111	0.266	15.45	36.07	0.74	0.135	0.304	18.25	34.06																
Elongation	*Diam*	All			2.23E-02	1.16E-03	1.85E-03	5.18	56.00	2.07E-02	8.69E-04	1.84E-03	4.19	36.85																
		ER			4.33E-02	3.18E-03	6.75E-03	7.34	41.96	4.51E-02	3.18E-03	6.40E-03	7.07	39.20																
		LR			2.18E-02	1.13E-03	1.76E-03	5.18	57.19	2.02E-02	7.93E-04	1.64E-03	3.93	37.73																
	DPD	✓			4.85	0.226	1.002	4.67	14.24	5.24	0.000	1.076	0.00	0.00																
	Emer	1LR			7.53	0.000	1.082	0.00	0.00	7.71	0.282	1.214	3.66	12.35																
		PR			2.64	0.296	0.845	11.23	28.61	2.41	0.469	0.774	19.44	48.84																
	ERate		ER												0.97	0.022	0.073	15.46	77.81	1.19	0.019	0.072	11.47	72.55						
		PR	PR		2.47	0.188	0.308	7.61	54.86	2.64	0.189	0.351	7.14	42.94	1.08	0.034	0.134	17.18	74.54	1.34	0.033	0.213	13.56	61.03						
			SR1												0.99	0.023	0.071	15.46	79.16	1.33	0.023	0.103	11.46	69.69						
			SR2												0.43	0.068	0.053	60.14	93.63	0.79	0.048	0.123	27.81	79.79						
	Length		PR												2.57	0.272	0.707	20.32	81.53	3.19	0.364	1.239	18.91	74.93						
			SR1												2.01	0.160	0.373	19.94	83.12	2.77	0.310	0.677	20.10	82.33						
			SR2												0.45	0.090	0.078	66.78	92.95	1.09	0.172	0.458	38.22	79.25						
	ARL		✓												2.02	0.132	0.363	17.98	80.67	2.41	0.181	0.383	17.62	82.76						
	MRL	@8 DAS		@9 DAS	14.20	1.377	3.215	9.699	37.41	15.57	1.615	4.275	10.37	27.09										27.38	3.29	73.00	29.06	3.84	81.00
	TRL		✓												6.76	2.121	4.201	21.56	85.28	10.34	5.660	8.004	23.00	87.79						
	Surf			@9 DAS																					16.07	4.03	74.00	16.86	4.78	68.00
Production	*LRD*	✓			2.17	0.197	0.622	9.076	24.59	2.23	0.337	0.686	15.10	38.55																
	Nb	ER	ER		4.42	0.412	0.843	9.325	43.71	4.82	0.364	0.710	7.554	40.64	3.35	0.147	0.299	11.45	84.97	4.26	0.262	0.611	12.04	81.37						
			SR1												/	/	/	/	/	/	/	/	/	/						
			SR2												1.53	0.245	0.198	32.37	93.41	1.74	0.045	0.131	12.10	77.51						
	Nb_{Leaves}			✓																					4.33	0.30	71.00	4.17	0.34	68.00
	$Nb_{Tillers}$			✓																					1.41	0.63	75.00	0.85	0.56	71.00
Tropism	*SRA*		ER												1.68	0.056	0.170	14.15	79.20	2.21	0.047	0.171	9.77	73.41						
		SR1	SR1		0.51	0.113	0.220	22.13	46.46	0.52	0.112	0.247	21.73	35.00	1.50	0.046	0.110	14.22	82.58	1.77	0.038	0.139	10.97	73.33						
			SR2												2.46	0.120	0.043	14.05	96.98	2.46	0.054	0.069	9.47	88.99						
	Theta		PR												0.12	0.002	0.009	35.14	68.85	0.17	0.003	0.019	30.94	61.45						
			SR1												0.75	0.012	0.030	14.44	81.82	0.88	0.008	0.039	10.47	68.86						
			SR2												1.19	0.067	0.029	21.67	96.38	1.21	0.015	0.042	10.16	78.77						
	CH		✓	@9 DAS											4.09	2.691	4.692	40.07	86.80	7.97	9.868	12.63	39.44	88.82	212.9	70.29	61.00	217.9	87.11	67.00
	Width			@9 DAS																					11.23	3.48	55.00	10.70	3.93	66.00

3.3.1.2. IMPACT OF CONTINENT OF ORIGIN AND KNOWN COLLECTIONS ON PHENOTYPING TRAITS

Very few effects were found that could be attributed to the continent of origin of the genotypes in both panels (Table 8). In the durum wheat panel, the genotypes with the highest R/S_{Dry} have been identified as the ones coming from Asia while the genotypes with the smallest R/S_{Dry} come from Africa (pval < 0.001). Also, in both panels, the genotypes showing significantly high grain yield under both controlled and stressed conditions (*GYC*, *GYS*) were from Europe (pval < 0.01 for durum wheat, and pval < 0.001 and < 0.01 for bread wheat, *GYC*, *GYS* respectively).

In term of genotype collections within the bread wheat panel, the hybrids genotypes and their parents appeared to have significantly shorter root lengths ($Length_{PR}$, $Length_{SR1}$, *TRL*, pval < 0.001 for all) than the other collections. In addition, the BreedWheat collection seemed to have the highest values for most traits, all collections confounded. The hybrids genotypes and their parents were not included in the field trials, so that no comparison between collections was carried out for the grain yields of the bread wheat panel (Table 8).

Regarding the collections within the durum wheat panel, the EPO lines seemed to have the shorter roots compared to other collections (pval < 0.001), followed by the UNIBO collection. The GPDUR collection stood out with genotypes having in general the highest traits values. This collection also seemed to be the most successful in the field with significantly higher *GYC*, *GYS* and *GYSI* values (pval < 0.001) than the other collections (Table 8).

Table 8 (next page). Results of the ANOVA analyses between platform traits and the collections, continent of origin and the cluster groups for both bread wheat and durum wheat panels separately (each letter corresponds to a different significant group, the darkest orange colours correspond to the groups with the highest values, the lightest to the lowest values: a>ab>b>bc>c>d); as well as the results of the linear correlations between the phenotyping traits and the year of release of the genotype (in green, positive correlations and in blue, negative ones) (Annexe 1); and the results of the comparison between bread wheat (BW) vs durum wheat (DW) (B=BreedWheat, Ch=Checks, H=Hybrids, L=Local variety, P=Parents, C=CREA, E=EPO, G=GPDUR, U=UNIBO; Af=Africa, Am=America, As=Asia, Eu=Europe, Oc=Oceania; pval < 0.1 (n.s.), pval < 0.05 (*), pval < 0.01 (**), pval < 0.001 (***); All = all root types confounded, DAS = days after sowing, ER = embryonic roots, PR = primary root, SR1 = first pair of seminal roots, SR2 = second pair of seminal roots, 1LR = first lateral root).

						Bread wheat																						Durum wheat														BW vs DW		
						Collections							Continents							Clustering groups								Collections					Continents					Clustering group									
Category	Trait	RootPhAir	Pouch	4PMI	Field	B	Ch	H	L	P	pval	Af	Am	As	Eu	Oc	pval	1	2	3	4	5	6	pval	Year	C	E	G	U	pval	Af	Am	As	Eu	pval	1	2	3	4	5	pval	Year	BW	DW	pval
Biomass	*R/S*	Dry				b	ab	ab	b	a	*	a	a	a	a	a	n.s.	a	b	ab	a	ab	a	***	n.s.	b	b	a	b	***	a	a	a	a	n.s.	a	b	b	b	b	***	** (+)	a	a	n.s.
				Dry		/	/	/	/	/	/	a	a	a	a	a	n.s.	ab	ab	a	b	ab	ab	*	n.s.	a	a	a	a	n.s.	c	bc	a	b	***	a	ab	ab	b	b	***	n.s.	a	b	***
		Fresh				a	a	a	a	a	*	a	a	a	a	a	n.s.	ab	c	bc	ab	ab	a	***	n.s.	b	b	a	b	***	a	a	a	a	n.s.	a	bc	c	bc	b	***	n.s.	a	a	n.s.
	RMass	Dry				a	a	a	a	a	n.s.	a	a	a	a	a	n.s.	b	d	bc	a	bc	c	***	n.s.	a	a	a	a	n.s.	a	a	a	a	n.s.	ab	b	c	a	b	***	n.s.	a	a	n.s.
				Dry		/	/	/	/	/	/	a	a	a	a	a	n.s.	a	a	b	a	a	a	***	n.s.	a	a	a	a	n.s.	a	a	a	a	n.s.	a	a	ab	b	a	***	n.s.	a	b	***
		Fresh				a	a	a	a	a	n.s.	a	a	a	a	a	n.s.	b	d	bc	a	bc	c	***	n.s.	a	a	a	a	n.s.	a	a	a	a	n.s.	a	a	b	a	a	***	n.s.	a	a	n.s.
	SMass	Dry				a	a	a	a	a	n.s.	a	a	a	a	a	n.s.	b	d	b	a	bc	c	***	n.s.	a	a	a	a	n.s.	a	a	a	a	n.s.	b	a	b	b	a	***	n.s.	a	b	***
				Dry		/	/	/	/	/	/	a	a	a	a	a	n.s.	a	a	b	a	a	a	***	n.s.	a	a	a	a	n.s.	a	a	a	a	n.s.	b	a	b	b	a	***	n.s.	a	b	***
		Fresh				a	a	a	a	a	n.s.	a	a	a	a	a	n.s.	b	d	b	a	bc	c	***	n.s.	a	a	a	a	n.s.	a	a	a	a	n.s.	b	b	c	a	b	***	n.s.	a	a	n.s.
Elongation	*Diam*	All				a	a	a	a	a	n.s.	a	a	a	a	a	n.s.	a	b	ab	a	a	a	***	n.s.	a	a	a	a	n.s.	a	a	a	a	n.s.	b	ab	ab	a	ab	*	n.s.	a	b	***
		ER				b	a	ab	ab	a	**	a	ab	ab	a	a	***	a	b	ab	a	a	ab	*	* (+)	a	a	a	a	n.s.	a	a	a	a	n.s.	a	a	a	a	a	n.s.	n.s.	b	a	**
		LR				a	a	a	a	a	n.s.	a	a	a	a	a	n.s.	a	b	a	a	a	a	***	n.s.	a	a	a	a	n.s.	a	a	a	a	n.s.	b	ab	b	a	ab	**	n.s.	a	b	***
	DPD	✓				a	a	a	a	a	n.s.	b	ab	ab	b	a	*	a	a	a	a	a	a	n.s.	n.s.	a	a	a	a	n.s.	a	a	a	a	n.s.	a	a	a	a	a	n.s.	n.s.	b	a	***
	Emer	1LR				a	a	a	a	a	n.s.	a	a	a	a	a	n.s.	/	/	/	/	/	/	n.s.	n.s.	a	a	a	a	n.s.	a	a	a	a	n.s.	/	/	/	/	/	/	n.s.	b	a	**
		PR				a	a	a	a	a	n.s.	a	a	a	a	a	*	/	/	/	/	/	/	n.s.	n.s.	b	b	b	a	***	ab	b	a	b	**	/	/	/	/	/	/	n.s.	a	b	*
	ERate		ER			a	a	a	a	a	n.s.	a	a	a	a	a	n.s.	c	c	ab	ab	b	a	***	n.s.	a	a	a	b	***	a	ab	a	a	*	a	a	b	c	a	***	n.s.	b	a	***
			PR			a	a	a	a	a	n.s.	a	ab	ab	a	ab	***	b	c	bc	a	bc	bc	***	n.s.	a	a	a	a	n.s.	a	a	a	a	n.s.	a	a	b	a	a	***	n.s.	b	a	***
			PR			a	a	a	a	a	n.s.	a	a	a	a	a	n.s.	d	d	bc	ab	c	a	***	n.s.	a	a	a	a	n.s.	a	a	a	a	n.s.	a	a	c	c	b	***	n.s.	b	a	***
			SR1			a	a	a	a	a	n.s.	a	a	a	a	a	n.s.	c	c	ab	a	b	a	***	n.s.	ab	ab	a	b	*	a	ab	ab	a	*	ab	a	c	d	bc	***	n.s.	b	a	***
			SR2			/	/	/	/	/	/	/	/	/	/	/	/	/	/	/	/	/	/	/	/	/	/	/	/	/	/	/	/	/	/	/	/	/	/	/	/	/	b	a	***
	Length		PR			a	ab	b	b	b	***	a	a	a	a	a	n.s.	d	d	bc	b	c	a	***	n.s.	a	c	a	b	***	a	a	a	a	n.s.	a	a	b	c	b	***	n.s.	b	a	***
			SR1			a	ab	b	ab	b	***	a	a	a	a	a	n.s.	c	c	b	a	b	a	***	* (-)	a	c	a	b	***	a	ab	a	a	*	a	a	b	c	b	***	n.s.	b	a	***
			SR2			/	/	/	/	/	/	/	/	/	/	/	/	/	/	/	/	/	/	/	/	/	/	/	/	/	/	/	/	/	/	/	/	/	/	/	/	b	a	***
	ARL		✓			a	ab	ab	ab	b	**	a	a	a	a	a	n.s.	c	c	b	b	b	a	***	n.s.	a	c	a	b	***	ab	ab	a	a	*	a	a	b	c	b	***	n.s.	b	a	***
	MRL	@8DAS				a	a	a	a	a	n.s.	a	ab	a	a	ab	*	b	c	b	a	bc	bc	***	n.s.	ab	ab	a	b	*	a	a	b	a	***	* (+)	b	a	***
				@9DAS		/	/	/	/	/	/	a	a	a	a	a	n.s.	a	a	b	a	a	a	***	n.s.	a	a	a	a	n.s.	a	a	a	a	**	a	b	c	c	ab	***	** (+)	b	a	***
	TRL		✓			a	ab	b	ab	b	***	a	a	a	a	a	n.s.	c	c	b	a	b	a	***	n.s.	a	c	a	b	***	a	a	a	a	n.s.	a	a	b	c	b	***	n.s.	b	a	***
	Surf			@9DAS		/	/	/	/	/	/	a	a	a	a	a	n.s.	a	a	b	a	a	a	***	n.s.	a	a	a	a	n.s.	a	a	a	a	n.s.	a	a	a	b	a	***	** (+)	b	a	*
Production	*LRD*	✓				a	a	a	a	a	n.s.	a	a	a	a	a	n.s.	a	a	a	a	a	a	*	n.s.	a	a	a	a	n.s.	a	a	a	a	n.s.	b	ab	ab	ab	a	*	n.s.	a	a	n.s.
		ER				a	a	a	a	a	n.s.	a	a	a	a	a	n.s.	b	c	b	a	ab	b	***	n.s.	a	a	a	a	n.s.	a	a	a	a	n.s.	a	a	b	a	a	***	n.s.	b	a	***
	Nb		ER			a	ab	b	b	b	***	a	a	a	a	a	n.s.	bc	bc	c	a	bc	ab	***	* (-)	a	b	a	ab	***	a	a	a	a	n.s.	ab	a	bc	d	c	***	n.s.	b	a	***
			SR1			a	a	a	a	a	n.s.	a	a	a	a	a	n.s.	/	/	/	/	/	/	n.s.	n.s.	a	a	a	a	*	a	a	a	a	n.s.	/	/	/	/	/	/	n.s.	a	a	n.s.
			SR2			/	/	/	/	/	/	/	/	/	/	/	/	/	/	/	/	/	/	/	/	/	/	/	/	/	/	/	/	/	/	/	/	/	/	/	/	b	a	***
	Nb_{Leaves}			✓		/	/	/	/	/	/	a	a	a	a	a	n.s.	a	a	a	a	a	a	n.s.	n.s.	a	a	ab	b	**	a	a	a	a	n.s.	a	a	a	a	a	**	n.s.	a	b	***
	$Nb_{Tillers}$			✓		/	/	/	/	/	/	a	a	a	a	a	n.s.	a	a	b	a	a	a	***	n.s.	a	a	a	a	n.s.	a	a	a	a	n.s.	a	a	a	a	a	.	n.s.	a	b	***
Tropism	*SRA*		ER			a	a	ab	a	a	*	a	a	a	a	a	n.s.	b	b	b	a	a	a	***	n.s.	a	a	a	a	n.s.	a	a	a	a	n.s.	a	a	b	b	a	***	n.s.	b	a	***
		SR1				a	a	a	a	a	n.s.	a	a	a	a	a	n.s.	ab	b	ab	ab	a	ab	*	* (+)	a	a	a	a	n.s.	a	a	a	a	n.s.	a	a	a	a	a	n.s.	n.s.	a	a	n.s.
			SR1			ab	ab	ab	a	a	***	a	a	a	a	a	n.s.	b	b	b	b	a	a	***	* (+)	a	a	a	a	n.s.	b	a	b	b	***	a	a	a	a	a	***	n.s.	b	a	***
			SR2			/	/	/	/	/	/	/	/	/	/	/	/	/	/	/	/	/	/	/	/	/	/	/	/	/	/	/	/	/	/	/	/	/	/	/	/	a	a	n.s.
	Theta		PR			a	a	a	a	a	n.s.	a	a	a	a	a	n.s.	/	/	/	/	/	/	/	n.s.	ab	a	b	ab	**	a	a	a	a	n.s.	/	/	/	/	/	/	n.s.	b	a	***
			SR1			ab	a	ab	a	a	**	a	a	a	a	a	n.s.	c	c	c	bc	a	ab	***	n.s.	b	a	ab	b	***	a	a	a	a	n.s.	ab	b	ab	b	ab	a	***	n.s.	b	a	***
			SR2			/	/	/	/	/	/	/	/	/	/	/	/	/	/	/	/	/	/	/	/	/	/	/	/	/	/	/	/	/	/	/	/	/	/	/	/	a	a	n.s.
	CH		✓			a	ab	b	ab	b	***	a	a	a	a	a	n.s.	d	d	c	b	bc	a	***	n.s.	a	c	a	b	***	a	a	a	a	n.s.	a	a	b	c	b	***	n.s.	b	a	***
				@9DAS		/	/	/	/	/	/	a	a	a	a	a	n.s.	b	b	c	b	a	b	***	n.s.	a	a	a	a	n.s.	a	a	a	a	n.s.	b	a	ab	b	a	***	* (+)	a	a	n.s.
	Width			@9DAS		/	/	/	/	/	/	a	a	a	a	a	n.s.	b	b	c	b	a	b	***	n.s.	a	a	a	a	n.s.	a	a	a	a	n.s.	b	a	a	ab	a	***	n.s.	a	a	n.s.
Field	*GYSI*				✓	/	/	/	/	/	/	a	a	a	a	a	n.s.	ab	b	ab	ab	a	ab	.	n.s.	c	ab	a	bc	***	a	a	a	a	n.s.	a	c	b	bc	b	***	*** (+)	/	/	/
	GYC				✓	/	/	/	/	/	/	b	a	a	a	a	***	a	a	a	a	a	a	n.s.	*** (+)	b	b	a	b	***	ab	b	ab	a	**	a	c	bc	bc	b	***	*** (+)	a	b	***
	GYS				✓	/	/	/	/	/	/	b	ab	ab	a	ab	**	ab	b	ab	ab	a	a	**	*** (+)	b	b	a	b	***	ab	b	ab	a	**	a	c	b	bc	b	***	*** (+)	b	a	***
	AMF				✓	/	/	/	/	/	/	/	/	/	/	/	/	/	/	/	/	/	/	/	/	/	a	a	a	n.s.	a	a	a	a	n.s.	a	a	a	a	a	n.s.	n.s.	/	/	/

3.3.1.3. CHARACTERISTICS OF CLUSTERS

From the hierarchical analysis of the complete set of data, the bread wheat panel has been divided into 6 clusters (Figure 14) and the durum wheat panel into five clusters (Figure 15). The main characteristics of (and differences between) the clusters are highlighted in Table 8. A tentative description of each cluster has been sketched in the Figure 14 – B and Figure 15 – B.

The first bread wheat cluster could be named as "Medium shoots with short and steep root system" plants on the basis of its most prominent features. This group is composed of genotypes with medium values for the traits of the biomass category, quite important ***Diam*** values but, surprisingly low traits values for ***ERate***, ***Length*** and Nb_{ER}. Genotypes of this cluster seem to invest a little less in roots than the other clusters and are slightly sensitive to stressed conditions in the field.

The second bread wheat cluster could be called "Short shoots with short, thin and steep root system". It is composed of genotypes with low values for the traits of the biomass category (lowest ***R/S***, ***RMass*** and ***SMass***), of the elongation category (thinner ***Diam***, lower growth rates ***ERate*** and ***Length***), of the production category (low Nb_{ER}), and lower values for the traits of the tropism category (lowest ***SRA***, ***CH,*** and quite low ***Width***). Genotypes in this group tend to invest more in shoots than roots and are the most sensitive to field stress conditions of all the cluster groups (lowest ***GYSI*** and ***GYS***).

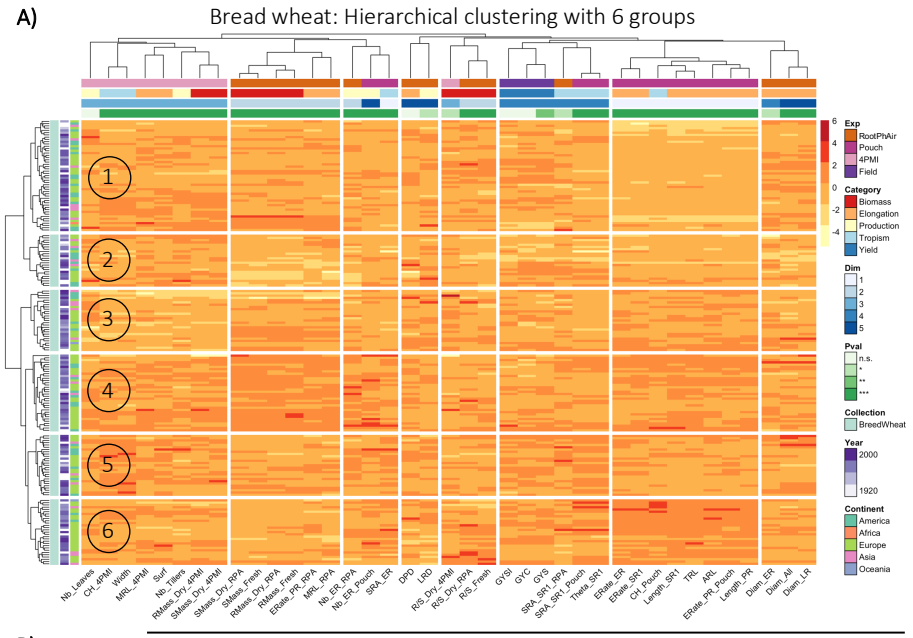
The third bread wheat cluster, "Medium shoots with steeper root system" plants, is mainly composed of genotypes having slightly higher ***SMass*** than ***RMass***, lower values for the traits of the elongation category (***ERate*** and ***Length***), low values for the traits of the production category (Nb_{ER}), steeper root system (lowest ***CH***, low ***SRA,*** and lowest ***Width***). This cluster invests more in shoots than in roots and is slightly susceptible to field stressed conditions.

The fourth bread wheat cluster can be named "Large shoots with deep and dense root system". It is composed of genotypes with the highest trait values in the biomass category, with quite high values for the traits of the elongation category (high ***Diam***, ***ERate***, ***Length***, ***TRL***, ***MRL***, ***Surf***), with the highest trait values in the production category (Nb_{ER}), and lower values for the traits of the tropism category, leading to moderately deeper root system then the other cluster groups (***SRA***, ***Width*** and ***CH***). This cluster invests a lot in roots but also lots in shoots and is a little susceptible to field stressed conditions.

The fifth bread wheat cluster, "Medium shoots with wider root system", includes genotypes with a good investment in ***RMass*** compared to ***SMass*** (quite high ***R/S***), medium values for the trait of the elongation category, widest root systems (highest ***SRA***, ***CH***, ***Width***) and among the most tolerant genotypes to field stresses (higher ***GYSI*** and ***GYS***).

The last bread wheat cluster could be called "Short shoots with deep and wide root system". It includes genotypes having high ***R/S***, but not the highest ***RMass*** and ***SMass***, with quite high trait values of the elongation category, with a wider root system expansion and an equivalent yield under both controlled and stressed conditions. This cluster seems to invest the most in roots and shows up as less susceptible to field stressed conditions.

For the bread wheat panel, the clusters that seem to be the most performant in the field under controlled and stressed conditions are the fifth and sixth cluster groups, that seem to invest a little more in their roots compared to the shoots but that have as main characteristic a wide (both clusters) and deep (sixth cluster) root system.



B)

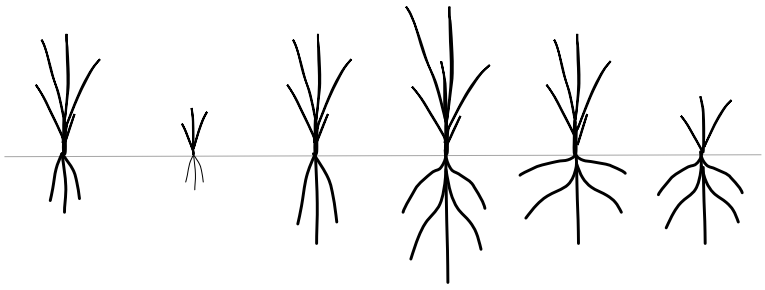
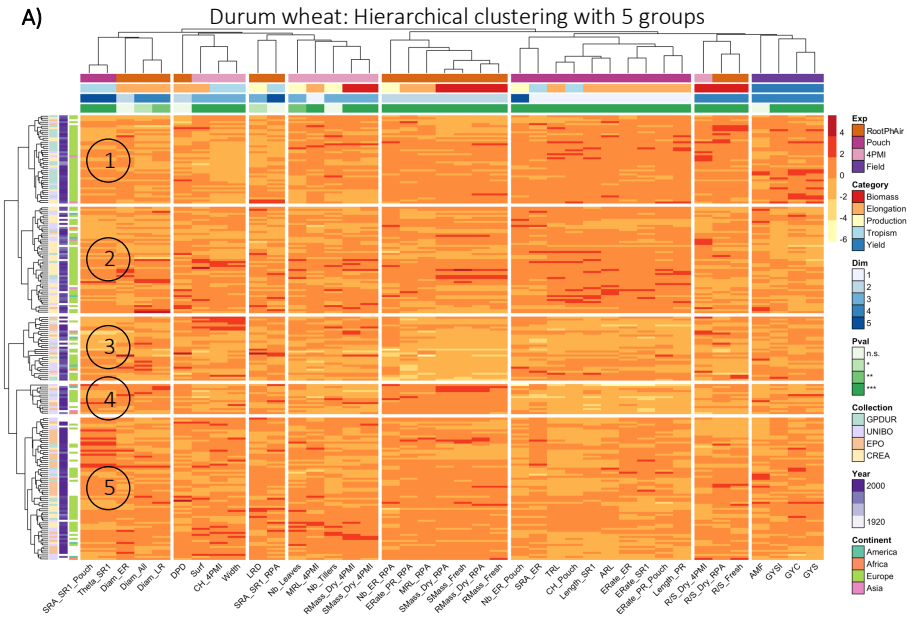
	Bread wheat clusters					
	1	2	3	4	5	6
Plant scheme						
Name of the cluster	Medium shoots with short and steep root system	Short shoots with short, thin and steep root system	Medium shoots with steeper root system	Large shoots with deep and dense root system	Medium shoots with wider root system	Short shoots with deep and wide root system
Carbon investment	Roots & Shoots	Shoots > Roots	Shoots > Roots	Roots & Shoots	Roots & Shoots	Roots > Shoots
Scale for field tolerance and yield productivity under stress	+	-	+	+	+ +	+ +

*Figure 14. Heatmaps of the hierarchical clustering performed for the bread wheat panel (**A**) followed by plant schemes to illustrate each cluster (**B**). **A)** The numbers on the left are the cluster groups number. "Exp" accounts for the different platforms; "Category" is the category within which the root trait has been attributed (section 3.2.3); "Dim" is the number of dimensions from PCA analysis (section 3.3.3.1), "Pval" is the p-value from the variance analyses performed between cluster groups, "Collection" is the collection to which belong the genotype, "Year" is the year of breeding and "Continent" the continent of origin of the genotype (section 3.2.1, Annexe 1). **B)** Plant schemes per cluster, their names, carbon investment preferences and a subjective scale estimated based on their field tolerance (**GYSI**) and yield productivity under stress (**GYS**). The scales and plant schemes have been set per plant species (intra comparison of the proportions only – not to be compared between species).*



B)

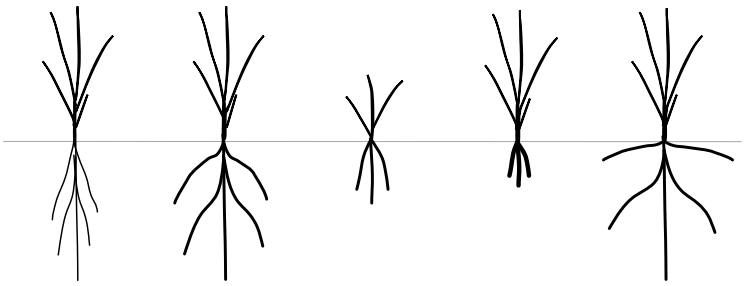
	Durum wheat clusters				
	1	2	3	4	5
Plant scheme					
Name of the cluster	Medium shoots with thin, deep and steep root system	Medium shoots with deep, wide and dense root system	Short shoots with short root system	Medium shoots with short, thick and steep root system	Medium shoots with wider root system
Carbon investment	Roots > Shoots	Roots & Shoots	Roots & Shoots	Shoots > Roots	Roots & Shoots
Scale for field tolerance and yield productivity under stress	+ +	- -	+	-	+

*Figure 15. Heatmaps of the hierarchical clustering performed for the durum wheat panel (**A**) followed by plant schemes to illustrate each cluster (**B**). **A)** The numbers on the left are the cluster groups number. "Exp" accounts for the different platforms; "Category" is the category within which the root trait has been attributed (section 3.2.3); "Dim" is the number of dimensions from PCA analysis (section 3.3.3.1), "Pval" is the p-value from the variance analyses performed between cluster groups, "Collection" is the collection to which belong the genotype, "Year" is the year of breeding and "Continent" the continent of origin of the genotype (section 3.2.1, Annexe 1). **B)** Plant schemes per cluster, their names, carbon investment preferences and a subjective scale estimated based on their field tolerance (**GYSI**) and yield productivity under stress (**GYS**). The scales and plant schemes have been set per plant species (intra comparison of the proportions only – not to be compared between species).*

The durum wheat genotypes were classified into five different clusters (Figure 15). The first one, labelled "Medium shoots with thin, deep and steep root system", is composed of genotypes having the highest ***R/S***, high values for the traits of the elongation category, lower ***Diam***, lower ***LRD***, lower ***Width***, and good tolerance to field stresses (***GYSI***). This cluster seems to invest most in roots compared to shoots, with a deeper root development, and is among the most tolerant clusters to field stresses.

The second durum wheat cluster is named "Medium shoots with deep, wide and dense root system". In this one, genotypes have medium values for the traits of the biomass category, high values for the elongation category (highest ***ERate***, ***ARL***, ***TRL***), high values for the production category (higher Nb_{ER}), wider and larger root systems (***SRA***, ***Width***) than other clusters and less grain yield in all environments. This cluster invests both in roots and shoots, has rapid expansion, very large root systems but is the less productive in the field and the most susceptible to field stresses.

The third durum wheat cluster, "Short shoots with short root system", includes genotypes with lower values for the traits of the biomass category (lower ***R/S***, ***RMass***, and ***SMass***), slightly lower traits in the elongation category (lower ***ERate*** and ***Length***), low values for the traits of the production category, most steeper root system and slightly susceptible to field stresses. These genotypes invest less in roots than the other clusters and are quite susceptible to field stresses.

The fourth durum wheat cluster is the "Medium shoots with short, thick and steep root system". Its genotypes have medium ***R/S*** ratio, thicker ***Diam*** values, and surprisingly lowest trait values from the elongation category (shorter ***Length***, ***ARL***, ***MRL***, ***TRL***), fewer Nb_{ER}, steeper root system compared to other clusters. Genotypes of this cluster invest a little less in roots compared to the shoots but maintain a quite good ***R/S*** thanks to thick root diameters. They are also slightly susceptible to field stressed conditions.

The last durum wheat cluster is called "Medium shoots with wider root system". It is composed of genotypes with medium ***R/S*** ratio, medium values for the traits of the elongation category (***ERate***, ***Length***, ***ARL***), widest (***SRA***) and largest (***CH*** and ***Width***) root systems compared to other clusters and are slightly less productive in terms of grain yield among all environments. Genotypes of this cluster invest both in roots and shoots, have very large root

systems, with medium expansion and are only slightly susceptible to field stresses.

For the durum wheat panel, the cluster that seems to be the most performant in the field under controlled and stressed conditions is the first one. And this cluster has some different main characteristics than the clusters pinned for the bread wheat panel. As for the bread wheat clusters, it seems to invest a little more in their roots compared to the shoots, but in contrast, it has a steep and deep root system expansion.

3.3.1.4. IMPACT OF BREEDING

Only one correlation was found between the traits of the biomass category and the genotype year of release. This correlation was a positive one between R/S_{Dry} estimated in RootPhAir for the durum wheat panel and the year of release (pval < 0.01) (Table 8).

However, some contrasting correlations were found for the traits of the elongation category between both species. Two correlations emerged for the bread wheat panel, a positive one for the RootPhAir $Diam_{ER}$ (pval < 0.05) and a negative one for the Pouch $Length_{SR1}$ (pval < 0.05), suggesting that genotypes with thicker embryonic roots but also with shorter first pair of seminal roots were selected over the years. This observation is contrary to what one would expect from the well-known relationship of higher growth potential with root diameter (Pagès, 1995), unless the root growth potential cannot be realised in the platform conditions. For the durum wheat panel, three correlations were found, all positive. For ***MRL***, which was estimated in both RootPhAir and 4PMI (pval < 0.05 and < 0.01, RootPhAir and 4PMI respectively), as well as for ***Surf*** (pval < 0.01) suggesting that genotypes with longer embryonic roots and a larger root system were selected over years (which is in line with the R/S_{Dry} positive evolution found above).

In term of production, only the bread wheat genotypes seem to have a Nb_{ER} slightly decreasing over years (pval < 0.05, which was confirmed only in the Pouch experiment).

Concerning the traits of the tropism category, for the bread wheat panel, genotypes with wider angle between the first pair of seminal SRA_{SR1} (in both RootPhAir and Pouch) were selected over years (pval < 0.05). And for the durum wheat panel, genotypes with a larger convex hull area (***CH***, in 4PMI)

and thus exploring a large soil surface, were selected over years (pval < 0.05), which is also in line with previous ***MRL*** and ***Surf*** correlations.

Finally, as excepted, positive correlations were found between the year of release and the traits related to yield in both species (***GYC*** and ***GYS***, pval < 0.001 for both species and both traits). Nevertheless, only the durum wheat panel show a clear positive evolution of the ***GYSI*** (pval < 0.001), indicating that more tolerant genotypes seem to have been selected over years for this panel only.

3.3.2. GENETICS

3.3.2.1. BROAD-SENSE HERITABILITY

The root traits classified in the biomass category show quite moderate to high heritabilities for both wheat species (~ 25% for $RMass_{Dry}$ in RootPhAir; ~ 70% for $SMass_{Dry}$ in 4PMI) (Table 7). For RootPhAir in particular, the ***R/S*** ratios show the highest H^2 of this trait category reaching almost 60%. This last observation could identify the ***R/S*** as a good candidate for breeding selection.

Concerning the traits in the elongation category, they also show relatively moderate to high heritabilities. For example, in RootPhAir, all diameter traits (***Diam***) reached H^2 values close to 40-50% for the bread wheat panel and 40% for the durum wheat panel, same observations for the $ERate_{PR}$. The ***MRL*** in RootPhAir showed slightly lower values with H^2 close to 40% for bread wheat, but 30% for durum wheat, however in 4PMI, the ***MRL*** values were quite higher with ~70% for bread wheat and 80% for durum wheat (Table 7). Very high H^2 were observed for the traits linked to the second pair of seminal roots in the Pouch experiment, but as already mentioned, it should be considered cautiously since only 40% of the genotypes owned this second pair of seminal root type. Finally in this category, the ***DPD*** and the $Emer_{1LR}$ estimated in RootPhAir are both traits showing the lowest H^2 for both species, indicating that these traits would be less genetically controlled.

As for the other categories, both the traits of the production category and the tropism category have very high heritabilities for the Pouch and 4PMI experiments (> 60%) (Table 7). Again, all traits related to the second pair of seminal roots record some of the highest H^2 for both species (SRA_{SR2} and $Theta_{SR2}$ > 90% for bread wheat and > 75% for durum wheat). By omitting these traits related to the second pair of seminal roots, the ***CH*** showed the

highest H^2 almost reaching 90% for the Pouch experiment within this tropism category.

A general trend is observed from the broad sense heritabilities (H^2) and the coefficients of variation (CV_g) measured in RootPhAir experiment compared to the other phenotyping experiments. Across all trait categories, most H^2 and CV_g are lower in RootPhAir than the ones estimated in Pouch and 4PMI experiments (Table 7). This difference could be trigger by the presence or absence of substrate in the platforms. RootPhAir has a substrate-free environment where plants evolve in 3D without any support, compared to the 2D-support given to the plants in both Pouch and 4PMI (pouches and Rhizotube, Figure 13). The fact it has been proven that the mechanical impedance of the soil increases the genetic variability of the root traits, could explained this difference (Colombi and Walter, 2017).

3.3.2.2. POTENTIAL HETEROSIS EFFECTS

Some significant differences were found in the results of the contrast analysis between the hybrid phenotypic values and the mean values of their parents within the bread wheat panel (Table 9). Most of the differences were negative which means the hybrids had significantly lower traits values than their mean parent value. The hybrid H15FR11757/SY MATTIS showed differences for three traits of the elongation category ($ERate_{PR}$, $Length_{PR}$, TRL) and three traits of the tropism category (SRA_{ER}, SRA_{SR1}, $Theta_{SR1}$), which were significantly lower than the mean of their parents. This suggests that H15FR11757/SY MATTIS have a smaller and steeper root system compared to the root system of their parents. All four H15FR13047/OREGRAIN, SUBLIM/GIAMBOLOGNA, SUBLIM/OREGRAIN and SY 117079/AKAMAR followed the same pattern of results but only for the traits of the tropism category, also suggesting more steeper root system than their parents. If the desired heterosis effect would be to have a root system that explores deeper horizons, then these last four hybrids could be potentially good candidates.

Concerning a greater investment in the root system, the hybrid BOLOGNA/GIAMBOLOGNA tended to have a superior R/S_{Dry} value than the parents (pval < 0.05). On the other hand, the two hybrids, SUBLIM/ATHLON and SY 117071/ARLEQUIN had significantly inferior R/S_{Dry} values than their parents (pval < 0.05 for both).

Table 9. Contrasts between the hybrids and their mean parent values to see if there is a heterosis effect. Green colour corresponds to positive correlations and blue colour to negative ones (pval < 0.1 (n.s.), pval < 0.05 (*), pval < 0.01 (**), pval < 0.001 (***); All = all root types confounded, DAS = days after sowing, ER = embryonic roots, PR = primary root, SR1 = first pair of seminal roots, SR2 = second pair of seminal roots, 1LR = first lateral root).

				Contrasts between hybrids and their mean parent values									
Category	**Trait**	**RootPhAir**	**Pouch**	**ANNIBALE/ AKAMAR**	**BOLOGNA/ GIAMBOLOGNA**	**H15FR11757/ SY MATTIS**	**H15FR13047/ OREGRAIN**	**SUBLIM/ ATHLON**	**SUBLIM/ GIAMBOLOGNA**	**SUBLIM/ OREGRAIN**	**SY 116464/ ATHLON**	**SY 117071/ ARLEQUIN**	**SY 117079 /AKAMAR**
Biomass	***R/S***	Dry		n.s.	* (+)	n.s.	n.s.	* (-)	n.s.	n.s.	n.s.	* (-)	n.s.
		Fresh		n.s.	n.s.	n.s.	n.s.	n.s.	n.s.	n.s.	n.s.	n.s.	n.s.
	RMass	Dry		n.s.	n.s.	n.s.	n.s.	n.s.	n.s.	n.s.	n.s.	n.s.	n.s.
		Fresh		n.s.	n.s.	n.s.	n.s.	n.s.	n.s.	n.s.	n.s.	n.s.	n.s.
	SMass	Dry		n.s.	n.s.	n.s.	n.s.	n.s.	n.s.	n.s.	n.s.	n.s.	n.s.
		Fresh		n.s.	n.s.	n.s.	n.s.	n.s.	n.s.	n.s.	n.s.	n.s.	n.s.
Elongation	***Diam***	All		n.s.	n.s.	n.s.	n.s.	n.s.	n.s.	n.s.	n.s.	n.s.	n.s.
		ER		n.s.	n.s.	n.s.	n.s.	n.s.	n.s.	n.s.	n.s.	n.s.	n.s.
		LR		n.s.	n.s.	n.s.	n.s.	n.s.	n.s.	n.s.	n.s.	* (-)	n.s.
	DPD	✓		n.s.	n.s.	n.s.	n.s.	n.s.	n.s.	n.s.	n.s.	n.s.	n.s.
	Emer	1LR		n.s.	n.s.	n.s.	n.s.	n.s.	n.s.	n.s.	n.s.	n.s.	n.s.
		PR		n.s.	n.s.	n.s.	n.s.	n.s.	n.s.	n.s.	n.s.	n.s.	n.s.
	ERate		ER	/	/	n.s.	n.s.	n.s.	n.s.	n.s.	n.s.	n.s.	n.s.
		PR		n.s.	n.s.	** (-)	n.s.	n.s.	n.s.	n.s.	n.s.	n.s.	n.s.
			PR	/	/	*** (-)	n.s.	n.s.	n.s.	n.s.	n.s.	n.s.	n.s.
			SR1	/	/	n.s.	n.s.	n.s.	n.s.	* (+)	n.s.	n.s.	n.s.
	Length		PR	/	/	** (-)	n.s.	n.s.	n.s.	n.s.	n.s.	n.s.	n.s.
			SR1	/	/	n.s.	n.s.	n.s.	n.s.	n.s.	n.s.	n.s.	n.s.
	ARL		✓	/	/	n.s.	n.s.	n.s.	n.s.	n.s.	n.s.	n.s.	n.s.
	MRL	@8 DAS		n.s.	n.s.	n.s.	n.s.	n.s.	n.s.	n.s.	n.s.	n.s.	n.s.
	TRL		✓	/	/	* (-)	n.s.	n.s.	n.s.	n.s.	n.s.	n.s.	n.s.
Production	***LRD***	✓		n.s.	n.s.	n.s.	n.s.	n.s.	n.s.	n.s.	n.s.	n.s.	n.s.
	Nb	ER		n.s.	n.s.	n.s.	n.s.	n.s.	n.s.	n.s.	n.s.	n.s.	n.s.
			ER	/	/	n.s.	n.s.	n.s.	n.s.	n.s.	n.s.	n.s.	n.s.
			SR1	/	/	n.s.	n.s.	n.s.	n.s.	n.s.	n.s.	n.s.	n.s.
Tropism	***SRA***		ER	/	/	*** (-)	* (-)	n.s.	*** (-)	* (-)	n.s.	n.s.	* (-)
		SR1		n.s.	n.s.	n.s.	n.s.	n.s.	n.s.	n.s.	n.s.	n.s.	*
			SR1	/	/	*** (-)	** (-)	n.s.	*** (-)	* (-)	n.s.	n.s.	** (-)
	Theta		PR	/	/	*** (+)	n.s.	*** (-)	*** (-)	*** (-)	n.s.	n.s.	n.s.
			SR1	/	/	*** (-)	** (-)	n.s.	*** (-)	** (-)	n.s.	n.s.	** (-)
	CH		✓	/	/	n.s.	n.s.	n.s.	n.s.	n.s.	n.s.	n.s.	n.s.

It is worth noting that SUBLIM, ARLEQUIN, ATHLON, OREGRAIN and SY MATTIS are genetically closed because they are all offspring of the bread wheat genotype APACHE (Y. Mannes, personal communication). Moreover, the hybrids SUBLIM/ATHLON, SY 117071/ARLEQUIN and SUBLIM/OREGRAIN are all genotypes that have been proved to be performant on field trials under stressed conditions (Y. Mannes, personal communication). This suggests that hybrids tending to invest more in their shoots in the early stages of life (as SUBLIM/ATHLON and SY 117071/ARLEQUIN) or having a steep root system (as SUBLIM/OREGRAIN) would better perform under stressed field conditions at latter stages. However, the fact that other hybrids displayed similar features

but were not recorded as performant under stress suggests that these features may not, by themselves, lead to superior performance.

3.3.2.3. GENETIC CORRELATIONS WITHIN PLATFORMS

Many genetic correlations emerged between the traits estimated within the same platform trial and this observation is verified for both panels (Figure 16 – A: bread wheat panel; Figure 16 – B: durum wheat panel).

Within the RootPhAir experiment:

- ***RMass*** (both fresh and dry) is highly positively correlated with ***SMass*** (both fresh and dry), which means that if one of these two trait increases, both will do (for both species). Interestingly, the R/S_{Dry} is positively correlated with $RMass_{Dry}$ only, indicating that R/S_{Dry} increases are the results of an increase of $RMass_{Dry}$ more than of a decrease of $SMass_{Dry}$. Slightly positive correlations are seen between biomass and diameter traits (e.g., $Diam_{ER}$) and stronger ones between biomass and $ERate_{PR}$, ***MRL*** and even Nb_{ER}. Negative ones are also seen between biomass and emergence traits (e.g., $Emer_{PR}$). These positive and negative correlations are not surprising since all these traits have a direct influence on root biomass.
- A strong correlation is seen between the $ERate_{PR}$ and the ***MRL*** which is quite evident. $ERate_{PR}$ and the $Diam_{ER}$, are closely linked, which fits with the fact that larger diameters confer higher root growth potential (Pagès, 1995). $Diam_{All}$ and $Diam_{LR}$ are also closely correlated, which is also not surprising, since the $Diam_{All}$ gather the diameters all root types confounded and that the lateral roots are the most represented root type (the number of embryonic roots never exceeding 7 roots and the number of lateral roots generally exceeding 100 roots per plant).
- The ***LRD*** is positively correlated with the ***DPD*** (durum wheat only) and the $Emer_{1LR}$. This result suggests that lateral roots initiated at higher densities would develop more slowly, which may reflect some degree of competition for assimilates between initiated lateral root primordia. The ***LRD*** is also negatively correlated with the Nb_{ER} which suggests that plants having fewer Nb_{ER} are able to initiate lateral roots at higher density on the remaining embryonic roots. The ***DPD*** is negatively correlated with $ERate_{PR}$ for both species, suggesting that faster growth of the primary root implies that lateral roots will appear more quickly. The ***DPD*** is also slightly

positively correlated with the ***Diam$_{ER}$*** (bread wheat only) which makes sense since the thicker the root is, the more time for the lateral root to emerge from the root tissues is needed.

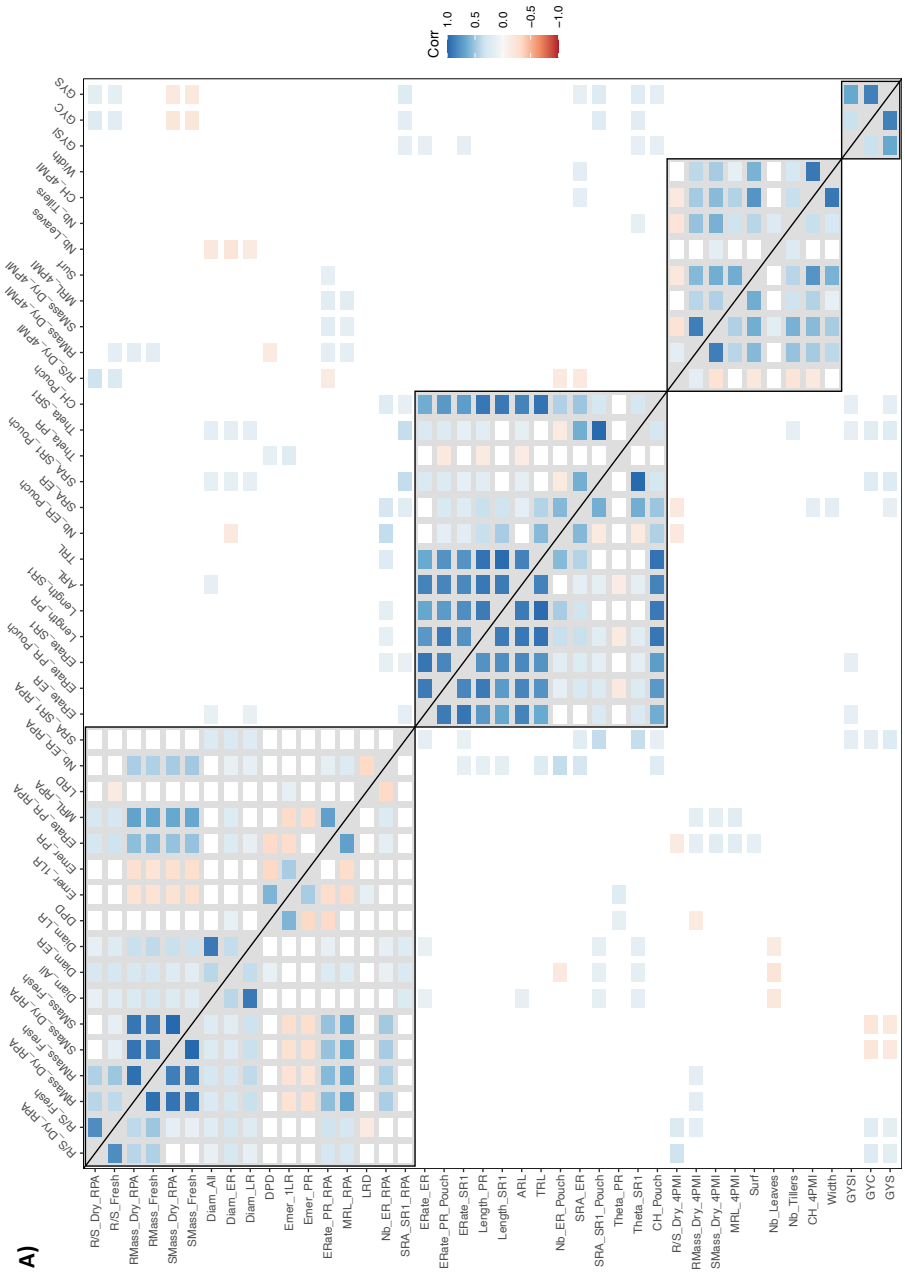
- The ***SRA$_{SR1}$*** seems in general relatively independent from most traits estimated in this RootPhAir experiment except the ***Diam*** traits (for both species). Indeed, slight positive correlations were found between the ***SRA$_{SR1}$*** and the ***Diam$_{ER}$*** but also with the ***LRD*** (durum wheat only) suggesting that the root systems having thicker embryonic roots, or with a higher density of lateral roots, tend to have wider amplitude between their first pair of seminal roots.

All these observations are confirmed for both wheat species (unless stated).

Within the Pouch experiment and for both species, strong positive correlations are excepted and observed between all traits of the elongation category (e.g., ***ERate***, ***Length***, ***ARL***, ***TRL***) and also with the ***CH***. The ***Nb$_{ER}$*** tends to be slightly negatively correlated with the ***SRA$_{SR1}$*** indicating that a genotype having more seminal roots will also have a narrower amplitude between its first pair of seminal roots, but a wider amplitude between the extreme roots (positive correlation between ***Nb$_{ER}$*** and ***SRA$_{ER}$***).

Within the 4PMI experiment, where a combined W and N stress was applied, ***R/S$_{Dry}$*** is positively correlated with ***RMass$_{Dry}$***. This suggests that for both species under stressed conditions, the increase of ***R/S$_{Dry}$*** is mainly due to as increase of ***RMass$_{Dry}$***. In the case of bread wheat, ***SMass$_{Dry}$*** also tend to slightly decrease as the ***R/S$_{Dry}$*** increases, since a negative correlation is seen between both last traits. Most of the traits are positively correlated together (except the ***R/S$_{Dry}$***) indicating that the traits of the elongation category (e.g., ***MRL***, ***Surf***), the production category (e.g., ***Nb$_{Leaves}$***, ***Nb$_{Tillers}$***) and the tropism category (e.g., ***CH***, ***Width***) seem to increase together. This suggests that, under stress, when a plant is able to have large shoot parts, it will also have large root parts.

The traits measured in the field show positive correlations between the ***GYSI*** and ***GYC*** and a more pronounced one between ***GYSI*** and ***GYS***. No correlations were found between the yield-related traits and the ***AMF*** percentage of the durum wheat panel.


Corr
1.0
0.5
0.0
−0.5
−1.0
A)
R/S_Dry_RPA
R/S_Fresh
RMass_Dry_RPA
RMass_Fresh
SMass_Dry_RPA
SMass_Fresh
Diam_All
Diam_ER
Diam_LR
DPD
Emer_1LR
Emer_PR
ERate_PR_RPA
MRL_RPA
LRD
Nb_ER_RPA
SRA_SR1_RPA
ERate_ER
ERate_PR_Pouch
ERate_SR1
Length_PR
Length_SR1
ARL
TRL
Nb_ER_Pouch
SRA_ER
SRA_SR1_Pouch
Theta_PR
Theta_SR1
CH_Pouch
R/S_Dry_4PMI
RMass_Dry_4PMI
SMass_Dry_4PMI
MRL_4PMI
Surf
Nb_Leaves
Nb_Tillers
CH_4PMI
Width
GYSI
GYC
GYS

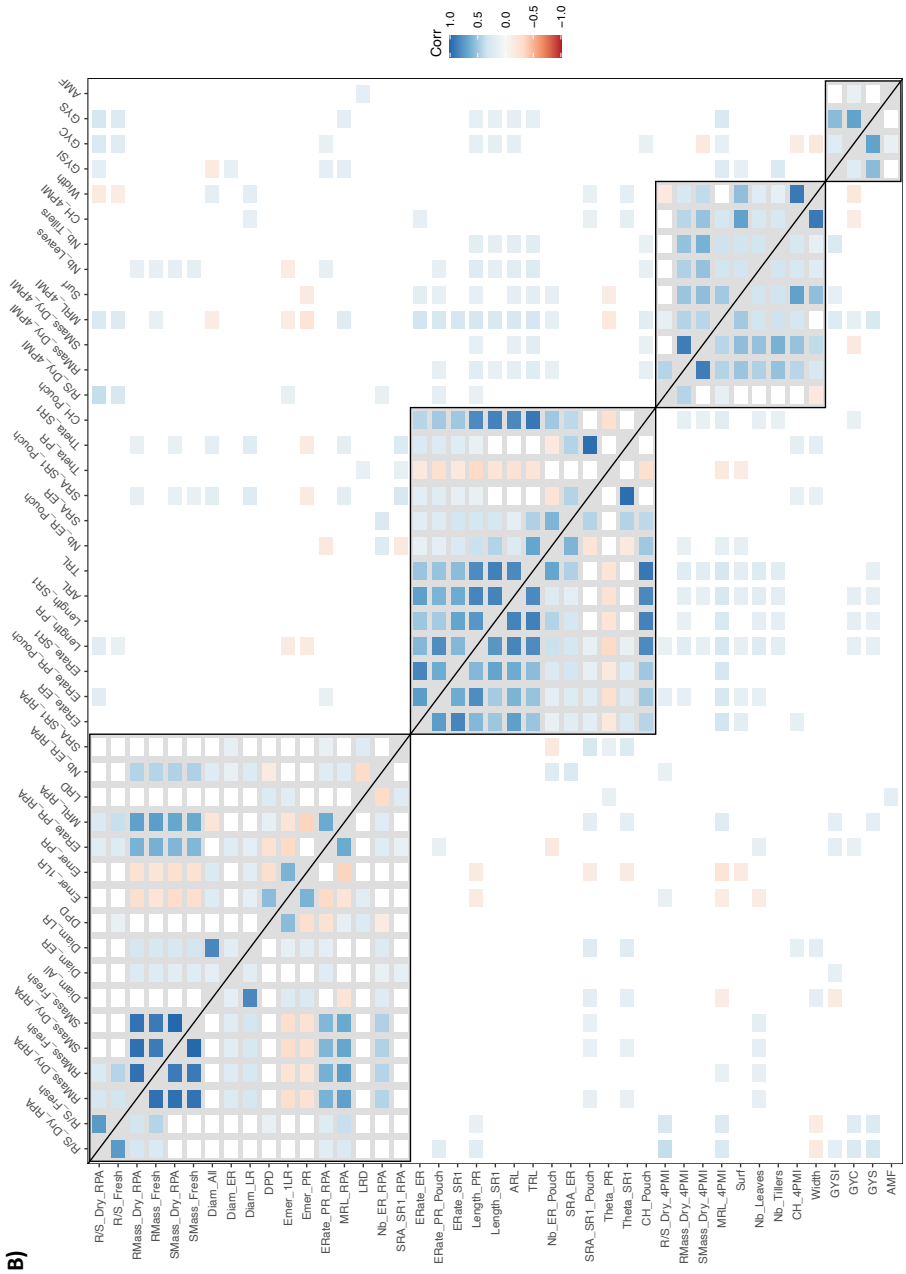


Figure 16 (from previous page). Genetic correlation matrices between phenotyping traits (platform and field traits): ***A)*** *Bread wheat panel, pval < 0.05;* ***B)*** *Durum wheat panel, pval < 0.05. The traits have been classified per experiment. Each surrounding black rectangle represents one experiment, from top left to bottom right: RootPhAir (RPA), Pouch, 4PMI and field trials.*

3.3.3. ENVIRONMENTAL IMPACTS

3.3.3.1. CONSISTENCY BETWEEN PLATFORMS (CORRELATIONS AND HERITABILITIES)

A principal component analysis was carried out with all platform and field traits and showed that most of the dimensions could be distinctly attributed to one of these experiments (Figure 17 & Figure 18).

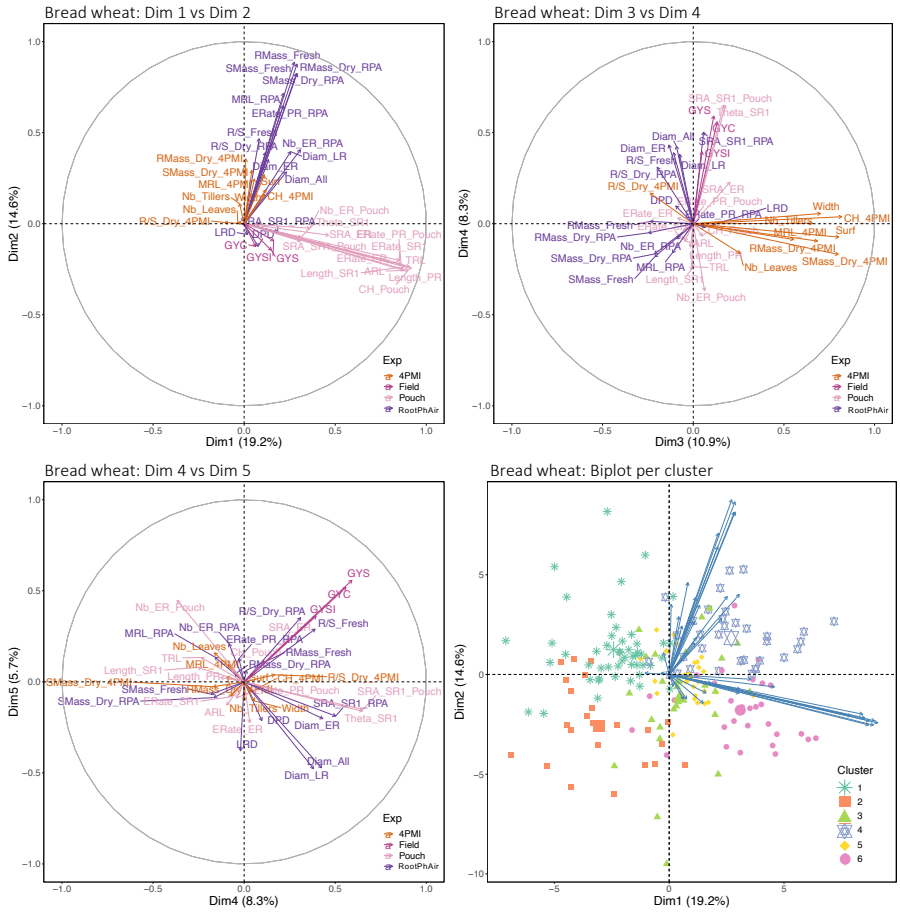


Figure 17. Principal component analysis carried out for the bread wheat panel for the traits measured in the three platforms (RootPhAir, Pouch and 4PMI) and the field trials (from top-left to bottom-right: Dim 1 vs Dim 2, Dim 3 vs Dim 4, Dim 4 vs Dim 5 and biplot). The colours correspond to the experiments for the first three graphics, and to the respective clustering groups for the last graphic (section 3.3.1.3).

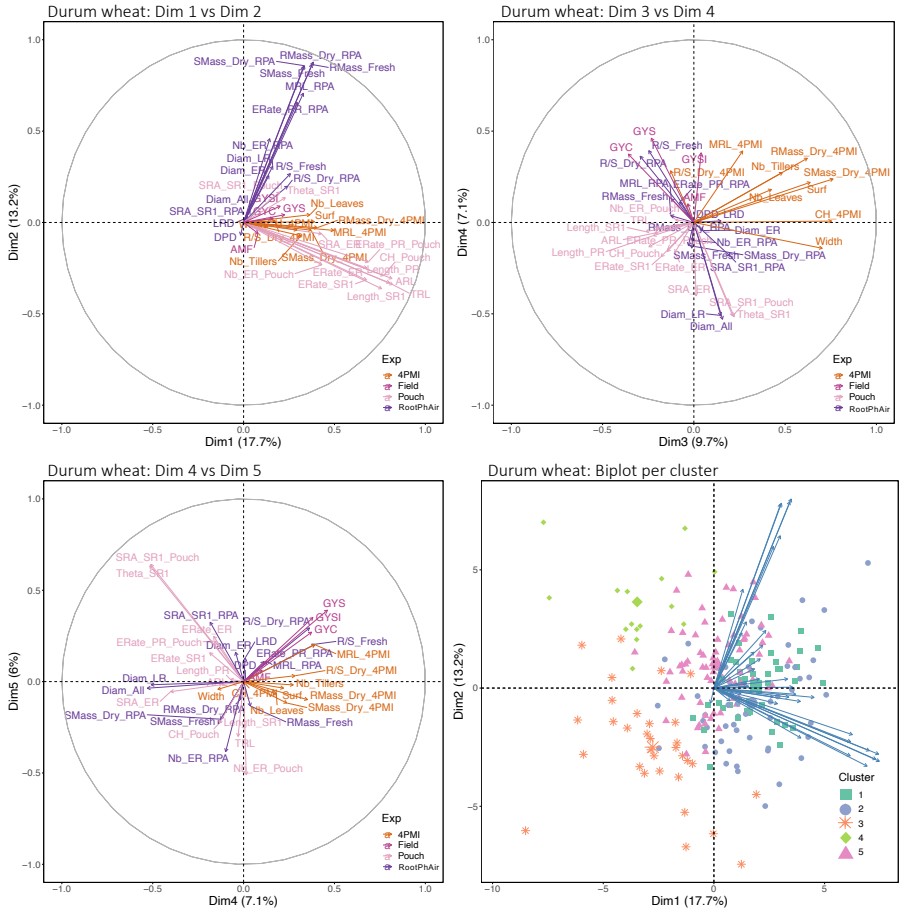


Figure 18. Principal component analysis carried out for the durum wheat panel for the traits measured in the three platforms (RootPhAir, Pouch and 4PMI) and the field (from top-left to bottom-right: Dim 1 vs Dim 2, Dim 3 vs Dim 4, Dim 4 vs Dim 5 and biplot). The colours correspond to the experiments for the first three graphics, and to the respective clustering groups for the last graphic section 3.3.1.3).

The first dimension accounts for most of the traits of the Pouch experiment (accounting for 19.2% or 17.7% of the variability for bread wheat and durum wheat panel respectively) while the second dimension is dominated by most of the traits of the RootPhAir experiment (explaining 14.6% or 13.2% of the variability observed for bread wheat and durum wheat panel respectively). The third dimension seems to be dominated by the traits of the 4PMI experiment and finally the fourth dimension by the field traits (Figure 17 & Figure 18). These patterns are confirmed for both wheat species (Figure 17: bread wheat; Figure 18: durum wheat).

The fact that each experiment seems to be associated to one different dimension suggests that the genotype by environment interactions are much larger than the average genotypic effect and, accordingly, that genotypic differences seem to be largely environment specific. This observation is confirmed by the low number of correlations found between traits estimated in different platforms (Figure 16). Indeed, in contrast to the multiple genetic correlations found between traits measured within the same platform, those found between different platforms are less numerous. This trend is seen for both panels but more pronounced for bread wheat (Figure 16 – A: bread wheat panel; Figure 16 – B: durum wheat panel).

The RootPhAir and Pouch trials were conducted under controlled conditions but with different growing environments. Corresponding traits measured in both experiments are positively correlated as for the $ERate_{PR}$ (durum wheat only), the Nb_{ER}, and the SRA_{SR1} (Figure 16). Some other plausible correlations are found for the durum wheat panel, e.g., the $Length_{PR}$ is negatively correlated with the $Emer_{PR}$ traits but positively with the R/S traits which seem to be logical. As already seen within the Pouch experiment, the Pouch Nb_{ER} is negatively correlated (durum wheat only) with the SRA_{SR1} of RootPhAir, which suggests that plants having more embryonic roots would also have a narrower amplitude between the first pair of seminal roots.

Some excepted correlations are seen between corresponding traits measured in both RootPhAir and 4PMI platforms such as R/S_{Dry}, $RMass_{Dry}$ (bread wheat only) and MRL. But for the rest of the traits very few correlations are seen between these two platforms where both conditions (controlled vs stressed) and environment (3D substrate-free of aeroponics vs 2D Rhizotubes) are completely different.

Finally, the Pouch and 4PMI experiments were both performed in a 2D device, but a combined stress was applied in the 4PMI trial. Almost no correlations were found between the two platforms for the bread wheat panel, in contrast to the many logical correlations seen for the durum wheat panel (e.g., MRL of 4PMI with $ERate_{PR}$ and $Length_{PR}$ of Pouch, or $RMass_{Dry}$ of 4PMI with ARL and TRL of Pouch). This suggests that the stress conditions may have induced a greater impact on the bread wheat panel and that the plasticity of the traits was expressed to a greater extent, leading to almost no correlations.

3.3.3.2. CORRELATIONS BETWEEN PLATFORM TRAITS AND YIELD-RELATED TRAITS

Over the 7 field trials, the bread wheat panel showed mean genotypic yield values ranging from 4.8 t/ha to 8.3 t/ha with a population mean of 7.0 t/ha in the control treatment, and from 3.8 t/ha to 6.2 t/ha with a population mean of 5.3 t/ha under combined stressed conditions. The impact of the stress for the bread wheat panel in the field was therefore clear (2.0 t/ha) and not exaggerated.

For the durum wheat panel, the impact of the stress was less clear. Indeed, the mean genotypic yield under controlled conditions ranged from 3.3 t/ha to 8.5 t/ha with a population mean of 5.8 t/ha while, under stressed conditions, the range was from 3.0 t/ha to 7.5 t/ha with a mean value of 5.5 t/ha.

Correlations between yield-related traits and platform traits are shown in Figure 16. Even if few significative results were found, some expected and unexpected weak correlations appeared and will be discussed in relation to the root ideotypes found in the literature. These relationships should be treated with caution as very different stages, traits and growing conditions are being compared.

a) BREAD WHEAT

For the bread wheat panel, positive correlations were observed between the ***R/S*** measured in RootPhAir and the grain yield under both controlled and stressed conditions (***GYC***, ***GYS***). This suggests that, in the early stages of development, plants investing more in roots (increased ***R/S***) would have a higher grain yield in the later stages under both conditions. These positive correlations were expected especially for ***GYS*** since it is well known that, under water or nitrogen limited conditions, genotypes investing in steep and deep roots are more likely to reach these mobile resources in soil depths and so to better withstand these unfavourable environments (Manschadi *et al.*, 2010; Lynch, 2013, 2019; Richard *et al.*, 2015). Surprisingly, no correlation was found between the yield sensitivity index ***GYSI*** and ***R/S*** of RootPhAir, which suggests that the beneficial effect of early ***R/S*** is observed constitutively in controlled and stressed conditions and does not contribute to improved response to the stressed condition. We have seen before that an increase of the ***R/S*** in RootPhAir was linked with an increase of ***RMass*** more than a decrease of ***SMass***. Surprisingly, no correlations were found between ***RMass***

and ***GYC*** or ***GYS*** and negative ones were observed for the ***SMass*** with ***GYC*** and ***GYS***. These correlations are, clearly, difficult to interpret.

For the 4PMI experiment, where a combined W and N stress was applied, correlations of platform ***R/S*** and ***GYS*** or ***GYSI*** were expected. Surprisingly, no correlations were found between none of the yield related traits and the traits estimated within the 4PMI experiment.

A positive correlation was found between the mean yield under both conditions (***GYC*** and ***GYS***) and the SRA_{SR1} evaluated in RootPhAir and Pouch experiments. The same positive correlation was found with the ***GYSI*** but only for the SRA_{SR1} of RootPhAir and the ***CH*** and $Theta_{SR1}$ of Pouch. This suggests that a plant having seminal roots developing more horizontally and allowing a larger aera of the soil to be explored at early stages, would have a higher grain yield in latter stages. This finding goes against the "steep-cheap-deep" root ideotype hypothesis that a plant with a steeper root development would achieve better performance under stress. However, it supports the "topsoil-foraging" ideotype that enhances phosphorus absorption since phosphorus is a highly immobile macronutrient mainly located in the topsoil. It could be that the latter ideotype is a fruitful strategy to cope with co-occurring water and nitrogen stresses, as experienced in the field trials. It was also suggested by Lynch (2019) that this last strategy might allow the plants to maximize their exploration of the soil and have access to all mobile and immobile resources across the whole profile.

The last correlation observed is a positive one between the $ERate_{ER}$ and $ERate_{SR1}$ of the Pouch experiment with the ***GYSI***. This result seems in line with the larger soil exploration hypotheses as plants having embryonic roots growing faster would explore faster diverse soil areas and could therefore be more tolerant to future stressed conditions (increased ***GYSI***).

b) DURUM WHEAT

A larger number of correlations have been observed for durum wheat compared to bread wheat. The same positive correlations were found between the ***R/S*** of RootPhAir with ***GYC*** and ***GYS***, but also with the ***GYSI***, suggesting that plants investing more in their roots, at early stages would be more performant in the field latter on, and would also be more tolerant to stressed conditions. The ***MRL*** (for both RootPhAir and 4PMI), the $ERate_{PR}$ of RootPhAir and the ***Surf*** of 4PMI are all positively correlated with ***GYSI***,

supporting that root systems exploring a larger soil area but also in depth, would better withstand combined stressed conditions (Palta *et al.*, 2011). This result is in line with the root "steep-cheap-deep" ideotype hypothesis as well as with the "top-soil foraging" ideotype (Lynch, 2013).

Plants that are more resilient to stress conditions seem to have in general thinner roots all types confounded (***Diam$_{All}$*** negatively correlated to ***GYSI***), but thicker embryonic roots (***Diam$_{ER}$*** positively correlated to ***GYSI***). The root type most represented in the calculation of the ***Diam$_{All}$*** are lateral roots, but their weight in the calculation also depends on the length of embryonic roots, the ***DPD*** and the ***LRD***. The negative correlation is therefore difficult to interpret and the lack of correlation between ***Diam$_{LR}$*** and ***GYSI*** is not necessarily in contradiction.

Surprisingly, almost no correlations were found between the arbuscular mycorrhizal fungi (***AMF***) colonisation and the platform traits or the yield-related traits. Yet it has been demonstrated that ***AMF*** strongly influence root characteristics (e.g., root biomass, root length, root volume, root branching and root diameters) but also improve nutrient capture of plants under stressed conditions (Sheng *et al.*, 2009; Chun-Yan Liu, A. K. Srivastava and Qiang-Sheng Wu, 2013; Xia *et al.*, 2020), and so more correlations were expected. The only slight correlation observed between ***AMF*** and platform traits was with ***LRD***, which may indicate that an increased probability of contact between roots and ***AMF***, or a larger number of branching points, actually promotes ***AMF*** colonisation.

3.4. DISCUSSION

3.4.1. MAIN MESSAGES

Phenotyping experiments of two large diversity panels of bread wheat and durum wheat have been performed in three singular platforms (RootPhAir, Pouch and 4PMI) leading to the characterisation of 45 phenotypic variables classified into four categories: biomass, elongation, production, or tropism. Even if the variables were relatively different across platforms, some trends could be identified.

Important genetic variabilities (CV_g) have been recorded for all traits but especially those in the tropism category (e.g., ***SRA***, ***CH***). The H^2 values were

variable but with a range going from moderate to high values. The RootPhAir experiment conducted in mechanically unconstrained aeroponics environment was the one showing the lowest CV_g and H^2 in comparison of the Pouch and Rhizotubes experiments.

Correlations dominated between variables of the same platforms and were scarce between variables of different platform, supporting the hypothesis that the genetic differences for root morphology could be largely environment specific.

Similar results were obtained for bread wheat and durum wheat in platform experiments. However, when the results from the different phenotyping platforms were pooled, the cluster groups that appeared to perform better under combined N and W stress showed very distinct root characteristics between the two species (discussed below in section 3.4.4).

3.4.2. NEW PROCESS VARIABLES VS INTEGRATIVE VARIABLES

The method developed in Chapter 2 combined with the unique conditions of the RootPhAir platform made it possible to estimate process variables related to root development processes and dynamics, namely the ***DPD***, ***LRD, Diam*** and ***ERate***. We expected variables that are closer to the development and growth mechanisms, but these new traits turned out to have had relatively small or equivalent H^2 compared to integrative variables, more widely estimated (Table 7).

First, the ***DPD***, which is defined as the time needed between the initiation and the emergence of a lateral root, is one of the traits showing the lowest genetic variability and heritability (Table 7). To our knowledge, this trait has never been estimated in other experiments on such large panels and, particularly, with wheat. The ***DPD*** can be defined as the equivalent of the length of apical unbranched zone (length of apical unbranched zone = ***ERate*** * ***DPD***) in the time domain. The length of apical unbranched zone is a well-known root characteristic that has been proven to be a good indicator of root growth in many species as banana (Lecompte, Ozier-Lafontaine and Pagès, 2001), maize (Pellerin and Pagès, 1994; Pellerin and Tabourel, 1995; Pagès *et al.*, 2010) or pea (Tricot, Crozat and Pellerin, 1997). It has been shown in Chapter 2 that the ***DPD*** is a constant parameter for a given plant, and this observation reinforces the positive relationship between the length of apical unbranched

zone and the root growth (section 2.2.6.4). The negative correlation found in our study between the ***DPD*** and the ***ERate$_{PR}$*** for both species suggests that genotypes having a faster primary root growth would also have a shorter time between the initiation and the emergence of a lateral root (at least their first growing lateral root, since ***DPD*** was computed on the newly emerging lateral root closest to the parent root tip).

The ***LRD*** is also a trait that is not often estimated in phenotyping experiments with such large panels and throughput. It was shown in Chapter 2 that the estimation of the branching density remains a complex task to be achieved because the local variability of this traits does not allow manual counting to be representative of the global density (cf. also Muller and Hong, unpublished). In maize, it has also been proven that the ***LRD*** varies according to the root diameter (larger diameter having higher densities) (Wu, Pagès and Wu, 2016). This is why ***LRD*** was estimated as a general lateral root production potential per genotype (Chapter 2, section 2.2.6.5). Unexpectedly, the values of H^2 remained quite low (Table 7, bread wheat ~25% and durum wheat ~39%) but were in the same magnitude as the ***LRD*** heritability estimated in hydroponics for bread wheat (25%) by Guo *et al.* (2021), in line with the fact that lateral root formation is highly influenced by the environment. The negative correlation between the ***LRD*** and the ***Nb$_{ER}$*** suggests that a higher share of assimilates for an embryonic root enables a greater lateral root production (***LRD***) which is in line with source-sink considerations (Bingham and Stevenson, 1993; Lynch, 2013; Guo *et al.*, 2021).

The ***Diam*** traits per root types, rarely found in the literature, were evaluated thanks to typical analysis pipeline developed in RootPhAir since the categorisation in the different root types was made based on the entire tip population. The H^2 values found were moderate but in line with the H^2 found for bread wheat grown in hydroponics (53%) in Guo *et al.*, (2021). Also, a positive correlation was found between the ***Diam$_{ER}$*** and the ***ERate$_{PR}$*** which confirms the relationships between root growth potential and root diameter (Cahn, Zobel and Bouldin, 1989; Pagès, 1995).

In view of the results of Chapter 2 (section 2.2.6.3), the ***ERate$_{PR}$*** was assessed to be generally constant for a given plant. This linearity has already been observed for the growth of axile roots in maize (Hund, Trachsel and Stamp, 2009) and also between the root length and the accumulated thermal time of

wheat grown in the field (Barraclough and Leigh, 1984). In terms of correlation, the ***ERate$_{PR}$*** was positively correlated with the ***MRL***, the ***RMass*** and ***SMass*** which suggests that plant with longer roots explore larger soil area and achieve a higher shoot biomass (***SMass***).

These process variables estimated by the pipeline in the RootPhAir platform bring new aspects of root system dynamics that are rarely approached with such large panels and throughput and that will ease the *in silico* evaluation of new genotypes by modelling approaches. Their H^2 values are moderate, but the relative effects of the intrinsic variability of these variables (Muller *et al.*, 2019) and of the mechanically unconstrained aeroponics environment of RootPhAir (cf. following section 3.4.3) on these heritabilities remain to be assessed.

3.4.3. DISCUSSION ON PLATFORMS HERITABILITIES

One of the most striking observations is that the traits measured in RootPhAir show globally lower H^2 than the traits measured in Pouch or 4PMI experiments (Table 7 & section 3.3.2.1). The origin of this clear difference will be discussed below, but the main hypothesis is that it might be due to the unique substrate-free environment of this platform.

Compared to the Pouch results, the heritabilities in RootPhAir were largely inferior. Between corresponding traits, such as ***MRL*** (H^2 ~40%) in RootPhAir and ***ARL*** (H^2 ~80%) in Pouch, the drop of H^2 was very strong (more than 40%). The most obvious difference to consider between these two experiments is a matter of time. Indeed, the plants in RootPhAir were at least 17 days old, while the plants in the Pouch were only four days old. The drop in H^2 must therefore have occurred relatively early. The effect that time has on plants can be seen as an accumulation of decisions that are continuously made during growth (e.g., the number of branching points, elongation rates, tropisms, etc.) and likely lead to increasingly diverse plant trajectories. As time elapses the heritability of some traits may therefore decrease. The differences between growing conditions in Pouches and RootPhAir may also have influenced their H^2 values. The Pouch environment could be associated to a drier environment compared to RootPhAir where roots were constantly moistened with nutritive solution. In term of mechanical impedance, the plants in RootPhAir grew in substrate-free environment and the plants in Pouch were growing in contact with the filter paper. Nevertheless, given the early stage of growth in Pouches,

we believe this mechanical effect did not have time to influence seedling growth significantly. In other words, RootPhAir can be seen here as an experiment at "advanced stage without mechanical constraint" compared to Pouch seen as an experiment at "young stage with very low constraint". Therefore, we would assume that main differences of H^2 between RootPhAir and Pouch are due to time and, to a lesser extent, to differences of root surface moisture.

Compared to the 4PMI results, RootPhAir also showed lower H^2 (e.g., H^2 of ***MRL*** were < 40% in RootPhAir and > 70% in 4PMI). These differences most likely originated in the mechanical impedance and in the low water and nitrogen conditions of 4PMI or, equivalently, in the lack of mechanical constraints in RootPhAir. It has been observed that, for root traits, genotypes tend to reveal their specificities when they are grown under stress (B. Foster, personal communication). The influence of the time is probably negligible here since both experiments have last for similar durations. Accordingly, RootPhAir would be an experiment at "advanced stage without mechanical constraint" compared to 4PMI that is seen as an experiment at "advanced stage with constraints". Accordingly, mechanical and abiotic constraints could be considered to be at the origin of the differences in heritabilities between the two platforms.

The fact that H^2 of Pouch and 4PMI were more in the same range of values (without considering the H^2 values related to the second pair of seminal roots, average H^2 of Pouch is ~80% and 4PMI ~70%) is therefore intriguing as the two platforms differ in terms of both time and constraints. We have seen before that the effects of time and constraints on H^2 are opposite. Therefore, the effects of longer time and constraints in 4PMI may have balanced one another, resulting in similar H^2 values.

An important question arises from these comparisons: is a constrained environment required, or better suited, to reveal differences between genotypes for root traits? It has been seen in the literature that genetic variances and heritabilities for yield-related, above-ground traits generally decrease when plants are exposed to stressed environments (Ceccarelli, 1989; Mathew *et al.*, 2018). We propose that paramount morphological plasticity of roots could make the question different for root morphology than the above-ground parts. The plasticity of the root system allows it to

constantly adapt to unpredictable and heterogeneous environment (Schneider and Lynch, 2020). Accordingly, a more constrained root environment would narrow the margin of plasticity that is being realised and thus lead to clearer differences between genotypes. Unfortunately, our experiment lacks a "young stage with constraint" scenario which could have been carried out for example in the RootPhAir experiment with an abiotic stress applied. It would have been appropriate to compare such environment with the others in order to confirm the hypotheses raised. Also, the new process variables estimated in RootPhAir (e.g., ***DPD***, ***ERate***, cf. previous section 3.4.2) were not measured in 4PMI and could not be used to compare the platforms.

3.4.4. CROSS-PLATFORM EXPERIMENTS OUTPERFORM SINGLE-PLATFORM EXPERIMENTS TO ACCOUNT FOR YIELD PERFORMANCE

High throughput phenotyping platforms have been developed to meet the throughput required by quantitative genetic analyses. However, variables estimated in different platforms, even if these are dedicated to the same plant organs, seem to be very different. Very low number of correlations were found in our study between variables of different platforms (section 3.3.3.1). This may mean that genotypic differences are largely environment-dependent and arise as genotype-by-environment interactions, or that the variables estimated in different platforms are highly independent. The latter does not seem plausible, because the variables in all platforms covered the same four classes of variables (biomass, elongation, production, and tropism).

If genotypic differences vary across phenotyping platforms, no platform should be better at predicting crop behaviour in the field, unless the environment of the high throughput phenotyping platforms is able to mimic the field, which seems rather unlikely. And, indeed, none of the three root phenotyping setups used here was better at predicting field observations. Nevertheless, the combination of the platforms has led to a larger set of variables in a wider set of growing conditions that, processed together in a clustering analysis, converged to define a small number of morphotypes that could be discussed in relationships with existing ideotypes. In particular, given that common root ideotypes are targeting a given single stress condition, and that they were, at least partly recognized among our clusters, our results were

useful to confront single stress ideotypes to their performance under combined stress conditions.

For bread wheat, genotypes that performed better under combined stresses displayed wide root systems, not necessarily deep, and a large investment in the roots compared to shoot parts. According to Lynch (2019), this type or root system architecture could be viewed as a compromise between the acquisition of top- and deep-soil resources. This hypothesis is aligning with the fact that bread wheat is grown in many different environments (Monneveux, Jing and Misra, 2012). On the contrary, for the durum wheat panel, the best performing group was characterised by genotypes also having a higher investment in roots compared to shoots, but with a deep root system expansion. This durum wheat cluster group matches the main characteristics of the "steep-dep-cheap" ideotype, proposed by Lynch (2013) to maximise water uptake under water limitations. Historically, durum wheat has been mainly cultivated in rainfed Mediterranean environments (Monneveux, Jing and Misra, 2012), where having deep roots to reach water resources at depth is generally considered as an asset (Hurd, 1974; O'Brien, 1979; Manske and Vlek, 2002). The fact that these characteristics would have been selected over years is confirmed by the positive evolution of the ***MRL*** estimated in both RootPhAir and 4PMI with the year of release of the durum wheat genotypes.

3.5. PERSPECTIVES BEYOND THE THESIS

- Other key field variables relative to wheat phenology, such as plant height, spike emergence date and flag leaf emergence date or condition, could have been added to enrich the field database in the analyses. These variables, whose appropriate values are crucial to ensure yield performance, could bring an additional aspect as they represent intermediate stages of plant development in the field (much before harvest) and could therefore reveal further correlations with the platform variables.
- In view of the plasticity of the traits and the fact that there is little or no correlation between the parameters estimated in the platform and in the field, it would also be important to verify that the platform traits can predict field behaviour. Indeed, this would validate our very exploratory approach to combining all the platform results that allowed us to define specific root morphotypes that are potentially more performant in the field by species. It would also be possible to bring different weights of the variables of interest (such as the yield) into this type of broad clustering approach.
- Finally, estimated heritabilities ranged from moderate to high, but unfortunately generally lower in RootPhAir compared to the other facilities. We could study and use the architectural models to identify and define more global parameters than atomic or development traits (e.g., characteristics such as a plant with deep roots and short shoots but not a specific elongation rate or angle between seminal roots) that might allow us to find higher heritabilities.

Interchapter 3-4

In the previous Chapter 3, moderate to high variabilities were revealed, suggesting that some genetic determinism could potentially be uncovered from the root traits estimated in three phenotyping platforms.

In the following Chapter 4, the genetic determinism of these traits will be investigated by genome-wide association studies (GWAS) to see whether root traits, and more specifically those related to root development processes and dynamics, are determined by a large number of regions in the genome with small effects, or whether their genetic architecture is determined by a few very strong regions in the genome. This GWAS analyses will only be performed for the bread wheat diversity panel, due to the unavailability of genomic data for the durum wheat panel.

The QTLs found in our study will be placed in a broader context on the basis of a literature review (gathering all QTLs for root traits found from 2005 to 2020 for the bread wheat species), to see, for example, whether they were found on the same chromosomes as QTLs of related traits, classified in the same trait category (e.g., Elongation, Branching, Length, etc.).

Chapter 4.

Root Phenotype Descriptors Close to Growth and Development Do Not Have Simpler Genetic Architecture than Shape Descriptors

4.1. INTRODUCTION

The advances in genetics and genomics coupled with the development of high throughput phenotyping technologies has streamlined the realisation of genome wide association studies (GWAS) to analyse the genetic architecture of complex traits (Kuijken *et al.*, 2015; Watt *et al.*, 2020; Saint Cast *et al.*, 2022). This evolution, combined with the development of genomic selection for quantitative traits, is likely to foster the genetic improvement of root morphology that is at the heart of water and nutrient uptake (Tuberosa *et al.*, 2003; de Dorlodot *et al.*, 2007; Sanguineti *et al.*, 2007; Kuijken *et al.*, 2015).

Obtaining accurate root morphological data at high throughput, however, remains a difficult venture and the variables that are ultimately analysed are generally highly integrative, e.g., total number of roots, convex hull, or biomass. One may expect that the genetic architecture of these traits comprises a larger number of contributing loci with more diluted effects than phenotypic variables that would closely approach the biological processes which generate root system architecture, such as growth, branching and tropisms (de Dorlodot *et al.*, 2007; Passot *et al.*, 2019; Freschet *et al.*, 2020; Tracy *et al.*, 2020). However, it has been recently reviewed that growth and development processes display an important intrinsic variability (Muller *et al.*, 2019) which should, in principle, blur the effects of individual loci on the root phenotype.

Linking biological processes to integrative variables has become increasingly natural with the advent of functional structural plant models (Draye *et al.*, 2010; Muller and Martre, 2019; Tracy *et al.*, 2020). Indeed, functional structural plant models are designed on the basis of (eco-)physiological knowledge to simulate plant architecture from the dynamic behaviour of growth and development processes operating at the meristem level (Louarn

and Song, 2020; Tracy *et al.*, 2020). In the case of root system architecture, these models have been used in synergy with phenotyping and genetics to elaborate root ideotypes with desired performance in given environmental scenarios (Lynch *et al.*, 1996; Postma, Jaramillo and Lynch, 2008; Lynch, 2013). Using model parameters as descriptors of the root phenotype upstream of GWAS, instead of highly integrative variables, would therefore pave the way to exploit the power of modelling (e.g., linking soil and plant hydraulics with architecture) to improve our prediction of the performance of new genotypes (Passot *et al.*, 2019).

In Chapter 2, we have presented a pipeline to estimate several parameters of architectural models such as ArchiSimple (Pagès *et al.*, 2012), CRootBox (Schnepf *et al.*, 2018) or RootTyp (Pagès *et al.*, 2004) from high throughput phenotyping experiments. In Chapter 3, we have illustrated this pipeline on bread and durum wheat cases. The traits showed large genetic variability and expressed from moderate to high heritabilities. In the present study, we will characterise the genetic architecture of these new variables, with the expectation that we would find fewer but stronger QTLs than what is usually found for conventional shape descriptors.

4.2. MATERIAL AND METHODS

4.2.1. PLANT MATERIAL AND GENETIC MAPS

This study was conducted with a panel of 200 bread wheat genotypes from the Diversity panel of the BreedWheat project, initially formed by 450 genotypes selected with the aim of representing global diversity while being adapted to European growing conditions (Rincent et al., 2019). The panel embraces various geographical origins: Africa, America, Asia, Europe or Oceania (information collected from partners of the SolACE project and online resources ('GRIS', 2017; 'EU Plant variety database (v.3.4)', 2022), Annexe 1).

The 200 genotypes were genotyped on an improved Axiom array based on the TaBW420K SNP chip with the position of 98,869 markers (all data were provided by the BreedWheat European project (Colombo *et al.*, 2022)).

4.2.2. PLATFORM EXPERIMENTS

The bread wheat panel has been phenotyped in three setups, described in Chapter 3.

Firstly, a well-known pouch-like system has been used to assess the seminal root angle diversity of young seedlings. In this setup, seeds were attached with a 1% agar drop on vertical filter paper pouches. Water was able to rise by capillarity throughout the filter paper. During the 4-day experiments, images of the pouches were taken daily for the last two or three days. Growing angle, length and elongation rate were computed from root tracings performed with the SmartRoot software (Lobet, Pagès and Draye, 2011). The experiment was repeated twice, and each genotype was replicated 6 times per experiment. The calculation of the genotypic means was done by correcting the observed values by the exact height at which each seed had been set on the pouch (for more details about the exact statistical model applied, cf. Chapter 3, sections 3.2.2.2 and 3.2.4.2).

Secondly, the panel was phenotyped in the RootPhAir platform to investigate the dynamics of root development up to 20 days after germination. RootPhAir provides a substrate-free environment where plants are moistened with an intermittent spray of 50% diluted Hoagland solution (Annexe 2). Whole root system images were captured every two hours during the entire experiment. Images were fed into an analysis pipeline (described in Chapter 2) to compute commonly measured variables (maximum root length, root length per root type and root angle between pair of seminal roots), as well as variables typically used as model parameters and closely linked to the development processes of the root systems (root diameter, elongation rate, lateral root density). Finally, root and shoot biomasses were measured at harvest and their ratio was computed. The experiment was repeated two times, leading to a total of four replicates per genotype. The platform and the statistical model applied to estimate the genotypic means are detailed in Chapter 3 (sections 3.2.2.1 and 3.2.4.1).

Finally, the panel has been phenotyped in the 4PMI platform (INRAE-Dijon). Plants were cultivated during 25 days in 2D cylindrical transparent Rhizotubes (Jeudy *et al.*, 2016) (Chapter 3 section 3.2.2.3). In this experiment, plants were submitted to a combined water and nitrogen deficit that was applied by stopping irrigation three days after the start of the experiment (Annexe 3). Images of the root systems were captured daily during the entire experiment. Images of the 11^{th} day after sowing were segmented using an artificial intelligence-based solution (Salon, Jeudy and Lamboeuf, unpublished) and the height, width and convex hull surface area occupied by the root system were

computed. Root and shoot biomasses were measured at harvest and their ratio was computed. Plants were replicated four times. The exact design and the statistical model applied to calculate the genotypic means are described in Chapter 3 (sections 3.2.2.3 and 3.2.4.3).

A total of 45 platform traits were estimated for all of the three setups. The full list of variables is shown in Table 6 of the Chapter 3 (section 3.2.3).

Finally, in addition to all these platform traits, three yield-related traits estimated from various field experiments under controlled or stressed conditions, were added to the dataset. These are the average grain yield under controlled conditions (***GYC***), the average grain yield under stressed conditions (***GYS***) and also a non-parametric index expressing the grain yield sensitivity to stress (***GYSI***) (large values attributed to more stress tolerant genotypes) (for the exact construction of this index, cf. Chapter 3 section 3.2.2.4).

4.2.3. GENETIC ANALYSIS: QTLS DETECTION VIA GWAS ANALYSIS

The GWAS analysis of the platform and field traits were performed using several models currently used in the literature. A first analysis was done with the EMMAX (Efficient Mixed-Model Association eXpredited) algorithm developed in R (R Core Team, 2021). This EMMAX algorithm reduces the running time of the analyses by making some simplification assumptions as it estimates the variances components only once for the entire dataset and globally apply it to each marker (instead of repeating it for each marker) (Kang *et al.*, 2010). The 6 other models were the standard ones included in the GAPIT package in R: MLM (Mixed Linear Model), CMLM (Compressed MLM), MLMM (Multiple Loci Mixed Model), FarmCPU (Fixed And Random Model Circulating Probability Unification), BLINK (Bayesian-information and Linkage-disequilibrium Iteratively Nested Keyway) and SUPER (Settlement of MLMs Under Progressively Exclusive Relationship) (Wang and Zhang, 2021).

The significant SNPs associated to the platform traits and yield traits were determined as the union of the SNPs declared significant by any of the different models. As our aim was not to accurately identify a gene to be cloned, the threshold to define the significance of the SNPs was set at a moderate-to-restrictive p-value of minimum 10^{-5}, which is less than a Bonferroni threshold assuming independent tests (R. Rincent, personal communication).

The QTLs boundaries were defined with a method inspired from Colombo *et al.* (2022). For each trait and for each chromosome, the linkage-disequilibrium between the significant SNPs (all models combined) was performed with the "LD" function in R. The linkage-disequilibrium function gave also the R^2 value per marker pair. The clustering of the QTLs was performed based on a R^2 critical (R^2c) value that has been set as the 99th percentile of the null distribution of R^2 of 10,000 pairs of markers, randomly sampled from different chromosomes (CHR). This threshold represents a 1% risk that two markers are in linkage-disequilibrium by chance (Colombo *et al.*, 2022). If the R^2 between two pairs of SNPs was higher than the R^2c, then, these two SNPs were in high linkage-disequilibrium, potentially very close to each other, and thus were considered as belonging to the same QTL. Among all SNPs belonging to the same QTL, those with the minimum and maximum position were used to define the QTL boundaries. At last, QTLs were considered as potential co-localisations when their physical distance was less than one tenth of the total chromosome physical length as in Colombo *et al.* (2022).

4.2.4. QTLS CLASSIFICATION

Each of the QTLs detected has been assigned to one of the 18 different trait categories (Table 10 that have been designed based on a review of 59 articles from the literature, Chapter 1, section 1.6.3).

Table 10. Categories created to classify the QTLs found in this study and be able to compare them with equivalent QTLs from the same categories found in the literature.

QTL categories	Definition	Examples of traits matching the category
Angle	Traits related to the root orientation angles (e.g., angles from the vertical or angle between pair of seminal roots)	$Theta_{PR}$, $Theta_{SR2}$, SRA_{SR2}
Area	Traits related to the surface area occupied by the root system (e.g., total root surface area)	*Surf*
Branching	Traits related to root branching (e.g., forks number)	*LRD*
Depth	Traits related to root system depth (e.g., maximum root length or root plate depth	*MRL*
Diameter	Traits related to root diameters (e.g., root diameter, average root diameter)	$Diam_{ER}$, $Diam_{LR}$
Distribution	Traits related to distribution of the root system within the soil (e.g., convex hull or root length density per cm^3 of soil)	*CH*, *Width*
Elongation	Traits related to root elongation (e.g., elongation or growth rate)	$ERate_{ER}$, $ERate_{PR}$
Length	Traits related to root length (e.g., total, primary, seminal root lengths)	*Length*
NbRoot	Traits related to root number (e.g., seminal, total, or average root number)	Nb_{ER}, Nb_{SR1}, Nb_{SR2}
NbLeaves	Leaf number	Nb_{Leaves}
NbTillers	Tiller number	$Nb_{Tillers}$
R/S	Root to shoot ratios (fresh or dry)	R/S_{Dry}, R/S_{Fresh}
RHair	Traits related to root hairs (e.g., root hair density)	/
RMass	Root biomass (fresh or dry)	$RMass_{Dry}$, $RMass_{Fresh}$
SMass	Shoot biomass (fresh or dry)	$SMass_{Dry}$, $SMass_{Fresh}$
TMass	Total plant biomass (fresh or dry)	/
Volume	Traits related to root volume (e.g., total root volume)	/
Yield	Traits related to yield (e.g., grain yield)	*GYC*, *GYS*

4.3. RESULTS

4.3.1. QTLS DETECTED FOR PLATFORM AND FIELD TRAITS

A total of 171 significant SNPs have been detected by the different models: 110 for platform traits (one extra unknown positioned SNP was detected for Nb_{Leaves} but will not be included in the results) and 61 for yield-related traits. They are represented in Figure 19, which represents multiple Manhattan plots (one per variable and model) viewed from top.

From the clustering of the significant SNPs, 59 QTLs have been defined, 39 and 20 for platform and for yield-related traits respectively (Figure 19 and Table 11, Annexe 5).

With the exception of grain yield (*GYC* and *GYS*) and angle ($Theta_{SR2}$ and $Theta_{PR}$ in Pouch), QTLs were detected in small number for most of the traits. We have seen in Chapter 3 (Table 7) that platform traits showed moderate to high broad sense heritabilities (H^2). Root traits for which at least one QTL was detected showed H^2 values between 25% and 97%, which spans the whole range of heritabilities. Interestingly, root traits for which no QTLs were detected displayed H^2 between 14 and 87%. Numerous QTLs were therefore not detected preferentially for traits with large heritabilities, except for $Theta_{PR}$ and $Theta_{SR2}$ in Pouch which had very large heritabilities. We can therefore conclude that (i) contrasting genetic architectures exist between these traits, even those that have large heritabilities, and that (ii) with the exception of root angle, most traits are likely to be controlled by a large number of loci with small individual effects which fall below the detection threshold of the GWAS.

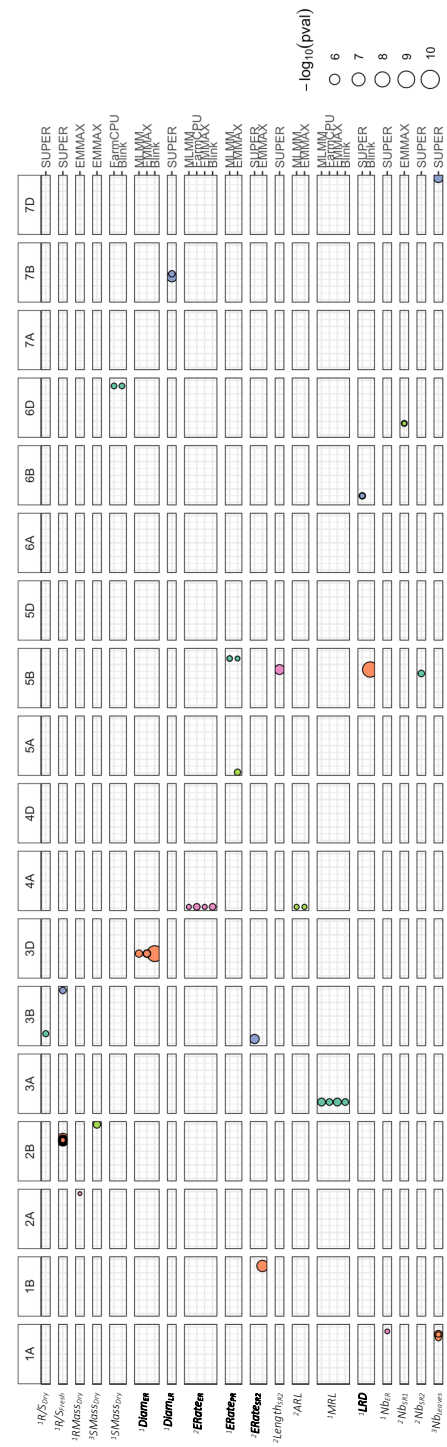


Figure 19. This representation corresponds to a Manhattan plot viewed from top with the set of all significant SNPs detected. Traits (and models) for which no QTLs were detected are not represented. In bold, all traits considered to be closely linked to root growth dynamic. Each dot corresponds to one SNP, the diameter being proportional to the -log10(pval). All SNPs belonging to the same QTL have the same colour. Five colours have been alternated to facilitate the visualisation of QTL successions. All SNP positions are relative since the widths of each chromosome have been scales from 0 to 1. One unknown positioned SNP for NB_{Leaves} was omitted (1= RootPhAir, 2= Pouch, 3= 4PMI, 4= Field, ARL = average root length, Diam = diameter, ER = embryonic roots, ERate = elongation rate, GYC = grain yield under controlled conditions, GYS = grain yield under stressed conditions, Length = root length, LR = lateral root, LRD = lateral root density, MRL = maximum root length, Nb = number, PR = primary root, R/S = root to shoot ratio, RMass = root biomass,, SMass = shoot biomass, SR1 = first pair of seminal roots, SR2 = second pair of seminal roots, SRA = seminal root angle, Theta = root angle from vertical).

Root category	Experiment	Trait	QTL number	Names of the QTL	CHR	Most significant SNP	Model detecting the most significant SNP	Models detecting the other SNPs	BP	pval	-log10(pval)	Lower BP	Higher BP	Nb SNP in the QTL	Effect
R/S	RootPhAir	$^{1}R/S_{DRY}$	1	QTL_R/SDry_3B	3B	cfn1974830	SUPER	/	14682885 10	7.76E-06	5.11	14682885 10	14682885 10	1	/
	RootPhAir	$^{1}R/S_{FRESH}$	2	QTL_R/SFresh_2B	2B	cfn1567967	SUPER	SUPER	571251128	1.32E-07	6.88	563861366	571251128	28	/
			3	QTL_R/SFresh_3B	3B	cfn0229829	SUPER	/	805258205	6.61E-06	5.18	805258205	805258205	1	/
RMass	RootPhAir	$^{1}RMASS_{DRY}$	4	QTL_RMassDry_2A	2A	cfn0378434	EMMAX	/	751553548	9.99E-06	5.00	751553548	751553548	1	/
SMass	4PMI	$^{1}SMASS_{DRY}$	5	QTL_SMassDry_2B	2B	tplb0053o16_935	EMMAX	/	79316721	5.30E-06	5.28	79316721	79316721	1	/
	RootPhAir	$^{1}SMASS_{DRY}$	6	QTL_SMassDry_6D	6D	cfn3167537	Blink, FarmCPU	/	42552380	8.35E-06	5.08	42552380	42552380	2	/
Diameter	RootPhAir	$^{1}DIAMTER$	7	QTL_DiamtER_3D	3D	cfn0374358	Blink, EMMAX, MLMM	EMMAX	25002058	3.31E-09	8.48	25002058	25002058	4	/
	RootPhAir	$^{1}DIAMTER$	8	QTL_DiamtER_7B	7B	cfn3514523	SUPER	SUPER	315910548	1.18E-06	5.93	315910548	315654909	2	/
Elongation	Pouch	$^{2}ERATEER$	9	QTL_ERateER_4A	4A	cfn0247843	Blink, FarmCPU, MLMM, EMMAX	/	18007093	6.52E-06	5.19	18007093	18007093	4	/
	RootPhAir	$^{1}ERATEEM$	10	QTL_ERatePR_5A	5A	cfn0778241	EMMAX	/	96172 82	7.14E-06	5.15	96172 82	96172 82	1	/
			11	QTL_ERatePR_5B	5B	cfn0791282	MLMM, EMMAX	MLMM, EMMAX	61195417 7	8.67E-06	5.06	61195417 7	61211333 9	6	/
	Pouch	$^{2}ERATEEM$	12	QTL_ERatePR2_1B	1B	cfn0329772	EMMAX	/	60455315 5	4.53E-07	6.34	60455315 5	60455315 5	1	/
			13	QTL_ERatePR2_3B	3B	cfn0685249	SUPER	/	66470105	2.00E-06	5.70	66470105	66470105	1	/
Length	Pouch	$^{2}LENGTHEM$	14	QTL_LengthSt2_5B	5B	cfn0361523	SUPER	/	46 78011 59	1.38E-06	5.86	46 78011 59	46 78011 59	1	/
	Pouch	^{2}ARL	15	QTL_ARL_4A	4A	cfn0247843	EMMAX, MLMM	/	18007093	9.19E-06	5.04	18007093	18007693	2	/
	RootPhAir	^{1}MRL	16	QTL_MRL_3A	3A	cfn0671417	MLMM, EMMAX, Blink, FarmCPU	/	12275454 0	4.12E-06	5.39	12275454 0	12275454 0	4	/
Branching	RootPhAir	^{1}LRD	17	QTL_LRD_5B	5B	cfn0154919	Blink	/	46 86413 56	6.79E-09	8.17	46 86413 56	46 86413 56	1	/
			18	QTL_LRD_6B	6B	cfn0264429	SUPER	SUPER	88963984	6.78E-06	5.17	88892096	88963984	2	/
NbRoot	RootPhAir	$^{1}NBTER$	19	QTL_NbTER_3A	3A	cfn0263877	SUPER	/	54 40847 86	9.55E-06	5.02	54 40847 86	54 40847 86	1	/
	Pouch	$^{2}NBSEG$	20	QTL_NbSt1_6D	6D	cfn0883079	EMMAX	EMMAX	10034613	7.91E-06	5.10	99858786	10034613	2	/
	Pouch	$^{2}NBSEG$	21	QTL_NbSR2_5B	5B	cfn0194999	SUPER	/	41683734	6.69E-06	5.17	41683734	41683734	1	/
NbLeaves	4PMI	$^{1}NBLEAVES$	22	QTL_NbLeaves_1A	1A	cfn0506233	SUPER	SUPER	51110098 07	3.92E-06	5.41	47 44406 81	51110183 2	3	/
	Pouch	$^{2}THETASEG$	23	QTL_NbLeaves_7D	7D	cfn3594533	SUPER	/	63666538 8	1.62E-06	5.79	63666538 8	63666538 8	1	/
	Pouch	$^{2}SRASEG$	24	QTL_SRASR2_4D	4D	cfn2447261	SUPER	/	42111325 3	6.53E-06	5.18	42057590 9	42111325 3	2	/
Angle	Pouch	$^{2}THETAEM$	25	QTL_ThetaPR_3A_1	1A	cfn1119723	FarmCPU	/	31531253	2.40E-07	6.62	31531253	31531253	1	0.01
			26	QTL_ThetaPR_3A_2	1A	cfn1053258	FarmCPU	/	54850 1006	3.87E-07	6.41	54850 1006	54851 0006	1	-0.01
			27	QTL_ThetaPR_3A_3	1A	cfn0500227	FarmCPU	/	52080 6631	8.98E-06	5.05	52080 6631	52080 6631	1	-0.01
			28	QTL_ThetaPR_3B_1	1B	cfn0545720	FarmCPU	/	65 12777 48	1.66E-06	5.78	65 12777 48	65 12777 48	1	-0.02
			29	QTL_ThetaPR_3B_2	1B	cfn0367316	FarmCPU	/	58 13509 23	3.94E-06	5.40	58 13509 23	58 13509 23	1	-0.01
			30	QTL_ThetaPR_2B	2B	cfn0607374	FarmCPU	/	70 81865 53	7.55E-07	6.12	70 81865 53	70 81865 53	1	0.01
			31	QTL_ThetaPR_3B	3B	cfn0215431	FarmCPU	/	50 39565 49	2.47E-06	5.61	50 39565 49	50 39565 49	1	0.01
			32	QTL_ThetaPR_5A	5A	cfn0106747	FarmCPU	/	43 95333 25	9.42E-07	6.03	43 95333 25	43 95333 25	1	-0.01
			33	QTL_ThetaPR_5B	5B	cfn2718043	Blink, FarmCPU, MLMM, EMMAX, CMLM, MLM	EMMAX, CMLM, MLM	59533552 59	1.08E-09	8.97	59533552 59	59563361 9	9	/
			34	QTL_ThetaSR2_2B_1	2B	cfn0638948	FarmCPU	/	57859597 0	1.01E-06	6.00	57859597 0	57859597 0	1	0.16
			35	QTL_ThetaSR2_2B_2	2B	cfn1597800	FarmCPU	/	71449203 8	8.11E-06	5.09	71449203 8	71449203 8	1	0.12
	Pouch	$^{2}THETASEG$	36	QTL_ThetaSR2_3A	3A	cfn1868786	Blink, MLMM, EMMAX, SUPER, MLM, CMLM, FarmCPU	/	72841919 5	4.77E-11	10.32	72841919 5	72841919 5	7	/
			37	QTL_ThetaSR2_6A_1	6A	cfn0835934	FarmCPU	/	60536016 5	5.05E-06	5.30	60536016 5	60536016 5	1	-0.06
			38	QTL_ThetaSR2_6A_2	6A	cfn2946025	SUPER	SUPER	85503884	9.96E-07	6.00	67497758	52394965	6	/
Distribution	4PMI	$^{1}WIDTH$	39	QTL_Width_3B	3B	cfn0152077	Blink, FarmCPU, EMMAX, MLMM	/	66678952 8	3.96E-06	5.40	66678952 8	66678952 8	4	/
Yield	Field	^{1}GYC	40	QTL_GYC_1A	1A	cfn0506636	SUPER	/	55174511 3	6.68E-06	5.18	55174511 3	55174511 3	1	/
			41	QTL_GYC_1B	1B	Ra_c17685_927	FarmCPU, SUPER	/	63171853 4	1.68E-06	5.77	63171853 4	63171853 4	2	-0.14
			42	QTL_GYC_2A_1	2A	cfn0132271	FarmCPU	/	76946614 5	1.58E-06	5.80	76946614 5	76946614 5	1	-0.21
			43	QTL_GYC_2A_2	2A	cfn1419842	FarmCPU	/	62956928 8	1.74E-06	5.76	62956928 8	62956928 8	1	-0.16
			44	QTL_GYC_2B_1	2B	cfn1731174	FarmCPU, SUPER, Blink	SUPER	47441611	2.21E-08	7.66	80018190 9	80018190 9	5	0.18
			45	QTL_GYC_2B_2	2B	cfn0617844	EMMAX	SUPER	80018190 9	6.38E-06	5.20	47436615	47441611	1	/
			46	QTL_GYC_4A	4A	cfn2316269	SUPER	SUPER	68542592 6	3.57E-06	5.45	68542592 6	68574257 0	3	/
			47	QTL_GYC_4D	4D	cfn2455779	FarmCPU	/	16747973	7.38E-08	7.13	16747973	16747973	1	-0.20
			48	QTL_GYC_5D	5D	cfn2823065	Blink	SUPER	11161627 0	6.20E-07	6.21	11161627 0	11437558 2	4	/
			49	QTL_GYC_6A	6A	bga0wk003057	SUPER, Blink	/	58327035 7	2.88E-06	5.54	58327035 7	58327035 7	2	/
			50	QTL_GYC_7B_1	7B	cfn3557823	FarmCPU, SUPER	SUPER	13422312 5	2.32E-07	6.63	13055047 1	13425735 1	12	0.15
			51	QTL_GYC_7B_2	7B	cfn0005566	SUPER	SUPER	72726950 2	3.95E-06	5.40	72726641 3	72726950 2	2	/
	Field	^{1}GYS	52	QTL_GYS_2B	2B	cfn1534443	Blink	/	64322414 7	2.38E-07	6.62	64322414 7	64322414 7	1	/
			53	QTL_GYS_3A	3A	cfn0670322	FarmCPU	/	6898028	7.20E-08	7.14	6898028	6898028	1	0.14
			54	QTL_GYS_4A	4A	cfn0726795	Blink, SUPER	SUPER	68170355 7	5.35E-09	8.27	68109610 4	68427400 9	13	/
			55	QTL_GYS_5A	5A	cfn0772299	FarmCPU	/	70844567 5	9.55E-06	5.02	70844567 5	70844567 5	1	-0.11
			56	QTL_GYS_7A	7A	cfn0910298	FarmCPU	/	31774759 2	2.38E-06	5.62	31774759 2	31774759 2	1	0.21
			57	QTL_GYS_7B_1	7B	cfn0933772	Blink, FarmCPU, SUPER	SUPER	88564142	5.78E-11	10.24	88564142	13424082 3	6	/
			58	QTL_GYS_7B_2	7B	cfn3446456	Blink, FarmCPU	/	73081244 7	3.16E-09	8.50	73081244 7	73081244 7	2	/
			59	QTL_GYS_7D	7D	cfn0446759	SUPER	/	55934330	5.37E-06	5.27	55934330	55934330	1	/

Table 11 (previous page). List of the QTLs found with a SNP significance threshold set at a p-value < 10^{-5} or $-\log_{10}(pval) > 5$ ([1]= RootPhAir, [2]= Pouch, [3]= 4PMI, [4]= Field, BP= base pair, CHR=chromosome, ER = embryonic root, LR = lateral root, PR = primary root, SR1 = first pair of seminal roots, SR2 = second pair of seminal roots).

It was not surprising to find a lot of QTLs for the traits in the Yield category (***GYC*** and ***GYS***) given the continued success of selection for years and the fact that the varieties used in this study were released many years ago. It is interesting to find many QTLs for root angle (9 for $Theta_{PR}$ and five for $Theta_{SR2}$). Indeed, $Theta_{PR}$ represents the absolute value of the angle of the primary root from the vertical and thus can be seen as an indication of a gravitropism bias of the primary root. Our result would indicate that this bias would be controlled by loci with large effects. The signed value of $Theta_{PR}$ was also investigated to test whether the root orientation would reflect a mechanical interaction at the root-pouch contact resulting from circumnutation. No QTLs was found for the signed $Theta_{PR}$ trait (results no showed), indicating that the $Theta_{PR}$ should be interpreted as a gravitropism bias. Concerning now the $Theta_{SR2}$, results have to be taken carefully, as mentioned in Chapter 3, since only 40% of the genotypes owned a second pair of seminal roots. No interpretation can therefore be drawn.

4.3.2. CORRELATIONS AND QTL CO-LOCATIONS FOR TRAITS SHOWING AT LEAST ONE QTL

The correlation matrix (created with just the subset of genotypes from the BreedWheat collection), is presented in Figure 20 including only the traits for which at least one QTL was detected. In addition, the number of QTL co-locations per pair of traits have been illustrated by adding a coloured square accordingly. We can see from Figure 20 that co-localising QTLs do not necessarily correspond to traits with strong genetic correlations, nor vice-versa.

The first exception concerns ***GYC*** and ***GYS*** that were highly correlated and showed three co-localising QTLs. This suggests, in the first place, that genotypes that tend to have a high grain yield under controlled conditions are likely to also have a great yield under stressed conditions. In a second stage, it also suggests that these two traits are, at least in part, controlled by similar genome regions. The second exception is a region on CHR 5B where one QTL for $Length_{SR2}$ co-localises with QTLs for ***LRD*** and Nb_{SR2}. This region would influence the number roots in the second pair of seminal roots, their length

as well as the lateral root density. Since these traits correspond to rather different biological processes but contribute to the total root system length, it is tempting to propose that this region would influence the allocation of assimilates to the root system. Unfortunately, this hypothesis is not supported by the lack of QTLs for ***RMass*** in the same region. Again, as mentioned above, the interpretation of traits for the second pair of seminal roots must be made with caution as they were observed on a reduced number of genotypes. The third exception, with one QTL co-localisation between ***ERate$_{ER}$*** and ***ARL***, is probably artefactual since the two variables are, by nature, very similar (a large ***ARL*** at four days means logically a large ***ERate$_{ER}$***).

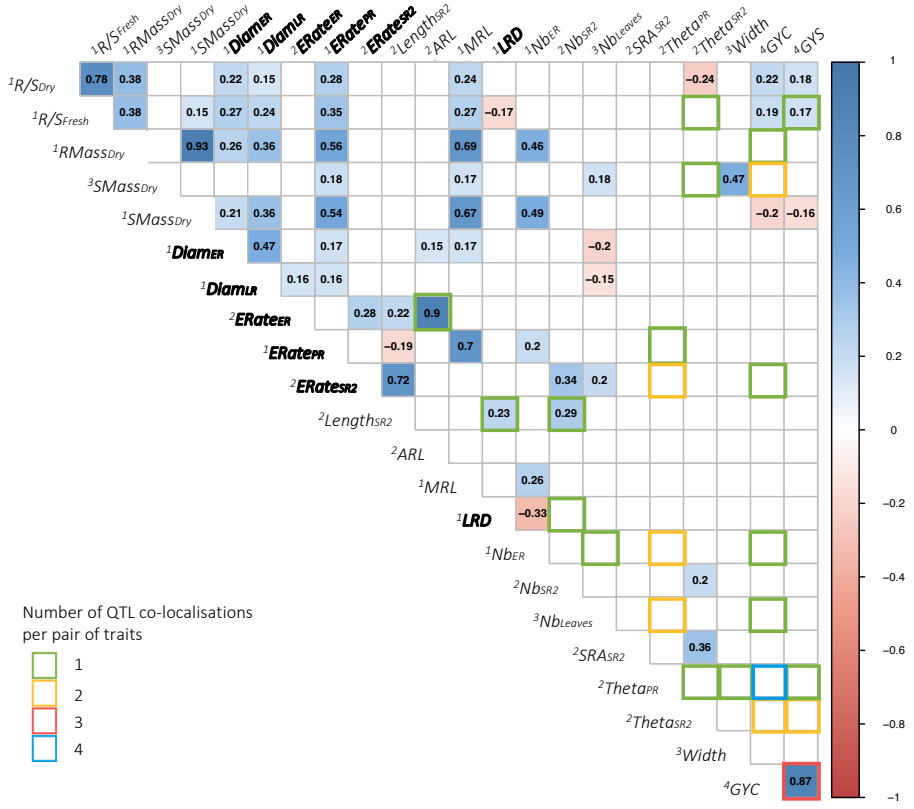


Figure 20. Matrix illustrating the genetic correlations (p-value > 0.05) and the number of QTL co-localisations found between pairs of root platform traits (bread wheat, BreedWheat collection only). Only the traits for which at least one QTL was found are present. The list of all traits is described in Table 6 of Chapter 3 (section 3.2.3). In bold, all traits considered to be closely linked to root growth dynamic. The coloured squares correspond to the number of QTL co-localisations per pair of traits ([1] = RootPhAir, [2] = Pouch, [3] = 4PMI, [4] = Field, ER = embryonic root, PR = primary root, SR1 = first pair of seminal roots, SR2 = first pair of seminal roots).

One can also note that several co-localisations occurred between QTLs for variables that are pointed as relatively independent (no or weak significant correlations seen). This is, for example, obvious between, on the one side, variables related to tropisms and directions (e.g., $Theta_{PR}$, $Theta_{SR2}$), and, on the other side, variables related to biomass (e.g., R/S_{Fresh}, $RMass_{Dry}$, $SMass_{Dry}$), elongation (e.g., $ERate_{PR}$ and $ERate_{SR2}$), root production (e.g., Nb_{ER}) and yield (*GYC* and *GYS*, cf. below, section 4.3.3).

With the exception of grain yield, these results seem to go against expectations that QTL co-localisation should parallel genetic correlations (Tuberosa *et al.*, 2002; Liu *et al.*, 2013). Nevertheless, if neighbour QTLs affecting different traits have small individual contribution to the trait variability, their co-localisation may have only a marginal contribution to the genetic correlation. On the other side, genetically correlated variables that show no co-localisations are likely to be variables controlled by a large number of loci with small individual effects that have small chances to be consistently detected.

4.3.3. CO-LOCATIONS OF QTLS FOR PLATFORM TRAITS WITH QTLS OF YIELD-RELATED TRAITS

Several co-localisations involve platform traits with yield and can be detailed from Annexe 6. A relatively large hotspot has been found at the right of CHR 2B (cf. insert Figure 22 in Annexe 6). A first cluster of R/S_{Fresh}, $Theta_{SR2}$ and *GYS* is found at the left side of the hotspot, which links grain yield under combined stress with root:shoot assimilate allocation and with the width of the root system, which does not come as a surprise but is rather interesting. The same *GYS* QTL also clusters with $Theta_{PR}$ and $Theta_{SR2}$, which further stresses a potential contribution of root angle and tropisms to crop yield under combined stress. The CHR 2B hotspot also comprises a cluster comprising *SMass* and *GYC*, which contributes to the positive correlation between *GYC* and *GYS* that was mentioned above.

Three other sites of co-localisations, on CHR 1A, 1B and 6A, link *GYC*, with the lateral expansion of the root system (Nb_{ER}, $ERate_{SR2}$ and $Theta_{SR2}$). This link has logical grounds given that irrigation and rainfall provided the crop with ample water supply and that nitrogen may have been a yield limiting factor in these trials, even in controlled conditions.

Finally, ***GYC*** and ***Theta$_{PR}$*** occurred in the clusters on CHR 1A and 1B, but are difficult to interpret given the unknown significance of a gravitropic bias of the primary root.

A last QTL cluster was found on CHR 1A, involving ***GYC***, ***Nb$_{ER}$*** and ***Nb$_{Leaves}$***. Again, this assumes that this region controlling the number of embryonics roots also controls the number of leaves and the grain yield under controlled conditions.

Nevertheless, one striking results from Figure 20 is that co-localisations between platform and yield occurred preferentially with yield in controlled conditions (12 QTLs) compared to yield under combined stress (4 QTLs) (cf. also Figure 22 in Annexe 6).

4.3.4. COMPARISON OF THE QTLS LOCATIONS FOUND WITH PREDOMINANT LOCATIONS IN THE LITERATURE FOR SIMILAR TRAITS

The QTLs detected in this study have been aligned with a survey of bread wheat QTLs from 59 root studies from 2005 to 2020 (Figure 21 & Annexe 4). The objective of this analysis was mainly to assess whether QTLs from our study tend to fall in the chromosomes where root QTLs are frequently detected. Accordingly, the alignment has been made at the chromosome scale. At this coarse level, numbers in Figure 21 cannot be considered as matches. The main difficulty in assembling this survey was the lack of consistency between descriptors used in different studies. This issue was handled by grouping variables arbitrarily in 18 trait categories that correspond to general terms commonly used in root phenotyping (Table 10). A small number of these root studies reported yield-related variables, which have been grouped in the Yield category (Chapter 1, section 1.6.3). Since all studies did not cover all categories with the same number of variables and as they used different populations, we distinguished the number of studies finding QTLs for a category in a given chromosome (Figure 21 – A), from the average number of QTLs reported by study for this category and chromosome (Figure 21 – B).

Figure 21 – A reveals a strong bias towards the RMass, Length and NbRoot categories which refer to integrative traits, relatively straightforward to measure. On the opposite, categories Elongation, Branching, RHair and Distribution are the least represented. In general, for most variables studied

in more than three studies, QTLs are detected in nearly all chromosomes with small chromosome preferences. It is only for categories with a large number of studies that QTL numbers tend to peak on certain chromosomes. Those may comprise QTLs that are polymorphic in several populations and/or whose expression is less environment-dependent and would, therefore, be more systematically detected across different studies.

Figure 21 – B, where the confounding effect of the number of studies has been removed, also indicates that, for most categories with a sufficient number of studies, QTLs tend to be evenly distributed across chromosomes, but further shows that usually less than three QTLs are reported per study and chromosome, irrespective of the number of studies. This reinforces the picture that many QTLs for root traits are environment and/or population dependent and that a large number of studies is needed to identify more constitutive or widespread QTLs. Several categories (R/S, Diameter, Area, Volume, Angle and Distribution), however tend to show a different trend with more contrasted numbers of QTLs across chromosomes. These may be characterized by a more constitutive behaviour, as for Diameter which represents a potential elongation rate (Cahn, Zobel and Bouldin, 1989; Pagès, 1995), and for Angle which, in most root phenotyping experiments, is measured at emergence, before the root is actually exposed to different conditions.

Our efforts to identify QTLs for novel variables have been rewarding as new QTLs have been detected in the Branching and Elongation categories. However, because very few QTLs had been reported before in these categories, and given the homogeneous distribution of QTLs for many traits, it was unlikely that our hits would occur in the same chromosomes as those previously reported.

However, with the exception of R/S whose QTLs landed in the chromosomes where a large number of QTLs were reported on average (Figure 21 – B), the other categories did not indicate a preference for our novel results, nor did they show a QTL enrichment of specific chromosomes.

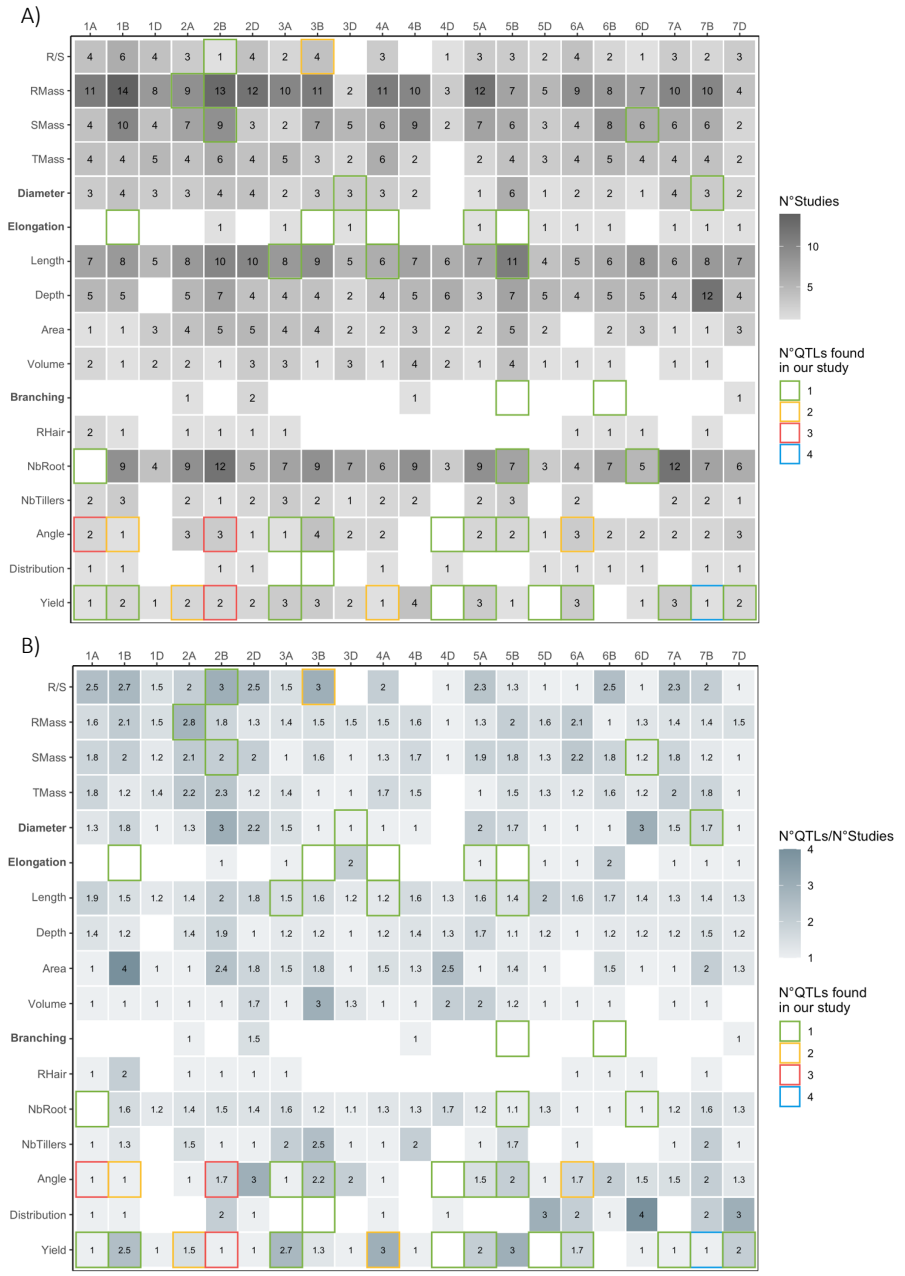


*Figure 21. Tables reviewing: **A)** the number of studies detecting QTLs on each chromosome per root trait category; **B)** the number of QTLs reported on each chromosome and category divided by the number of studies where at least one QTL was reported (for the same category and chromosome). The root categories that are on the left are described in the text, the ones in bold are the ones that are considered as associated to root growth dynamic. The coloured squares represent the number of QTLs found in this study, for the chromosome and for the root trait concerned. The number of articles reviewed is 59 and the total number of QTLs reviewed is 1700.*

4.4. DISCUSSION

We have explored the genetic architecture of several descriptors of the root morphology of bread wheat, with a focus on process variables used as parameters of root system architecture models (models which are thought to capture root growth dynamic with few variables). The GWAS results and a large QTL literature survey indicate that root traits are controlled by a large number of small effect loci distributed along the genome. It appears that increasing the number of variables and studies leads to an enrichment of QTLs on a small number of chromosomes, which suggests that some QTLs are likely to be less population- and context-dependent. However, no clear differences were found between the most commonly estimated integrative root variables and the process variables.

4.4.1. CONSEQUENCES OF MISSING CONSENSUS ON TERMS AND DESCRIPTORS

Quantitative trait loci do not always show up in genetic analyses for well-known reasons largely related to genetic background, phenotyping environment, genetic polymorphism, and experimental design. Our results indicate that, by increasing the number of studies or by grouping similar traits into categories, one is able to enrich specific chromosomes with larger number of QTL hits. Whether this enrichment can be exploited to, for example, differentiate constitutive from context-dependent QTLs will depend on our ability to demonstrate that QTLs assigned to the same chromosome are true co-localisations.

However, the situation seems to become more complicated when it comes to root traits because the phenotyping community still lacks agreements on what to measure and how. Several factors can explain this situation:

- roots are observed in very different substrates (from air to natural soils) and, in link with that, the objects of measurement can be individual roots or root segments, whole root systems or parts of root systems,
- these objects may, or may not, be identified,
- their conceptual representations are still very diverse (from biomasses to detailed architectural features),

- there are as many image analysis pipelines and resulting variables as there are studies,
- the terminology is far from being stabilized and, where it is (e.g., plant ontologies), it is generally not used.

As a consequence, aligning results from different genetic studies in order to confirm QTLs or to differentiate context-dependent QTLs remains a daunting task, despite the fact that it is the main avenue for QTL analysis.

4.4.2. QTL CO-LOCALISATION - A PROMISING TOOL TO LINK ROOT FEATURES AND CROP PERFORMANCE?

Linking root features with crop performance in different environmental scenarios is commonly achieved via modelling approaches, leading to the definition of specific characteristics of ideotypes that can be validated in the field. However, the success of ideotype breeding depends on our ability to define heritable variables that can be evaluated easily and at a high throughput. In the case of root variables, such throughput is mainly achievable in phenotyping platforms, yet these involve highly artificial environments to which the root phenotype is very sensitive. An extra step is therefore needed, which consists in linking the root phenotype in platform with the root phenotype in the field.

This extra-step may be by-passed if we are able to link the platform phenotype directly with field performance. Our results and the QTL literature survey indicate that platform traits have a complex genetic architecture with many contributing loci, potentially context-dependent. However, in Chapter 3, based on platform variables, we were able to cluster genotypes and propose ideotype-like descriptions, based on platform variables, that were interpreted with field performance. The enrichment of QTLs on a small number of chromosomes that we observed here further suggests that QTL co-localisation might also help identifying trait categories for which some reproducible QTLs are co-localising with yield QTLs – co-localisation which remains to be confirmed.

4.4.3. GENETIC ARCHITECTURE OF ROOT TRAITS

Our study was designed and conducted in a way that should deliver an important QTL detection power. This involved the recourse of a large diversity panel, the use of a large phenotypic dataset with 45 different platform traits

with reasonably large heritabilities (Chapter 3) and the combination of three complementary phenotyping setups in controlled conditions. The number of QTLs detected for the 45 platform traits (42 for root traits only) is rather low in comparison to the 100 QTLs for 13 traits (10 for root traits only) measured in a single platform (4PMI) reported by Colombo *et al.* (2022).The main differences are that they used an extended version of the same bread wheat diversity panel (comprising 450 lines instead of the 200 used in this study) and 265 additional bread wheat lines from an elite panel (thus 715 lines in total), and that plants were grown in full nitrogen and well-watered conditions. The population structure and the population size are important factors influencing the power of QTL detection (Rafalski, 2010; Kushwaha *et al.*, 2017) and it is likely that the design of their experiment influenced favourably the detection power. In addition, they used a less conservative method to define the threshold of SNPs significance based on the false-discovery rate (FDR) method, with a 30% of risk of false positive (Benjamini, 2010). We tried to relax the threshold to a similar level and we obtained roughly more than 250 QTLs, which suggests that the threshold method is the main reason for the contrasted numbers of QTLs (Annexe 7, Figure 23).

In addition to the low number of QTLs, we also found that the QTLs above the threshold had relatively large associated p-values (the $-\log_{10}$(pval) median value being 5.6 and the $-\log_{10}$(pval) maximum value being 10.3, Table 11) and were often composed of one or only few significant SNPs (median value being one SNP per QTL). This result is in line with de Dorlodot *et al.* (2007) who reported that root morphology was often found to be controlled by a series of small effect loci, also interacting with the environment. Therefore, only a powerful test would reveal them. As mentioned above, it is possible that, with a larger population, more QTLs would be discovered (Rafalski, 2010; Kushwaha *et al.*, 2017). Nevertheless, it seems that the finding of major effects and reproducible QTLs for root traits (Soriano and Alvaro, 2019; Alemu *et al.*, 2021; Daryani *et al.*, 2022) would rather be an exception.

4.4.4. TRAITS CLOSE TO DEVELOPMENT PROCESSES DO NOT NECESSARILY WARRANT SIMPLE GENETIC ARCHITECTURE

Our QTL survey indicated that a majority of root phenotyping experiments focus on three trait categories (Biomass, Length and Production). Not

surprisingly, these categories correspond to integrative traits that are easily measurable in simple setups (Freschet *et al.*, 2020; Tracy *et al.*, 2020).

Upstream of our study, we assumed that dynamic mathematical models of root architecture, which integrate current physiological understanding of root growth and development, rely on parameters that should be closer to the biological and development processes than common integrative variables (de Dorlodot *et al.*, 2007; Passot *et al.*, 2019). Based on this assumption, we predicted that model-based variables would lead to improved QTL detection in addition to leading naturally to a wide range of applications (Muller and Martre, 2019). However, we found little evidence that the genetic architecture of such variables should be different from that of conventional integrative variables. The paper of Muller *et al.* (2019) proposes a different reading frame of the root phenotype that would pay attention to the intrinsic variability of root growth and development processes. If we follow their proposition, traits close to biological processes might be intrinsically more noisy than integrative ones and, if this is the case, phenotyping experiments should be re-designed accordingly.

4.5. PERSPECTIVES BEYOND THE THESIS

- Further investigations could be carried out with a lower SNP detection threshold as with the false discovery rate method and by extending the analysis to collocate the significant SNPs found to fix the exact number of QTLs.
- A next step would also be to compare the position of the QTLs found here with some important genes related to wheat phenology such as plant height or flag leaf appearance.
- For sure it would also have been really interesting to carry out the exact same analysis with the durum wheat panel to see if the same trends would have been discovered or if totally different results would have been found.

Interchapter 4-5

In Chapter 4, the genetic architecture of several descriptors of root system architecture was investigated in bread wheat. We found that root traits are controlled by several small-effect loci distributed along the genome and that no clear difference was observed between the determinism of most commonly estimated morphological traits and those related to root growth dynamics, although they are supposed to be closer to development functions.

In continuation, in Chapter 5, we will gather the main findings discussed along previous chapters and discussed them. Eventually, we will conclude by proposing some avenues of exploration.

Chapter 5.

General discussion

5.1. MAIN FINDINGS

The main themes addressed in this thesis were the quantification and the genetics of root system architecture, with a deliberate emphasis on a selection of traits related to root growth development processes, inspired by root architectural models. The major findings were the following:

- We showed that simple features as locations of root tips over time, are sufficient to build a reasonably correct representation of a root system architecture and we illustrated this principle with a novel image and data analysis pipeline traits (Chapter 2).
- We applied this pipeline to bread and durum wheat diversity panels and found that integrative and process root traits displayed a wide genetic diversity and moderate heritabilities. We also observed that process variables had similar, but not higher, heritabilities than conventional integrative variables (Chapter 3).
- The phenotypic evaluation of the same panels in different platforms indicated that genotypic differences were largely environment-specific and resulted from interactions between genotype and environment. Despite this, the combination of platforms allowed us to assemble groups of genotypes whose morphotypes could be interpreted in relation to yield performance under combined stress (Chapter 3).
- Genome wide association studies indicated that, similarly to integrative variables, process variables are controlled by several small effect loci distributed along the entire genome (Chapter 4).

5.2. DISCUSSION

In the first part of the discussion, we will discuss whether we could achieve the objectives set at the beginning of this work (section 5.2.1). Then we will raise some results that have challenged us (section 5.2.2). Finally, we will add some ideas for future research (section 5.3).

5.2.1. ACHIEVEMENT OF THE OBJECTIVES

5.2.1.1. FROM TIPS TO INPUT PARAMETERS OF ROOT ARCHITECTURAL MODELS

The first objective was, from simple features as root tip coordinates, to estimate root architectural traits with an emphasis on process variables selected from input parameters of root architectural models (Chapter 2).

From the representation of root system architecture developed in the analysis pipeline, we managed to estimate most of the variables needed to run the ArchiSimple model (more or less 7 out of the 11 variables listed in the Table 3 & Table 4 (Chapter 2)). For the growth parameters, the duration of primordium development (***DPD***), the diameter (***Diam***) of the roots per root type (all types confounded or embryonic roots and lateral roots separately), the elongation rate (***ERate***, also per root type except for the lateral roots) and the maximal root length (***MRL***) could be estimated (Chapter 2). However, the sensitivity to mechanical constraints was not estimated as the pipeline was dedicated to analyse aeroponically-grown plants (without mechanical constraints). For the shape and direction variables, only the angle between the first pair of seminal roots was obtained here ($\boldsymbol{SRA_{SR1}}$). The gravitropism influence and the insertion angle per root type (***Theta***) could not be assessed (especially for the lateral roots). Then, for variables linked to branching, the pipeline was able to perform a root categorisation and to estimate lateral root density (***LRD***). Finally, target plants were too young to show senescence, which was therefore not estimated.

Despite that all the parameters were not obtained, we were able to go quite far and both integrative but also process variables were assessed. In its current form, the pipeline can be used routinely to estimate several input parameters on large collections of wheat genotypes and should be adaptable to other species.

5.2.1.2. WHAT ARE THE BENEFITS OF CROSS-PLATFORM ANALYSIS?

As root traits are known to be largely influenced by the environment, our second objective (Chapter 3) was to cross-analyse root characteristics measured in different phenotyping conditions (RootPhAir, Pouches and 4PMI).

One would hope that, from controlled environments provided by the conditions of high throughput phenotyping platforms, traits that are close to

or belonging to the same root category (e.g., Biomass, Elongation, Production) would be consistently correlated within and between platform trials. Although this was verified within each experiment, very few significant correlations were found between variables of the different platforms. In other words, the platforms conditions had a dramatic impact on root growth and development.

This relative independence can hardly be attributed to noise given the fairly moderate heritabilities found for these traits. It should rather be attributed to large plasticity. This means that genotypic differences were largely dependent on the environment and expressed through interactions between genotype and environment.

Nevertheless, the combination of platforms enabled a greater number of variables to be obtained under a various number of growing conditions. Interestingly, a clustering of all the platforms data allowed the identification of some characteristics for best performing groups under combined field stress conditions, which were found to be different between the two wheat species. Without any special precautions, this pooling method clearly allowed for the assessment of "ideotype" groups close to the well-known root ideotypes such as the "steep-cheap-deep" root or "topsoil foraging" root ideotype (Chapter 3, section 3.3.1.3).

Thus, even though root traits were estimated and measured differently in each platform, their (naive) combination allowed to draw certain conclusions regarding field performance. It was therefore shown that stable controlled conditions (from the phenotyping platforms) might be useful for predicting field performance.

5.2.1.3. WHAT IS THE ADDED VALUE OF VARIABLES RELATED TO ROOT DEVELOPMENT PROCESSES?

Our third objective was to investigate the genetic architecture of process variables and see if it differs from that of the integrative variables that are most commonly used (Chapter 3 & Chapter 4).

Our pipeline allowed to estimate process variables, corresponding to input parameters of root architectural models (e.g., ***Diam***, ***DPD***, ***LRD***, ***ERate***) in addition to integrative variables (Chapter 2). We believe that process variables are closer to growth and development processes than integrative variables. Surprisingly, these process variables showed quite large genetic variabilities

but not necessarily larger heritabilities (H^2) than the integrative ones (Chapter 3) and only a handful of QTLs at few genome locations were detected for these variables (Chapter 4). It is possible that loci with large effects have already been fixed through selection and that the remaining variability is controlled by a multitude of small effect loci, for both integrative and process variables. It would therefore mean that the traits related to root development processes have not necessarily a different genetic determinism than the integrative root traits (de Dorlodot *et al.*, 2007).

Alternative, non-genetic, explanations deserve to be explored. Since process variables describe dynamic process that are expected to change over time, their manifestation could be more noisy than integrative variables which are the cumulative outcome of dynamic processes whose variations could smooth out over time. Finally, we observed in our experimental setups that process variables were rather stable over time, which means that they should be approximately proportional to integrative variables.

5.2.2. OUTSTANDING RESULTS

5.2.2.1. UNEXPECTED ELONGATION STABILITY

Surprisingly, and despite their dynamic aspects, relatively constant and stable values were found for the process variables newly estimated.

Indeed, a clear linear relationship emerged with consistency from the assessment of $\boldsymbol{ERate_{PR}}$, expressing the elongation rate of the primary root. In addition, other evidence suggests that this linear relationship may be true for all embryonic roots (due to the parallelism of the seminal root regressions). Therefore, the throughput given by the RootPhAir platform and used to achieve such a constant feature does not seem necessary. Much less dense image time series could therefore be used to simplify the estimation of this constant $\boldsymbol{ERate_{PR}}$ value.

Nevertheless, it must be pointed out that the linearity hypothesis may have limited the detection of other evolution trends of the $\boldsymbol{ERate_{PR}}$ for few genotypes. Similarly, the last points detected suggest the beginning of a change in the trajectory followed and that the linearity might have stopped if we had observed root growth over a longer period of time.

The density of the image series was, however, essential for the determination of the ***LRD*** and ***Diam*** characteristics since the categorisation into different

root types, necessary for their estimation, was possible on the basis of the entire population of tips. More specifically, it was shown that the estimation of the lateral branching density remains a complex task to be achieved because the local variability of this traits does not allow manual counting to be representative of the global density (Muller and Hong, unpublished). The linearity of the regression used to estimate the ***LRD*** was consistent across both panels and revealed the possibility to define a "global lateral root production" per plant based on the whole tip population detected in the experiment. With this variable, we have somehow simplified an indicator that is rather difficult to estimate locally, because of its great variability, into a global one that expresses quite clearly the general lateral root formation behaviour of a genotype.

Finally, we also found that the ***DPD*** (which expresses the time needed between the initiation and the emergence of a lateral root) is constant over time for all embryonic roots of a given plant. Again, for a trait expressing a real dynamic aspect of the root system, a possible simplification was suggested by our studies.

5.2.2.2. FROM SEEDLING ROOT TRAITS TO FIELD PERFORMANCE

The effectiveness of using root traits estimated at relatively early stages to predict field performance at later stages is controversial in the literature and this was also the case for our study.

All the traits of this study remained estimated at very young growth stage and thus were almost exclusively related to embryonic root type. The nodal roots, appearing at latter stages were not addressed here (except through biomass traits estimated at the end of the 4PMI experiment). It is known that the embryonic roots only represent a small proportion of the entire root system (< 14% according to Manske and Vlek (2002)) and that their roles are usually associated with early and deep root growth for resources acquisition of the first stages (Manske and Vlek, 2002; Atkinson *et al.*, 2014). They are believed to be mainly active during the vegetative phase, but their role after the apparition of nodal roots is not so clear (Hochholdinger and Zimmermann, 2008; Atkinson *et al.*, 2014). At the 4-leaf stage, the nodal roots start to emerge and to develop in the shallow soil layers, the number of nodal roots being highly dependent on the number of tillers (Hockett, 1986; Manske and Vlek, 2002). Often, for cereal plants, it is thought that even though the seminal

roots remain active after the apparition of the nodal roots, their contribution to resource acquisition is much less compared than that of the nodal roots, and that the latter take over with a much greater water absorption capacity (Chochois *et al.*, 2015; Ahmed *et al.*, 2018; Z. Liu *et al.*, 2020).

Since weak correlations were found between yield traits and platform traits estimated before the emergence of nodal roots, the study of later growth stages may help in revealing more correlations with field behaviour.

However, by crossing the results obtained from the three platforms, some characteristics of best performing groups in the field were linked with platform traits values at an early growth stage (as discussed in previous section 5.2.1.2). Additionally, the characteristics highlighted with our crude clustering method, were linked to well-known root ideotypes (Chapter 3, section 3.3.1.3).

5.2.3. A BRIEF CONCLUSION ON THE OBJECTIVES

To sum up, the traits estimated in the RootPhAir platform and this analysis pipeline brings new aspects of root dynamics and development that are rarely approached: (i) the root traits studied have been precisely selected to match most of the input parameters needed for root models, and this is worthwhile as it allows us to investigate these genotypes in a wider context through model simulation and, (ii) under heterogeneous conditions, in contrast to the stable conditions provided by the RootPhAir platform, these process variables would probably no longer simplify to constant values. Therefore, it would be premature not to explore this approach further.

Although all this work has been developed around two wheat species (bread wheat and durum wheat), we believe that the analysis pipeline created could be extended to other species such as cereal-like architecture, but probably not to tap-root systems (because the distinction between the emergence of seminal and lateral roots and the use of tip-collar distance to approximate their length are two essential conditions on which the determination of many variables is based).

5.3. AVENUES OF EXPLORATION

5.3.1. ONE STEP FURTHER TO MODELLING

Despite the effort that was made to estimate traits useful as inputs of models in Chapter 2 and Chapter 3, and to study their genetic determinism in Chapter 4, the estimation for traits related to the lateral root growth remained incomplete. A further step would be to estimate the ***ERate***, the ***Length*** and even the ***Theta*** of this lateral root type, whose role in resource acquisition is crucial and whose intrinsic variability has recently been proven to be at the origin of a huge phenotypic plasticity (Muller *et al.*, 2019). It would therefore be desirable to focus on accessing these features to fulfil all the input parameters of root architectural models.

Ecophysiology and modelling are intrinsically linked and largely complementary to address the complexity of root and root system processes (de Dorlodot *et al.*, 2007; Dunbabin *et al.*, 2013; Lynch, 2013; Muller *et al.*, 2019). Investigations that integrate these fields successfully can be seen as key gear that has and will continue to improve our knowledge of the essential functions of plants (especially root system architecture) needed to withstand changing and challenging environments, including combined stresses. This is why, even without the exact estimation of lateral parameters, it would already be very interesting to examine the results of some root architectural models run with our newly estimated variables in the hope that the simulated scenarios will reflect more accurately what is happening in the field or help us understand new processes. This point is currently being investigated within the SolACE project.

5.3.2. MAKE PLATFORMS HOMOGENEOUS

Although the phenotypic and genetic analyses combined root traits coming from three different platform setups, they were hardly comparable as they were not estimated in the exact same way. Likewise, many platforms exists but each with their own root system representation and with their own way to estimate phenotyping traits. For this reason, making phenotyping platforms more comparable could represent a considerable additional asset, e.g., by precisely defining a set of base variables to be estimated, following the similar root system capture methods (2D-3D, temporal resolution) and image time series analysis methods.

First, this might help in revealing more correlations between close traits, reveal more genetic variability and dissociate it from environmental variability. And secondly, it could also allow for a more robust meta-analysis by increasing the potential number of QTLs found, which could lead to the discovery of more co-localisations sites. This could therefore represent a parallel approach to the enrichment that can be achieved by cross-analysing various traits from different platforms (as discussed above in section 5.2.1.2).

This homogenisation, both in terms of the variables measured and the data format, has already been mentioned several times as a future opportunity to improve phenotyping but also to allow for data durability (Kuijken *et al.*, 2015; Lobet *et al.*, 2015; Lobet, 2017a; Muller *et al.*, 2019; Pieruschka and Schurr, 2019; Watt *et al.*, 2020). However, it seems that this homogenisation has hardly been implemented in practice and we still do not really know why, except for the diversity of the disciplinary fields involved and the fact that they all have to work together.

5.3.3. REPOSITIONING THE ROOT SYSTEM ARCHITECTURE

During this thesis, much attention was paid to the root system and its functioning. However, the architecture of the root system is part of a much larger and more complex plant system. Therefore, we believe it is also important to reposition the root system architecture within:

(i) THE PLANT SYSTEM AS A WHOLE

The development of phenotyping experiments looking at both above- and below-ground aspects of the plant has already been attempted or suggested in literature (Nagel *et al.*, 2014; Chochois *et al.*, 2015; Gioia *et al.*, 2015) and we believe it could better picture the whole plant system in terms of source-sink dynamics and stress resilience.

(ii) THE DYNAMIC PROCESSES THAT SURROUND IT

Likewise, root system architecture has become increasingly studied, but no one really has succeeded in estimating the set of variables needed to describe this root system architecture properly, because everyone is only interested in a few variables, measured in different ways and therefore not very comparable (as discussed above, section 5.3.2). The root system architecture is not a static concept and should perhaps be considered as one of the many aspects of root systems. Therefore, we should replace it among the dynamic

processes that surround it and especially with its interaction with soil resources and rhizosphere microbiome (Dunbabin *et al.*, 2013; McGrail, Van Sanford and McNear, 2020).

Nonetheless, many modelling approaches have already started to explore this path via, for example, hydraulic root architecture models that combine aspects of the architecture and hydraulic conductivity of the soil-root system (Lobet, Pagès and Draye, 2014). Enhancing the accuracy with which the root system architecture is described in these models, e.g., by incorporating our newly estimated dynamic traits, could therefore improve the quality of the prediction of resource extraction in soil-plant systems or root interaction with soil biome.

We also believe that in such multidisciplinary approaches, joint work between many actors and fields (e.g., phenotyping, image analysis, modelling, breeding but also especially farming) will indeed continue to be necessary to better understand the complex and adaptive processes of root systems and their implications for plant performance under heterogenous field conditions (de Dorlodot *et al.*, 2007; Tracy *et al.*, 2020; Watt *et al.*, 2020).

References

Ahmad, I. *et al.* (2014) 'Screening of spring wheat (Triticum aestivum L.) genotypes for drought tolerance on the basis of seedling traits', *Pakistan Journal of Agricultural Sciences*, 51(2), pp. 367–372.

Ahmed, M.A. *et al.* (2018) 'Root type matters: measurement of water uptake by seminal, crown, and lateral roots in maize', *Journal of Experimental Botany*, 69(5), pp. 1199–1206. https://doi.org/10.1093/jxb/erx439.

Alabart, C. (2017) *Tracking of the growth of roots based on multi-object tracking techniques*. Université Catholique de Louvain.

Albert, A. and Zhang, L. (2010) 'A novel definition of the multivariate coefficient of variation', Biometrical Journal, 52(5), pp. 667–675. Available at: https://doi.org/10.1002/bimj.201000030.

Alemu, A. *et al.* (2021) 'Genome-wide association analysis unveils novel QTLs for seminal root system architecture traits in Ethiopian durum wheat', *BMC Genomics*, 22(1), p. 20. https://doi.org/10.1186/s12864-020-07320-4.

An, D. *et al.* (2006) 'Mapping QTLs for nitrogen uptake in relation to the early growth of wheat (Triticum aestivum L.)', *Plant and Soil*, 284(1–2), pp. 73–84. https://doi.org/10.1007/s11104-006-0030-3.

Anwar, K. *et al.* (2021) 'Elucidating the Response of Crop Plants towards Individual, Combined and Sequentially Occurring Abiotic Stresses', *International Journal of Molecular Sciences*, 22(11), p. 6119. https://doi.org/10.3390/ijms22116119.

Arsova, B. *et al.* (2020) 'Dynamics in plant roots and shoots minimize stress, save energy and maintain water and nutrient uptake', *New Phytologist*, 225(3), pp. 1111–1119. https://doi.org/10.1111/nph.15955.

Atkinson, D. (2000) 'Root Characteristics: Why and What to Measure', in A.L. Smit et al. (eds) *Root Methods: A Handbook*. Berlin, Heidelberg: Springer, pp. 1–32. https://doi.org/10.1007/978-3-662-04188-8_1.

Atkinson, J.A. *et al.* (2014) 'Branching Out in Roots: Uncovering Form, Function, and Regulation', *Plant Physiology*, 166(2), pp. 538–550. https://doi.org/10.1104/pp.114.245423.

Atkinson, J.A. *et al.* (2015) 'Phenotyping pipeline reveals major seedling root growth QTL in hexaploid wheat', *Journal of Experimental Botany*, 66(8), pp. 2283–2292. https://doi.org/10.1093/jxb/erv006.

Atkinson, J.A. *et al.* (2019) 'Uncovering the hidden half of plants using new advances in root phenotyping', *Current Opinion in Biotechnology*, 55, pp. 1–8. https://doi.org/10.1016/j.copbio.2018.06.002.

Atwell, B.J. (1990) 'The effect of soil compaction on wheat during early tillering', *New Phytologist*, 115(1), pp. 29–35. https://doi.org/10.1111/j.1469-8137.1990.tb00918.x.

Bai, C. *et al.* (2019) 'The relationships between seedling root screens, root growth in the field and grain yield for wheat', *Plant and Soil*, 440(1), pp. 311–326. https://doi.org/10.1007/s11104-019-04088-9.

Barczi, J.-F. *et al.* (2018) 'DigR: a generic model and its open source simulation software to mimic three-dimensional root-system architecture diversity', *Annals of Botany*, 121(5), pp. 1089–1104. https://doi.org/10.1093/aob/mcy018.

Barraclough, P.B. and Leigh, R.A. (1984) 'The growth and activity of winter wheat roots in the field: the effect of sowing date and soil type on root growth of high-yielding crops', *The Journal of Agricultural Science*, 103(1), pp. 59–74. https://doi.org/10.1017/S002185960004332X.

Bekkering, C.S., Huang, J. and Tian, L. (2020) 'Image-Based, Organ-Level Plant Phenotyping for Wheat Improvement', *Agronomy*, 10(9), p. 1287. https://doi.org/10.3390/agronomy10091287.

Bengough, A.G. *et al.* (2011) 'Root elongation, water stress, and mechanical impedance: a review of limiting stresses and beneficial root tip traits', *Journal of Experimental Botany*, 62(1), pp. 59–68. https://doi.org/10.1093/jxb/erq350.

Benjamini, Y. (2010) 'Discovering the false discovery rate', *Journal of the Royal Statistical Society: Series B (Statistical Methodology)*, 72(4), pp. 405–416. https://doi.org/10.1111/j.1467-9868.2010.00746.x.

Bingham, I.J. and Stevenson, E.A. (1993) 'Control of root growth: effects of carbohydrates on the extension, branching and rate of respiration of different fractions of wheat roots', *Physiologia Plantarum*, 88(1), pp. 149–158. https://doi.org/10.1111/j.1399-3054.1993.tb01772.x.

van der Bom, F.J.T. van der, Williams, A. and Bell, M.J. (2020) 'Root architecture for improved resource capture: trade-offs in complex environments', *Journal of Experimental Botany*, 71(19), pp. 5752–5763. https://doi.org/10.1093/jxb/eraa324.

Bonser, A.M., Lynch, J. and Snapp, S. (1996) 'Effect of phosphorus deficiency on growth angle of basal roots in Phaseolus vulgaris', *The New Phytologist*, 132(2), pp. 281–288. https://doi.org/10.1111/j.1469-8137.1996.tb01847.x.

Bragg, P.L., Govi, G. and Cannell, R.Q. (1983) 'A comparison of methods, including angled and vertical minirhizotrons, for studying root growth and distribution in a spring oat crop', *Plant and Soil*, 73(3), pp. 435–440. https://doi.org/10.1007/BF02184322.

Brancourt-Hulmel, M. *et al.* (2003) 'Genetic Improvement of Agronomic Traits of Winter Wheat Cultivars Released in France from 1946 to 1992', *Crop Science*, 43(1), pp. 37–45. https://doi.org/10.2135/cropsci2003.3700.

Brunelle, T. *et al.* (2015) 'Evaluating the impact of rising fertilizer prices on crop yields', *Agricultural Economics*, 46(5), pp. 653–666. https://doi.org/10.1111/agec.12161.

Cahn, M.D., Zobel, R.W. and Bouldin, D.R. (1989) 'Relationship between root elongation rate and diameter and duration of growth of lateral roots of maize', *Plant and Soil*, 119(2), pp. 271–279. https://doi.org/10.1007/BF02370419.

Ceccarelli, S. (1989) 'Wide adaptation: How wide?', *Euphytica*, 40(3), pp. 197–205. https://doi.org/10.1007/BF00024512.

Chen, Y. et al. (2020) 'Phenotypic variability in bread wheat root systems at the early vegetative stage', BMC Plant Biology, 20(1), p. 185. Available at: https://doi.org/10.1186/s12870-020-02390-8.

Chochois, V. *et al.* (2015) 'Variation in Adult Plant Phenotypes and Partitioning among Seed and Stem-Borne Roots across Brachypodium distachyon Accessions to Exploit in Breeding Cereals for Well-Watered and Drought Environments', *Plant Physiology*, 168(3), pp. 953–967. https://doi.org/10.1104/pp.15.00095.

Christopher, J. *et al.* (2013) 'QTL for root angle and number in a population developed from bread wheats (Triticum aestivum) with contrasting adaptation to water-limited environments', *Theoretical and Applied Genetics*, 126(6), pp. 1563–1574. https://doi.org/10.1007/s00122-013-2074-0.

Chun-Yan Liu, A. K. Srivastava and Qiang-Sheng Wu (2013) 'Effects of arbuscular mycorrhizal inoculation on growth, yield, nutrient uptake and irrigation water productivity of sunflowers grown under drought stress', *Agricultural Water Management*, 117, pp. 106–114. https://doi.org/10.1016/j.agwat.2012.11.007.

Collet, C. (2022) 'Review of QTLs found in studies aimed at finding QTLs for bread wheat root traits (from 2005 to mid-2020)'. Zenodo. https://doi.org/10.5281/zenodo.6671793.

Colombi, T. and Walter, A. (2016) 'Root responses of triticale and soybean to soil compaction in the field are reproducible under controlled conditions', *Functional plant biology: FPB*, 43(2), pp. 114–128. https://doi.org/10.1071/FP15194.

Colombi, T. and Walter, A. (2017) 'Genetic Diversity under Soil Compaction in Wheat: Root Number as a Promising Trait for Early Plant Vigor', *Frontiers in Plant Science*, 8, p. 420. https://doi.org/10.3389/fpls.2017.00420.

Colombo, M. *et al.* (2022) 'Genetic Analysis of Platform-Phenotyped Root System Architecture of Bread and Durum Wheat in Relation to Agronomic Traits', *Frontiers in Plant Science*, 13. Available at: https://www.frontiersin.org/article/10.3389/fpls.2022.853601 (Accessed: 5 April 2022).

Daryani, P. *et al.* (2022) 'Pinpointing genomic regions associated with root system architecture in rice through an integrative meta-analysis approach', *Theoretical and Applied Genetics*, 135(1), pp. 81–106. https://doi.org/10.1007/s00122-021-03953-5.

David, J. *et al.* (2014) 'Genotyping by sequencing transcriptomes in an evolutionary pre-breeding durum wheat population', *Molecular Breeding*, 34, pp. 1531–1548. https://doi.org/10.1007/s11032-014-0179-z.

Deacon, J.W. and Mitchell, R.T. (1985) 'Comparison of rates of natural senescence of the root cortex of wheat (with and without mildew infection), barley, oats and rye', Plant and Soil, 84(1), pp. 129–131. Available at: https://doi.org/10.1007/BF02197874.

Dhanda, S.S., Sethi, G.S. and Behl, R.K. (2004) 'Indices of Drought Tolerance in Wheat Genotypes at Early Stages of Plant Growth', *Journal of Agronomy and Crop Science*, 190(1), pp. 6–12. https://doi.org/10.1111/j.1439-037X.2004.00592.x.

Donmez, E. *et al.* (2001) 'Genetic Gain in Yield Attributes of Winter Wheat in the Great Plains', *Crop Science*, 41(5), pp. 1412–1419. https://doi.org/10.2135/cropsci2001.4151412x.

de Dorlodot, S. (2007) *Root system architecture: a genetic analysis in rice*. PhD Thesis. Université catholique de Louvain.

de Dorlodot, S. *et al.* (2007) 'Root system architecture: opportunities and constraints for genetic improvement of crops', *Trends in Plant Science*, 12(10), pp. 474–481. https://doi.org/10.1016/j.tplants.2007.08.012.

Draye, X. *et al.* (2010) 'Model-assisted integration of physiological and environmental constraints affecting the dynamic and spatial patterns of root water uptake from soils', *Journal of Experimental Botany*, 61(8), pp. 2145–2155. https://doi.org/10.1093/jxb/erq077.

Dubrovsky, J.G. and Rost, T.L. (2003) 'Root development | Lateral Root Initiation', in B. Thomas (ed.) Encyclopedia of Applied Plant Sciences. Oxford: Elsevier, pp. 1101–1107. Available at: https://doi.org/10.1016/B0-12-227050-9/00042-9.

Dunbabin, V.M. *et al.* (2013) 'Modelling root–soil interactions using three–dimensional models of root growth, architecture and function', *Plant and Soil*, 372(1–2), pp. 93–124. https://doi.org/10.1007/s11104-013-1769-y.

Dupuy, L., Gregory, P.J. and Bengough, A.G. (2010) 'Root growth models: towards a new generation of continuous approaches', *Journal of Experimental Botany*, 61(8), pp. 2131–2143. https://doi.org/10.1093/jxb/erp389.

Dupuy, L.X. (2011) 'Modelling Root Systems Using Oriented Density Distributions', *AIP Conference Proceedings*, 1389(1), pp. 726–729. https://doi.org/10.1063/1.3636834.

Emphasis (2022) 'Emphasis Phenotyping Landscape : Infrastructure Map'. Available at: https://emphasis.plant-phenotyping.eu/phenotyping-landscape/infrastructure-map (Accessed: 27 June 2022).

'EU Plant variety database (v.3.4)' (2022). Available at: https://ec.europa.eu/food/plant/plant_propagation_material/plant_variety_catalogues_databases/search/public/index.cfm?event=SearchForm&ctl_type=A (Accessed: 17 January 2022).

Eziz, A. *et al.* (2017) 'Drought effect on plant biomass allocation: A meta-analysis', *Ecology and Evolution*, 7(24), pp. 11002–11010. https://doi.org/10.1002/ece3.3630.

Fahlgren, N., Gehan, M.A. and Baxter, I. (2015) 'Lights, camera, action: high-throughput plant phenotyping is ready for a close-up', *Current Opinion in Plant Biology*, 24, pp. 93–99. https://doi.org/10.1016/j.pbi.2015.02.006.

Fiorani, F. and Schurr, U. (2013) 'Future Scenarios for Plant Phenotyping', *Annual Review of Plant Biology*, 64(1), pp. 267–291. https://doi.org/10.1146/annurev-arplant-050312-120137.

Fitter, A.H. (1994) 'Architecture and Biomass Allocation as Components of the Plastic Response of Root Systems to Soil Heterogeneity', in *Exploitation of Environmental Heterogeneity by Plants*. Elsevier, pp. 305–323. https://doi.org/10.1016/B978-0-12-155070-7.50016-0.

Fitter, A.H. (2002) 'Characteristics and Functions of Root Systems', in *Plant Roots - The hidden half*. Third Edition. https://doi.org/10.1201/9780203909423.ch2.

Flintham, J.E. *et al.* (1997) 'Optimizing wheat grain yield: effects of Rht (gibberellin-insensitive) dwarfing genes', *The Journal of Agricultural Science*, 128(1), pp. 11–25. https://doi.org/10.1017/S0021859696003942.

Freschet, G.T. *et al.* (2020) 'Root traits as drivers of plant and ecosystem functioning: current understanding, pitfalls and future research needs', *New Phytologist*. https://doi.org/10.1111/nph.17072.

Gerwitz, A. and Page, E.R. (1974) 'An Empirical Mathematical Model to Describe Plant Root Systems', *Journal of Applied Ecology*, 11(2), pp. 773–781. https://doi.org/10.2307/2402227.

Gioia, T. *et al.* (2015) 'Impact of domestication on the phenotypic architecture of durum wheat under contrasting nitrogen fertilization', *Journal of Experimental Botany*, 66(18), pp. 5519–5530. https://doi.org/10.1093/jxb/erv289.

Gregory, P.J. *et al.* (1978) 'Water relations of winter wheat: 1. Growth of the root system', *The Journal of Agricultural Science*, 91(1), pp. 91–102. https://doi.org/10.1017/S0021859600056653.

'GRIS' (2017). Available at: http://www.wheatpedigree.net/sort/index?search=&_action_list=Search (Accessed: 27 January 2022).

Guo, H. *et al.* (2021) 'Functional phenomics and genetics of the root economics space in winter wheat using high-throughput phenotyping of respiration and architecture', *New Phytologist*, 232(1), pp. 98–112. https://doi.org/10.1111/nph.17329.

Guo, X. *et al.* (2020) 'Genomic prediction of yield and root development in wheat under changing water availability', *Plant Methods*, 16(1), p. 90. https://doi.org/10.1186/s13007-020-00634-0.

Guo, Y. *et al.* (2012) 'QTL mapping for seedling traits in wheat grown under varying concentrations of N, P and K nutrients', *Theoretical and Applied Genetics*, 124(5), pp. 851–865. https://doi.org/10.1007/s00122-011-1749-7.

Hoagland, D.R. (Dennis R. and Arnon, D.I. (Daniel I. (1950) *The water-culture method for growing plants without soil*. Berkeley, Calif. : College of Agriculture, University of California. Available at: http://archive.org/details/watercultureme3450hoag (Accessed: 29 July 2017).

Hochholdinger, F. and Zimmermann, R. (2008) 'Conserved and diverse mechanisms in root development', *Current Opinion in Plant Biology*, 11(1), pp. 70–74. https://doi.org/10.1016/j.pbi.2007.10.002.

Hockett, E.A. (1986) 'Relationship of adventitious roots and agronomic characteristics in barley', *Canadian Journal of Plant Science*, 66(2), pp. 257–280. https://doi.org/10.4141/cjps86-040.

Hohn, C.E. and Bektas, H. (2020) 'Genetic Mapping of Quantitative Trait Loci (QTLs) Associated with Seminal Root Angle and Number in Three Populations of Bread Wheat (Triticum aestivum L.) with Common Parents', *Plant Molecular Biology Reporter*. https://doi.org/10.1007/s11105-020-01214-1.

Hounsfield Facility (2022) 'Hounsfield Facility: 3D X-ray imaging'. Available at: https://www.nottingham.ac.uk/microct/index.aspx (Accessed: 27 June 2022).

Humbert, S. *et al.* (2013) 'Genome-wide expression profiling of maize in response to individual and combined water and nitrogen stresses', *BMC Genomics*, 14(1), p. 3. https://doi.org/10.1186/1471-2164-14-3.

Hund, A., Trachsel, S. and Stamp, P. (2009) 'Growth of axile and lateral roots of maize: I development of a phenotying platform', *Plant and Soil*, 325, pp. 335–349. https://doi.org/10.1007/s11104-009-9984-2.

Hurd, E.A. (1974) 'Phenotype and drought tolerance in wheat', *Agricultural Meteorology*, 14(1), pp. 39–55. https://doi.org/10.1016/0002-1571(74)90009-0.

IPPN (2022) 'IPPN Phenotyping: Infrastructure'. Available at: https://www.plant-phenotyping.org/Infrastructure_Categories (Accessed: 27 June 2022).

IPPN Aeroponics (2022) 'Aeroponics (RootPhAir)'. Available at: https://www.plant-phenotyping.org/db_infrastructure#/tool/55 (Accessed: 27 June 2022).

Izzo, L.G. and Aronne, G. (2021) 'Root Tropisms: New Insights Leading the Growth Direction of the Hidden Half', Plants, 10(2), p. 220. Available at: https://doi.org/10.3390/plants10020220.

Jeudy, C. *et al.* (2016) 'RhizoTubes as a new tool for high throughput imaging of plant root development and architecture: test, comparison with pot grown plants and validation', *Plant Methods*, 12, p. 31. https://doi.org/10.1186/s13007-016-0131-9.

Jiang, G.M. *et al.* (2003) 'Changes in the rate of photosynthesis accompanying the yield increase in wheat cultivars released in the past 50 years', *Journal of Plant Research*, 116(5), pp. 347–354. https://doi.org/10.1007/s10265-003-0115-5.

Jiang, Y. and Li, C. (2020) 'Convolutional Neural Networks for Image-Based High-Throughput Plant Phenotyping: A Review', *Plant Phenomics*, 2020. https://doi.org/10.34133/2020/4152816.

Johnson, M.G. *et al.* (2001) 'Advancing fine root research with minirhizotrons', *Environmental and Experimental Botany*, 45(3), pp. 263–289. https://doi.org/10.1016/s0098-8472(01)00077-6.

Kalogiros, D.I. *et al.* (2016) 'Analysis of root growth from a phenotyping data set using a density-based model', *Journal of Experimental Botany*, 67(4), pp. 1045–1058. https://doi.org/10.1093/jxb/erv573.

Kang, H.M. *et al.* (2010) 'Variance component model to account for sample structure in genome-wide association studies', *Nature Genetics*, 42(4), pp. 348–354. https://doi.org/10.1038/ng.548.

Kelly, A. *et al.* (2020) 'Genetic selection for spatial and temporal characteristics of root growth in plants using a highthroughput phenotyping platform', in. *International Biometrics Conference*. Available at: https://dial.uclouvain.be/pr/boreal/object/boreal:236012 (Accessed: 16 November 2021).

Khokhar, J.S. *et al.* (2019) 'Juvenile root traits show limited correlation with grain yield, yield components and grain mineral composition traits in Indian wheat under hostile soils', *Cereal Research Communications*, 47(2), pp. 369–382. https://doi.org/10.1556/0806.47.2019.10.

Klepper, B., Belford, R.K. and Rickman, R.W. (1984) 'Root and Shoot Development in Winter Wheat', *Agronomy Journal*, 76(1), pp. 117–122. https://doi.org/10.2134/agronj1984.00021962007600010029x.

Kronenberg, L. et al. (2020) 'Temperature response of wheat affects final height and the timing of stem elongation under field conditions', Journal of Experimental Botany, 72(2), pp. 700–717. Available at: https://doi.org/10.1093/jxb/eraa471.

Kubo, K. *et al.* (2007) 'Quantitative trait loci for soil-penetrating ability of roots in durum wheat', *Plant Breeding*, 126(4), pp. 375–378. https://doi.org/10.1111/j.1439-0523.2007.01368.x.

Kuijken, R.C.P. *et al.* (2015) 'Root phenotyping: from component trait in the lab to breeding', *Journal of Experimental Botany*, 66(18), pp. 5389–5401. https://doi.org/10.1093/jxb/erv239.

Kushwaha, U. *et al.* (2017) 'Association Mapping, Principles and Techniques', *Journal of Biological and Environmental Engineering*, 2, pp. 1–9.

Lecompte, F., Ozier-Lafontaine, H. and Pagès, L. (2001) 'The relationships between static and dynamic variables in the description of root growth. Consequences for field interpretation of rooting variability', *Plant and Soil*, 236(1), pp. 19–31. https://doi.org/10.1023/A:1011924529885.

Li, K.Y., Boisvert, J.B. and Jong, R.D. (1999) 'An exponential root-water-uptake model', *Canadian Journal of Soil Science*, 79(2), pp. 333–343. https://doi.org/10.4141/S98-032.

Li, L., Zhang, Q. and Huang, D. (2014) 'A Review of Imaging Techniques for Plant Phenotyping', *Sensors*, 14(11), pp. 20078–20111. https://doi.org/10.3390/s141120078.

Liu, R. *et al.* (2020) 'Quantitative trait loci analysis for root traits in synthetic hexaploid wheat under drought stress conditions', *Journal of Integrative Agriculture*, 19(8), pp. 1947–1960. https://doi.org/10.1016/S2095-3119(19)62825-X.

Liu, X. *et al.* (2013) 'Mapping QTLs for seedling root traits in a doubled haploid wheat population under different water regimes', *Euphytica*, 189(1), pp. 51–66. https://doi.org/10.1007/s10681-012-0690-4.

Liu, Z. *et al.* (2020) 'Seminal and Nodal Roots of Barley Differ in Anatomy, Proteome and Nitrate Uptake Capacity', *Plant and Cell Physiology*, 61(7), pp. 1297–1308. https://doi.org/10.1093/pcp/pcaa059.

Lobet, G. *et al.* (2015) 'Root System Markup Language: Toward a Unified Root Architecture Description Language', *Plant Physiology*, 167(3), pp. 617–627. https://doi.org/10.1104/pp.114.253625.

Lobet, G. (2017a) 'Image Analysis in Plant Sciences: Publish Then Perish', *Trends in Plant Science*, 22(7), pp. 559–566. https://doi.org/10.1016/j.tplants.2017.05.002.

Lobet, G. *et al.* (2017) 'Using a Structural Root System Model to Evaluate and Improve the Accuracy of Root Image Analysis Pipelines', *Frontiers in Plant Science*, 8, p. 447. https://doi.org/10.3389/fpls.2017.00447.

Lobet, G. (2017b) 'Using structural models to validate and improve root image analysis pipelines', *Poster*. https://doi.org/10.6084/m9.figshare.5167672.v1.

Lobet, G., Draye, X. and Périlleux, C. (2013) 'An online database for plant image analysis software tools', *Plant Methods*, 9(1), p. 38. https://doi.org/10.1186/1746-4811-9-38.

Lobet, G., Pagès, L. and Draye, X. (2011) 'A Novel Image-Analysis Toolbox Enabling Quantitative Analysis of Root System Architecture', *Plant Physiology*, 157(1), pp. 29–39. https://doi.org/10.1104/pp.111.179895.

Lobet, G., Pagès, L. and Draye, X. (2014) 'A modeling approach to determine the importance of dynamic regulation of plant hydraulic conductivities on the water uptake dynamics in the soil-plant-atmosphere system', *Ecological Modelling*, 290, pp. 65–75. https://doi.org/10.1016/j.ecolmodel.2013.11.025.

Louarn, G. and Song, Y. (2020) 'Two decades of functional–structural plant modelling: now addressing fundamental questions in systems biology and predictive ecology', *Annals of Botany*, 126(4), pp. 501–509. https://doi.org/10.1093/aob/mcaa143.

Lynch, J.P. *et al.* (1996) 'SimRoot: Modelling and visualization of root systems', *Plant and Soil*, 188, p. 13.

Lynch, J.P. (2007) 'Roots of the Second Green Revolution', *Australian Journal of Botany*, 55(5), pp. 493–512. https://doi.org/10.1071/BT06118.

Lynch, J.P. (2013) 'Steep, cheap and deep: an ideotype to optimize water and N acquisition by maize root systems', *Annals of Botany*, 112(2), pp. 347–357. https://doi.org/10.1093/aob/mcs293.

Lynch, J.P. (2015) 'Root phenes that reduce the metabolic costs of soil exploration: opportunities for 21st century agriculture', *Plant, Cell & Environment*, 38(9), pp. 1775–1784. https://doi.org/10.1111/pce.12451.

Lynch, J.P. (2019) 'Root phenotypes for improved nutrient capture: an underexploited opportunity for global agriculture', *New Phytologist*, 223(2), pp. 548–564. https://doi.org/10.1111/nph.15738.

Lynch, J.P. and Brown, K.M. (2001) 'Topsoil foraging – an architectural adaptation of plants to low phosphorus availability', *Plant and Soil*, 237(2), pp. 225–237. https://doi.org/10.1023/A:1013324727040.

Ma, H.-X. *et al.* (2005) 'Molecular mapping of a quantitative trait locus for aluminum tolerance in wheat cultivar Atlas 66', *Theoretical and Applied Genetics*, 112(1), p. 51. https://doi.org/10.1007/s00122-005-0101-5.

Maccaferri, M. *et al.* (2005) 'Population structure and long-range linkage disequilibrium in a durum wheat elite collection', *Molecular Breeding*, 15, pp. 271–290. https://doi.org/10.1007/s11032-004-7012-z.

Maccaferri, M. *et al.* (2006) 'A panel of elite accessions of durum wheat (Triticum durum Desf.) suitable for association mapping studies', *Plant Genetic Resources: Characterization and Utilization*, 4, pp. 79–85. https://doi.org/10.1079/PGR2006117.

Maccaferri, M. *et al.* (2011) 'Association mapping in durum wheat grown across a broad range of water regimes', *Journal of Experimental Botany*, 62(2), pp. 409–438. https://doi.org/10.1093/jxb/erq287.

Manschadi, A.M. *et al.* (2008) 'Genotypic variation in seedling root architectural traits and implications for drought adaptation in wheat (Triticum aestivum L.)', *Plant and Soil*, 303(1), pp. 115–129. https://doi.org/10.1007/s11104-007-9492-1.

Manschadi, A.M. *et al.* (2010) 'Experimental and modelling studies of drought-adaptive root architectural traits in wheat (Triticum aestivum L.)', *Plant Biosystems - An International Journal Dealing with all Aspects of Plant Biology*, 144(2), pp. 458–462. https://doi.org/10.1080/11263501003731805.

Manske, G. and Vlek, P. (2002) 'Root Architecture-Wheat as a Model Plant', in *Plant Roots: The Hidden Half*. Third Edition. New York: Yoav Waisel, Amram Eshel, Uzi Kafkafi, pp. 249–259.

Martins, S.M. *et al.* (2020) 'PhenoRoots: an inexpensive non-invasive phenotyping system to assess the variability of the root system architecture', *Scientia Agricola*, 77(5). https://doi.org/10.1590/1678-992x-2018-0420.

Masson-Delmotte, V. *et al.* (2018) 'Global Warming of 1.5°C', in *An IPCC Special Report on the impacts of global warming of 1.5°C above pre-industrial levels and related global greenhouse gas emission pathways, in the context of strengthening the global response to the threat of climate change, sustainable development, and efforts to eradicate poverty*. In Press.

Mathew, I. *et al.* (2018) 'Variance components and heritability of traits related to root: shoot biomass allocation and drought tolerance in wheat', *Euphytica*, 214(12), p. 225. https://doi.org/10.1007/s10681-018-2302-4.

Mbow, C. *et al.* (2019) 'IPCC Special Report on Land and Climate Change. Chapter 5: Food Security', in.

McGrail, R.K., Van Sanford, D.A. and McNear, D.H. (2020) 'Trait-Based Root Phenotyping as a Necessary Tool for Crop Selection and Improvement', *Agronomy*, 10(9), p. 1328. https://doi.org/10.3390/agronomy10091328.

Möller, B. *et al.* (2019) 'rhizoTrak: a flexible open source Fiji plugin for user-friendly manual annotation of time-series images from minirhizotrons', *Plant and Soil*, 444(1), pp. 519–534. https://doi.org/10.1007/s11104-019-04199-3.

Monneveux, P., Jing, R. and Misra, S. (2012) 'Phenotyping for drought adaptation in wheat using physiological traits', *Frontiers in Physiology*, 3. Available at: https://www.frontiersin.org/article/10.3389/fphys.2012.00429 (Accessed: 7 May 2022).

Morris, E.C. *et al.* (2017) 'Shaping 3D Root System Architecture', *Current Biology*, 27(17), pp. R919–R930. https://doi.org/10.1016/j.cub.2017.06.043.

Muller, B. *et al.* (2019) 'Lateral Roots: Random Diversity in Adversity', *Trends in Plant Science*, 24(9), pp. 810–825. https://doi.org/10.1016/j.tplants.2019.05.011.

Muller, B. and Martre, P. (2019) 'Plant and crop simulation models: powerful tools to link physiology, genetics, and phenomics', *Journal of Experimental Botany*, 70(9), pp. 2339–2344. https://doi.org/10.1093/jxb/erz175.

Nagel, K.A. *et al.* (2012) 'GROWSCREEN-Rhizo is a novel phenotyping robot enabling simultaneous measurements of root and shoot growth for plants grown in soil-filled rhizotrons', *Functional plant biology: FPB*, 39(11), pp. 891–904. https://doi.org/10.1071/FP12023.

Nagel, M. *et al.* (2014) 'The genetic basis of durum wheat germination and seedling growth under osmotic stress', *Biologia Plantarum*, 58(4), pp. 681–688. https://doi.org/10.1007/s10535-014-0436-3.

Oakey, H. *et al.* (2006) 'Joint modeling of additive and non-additive genetic line effects in single field trials', *Theoretical and Applied Genetics*, 113(5), pp. 809–819. https://doi.org/10.1007/s00122-006-0333-z.

O'Brien, L. (1979) 'Genetic variability of root growth in wheat (Triticum aestivum L.)', *Australian Journal of Agricultural Research*, 30(4), pp. 587–595. https://doi.org/10.1071/ar9790587.

O'Brien, L. and DePauw, R. (2004) 'WHEAT | Breeding', in C. Wrigley (ed.) *Encyclopedia of Grain Science*. Oxford: Elsevier, pp. 330–336. https://doi.org/10.1016/B0-12-765490-9/00183-X.

Pagès, L. (1995) 'Growth patterns of the lateral roots of young oak (Quercus robur) tree seedlings Relationship with apical diameter', *The New Phytologist*, 130(4), pp. 503–509. https://doi.org/10.1111/j.1469-8137.1995.tb04327.x.

Pagès, L. *et al.* (2004) 'Root Typ: a generic model to depict and analyse the root system architecture', *Plant and Soil*, 258(1), pp. 103–119. https://doi.org/10.1023/B:PLSO.0000016540.47134.03.

Pagès, L. *et al.* (2010) 'Estimating root elongation rates from morphological measurements of the root tip', *Plant and Soil*, 328(1), pp. 35–44. https://doi.org/10.1007/s11104-009-0079-x.

Pagès, L. *et al.* (2012) 'ArchiSimple: A parsimonious model of the root system architecture', in. *2012 IEEE 4th International Symposium on Plant Growth Modeling, Simulation, Visualization and Applications*, pp. 297–303. https://doi.org/10.1109/PMA.2012.6524849.

Pagès, L., Bernert, M. and Pagès, G. (2020) 'Modelling time variations of root diameter and elongation rate as related to assimilate supply and demand', *Journal of Experimental Botany*, 71(12), pp. 3524–3534. https://doi.org/10.1093/jxb/eraa122.

Palta, J.A. *et al.* (2011) 'Large root systems: are they useful in adapting wheat to dry environments?', *Functional Plant Biology*, 38(5), pp. 347–354. https://doi.org/10.1071/FP11031.

Passioura, J. (2010) 'Scaling up: The essence of effective agricultural research', *Functional Plant Biology - FUNCT PLANT BIOL*, 37. https://doi.org/10.1071/FP10106.

Passioura, J.B. (2020) 'Translational research in agriculture. Can we do it better?', *Crop and Pasture Science*, 71(6), pp. 517–528. https://doi.org/10.1071/CP20066.

Passot, S. et al. (2018) 'A New Phenotyping Pipeline Reveals Three Types of Lateral Roots and a Random Branching Pattern in Two Cereals', Plant Physiology, 177(3), pp. 896–910. Available at: https://doi.org/10.1104/pp.17.01648.

Passot, S. *et al.* (2019) 'Connecting the dots between computational tools to analyse soil–root water relations', *Journal of Experimental Botany*, 70(9), pp. 2345–2357. https://doi.org/10.1093/jxb/ery361.

Pellerin, S. and Pagès, L. (1994) 'Evaluation of parameters describing the root system architecture of field grown maize plants (Zea mays L.)', *Plant and Soil*, 164(2), pp. 155–167. https://doi.org/10.1007/BF00010067.

Pellerin, S. and Tabourel, F. (1995) 'Length of the apical unbranched zone of maize axile roots: Its relationship to root elongation rate', *Environmental and Experimental Botany*, 35(2), pp. 193–200. https://doi.org/10.1016/0098-8472(94)00043-5.

Pieruschka, R. and Schurr, U. (2019) *Plant Phenotyping: Past, Present, and Future*, *Plant Phenomics*. Science Partner Journal. https://doi.org/10.34133/2019/7507131.

Pioneer (2022) 'Pioneer, Optimum, AQUAmax', *Optimum® AQUAmax® Hybrids*. Available at: https://www.pioneer.com/us/products/corn/traits-technologies/aquamax.html (Accessed: 19 June 2022).

Postma, J., Jaramillo, R. and Lynch, J. (2008) *Towards Modeling the Function of Root Traits for Enhancing Water Acquisition by Crops*.

Postma, J.A. *et al.* (2017) 'OpenSimRoot: widening the scope and application of root architectural models', *New Phytologist*, 215(3), pp. 1274–1286. https://doi.org/10.1111/nph.14641.

Price, A.H. *et al.* (2002) 'Upland rice grown in soil-filled chambers and exposed to contrasting water-deficit regimes: I. Root distribution, water use and plant water status', *Field Crops Research*, 76(1), pp. 11–24. https://doi.org/10.1016/S0378-4290(02)00012-6.

R Core Team (2021) *R: A language and Environment for Statistical Computing*. Vienna, Austria: R Foundation for Statistical Computing. Available at: https://www.R-project.org/.

Raats, P.A.C. (1974) 'Steady Flows of Water and Salt in Uniform Soil Profiles with Plant Roots', *Soil Science Society of America Journal*, 38(5), pp. 717–722. https://doi.org/10.2136/sssaj1974.03615995003800050012x.

Rafalski, J.A. (2010) 'Association genetics in crop improvement', *Current Opinion in Plant Biology*, 13(2), pp. 174–180. https://doi.org/10.1016/j.pbi.2009.12.004.

Rajurkar, A.B. *et al.* (2022) 'Installation and imaging of thousands of minirhizotrons to phenotype root systems of field-grown plants', *Plant Methods*, 18(1), p. 39. https://doi.org/10.1186/s13007-022-00874-2.

Rangarajan, H. *et al.* (2022) 'Multi-objective optimization of root phenotypes for nutrient capture using evolutionary algorithms', *The Plant Journal*. https://doi.org/10.1111/tpj.15774.

Rasband W.S. (2011) 'ImageJ'. Available at: https://imagej.nih.gov/ij/ (Accessed: 17 June 2022).

Rellán-Álvarez, R. *et al.* (2015) 'GLO-Roots: an imaging platform enabling multidimensional characterization of soil-grown root systems', *eLife*, 4. https://doi.org/10.7554/eLife.07597.

Rich, S.M. *et al.* (2020) 'Root phenotypes of young wheat plants grown in controlled environments show inconsistent correlation with mature root traits in the field', *Journal of Experimental Botany*, 71(16), pp. 4751–4762. https://doi.org/10.1093/jxb/eraa201.

Rich, S.M. and Watt, M. (2013) 'Soil conditions and cereal root system architecture: review and considerations for linking Darwin and Weaver', *Journal of Experimental Botany*, 64(5), pp. 1193–1208. https://doi.org/10.1093/jxb/ert043.

Richard, C.A. *et al.* (2015) 'High-throughput phenotyping of seminal root traits in wheat', *Plant Methods*, 11(1), p. 13. https://doi.org/10.1186/s13007-015-0055-9.

Rincent, R. *et al.* (2019) 'Using crop growth model stress covariates and AMMI decomposition to better predict genotype-by-environment interactions', *Theoretical and Applied Genetics*, 132(12), pp. 3399–3411. https://doi.org/10.1007/s00122-019-03432-y.

Rivington, M. *et al.* (2015) *Extreme weather and resilience of the global food system - Synthesis Report*.

RStudio Team (2019) *RStudio: Integrated Development Environment for R*. Boston, MA: RStudio, PBC. Available at: http://www.rstudio.com/.

Sáenz Rodríguez, M.N. and Cassab, G.I. (2021) 'Primary Root and Mesocotyl Elongation in Maize Seedlings: Two Organs with Antagonistic Growth below the Soil Surface', Plants, 10(7), p. 1274. Available at: https://doi.org/10.3390/plants10071274.

Saint Cast, C. *et al.* (2022) 'Connecting plant phenotyping and modelling communities: lessons from science mapping and operational perspectives', *in silico Plants*, 4(1), p. diac005. https://doi.org/10.1093/insilicoplants/diac005.

Salim, M.H., Todd, G.W. and Schlehuber, A.M. (1965) 'Root Development of Wheat, Oats, and Barley Under Conditions of Soil Moisture Stress1', *Agronomy Journal*, 57(6), pp. 603–607. https://doi.org/10.2134/agronj1965.00021962005700060026x.

Sanguineti, M.C. *et al.* (2007) 'Genetic dissection of seminal root architecture in elite durum wheat germplasm', *Annals of Applied Biology*, 151(3), pp. 291–305. https://doi.org/10.1111/j.1744-7348.2007.00198.x.

Schneider, H.M. and Lynch, J.P. (2020) 'Should Root Plasticity Be a Crop Breeding Target?', *Frontiers in Plant Science*, 11. https://doi.org/10.3389/fpls.2020.00546.

Schnepf, A. *et al.* (2018) 'CRootBox: A structural-functional modelling framework for root systems', *Annals of botany*, 121. https://doi.org/10.1093/aob/mcx221.

Sharma, S. *et al.* (2011) 'Dissection of QTL effects for root traits using a chromosome arm-specific mapping population in bread wheat', *Theoretical and Applied Genetics*, 122(4), pp. 759–769. https://doi.org/10.1007/s00122-010-1484-5.

Sharp, R.E. et al. (2004) 'Root growth maintenance during water deficits: physiology to functional genomics', Journal of Experimental Botany, 55(407), pp. 2343–2351. Available at: https://doi.org/10.1093/jxb/erh276.

Sheng, M. *et al.* (2009) 'Influence of arbuscular mycorrhizae on the root system of maize plants under salt stress', *Canadian Journal of Microbiology*, 55(7), pp. 879–886. https://doi.org/10.1139/w09-031.

Shewry, P.R. (2009) 'Wheat', *Journal of Experimental Botany*, 60(6), pp. 1537–1553. https://doi.org/10.1093/jxb/erp058.

Shi, J. *et al.* (2014) 'Dynamic responses of wheat to drought and nitrogen stresses during re-watering cycles', *Agricultural Water Management*, 146, pp. 163–172. https://doi.org/10.1016/j.agwat.2014.08.006.

Shrestha, R. *et al.* (2014) 'Comparing simple root phenotyping methods on a core set of rice genotypes', *Plant Biology*, 16(3), pp. 632–642. https://doi.org/10.1111/plb.12096.

Sjulgård, H. *et al.* (2021) 'Reversible and irreversible root phenotypic plasticity under fluctuating soil physical conditions', *Environmental and Experimental Botany*, 188, p. 104494. https://doi.org/10.1016/j.envexpbot.2021.104494.

Smith, A.G. *et al.* (2020) 'RootPainter: Deep Learning Segmentation of Biological Images with Corrective Annotation', *bioRxiv*, p. 2020.04.16.044461. https://doi.org/10.1101/2020.04.16.044461.

SolACE (2022) 'SolACE website'. Available at: https://www.solace-eu.net (Accessed: 17 June 2022).

Soriano, J.M. and Alvaro, F. (2019) 'Discovering consensus genomic regions in wheat for root-related traits by QTL meta-analysis', *Scientific Reports*, 9(1), pp. 1–14. https://doi.org/10.1038/s41598-019-47038-2.

Steffen, W. *et al.* (2015) 'Planetary boundaries: Guiding human development on a changing planet', *Science*, 347(6223), p. 1259855. https://doi.org/10.1126/science.1259855.

Su, S.-H. et al. (2017) 'Molecular Mechanisms of Root Gravitropism', Current Biology, 27(17), pp. R964–R972. Available at: https://doi.org/10.1016/j.cub.2017.07.015.

Suzuki, N. *et al.* (2014) 'Abiotic and biotic stress combinations', *New Phytologist*, 203(1), pp. 32–43. https://doi.org/10.1111/nph.12797.

Tardieu, F. (2010) 'Why work and discuss the basic principles of plant modelling 50 years after the first plant models?', *Journal of Experimental Botany*, 61(8), pp. 2039–2041. https://doi.org/10.1093/jxb/erq135.

Tardieu, F. *et al.* (2017) 'Plant Phenomics, From Sensors to Knowledge', *Current Biology*, 27(15), pp. R770–R783. https://doi.org/10.1016/j.cub.2017.05.055.

Thaler, P. and Pagès, L. (1996) 'Root apical diameter and root elongation rate of rubber seedlings (Hevea brasiliensis) show parallel responses to photoassimilate availability', *Physiologia Plantarum*, 97(2), pp. 365–371. https://doi.org/10.1034/j.1399-3054.1996.970222.x.

Tracy, S.R. *et al.* (2020) 'Crop Improvement from Phenotyping Roots: Highlights Reveal Expanding Opportunities', *Trends in Plant Science*, 25(1), pp. 105–118. https://doi.org/10.1016/j.tplants.2019.10.015.

Tricot, F., Crozat, Y. and Pellerin, S. (1997) 'Root system growth and nodule establishment on pea (Pisum sativum L.)', *Journal of Experimental Botany*, 48(11), pp. 1935–1941. https://doi.org/10.1093/jxb/48.11.1935.

Tsegaye, D. *et al.* (2012) 'Genetic variability, correlation and path analysis in durum wheat germplasm (Triticum durum Desf)'.

Tuberosa, R. *et al.* (2002) 'Identification of QTLs for root characteristics in maize grown in hydroponics and analysis of their overlap with QTLs for grain yield in the field at two water regimes', *Plant Molecular Biology*, 48(5), pp. 697–712. https://doi.org/10.1023/A:1014897607670.

Tuberosa, R. *et al.* (2003) 'Searching for quantitative trait loci controlling root traits in maize: a critical appraisal', *Plant and Soil*, 255(1), pp. 35–54. Available at: https://www.jstor.org/stable/24121101 (Accessed: 19 May 2022).

Tuberosa, R. and Salvi, S. (2005) 'QTLs and Genes for Tolerance to Abiotic Stress in Cereals', in P.K. Gupta and R.K. Varshney (eds) *Cereal Genomics*. Dordrecht: Springer Netherlands, pp. 253–315. https://doi.org/10.1007/1-4020-2359-6_9.

Ubbens, J.R. and Stavness, I. (2017) 'Deep Plant Phenomics: A Deep Learning Platform for Complex Plant Phenotyping Tasks', *Frontiers in Plant Science*, 8. Available at: https://www.frontiersin.org/article/10.3389/fpls.2017.01190 (Accessed: 19 April 2022).

Verma, V. *et al.* (2005) 'Identification and characterization of quantitative trait loci related to lodging resistance and associated traits in bread wheat', *Plant Breeding*, 124(3), pp. 234–241. https://doi.org/10.1111/j.1439-0523.2005.01070.x.

Wacker, T.S. *et al.* (2022) 'Semifield root phenotyping: Root traits for deep nitrate uptake', *Plant, Cell & Environment*, 45(3), pp. 823–836. https://doi.org/10.1111/pce.14227.

Waisel, Y. *et al.* (2002) *Plant Roots: The Hidden Half, Third Edition*. CRC Press.

Wang, J. and Zhang, Z. (2021) 'GAPIT Version 3: Boosting Power and Accuracy for Genomic Association and Prediction', *Genomics, Proteomics & Bioinformatics*, 19(4), pp. 629–640. https://doi.org/10.1016/j.gpb.2021.08.005.

Wasaya, A. *et al.* (2018) 'Root Phenotyping for Drought Tolerance: A Review', *Agronomy*, 8(11), p. 241. https://doi.org/10.3390/agronomy8110241.

Watt, M. *et al.* (2013) 'A rapid, controlled-environment seedling root screen for wheat correlates well with rooting depths at vegetative, but not reproductive, stages at two field sites', *Annals of Botany*, 112(2), pp. 447–455. https://doi.org/10.1093/aob/mct122.

Watt, M. *et al.* (2020) 'Phenotyping: New Windows into the Plant for Breeders', *Annual Review of Plant Biology*, 71(1), pp. 689–712. https://doi.org/10.1146/annurev-arplant-042916-041124.

White, P.J. *et al.* (2013) 'Matching roots to their environment', *Annals of Botany*, 112(2), pp. 207–222. https://doi.org/10.1093/aob/mct123.

Wu, Q., Pagès, L. and Wu, J. (2016) 'Relationships between root diameter, root length and root branching along lateral roots in adult, field-grown maize', *Annals of Botany*, 117(3), pp. 379–390. https://doi.org/10.1093/aob/mcv185.

Xia, T. *et al.* (2020) 'An invasive plant experiences greater benefits of root morphology from enhancing nutrient competition associated with arbuscular mycorrhizae in karst soil than a native plant', *PLOS ONE*, 15(6), p. e0234410. https://doi.org/10.1371/journal.pone.0234410.

Xie, Q. *et al.* (2017) 'Identifying seedling root architectural traits associated with yield and yield components in wheat', *Annals of Botany*, 119(7), pp. 1115–1129. https://doi.org/10.1093/aob/mcx001.

Yasrab, R. *et al.* (2019) 'RootNav 2.0: Deep learning for automatic navigation of complex plant root architectures', *GigaScience*, 8(11), p. giz123. https://doi.org/10.1093/gigascience/giz123.

Zang, J., Elliott, R. and Ketring, D.L. (1993) 'Root Distribution Models Applied to Peanuts', *Transactions of the ASAE.*, (36(3)), pp. 727–734. https://doi.org/10.13031/2013.28391.

Zhang, H. and Sonnewald, U. (2017) 'Differences and commonalities of plant responses to single and combined stresses', *The Plant Journal*, 90(5), pp. 839–855. https://doi.org/10.1111/tpj.13557.

Annexes

1. PANEL COMPOSITION

1.1. BREAD WHEAT PANEL

Table 12. Composition of the bread wheat panel, names of the genotypes, their category of origin, their country and continent of origin, as well as their year of release.

Number	SolACE.Code	Name	Origin	Country	Continent	Year
1	SBW1001	BENNI	BreedWheat	United States	America	1980
2	SBW1002	BONNY	BreedWheat	Kenya	Africa	1966
3	SBW1007	JACOMETTI 49	BreedWheat	Italy	Europe	1966
4	SBW1008	KLEIN 32	BreedWheat	Argentina	America	1932
5	SBW1010	MCNAIR 1587	BreedWheat	United States	America	1973
6	SBW1011	MONON	BreedWheat	United States	America	1959
7	SBW1012	MV03-86	BreedWheat	Hungary	Europe	1986
8	SBW1014	OBRII	BreedWheat	Ukraine	Asia	1983
9	SBW1016	ROMA	BreedWheat	Italy	Europe	1935
10	SBW1019	ZG7865/83	BreedWheat	Croatia	Europe	1983
11	SBW1021	BOURGOGNE	BreedWheat	France	Europe	1995
12	SBW1023	TALDOR	BreedWheat	France	Europe	1997
13	SBW1024	MIRONOVSKAIA 31	BreedWheat	Ukraine	Asia	1992
14	SBW1026	FRUNZENSKAIA 60	BreedWheat	Kyrgyzstan	Asia	1982
15	SBW1027	GONCHA	BreedWheat	Turkmenistan	Asia	-
16	SBW1028	308.02.2/WEAVER//F362K2.121	BreedWheat	Turks and Caicos Islands	America	-
17	SBW1029	DEMAR-4	BreedWheat	Italy	Europe	1965
18	SBW1030	ZG3073/84	BreedWheat	Croatia	Europe	1984
19	SBW1031	OWL/COL NO.3625//SOISSONS	BreedWheat	Iran	Asia	-
20	SBW1034	BOLAL	BreedWheat	United States	America	1970
21	SBW1038	HATVANI 40/25	BreedWheat	Hungary	Europe	-
22	SBW1039	KARCAGI 149	BreedWheat	Hungary	Europe	1967
23	SBW1040	MCNAIR 701	BreedWheat	United States	America	1973
24	SBW1041	MONTJOIE	BreedWheat	France	Europe	1969
25	SBW1045	SCOUT66	BreedWheat	United States	America	1967
26	SBW1047	TAM108	BreedWheat	United States	America	1984
27	SBW1048	TRAYANA	BreedWheat	Bulgaria	Europe	1981
28	SBW1049	LORETO	BreedWheat	Italy	Europe	1982
29	SBW1051	MACNAIR1813	BreedWheat	United States	America	1981
30	SBW1055	ZITNICA	BreedWheat	Yugoslavia	Europe	1982
31	SBW1056	BERMET	BreedWheat	Kyrgyzstan	Asia	1998
32	SBW1058	SWM89Y074H	BreedWheat	Armenia	Asia	-
33	SBW1060	AKULA/BONITO//F10S-3	BreedWheat	Turks and Caicos Islands	America	-
34	SBW1061	BONITO//KAREE/TUGELA	BreedWheat	Turks and Caicos Islands	America	-
35	SBW1062	KL.ESTRELLA	BreedWheat	Argentina	America	1995
36	SBW1064	MUSTANG	BreedWheat	United States	America	1983
37	SBW1066	2109-36	BreedWheat	Bulgaria	Europe	1976
38	SBW1067	2678-6	BreedWheat	Bulgaria	Europe	-
39	SBW1068	2838-39	BreedWheat	Bulgaria	Europe	-
40	SBW1069	ALBIDUM	BreedWheat	Uzbekistan	Asia	1974
41	SBW1070	ARPADHALOM-16	BreedWheat	Hungary	Europe	-
42	SBW1071	AUTONOMIA	BreedWheat	Italy	Europe	1938
43	SBW1072	BUCKSKIN	BreedWheat	United States	America	1973
44	SBW1073	CARSON	BreedWheat	United States	America	1986
45	SBW1080	STACY	BreedWheat	United States	America	1980
46	SBW1081	WHEELER	BreedWheat	United States	America	1980
47	SBW1082	ZGIPK.4387	BreedWheat	Croatia	Europe	-
48	SBW1083	VIENOY	BreedWheat	France	Europe	1994
49	SBW1085	GEREK79	BreedWheat	Turkey	Asia	1979
50	SBW1091	TAMEX	BreedWheat	United States	America	1980

51	SBW1094	COUGAR	BreedWheat	United States	America	1999
52	SBW1096	SKOPJANKA	BreedWheat	Macedonia	Europe	1982
53	SBW1101	CAPET	BreedWheat	France	Europe	1989
54	SBW1102	COLORBEN-4	BreedWheat	Italy	Europe	1966
55	SBW1105	DACIA	BreedWheat	Romania	Europe	1971
56	SBW1108	FOISON	BreedWheat	France	Europe	1985
57	SBW1110	GK-KALAKA	BreedWheat	Hungary	Europe	1990
58	SBW1111	HOKUEI	BreedWheat	Japan	Asia	1965
59	SBW1112	MUTSUBENKEY	BreedWheat	Japan	Asia	1950
60	SBW1114	NECTAR	BreedWheat	France	Europe	1985
61	SBW1115	NS RANA 1	BreedWheat	Yugoslavia	Europe	1975
62	SBW1119	ROSE	BreedWheat	United States	America	1981
63	SBW1120	RUBIS	BreedWheat	Sweden	Europe	1962
64	SBW1121	SADOVOSUPER	BreedWheat	Bulgaria	Europe	1979
65	SBW1124	TECUMSEH	BreedWheat	United States	America	1974
66	SBW1126	SALMONE	BreedWheat	Italy	Europe	1980
67	SBW1127	KOTARE	BreedWheat	New Zealand	Oceania	1984
68	SBW1129	MADRIGAL	BreedWheat	Great Britain	Europe	1995
69	SBW1135	TILEK	BreedWheat	Kyrgyzstan	Asia	2001
70	SBW1137	MCGUIRE	BreedWheat	United States	America	1996
71	SBW1144	TCI960735	BreedWheat	Turkey	Asia	-
72	SBW1146	AGROUNIA	BreedWheat	Yugoslavia	Europe	1987
73	SBW1147	BRACO	BreedWheat	France	Europe	1977
74	SBW1148	CEREALOR	BreedWheat	France	Europe	1964
75	SBW1149	CHAMBORD	BreedWheat	France	Europe	1960
76	SBW1150	DECLIC	BreedWheat	France	Europe	1985
77	SBW1151	HOROSHIRI KOMUGI	BreedWheat	Japan	Asia	1974
78	SBW1154	SOLARIS	BreedWheat	Czech Republic	Europe	1976
79	SBW1158	MIRONOVSKAIA 30	BreedWheat	Ukraine	Asia	1995
80	SBW1163	MV309-99	BreedWheat	Hungary	Europe	1999
81	SBW1165	GR915	BreedWheat	United States	America	1991
82	SBW1169	ES14/SITTA//AGRI/NAC	BreedWheat	Turks and Caicos Islands	America	-
83	SBW1170	BILINMIYEN96.40	BreedWheat	Turks and Caicos Islands	America	-
84	SBW1171	TCI962395	BreedWheat	Turks and Caicos Islands	America	-
85	SBW1172	QUENOA INIA	BreedWheat	Chile	America	1995
86	SBW1173	ADENA	BreedWheat	United States	America	1984
87	SBW1178	ALBATROS	BreedWheat	Belgium	Europe	1950
88	SBW1179	LUNA	BreedWheat	Poland	Europe	1970
89	SBW1181	LUTESCENS CH65/85	BreedWheat	Ukraine	Asia	1985
90	SBW1186	REDLAND	BreedWheat	United States	America	1986
91	SBW1188	SALUDA	BreedWheat	United States	America	1983
92	SBW1194	BRANKA	BreedWheat	Czech Republic	Europe	1988
93	SBW1196	NOBLET	BreedWheat	France	Europe	1995
94	SBW1199	WWL860104	BreedWheat	Turkey	Asia	-
95	SBW1201	BRUTA	BreedWheat	Czech Republic	Europe	1994
96	SBW1204	CIT89073	BreedWheat	Turkey	Asia	-
97	SBW1206	GK ZUGOLY	BreedWheat	Hungary	Europe	1994
98	SBW1207	ODESKA 161	BreedWheat	Ukraine	Asia	1995
99	SBW1211	MV314-99	BreedWheat	Hungary	Europe	1999
100	SBW1213	P29	BreedWheat	United States	America	1996
101	SBW1216	PROWERS 99	BreedWheat	United States	America	1999
102	SBW1217	TAISETSU KOMUGI	BreedWheat	Japan	Asia	1990
103	SBW1218	MAGISTRAL	BreedWheat	Romania	Europe	1998
104	SBW1219	GARAGUM	BreedWheat	Turkmenistan	Asia	2000
105	SBW1220	PAT	BreedWheat	United States	America	2001
106	SBW1221	CRVENA ZVESDA	BreedWheat	Yugoslavia	Europe	1967
107	SBW1224	HOSAR	BreedWheat	United States	America	1930
108	SBW1225	SUSQUEHANNA	BreedWheat	United States	America	1988
109	SBW1228	DI7003-1-12	BreedWheat	France	Europe	-
110	SBW1231	LUTESCENS EG16/82	BreedWheat	Ukraine	Asia	1984
111	SBW1234	MV23-77	BreedWheat	Hungary	Europe	1978
112	SBW1235	NEUHOF 1	BreedWheat	Austria	Europe	1969
113	SBW1241	TORRIL	BreedWheat	France	Europe	1989
114	SBW1245	ARTHUR	BreedWheat	United States	America	1968
115	SBW1249	MV-MAGVAS	BreedWheat	Hungary	Europe	1998

116	SBW1250	ALKA	BreedWheat	Czech Republic	Europe	1995
117	SBW1255	MIRLEBEN	BreedWheat	Ukraine	Asia	1993
118	SBW1258	RAMPART	BreedWheat	United States	America	1996
119	SBW1266	ECRIN	BreedWheat	France	Europe	1985
120	SBW1268	HERKULES	BreedWheat	Hungary	Europe	-
121	SBW1276	LANGUEDOC	BreedWheat	France	Europe	1962
122	SBW1279	MV33-86	BreedWheat	Hungary	Europe	1986
123	SBW1280	PROBSTDORFER MARTIN	BreedWheat	Austria	Europe	1982
124	SBW1282	TIMMO	BreedWheat	Sweden	Europe	1982
125	SBW1283	UTE	BreedWheat	United States	America	1983
126	SBW1284	SIROKA	BreedWheat	Croatia	Europe	1984
127	SBW1287	830-22	BreedWheat	Bulgaria	Europe	-
128	SBW1288	MV30-86	BreedWheat	Hungary	Europe	1986
129	SBW1292	PROBSTDORFER ACCORD	BreedWheat	Austria	Europe	1967
130	SBW1297	SANRAFAEL	BreedWheat	Spain	Europe	1964
131	SBW1300	ORMIL	BreedWheat	France	Europe	1996
132	SBW1301	BEHERT	BreedWheat	France	Europe	1994
133	SBW1302	MIRONIVSKA 68	BreedWheat	Ukraine	Asia	1999
134	SBW1304	CDC-CLAIR	BreedWheat	Canada	America	1997
135	SBW1308	MALYSA	BreedWheat	Slovakia	Europe	1998
136	SBW1310	SANSA	BreedWheat	Spain	Europe	1988
137	SBW1311	CAMINO	BreedWheat	Switzerland	Europe	1993
138	SBW1314	ALTERNA-TOURNEUR	BreedWheat	France	Europe	1957
139	SBW1315	ARGEE	BreedWheat	United States	America	1976
140	SBW1316	CH73641	BreedWheat	Switzerland	Europe	1982
141	SBW1317	DI7202-103	BreedWheat	France	Europe	-
142	SBW1319	DRUZHBA	BreedWheat	Russia	Asia	1981
143	SBW1320	GERMINAL	BreedWheat	France	Europe	1969
144	SBW1324	NUGAINES	BreedWheat	United States	America	1965
145	SBW1325	OVEST	BreedWheat	Italy	Europe	1961
146	SBW1326	P4523-80	BreedWheat	Austria	Europe	-
147	SBW1327	PAGEANT	BreedWheat	Great Britain	Europe	1981
148	SBW1328	PEGASUS	BreedWheat	New Zealand	Oceania	1985
149	SBW1332	RIDA	BreedWheat	Norway	Europe	1977
150	SBW1334	ULM	BreedWheat	France	Europe	1983
151	SBW1338	CH73425	BreedWheat	Switzerland	Europe	1979
152	SBW1341	HOLZAPFELS FRUH WEIZEN	BreedWheat	Germany	Europe	1917
153	SBW1345	SIMONA	BreedWheat	Czech Republic	Europe	1991
154	SBW1346	SEMPER	BreedWheat	Netherlands	Europe	1998
155	SBW1348	ABEL	BreedWheat	France	Europe	1961
156	SBW1353	CHARMANY	BreedWheat	United States	America	1984
157	SBW1354	COURTAL	BreedWheat	France	Europe	1943
158	SBW1355	ERSHOVSKAJA-3	BreedWheat	Russia	Asia	1973
159	SBW1356	FANION	BreedWheat	France	Europe	1978
160	SBW1358	FLORIO	BreedWheat	Great Britain	Europe	1993
161	SBW1359	MALACCA	BreedWheat	Great Britain	Europe	1997
162	SBW1360	PRESTIGE	BreedWheat	France	Europe	1969
163	SBW1361	PRIMEPI	BreedWheat	France	Europe	1962
164	SBW1362	PROBSTDORFER GEBER	BreedWheat	Austria	Europe	1969
165	SBW1364	RINNER WINTERWEISEN	BreedWheat	Austria	Europe	1972
166	SBW1365	STADLER	BreedWheat	United States	America	1964
167	SBW1366	STETSON	BreedWheat	Great Britain	Europe	1981
168	SBW1370	YORKSTAR	BreedWheat	United States	America	1968
169	SBW1372	MAXIMUM CAMBIER	BreedWheat	France	Europe	1936
170	SBW1373	FERDINAND	BreedWheat	Austria	Europe	1982
171	SBW1374	ROD	BreedWheat	United States	America	1992
172	SBW1377	EDWIN	BreedWheat	United States	America	1999
173	SBW1378	BOVICTUS	BreedWheat	Germany	Europe	1993
174	SBW1380	DI37-12-2	BreedWheat	France	Europe	-
175	SBW1390	FROIDURE	BreedWheat	France	Europe	1960
176	SBW1392	SIRIA	BreedWheat	Czech Republic	Europe	1994
177	SBW1393	REGINA	BreedWheat	Czech Republic	Europe	1981
178	SBW1398	IWWRN(85)198	BreedWheat	Chile	America	-
179	SBW1403	MIRONOVSKAIA 264	BreedWheat	Ukraine	Asia	1960
180	SBW1406	RENVAL	BreedWheat	Belgium	Europe	1977

181	SBW1407	ROISEL	BreedWheat	France	Europe	1967
182	SBW1408	TAMBO	BreedWheat	Switzerland	Europe	1985
183	SBW1410	VERBESSERTER ST.JOHANNER	BreedWheat	Austria	Europe	1962
184	SBW1411	BIZEL	BreedWheat	France	Europe	1966
185	SBW1412	CAROLUS	BreedWheat	Germany	Europe	1985
186	SBW1413	CH73241	BreedWheat	Switzerland	Europe	1979
187	SBW1415	DANKOWSKA IDEALNA	BreedWheat	Poland	Europe	1920
188	SBW1417	DI7210-15-11	BreedWheat	France	Europe	-
189	SBW1425	ZETA	BreedWheat	Poland	Europe	1978
190	SBW1426	ALTER DE GEMBLOUX	BreedWheat	Belgium	Europe	-
191	SBW1427	COMPACT	BreedWheat	United States	America	1974
192	SBW1428	FERMO	BreedWheat	Switzerland	Europe	1978
193	SBW1429	GELPA	BreedWheat	France	Europe	1967
194	SBW1435	PROTEKTOR	BreedWheat	Austria	Europe	1974
195	SBW1436	TRUBILO	BreedWheat	Germany	Europe	1948
196	SBW1437	VAKKA	BreedWheat	Finland	Europe	1953
197	SBW1439	REICHERSBERG 42	BreedWheat	Austria	Europe	1955
198	SBW1441	AUBE	BreedWheat	France	Europe	1960
199	SBW1444	BONTARIS	BreedWheat	Germany	Europe	1990
200	SBW1446	ATUT-II	BreedWheat	Austria	Europe	1974
201	SBW2001	ALLEZ Y	Checks	France	Europe	2010
202	SBW2002	APACHE	Checks	France	Europe	1998
203	SBW2003	BERMUDE	Checks	France	Europe	2007
204	SBW2004	RUBISKO	Checks	France	Europe	2011
205	SBW2005	TRAPEZ	Checks	France	Europe	2009
206	SBW3001	ANTEQUERA	Local variety	Spain	Europe	2008
207	SBW3002	CH NARA	Local variety	Switzerland	Europe	2007
208	SBW3003	LUDWIG	Local variety	Austria	Europe	1997
209	SBW3004	NOGAL	Local variety	France	Europe	2010
210	SBW3005	WIWA	Local variety	Switzerland	Europe	2005
211	SBW4001	AKAMAR	Parents	Italy	Europe	2010
212	SBW4002	ARLEQUIN:B-	Parents	France	Europe	2007
213	SBW4003	ATHLON:B-	Parents	France	Europe	2010
214	SBW4004	BOLOGNA:B-	Parents	Spain	Europe	2002
215	SBW4005	CCB09H046:B-	Parents	-	-	-
216	SBW4006	GIAMBOLOGNA:B-	Parents	Italy	Europe	2016
217	SBW4007	H15FR11757:B-	Parents	-	-	-
218	SBW4008	H15FR13047:B-	Parents	-	-	-
219	SBW4009	OREGRAIN:B-	Parents	France	Europe	2011
220	SBW4010	SUBLIM:B-	Parents	France	Europe	2009
221	SBW4011	SY 116464:B-	Parents	-	-	-
222	SBW4012	SY 117071:B-	Parents	-	-	-
223	SBW4013	SY 117079:B-	Parents	-	-	-
224	SBW4014	SY MATTIS:B-	Parents	France	Europe	2010
225	SBW5001	ANNIBALE/AKAMAR	Hybrids	-	-	-
226	SBW5002	BOLOGNA/GIAMBOLOGNA	Hybrids	-	-	-
227	SBW5003	H15FR11757/SY MATTIS	Hybrids	-	-	-
228	SBW5004	H15FR13047/OREGRAIN	Hybrids	-	-	-
229	SBW5005	SUBLIM/ATHLON	Hybrids	-	-	-
230	SBW5006	SUBLIM/GIAMBOLOGNA	Hybrids	-	-	-
231	SBW5007	SUBLIM/OREGRAIN	Hybrids	-	-	-
232	SBW5008	SY 116464/ATHLON	Hybrids	-	-	-
233	SBW5009	SY 117071/ARLEQUIN	Hybrids	-	-	-
234	SBW5010	SY 117079/AKAMAR	Hybrids	-	-	-

1.2. DURUM WHEAT PANEL

Table 13. Composition of the durum wheat panel (DW), names of the genotypes, their category of origin, their country and continent of origin, as well as their year of release.

Number	SolACE.Code	Name	Origin	Country	Continent	Year
1	SDW1001	AGATHE	GPDUR	France	Europe	1970
2	SDW1002	ALEXIS	GPDUR	France	Europe	2010
3	SDW1003	ANVERGUR	GPDUR	France	Europe	2012
4	SDW1004	ARCOUR	GPDUR	France	Europe	1981
5	SDW1005	ARGELES	GPDUR	France	Europe	1997
6	SDW1006	ATHORIS	GPDUR	Spain	Europe	2011
7	SDW1007	ATOUDUR	GPDUR	France	Europe	2010
8	SDW1008	AVENTUR	GPDUR	France	Europe	2010
9	SDW1009	BABYLONE	GPDUR	France	Europe	2009
10	SDW1010	BYBLOS	GPDUR	France	Europe	2003
11	SDW1011	CHISTERA	GPDUR	France	Europe	2012
12	SDW1012	CLOVIS	GPDUR	France	Europe	2009
13	SDW1013	COUSSUR	GPDUR	France	Europe	2010
14	SDW1014	CULTUR	GPDUR	France	Europe	2007
15	SDW1015	DAKTER	GPDUR	France	Europe	2005
16	SDW1016	DAURUR	GPDUR	Italy	Europe	2013
17	SDW1017	DURIAC	GPDUR	France	Europe	1991
18	SDW1018	DUROBONUS	GPDUR	Austria	Europe	2004
19	SDW1019	FLORIDOU	GPDUR	France	Europe	2011
20	SDW1020	GIBUS	GPDUR	France	Europe	2012
21	SDW1021	ISILDUR	GPDUR	France	Europe	2007
22	SDW1022	KARUR	GPDUR	France	Europe	2002
23	SDW1023	LAHAN	GPDUR	-	-	-
24	SDW1024	LGBORIS	GPDUR	France	Europe	2016
25	SDW1025	LIBERDUR	GPDUR	France	Europe	2007
26	SDW1026	LUMINUR	GPDUR	France	Europe	2011
27	SDW1027	MEMPHIS	GPDUR	France	Europe	2009
28	SDW1028	MIRADOUX	GPDUR	France	Europe	2007
29	SDW1029	MONASTIR	GPDUR	Italy	Europe	2009
30	SDW1030	MONDUR	GPDUR	France	Europe	1977
31	SDW1031	MURANO	GPDUR	France	Europe	2010
32	SDW1032	NEMESIS	GPDUR	France	Europe	2009
33	SDW1033	NOBILIS	GPDUR	France	Europe	2013
34	SDW1034	PASTADOU	GPDUR	France	Europe	2013
35	SDW1035	PESCADOU	GPDUR	France	Europe	2002
36	SDW1036	PHARAON	GPDUR	France	Europe	2007
37	SDW1037	PICTUR	GPDUR	France	Europe	2009
38	SDW1038	PLUSSUR	GPDUR	France	Europe	2011
39	SDW1039	QUALIDOU	GPDUR	France	Europe	2011
40	SDW1040	RELIEF	GPDUR	France	Europe	2013
41	SDW1041	RGTFABIONUR	GPDUR	France	Europe	2013
42	SDW1042	RGTVOILUR	GPDUR	France	Europe	2016
43	SDW1043	SCULPTUR	GPDUR	France	Europe	2007
44	SDW1044	SYBANCO	GPDUR	France	Europe	2010
45	SDW1045	SYCISCO	GPDUR	France	Europe	2010
46	SDW1046	TABLUR	GPDUR	France	Europe	2010
47	SDW1047	TOMCLAIR	GPDUR	France	Europe	1975
48	SDW2001	ADONE	CREA	Italy	Europe	2012
49	SDW2002	AKENATON	CREA	France	Europe	2005
50	SDW2003	ALEMANNO	CREA	Italy	Europe	2006
51	SDW2004	AMBRAL	CREA	France	Europe	1986
52	SDW2005	ANCO_MARZIO=YUPARE	CREA	Italy	Europe	2003
53	SDW2006	ANTALIS	CREA	Italy	Europe	2013
54	SDW2007	ARNACORIS	CREA	Italy	Europe	2005
55	SDW2008	ARTEMIDE	CREA	Italy	Europe	2007
56	SDW2009	AUREO	CREA	Italy	Europe	2009
57	SDW2010	BALIDURO	CREA	Italy	Europe	1996

58	SDW2011	BRONTE	CREA	Italy	Europe	1996
59	SDW2012	CAPPELLI	CREA	Italy	Europe	1915
60	SDW2013	CASANOVA	CREA	Italy	Europe	2003
61	SDW2014	CICLOPE	CREA	Italy	Europe	2006
62	SDW2015	CORE	CREA	Italy	Europe	2008
63	SDW2016	CUSPIDE	CREA	Italy	Europe	2010
64	SDW2017	DARIO	CREA	Italy	Europe	2006
65	SDW2018	DESERT_KING_(ORO)	CREA	United States	America	2005
66	SDW2019	DORATO	CREA	Italy	Europe	2004
67	SDW2020	DYLAN	CREA	Italy	Europe	2002
68	SDW2021	ERCOLE	CREA	Italy	Europe	2003
69	SDW2022	FABULIS	CREA	France	Europe	2010
70	SDW2023	FURIO_CAMILLO	CREA	Italy	Europe	2012
71	SDW2024	GENNARO	CREA	-	-	2009
72	SDW2025	GHIBLI	CREA	Italy	Europe	2003
73	SDW2026	GIUSTO	CREA	Italy	Europe	2001
74	SDW2027	GLOCODUR	CREA	Italy	Europe	2011
75	SDW2028	ISMUR	CREA	France	Europe	2007
76	SDW2029	KANAKIS	CREA	Italy	Europe	2008
77	SDW2030	KARALIS	CREA	Italy	Europe	2002
78	SDW2031	KRONOS	CREA	United States	America	1992
79	SDW2032	L22D84=PR22D84	CREA	Italy	Europe	2016
80	SDW2033	L2574	CREA	Italy	Europe	-
81	SDW2034	MARAKAS	CREA	Italy	Europe	2012
82	SDW2035	MG_54	CREA	Italy	Europe	-
83	SDW2036	MIDYNU	CREA	-	-	-
84	SDW2037	MINOSSE	CREA	Italy	Europe	2008
85	SDW2038	NEGRIDURO	CREA	Greece	Europe	2002
86	SDW2039	OFANTO	CREA	Italy	Europe	1990
87	SDW2040	OVIDIO	CREA	Italy	Europe	2012
88	SDW2041	PAPADAKIS	CREA	Greece	Europe	2000
89	SDW2042	PICENO	CREA	Italy	Europe	1983
90	SDW2043	PR22D89	CREA	Italy	Europe	2005
91	SDW2044	QUADRATO	CREA	Italy	Europe	1999
92	SDW2045	RAMIREZ	CREA	Italy	Europe	2007
93	SDW2046	SACHEM	CREA	France	Europe	2000
94	SDW2047	SAN_CARLO	CREA	Italy	Europe	1996
95	SDW2048	SERAFO_NICK	CREA	Italy	Europe	2010
96	SDW2049	SIJAH_KILAKLI	CREA	-	-	-
97	SDW2050	SILUR	CREA	Italy	Europe	2001
98	SDW2051	STRONGFIELD	CREA	Canada	America	2003
99	SDW2052	SURAKA	CREA	Mexico	America	1991
100	SDW2053	SURMESUR	CREA	France	Europe	2010
101	SDW2054	SVEVO	CREA	Italy	Europe	1996
102	SDW2055	TIREX	CREA	Italy	Europe	2007
103	SDW2056	TIZIANA	CREA	Italy	Europe	2001
104	SDW2057	TORRESE	CREA	Italy	Europe	2008
105	SDW2058	VETRODUR	CREA	Italy	Europe	2000
106	SDW2059	ARIOSTO	CREA	Italy	Europe	2005
107	SDW2060	DORAL	CREA	France	Europe	1992
108	SDW2061	ASTERIX	CREA	Italy	Europe	2010
109	SDW2062	BALSAMO	CREA	Italy	Europe	1993
110	SDW2063	CAPDUR	CREA	France	Europe	1981
111	SDW2064	ELIOS	CREA	Italy	Europe	1993
112	SDW2065	FENICE	CREA	Italy	Europe	1993
113	SDW2066	MATT	CREA	Greece	Europe	2003
114	SDW2067	OLIVER	CREA	Italy	Europe	2010
115	SDW2068	SELCUKLU-97	CREA	Turkey	Asia	1997
116	SDW2069	SY_EXPERT	CREA	Italy	Europe	2008
117	SDW3001	JOYAU	UNIBO	France	Europe	2002
118	SDW3002	SARAGOLLA	UNIBO	Italy	Europe	2004
119	SDW3003	NADIF	UNIBO	Italy	Europe	2016
120	SDW3004	CICCIO	UNIBO	Italy	Europe	1999
121	SDW3005	TEXUR	UNIBO	Italy	Europe	2012
122	SDW3006	TEODORICO	UNIBO	Italy	Europe	2015

123	SDW3007	ACADUR	UNIBO	Italy	Europe	2015
124	SDW3008	ACHILLE	UNIBO	Italy	Europe	2006
125	SDW3009	ALDEANO-DP028	UNIBO	Italy	Europe	1998
126	SDW3010	AMMAR-1-DP122	UNIBO	Algeria	Africa	2010
127	SDW3011	AW12/BIT-DP060	UNIBO	-	-	-
128	SDW3012	BOLIDO-DP034	UNIBO	Spain	Europe	1998
129	SDW3013	CASTELDOUX	UNIBO	France	Europe	2015
130	SDW3014	CESARE	UNIBO	Italy	Europe	2010
131	SDW3015	CYMMIT67-PLATA16-DP016	UNIBO	-	-	-
132	SDW3016	COLOMBO	UNIBO	Italy	Europe	2011
133	SDW3017	CREDIT	UNIBO	Italy	Europe	2009
134	SDW3018	GEROMTEL-1-DP139	UNIBO	Syria	Asia	-
135	SDW3019	GIBRALTAR	UNIBO	Italy	Europe	2011
136	SDW3020	GIDARA-2-DP141	UNIBO	Turkey	Asia	2004
137	SDW3021	H.MOUL(MOR)/CHABA88-DP065	UNIBO	-	-	-
138	SDW3022	INRAM1808=AMRIA-DP049	UNIBO	Morocco	Africa	-
139	SDW3023	JAWHAR-DP053	UNIBO	Morocco	Africa	1994
140	SDW3024	JORDAN-DP150	UNIBO	-	-	-
141	SDW3025	KIKO-NICK	UNIBO	Italy	Europe	2009
142	SDW3026	LAGONIL-2	UNIBO	-	-	-
143	SDW3027	LLOYD	UNIBO	France	Europe	1992
144	SDW3028	LOUKOS-1_DP157	UNIBO	Mexico	America	1990
145	SDW3029	MARJANA-DP054	UNIBO	Morocco	Africa	1996
146	SDW3030	NEFER-DP205	UNIBO	France	Europe	1995
147	SDW3031	OBELIX	UNIBO	Italy	Europe	2012
148	SDW3032	OMGENIL-3_DP166	UNIBO	-	-	-
149	SDW3033	OMRABI-5_DP071	UNIBO	Syria	Asia	1994
150	SDW3034	ORT-1_DP170	UNIBO	-	-	-
151	SDW3035	PLINIO_DP107	UNIBO	Italy	Europe	1988
152	SDW3036	ROQUENO_DP110	UNIBO	Spain	Europe	1991
153	SDW3037	TITO_FLAVIO	UNIBO	Italy	Europe	2013
154	SDW3038	ATIL_C2000_DP252	UNIBO	Mexico	America	2001
155	SDW3039	CHAM-1_DP136	UNIBO	Syria	Asia	1984
156	SDW3040	CRESO_DP089	UNIBO	Italy	Europe	1974
157	SDW3041	GALLARETA_DP041	UNIBO	Mexico	America	1982
158	SDW3042	KOFA	UNIBO	United States	America	1995
159	SDW3043	ARDENTE	UNIBO	France	Europe	1985
160	SDW3044	AZEGHAR-2_DP128	UNIBO	-	-	-
161	SDW3045	BOLO_DP035	UNIBO	Spain/Italy	Europe	1997
162	SDW3046	CIMMYT23 BISU_1/PATKA_3_DP011	UNIBO	-	-	-
163	SDW3047	CLAUDIO	UNIBO	Italy	Europe	1998
164	SDW3048	COLORADO_DP086	UNIBO	Italy	Europe	2007
165	SDW3049	CORTEZ_DP088	UNIBO	United States	America	1995
166	SDW3050	DURCAL _DP039	UNIBO	Spain	Europe	2000
167	SDW3051	GRAZIA_DP096	UNIBO	Italy	Europe	1985
168	SDW3052	GUEROU-1_DP142	UNIBO	Syria	Asia	-
169	SDW3053	IRIDE	UNIBO	Italy	Europe	1996
170	SDW3054	KARIM_DP064	UNIBO	Tunisia	Africa	1985
171	SDW3055	LEVANTE	UNIBO	Italy	Europe	2002
172	SDW3056	MERIDIANO_DP005	UNIBO	Italy	Europe	1999
173	SDW3057	MIKI-1_DP161	UNIBO	-	-	-
174	SDW3058	MOHAWK_DP104	UNIBO	United States	America	1998
175	SDW3059	SIMETO_DP248	UNIBO	Italy	Europe	1988
176	SDW3060	ZEINA-1_DP075	UNIBO	Syria	Asia	-
177	SDW3061	ACALOU_DP190	UNIBO	France	Europe	1990
178	SDW3062	ARCOBALENO_DP080	UNIBO	Spain/Italy	Europe	1995
179	SDW3063	COLOSSEO_DP087	UNIBO	Italy	Europe	1995
180	SDW3064	ITALO_DP098	UNIBO	Italy	Europe	1993
181	SDW3065	KABIR-1_DP151	UNIBO	Syria	Asia	1990
182	SDW3066	MASSARA-1_DP160	UNIBO	Morocco	Africa	
183	SDW3067	MEXICALI-75_DP103	UNIBO	Mexico	America	1975
184	SDW3068	NEODUR	UNIBO	France	Europe	1987
185	SDW3069	NORMANNO	UNIBO	Italy	Europe	2002
186	SDW3070	ODISSEO	UNIBO	Italy	Europe	2011
187	SDW3071	OUASERL-1_DP172	UNIBO	-	-	-

188	SDW3072	QUADALETE_DP176	UNIBO	-	-	-
189	SDW3073	VALNOVA_DP114	UNIBO	Italy	Europe	1975
190	SDW3074	WB881_DP116	UNIBO	United States	America	1982
191	SDW3075	AUS1_DP125	UNIBO	-	-	-
192	SDW3076	MARZAK_DP055	UNIBO	Morocco	Africa	1984
193	SDW4001	EL4X_27	EPO	-	-	-
194	SDW4002	EL4X_29	EPO	-	-	-
195	SDW4003	EL4X_31	EPO	-	-	-
196	SDW4004	EL4X_35	EPO	-	-	-
197	SDW4005	EL4X_41	EPO	-	-	-
198	SDW4006	EL4X_117	EPO	-	-	-
199	SDW4007	EL4X_118	EPO	-	-	-
200	SDW4008	EL4X_120	EPO	-	-	-
201	SDW4009	EL4X_130	EPO	-	-	-
202	SDW4010	EL4X_145	EPO	-	-	-
203	SDW4011	EL4X_146	EPO	-	-	-
204	SDW4012	EL4X_176	EPO	-	-	-
205	SDW4013	EL4X_179	EPO	-	-	-
206	SDW4014	EL4X_182	EPO	-	-	-
207	SDW4015	EL4X_188	EPO	-	-	-
208	SDW4016	EL4X_192	EPO	-	-	-
209	SDW4017	EL4X_194	EPO	-	-	-
210	SDW4018	EL4X_195	EPO	-	-	-
211	SDW4019	EL4X_198	EPO	-	-	-
212	SDW4020	EL4X_207	EPO	-	-	-
213	SDW4021	EL4X_212	EPO	-	-	-
214	SDW4022	EL4X_222	EPO	-	-	-
215	SDW4023	EL4X_227	EPO	-	-	-
216	SDW4024	EL4X_229	EPO	-	-	-
217	SDW4025	EL4X_233	EPO	-	-	-
218	SDW4026	EL4X_240	EPO	-	-	-
219	SDW4027	EL4X_241	EPO	-	-	-
220	SDW4028	EL4X_243	EPO	-	-	-
221	SDW4029	EL4X_250	EPO	-	-	-
222	SDW4030	EL4X_252	EPO	-	-	-
223	SDW4031	EL4X_262	EPO	-	-	-
224	SDW4032	EL4X_268	EPO	-	-	-
225	SDW4033	EL4X_278	EPO	-	-	-
226	SDW4034	EL4X_292	EPO	-	-	-
227	SDW4035	EL4X_305	EPO	-	-	-
228	SDW4036	EL4X_316	EPO	-	-	-
229	SDW4037	EL4X_331	EPO	-	-	-
230	SDW4038	EL4X_344	EPO	-	-	-
231	SDW4039	EL4X_350	EPO	-	-	-
232	SDW4040	EL4X_368	EPO	-	-	-
233	SDW4041	EL4X_370	EPO	-	-	-
234	SDW4042	EL4X_372	EPO	-	-	-
235	SDW4043	EL4X_373	EPO	-	-	-
236	SDW4044	EL4X_401	EPO	-	-	-
237	SDW4045	EL4X_402	EPO	-	-	-
238	SDW4046	EL4X_407	EPO	-	-	-
239	SDW4047	EL4X_412	EPO	-	-	-
240	SDW4048	EL4X_426	EPO	-	-	-
241	SDW4049	EL4X_428	EPO	-	-	-
242	SDW4050	EL4X_435	EPO	-	-	-
243	SDW4051	EL4X_460	EPO	-	-	-
244	SDW4052	EL4X_464	EPO	-	-	-
245	SDW4053	EL4X_474	EPO	-	-	-
246	SDW4054	EL4X_476	EPO	-	-	-
247	SDW4055	EL4X_483	EPO	-	-	-
248	SDW4056	EL4X_488	EPO	-	-	-
249	SDW4057	GQ4X_75	EPO	-	-	-
250	SDW4058	GQ4X_139	EPO	-	-	-

2. ROOTPHAIR NUTRITIVE SOLUTION

The nutritive solution used in the RootPhAir experiments is the Hoagland solution ½ concentrated (Hoagland and Arnon, 1950). The mother solutions usually added to 25L of demineralized water were diluted to 50%. The exact quantities added are in the last column of the next table (daughter solutions):

Table 14. RootPhAir nutritive solution (½ Hoagland).

Product information			Mother solutions		Daughter solutions
N° product	Product	Molar mass of the product (g/mol)	g of product per 1L of mother solution (g/L)	mol of product per 1L of mother solution (mol/L)	mL of mother solution per 25L of daughter solution ½ Hoagland (mL/25L)
1	KNO_3	101	202	2	31.25
2	$Ca(NO_3)_2.4H_2O$	236	472	2	31.25
3	$Mg.SO_4.7H_20$	246.5	493	2	12.5
4	NH_4NO_3	80	80	1	12.5
5	H_3BO_3	61.8	2.86	0.046	12.5
	$MnCl_2.4H_2O$	198	1.81	0.009	
	$ZnSO_4.7H_2O$	287.5	0.22	0.00076	
	$CuSO_4.5H_2O$	250	0.051	0.0002	
	$Na_2MoO_4.2H_2O$	242	0.12	0.0005	
6	KH_2PO_4 (pH to 6.0 with 3M KOH)	136	136	1	6.25
7	Iron (Sprint 138 iron chelate) Fe EDDHA	375	15	*0.04*	37.5

3. 4PMI NUTRITIVE SOLUTION

The nutritive solution used in the 4PMI experiments is detailed in the following table:

Table 15. 4PMI nutritive solution.

Product information			Mother solutions		Daughter solutions	
N° product	Product	Molar mass of the product (g/mol)	g of product per 1L of mother solution (g/L)	mol of product per 1L of mother solution (mol/L)	mM of the daughter solution (mM)	mL of mother solution per 25L of daughter solution (mL/25L)
1	K_2HPO_4	174.18	580	3.33	1	7.5
2	KNO_3	101.1	201	2	5	62.75
3	$Ca(NO_3)_2.4H_2O$	236.15	472	2	2.5	31.25
4	$Mg.SO_4.7H_2O$	246	246	1	2	50
5	$CaCl_2.2H2O$	147.01	588.04	4	2	12.5
6	H_3BO_3	61.83	0.62	0.01	0.01	25
7	$MnCl_2.4H_2O$	197.91	0.89	0.005	0.0045	25
8	$ZnCl_2$	138	0.097	0.0007	0.0007	25
9	$Mo(Na)_2O_4$	241.95	0.0485	0.0002	0.0002	25
10	$CuCl_2.2H_2O$	170.48	0.068	0.0004	0.0004	25
11	Fe EDTA	403.08	20.66	0.051	0.05	25

4. LIST OF ARTICLES USED FOR THE ROOT QTLS REVIEW

The complete list of 1700 QTLs reviewed from these 59 articles is available on Zenodo (Collet, 2022).

Table 16. Articles selected for the review of studies aimed at finding QTLs for bread wheat root traits (from 2005 to 2020).

N° Article	Authors	Year	DOI
1	Alahmad et al.	2019	10.3389/fpls.2019.00436
2	An et al.	2006	10.1007/s11104-006-0030-3
3	Atkinson et al.	2015	10.1093/jxb/erv006
4	Ayalew et al.	2018	10.3389/fpls.2018.01759
5	Ayalew et al.	2017	10.1007/s10681-017-1914-4
6	Bai et al.	2013	10.1093/jxb/ert041
7	Ballesteros et al.	2015	10.1007/s10681-014-1184-3
8	Batool et al.	2018	10.21162/PAKJAS/18.5426
9	Berry and Berry	2015	10.1007/s10681-015-1387-2
10	Botwright Acuña et al.	2014	10.1007/s11032-014-0063-x
11	Chesnokov et al	2014	10.1134/S1021443714060041
12	Christopher et al.	2013	10.1007/s00122-013-2074-0
13	Ci et al.	2012	10.1007/s11738-011-0818-5
14	Clarke et al.	2017	10.1093/aob/mcx068
15	Czyczylo-Mysza et al.	2014	10.2478/s11535-013-0273-y
16	Ehdaie et al.	2016	10.1007/s10681-016-1670-x
17	Fan et al.	2018	10.1007/s00122-018-3183-6
18	García-Suárez et al.	2010	10.1556/CRC.38.2010.2.2
19	Guo et al.	2012	10.1007/s00122-011-1749-7
20	Guo et al.	2013	10.1016/j.fcr.2013.07.012
21	Hamada et al.	2012	10.1007/s11104-011-1075-5
22	Hohn and Bektas	2020	10.1007/s11105-020-01214-1
23	Horn et al.	2016	10.1093/jxb/erw228
24	Huang et al.	2020	10.1016/j.cj.2020.02.007
25	Ibrahim et al.	2012	-
26	Kabir et al.	2015	10.1007/s10681-015-1495-z
27	Kadam et al.	2012	10.1007/s10142-012-0276-1
28	Khalid et al.	2018	10.1017/S1479262118000023
29	Kong et al.	2013	10.1007/s11104-013-1844-4
30	Landjeva et al.	2008	10.1007/s10535-008-0056-x
31	Landjeva et al.	2009	10.1007/s10681-009-0016-3
32	Laperche et al.	2006	10.1007/s00122-006-0373-4
33	Li et al.	2007	-
34	Li et al.	2018	10.21162/PAKJAS/18.4488
35	Li et al.	2011	10.2135/cropsci2011.03.0116
36	Li et al.	2020	10.1139/gen-2019-0116
37	Liu et al.	2013	10.1007/s10681-012-0690-4
38	Liu et al.	2019	10.1007/s10681-019-2452-z
39	Liu et al.	2020	10.1016/S2095-3119(19)62825-X
40	Ma et al.	2017	10.1139/gen-2017-0097
41	Pu et al.	2018	10.1007/s11104-017-3556-7
42	Ren et al.	2012	10.1007/s11032-011-9605-7
43	Ren et al.	2017	10.3389/fpls.2017.02096
44	Ren et al.	2018	10.3389/fpls.2018.00845
45	Ren et al.	2018	10.1590/0103-8478cr20170446
46	Rufo et al.	2020	10.3390/agronomy10050613
47	Salarpour et al.	2020	10.1007/s10681-020-02627-5
48	Sharma et al.	2011	10.1007/s00122-010-1484-5
49	Sun et al.	2013	10.1007/s10681-012-0834-6

50	Verma et al.	2005	10.1111/j.1439-0523.2005.01070.x
51	Wu et al.	2017	10.1007/s13353-017-0406-5
52	Xie et al.	2017	10.1093/aob/mcx001
53	Xu et al.	2013	10.1111/pbr.12048
54	Yang et al.	2018	10.1139/gen-2017-0159
55	Zhang et al.	2014	10.1007/s10681-013-1035-7
56	Zhang et al.	2013	10.1007/s12041-013-0253-z
57	Zhao et al.	2014	10.1007/s10681-014-1091-7
58	Zheng et al.	2019	10.1007/s00425-019-03154-x
59	Zhou et al.	2016	10.3724/SP.J.1006.2016.01764

5. LIST OF SIGNIFICANT SNPS DETECTED WITH GWAS

Table 17. List of all significant SNPs detected within the bread wheat panel. The threshold set for the SNP significance is a p-value <10^{-5}. "Exp" is the name of the experiment, "Trait" is the name of the trait, "Model" is the model used to detect the SNP, "SNP" is the significant SNs detected, "pval" is the p-value, "R^2" is the R-square, "CHR" is the chromosome on which the SNPs was detected, "BP" is it position of the SNP, "effect" is the effect of the SNPs on the phenotypic value when present and "QTL number" is the unique number given to each QTL (B= Blink, BP= base pair, C=CLMM, CHR=chromosome, E= EMMAX, F = FarmCPU, M1=MLM, M2= MLMM, S=SUPER).

Exp	Trait	Model	SNP	pval	R^2	CHR	BP	-log_{10}(pval)	effect	QTL number
RootPhAir	R/S_{Dry}	S	cfn1974830	7.76E-06	-	3B	146828510	5.11	-	1
RootPhAir	R/S_{Fresh}	S	cfn1567967	1.32E-07	-	2B	571251128	6.88	-	2
		S	cfn0603844	1.09E-06	-	2B	564236062	5.96	-	
		S	cfn1565494	1.60E-06	-	2B	563928015	5.80	-	
		S	contig81860_71_BS00100563	1.76E-06	-	2B	564877374	5.76	-	
		S	cfn0615174	1.84E-06	-	2B	563861366	5.74	-	
		S	cfn0388794	1.86E-06	-	2B	564430834	5.73	-	
		S	cfn0124313	1.87E-06	-	2B	564853399	5.73	-	
		S	cfn0615269	1.94E-06	-	2B	564234541	5.71	-	
		S	cfn0626606	2.11E-06	-	2B	569016998	5.68	-	
		S	cfn1565462	2.14E-06	-	2B	563924861	5.67	-	
		S	cfn0246832	2.40E-06	-	2B	568633537	5.62	-	
		S	cfn1632025	2.46E-06	-	2B	563867183	5.61	-	
		S	cfn1615178	2.55E-06	-	2B	568474555	5.59	-	
		S	cfn0605151	2.59E-06	-	2B	568745799	5.59	-	
		S	cfn1615174	2.77E-06	-	2B	568476344	5.56	-	
		S	cfn0204366	2.77E-06	-	2B	569063944	5.56	-	
		S	cfn0626458	2.77E-06	-	2B	569151171	5.56	-	
		S	cfn0615286	4.06E-06	-	2B	564229532	5.39	-	
		S	cfn0603839	4.26E-06	-	2B	564236597	5.37	-	
		S	cfn0246833	4.80E-06	-	2B	568633434	5.32	-	
		S	cfn0626607	5.16E-06	-	2B	569017027	5.29	-	
		S	cfn1587562	6.01E-06	-	2B	569142808	5.22	-	
		S	cfn0626614	7.04E-06	-	2B	569018962	5.15	-	
		S	cfn0117834	9.04E-06	-	2B	568826336	5.04	-	
		S	cfn1580947	9.15E-06	-	2B	569243870	5.04	-	
		S	cfn1586540	9.15E-06	-	2B	569140845	5.04	-	
		S	cfn0614533	9.34E-06	-	2B	569132068	5.03	-	
		S	cfn0603062	9.52E-06	-	2B	564439506	5.02	-	
		S	cfn0229829	6.61E-06	-	3B	805258205	5.18	-	3
RootPhAir	$RMass_{Dry}$	E	cfn0378434	9.99E-06	0.096	2A	751553548	5.00	-	4
4PMI	$SMass_{Dry}$	E	tplb0053o16_915	5.30E-06	0.101	2B	793167721	5.28	-	5
RootPhAir	$SMass_{Dry}$	B	cfn3167537	8.35E-06	-	6D	425522380	5.08	-	6
		F	cfn3167537	8.35E-06	-	6D	425522380	5.08	0.01	
RootPhAir	$Diam_{ER}$	B	cfn0374358	3.31E-09	-	3D	250023058	8.48	-	7
		E	cfn0374358	4.60E-06	0.103	3D	250023058	5.34	-	
		M2	cfn0374358	5.24E-06	-	3D	250023058	5.28	-	
		E	BGABW024629	5.92E-06	0.101	3D	250023058	5.23	-	
RootPhAir	$Diam_{LR}$	S	cfn3514523	1.18E-06	-	7B	315910548	5.93	-	8
		S	cfn0922215	7.00E-06	-	7B	357654909	5.15	-	
Pouch	$ERate_{ER}$	B	cfn0247843	6.52E-06	-	4A	18007093	5.19	-	9
		F	cfn0247843	6.52E-06	-	4A	18007093	5.19	0.00	
		M2	cfn0247843	9.27E-06	-	4A	18007093	5.03	-	
		E	cfn0247843	9.27E-06	0.096	4A	18007093	5.03	-	
RootPhAir	$ERate_{PR}$	E	cfn0778241	7.14E-06	0.09	5A	9617282	5.15	-	10
		M2	cfn0791282	8.67E-06	-	5B	611954177	5.06	-	11
		M2	cfn0800032	8.67E-06	-	5B	612014811	5.06	-	
		M2	cfn2757529	8.67E-06	-	5B	612113339	5.06	-	

		E	cfn0791282	9.59E-06	0.097	5B	611954177	5.02	-	
		E	cfn0800032	9.59E-06	0.097	5B	612014811	5.02	-	
		E	cfn2757529	9.59E-06	0.097	5B	612113339	5.02	-	
Pouch	$ERate_{SR2}$	E	cfn0329772	4.53E-07	0.201	1B	604553155	6.34	-	12
		S	cfn0685249	2.00E-06	-	3B	66470105	5.70	-	13
Pouch	$Length_{SR2}$	S	cfn0361523	1.38E-06	-	5B	467801159	5.86	-	14
Pouch	*ARL*	E	cfn0247843	9.19E-06	0.096	4A	18007093	5.04	-	15
		M2	cfn0247843	9.19E-06	-	4A	18007093	5.04	-	
RootPhAir	*MRL*	M2	cfn0671417	4.12E-06	-	3A	122754540	5.39	-	16
		E	cfn0671417	4.15E-06	0.104	3A	122754540	5.38	-	
		B	cfn0671417	6.40E-06	-	3A	122754540	5.19	-	
		F	cfn0671417	6.40E-06	-	3A	122754540	5.19	1.63	
RootPhAir	*LRD*	B	cfn0154919	6.79E-09	-	5B	468641356	8.17	-	17
		S	cfn0264429	6.78E-06	-	6B	88963984	5.17	-	18
		S	cfn0264538	8.55E-06	-	6B	88892096	5.07	-	
RootPhAir	Nb_{ER}	S	cfn0263877	9.55E-06	-	1A	544084786	5.02	-	19
Pouch	Nb_{SR1}	E	cfn0883079	7.91E-06	0.097	6D	100346813	5.10	-	20
		E	cfn3172155	9.55E-06	0.095	6D	99858786	5.02	-	
Pouch	Nb_{SR2}	S	cfn0194999	6.69E-06	-	5B	416837438	5.17	-	21
4PMI	Nb_{Leaves}	S	cfn0506233	3.92E-06	-	1A	511100907	5.41	-	22
		S	cfn0982769	7.75E-06	-	1A	474440681	5.11	-	
		S	cfn0506230	8.89E-06	-	1A	511101832	5.05	-	
		S	cfn3594533	1.62E-06	-	7D	636665388	5.79	-	23
		E	GENE-2673_1457	9.52E-06	0.095	Un	-	5.02	-	40
Pouch	SRA_{SR2}	S	cfn2447261	6.53E-06	-	4D	421113253	5.18	-	24
		S	cfn2444032	7.02E-06	-	4D	420575909	5.15	-	
Pouch	$Theta_{PR}$	F	cfn1119723	2.40E-07	-	1A	31531253	6.62	0.01	25
		F	cfn1053258	3.87E-07	-	1A	548501006	6.41	-0.01	26
		F	cfn0500227	8.98E-06	-	1A	520806631	5.05	-0.01	27
		F	cfn0545720	1.66E-06	-	1B	651277748	5.78	-0.02	28
		F	cfn0367316	3.94E-06	-	1B	581350923	5.40	-0.01	29
		F	cfn0607374	7.55E-07	-	2B	708186553	6.12	0.01	30
		F	cfn0215431	2.47E-06	-	3B	503956549	5.61	0.01	31
		F	cfn0106747	9.42E-07	-	5A	439533325	6.03	-0.01	32
		B	cfn2718043	1.08E-09	-	5B	595335259	8.97	-	
		F	cfn2718043	1.22E-08	-	5B	595335259	7.92	-0.02	
		M2	cfn2718043	1.03E-07	-	5B	595335259	6.99	-	
		E	cfn2718043	1.16E-07	0.134	5B	595335259	6.94	-	
		C	cfn2718043	6.78E-07	0.138	5B	595335259	6.17	-0.02	33
		M1	cfn2718043	6.78E-07	0.138	5B	595335259	6.17	-0.02	
		E	bgabw004229	2.76E-06	0.106	5B	595633361	5.56	-	
		C	bgabw004229	8.37E-06	0.111	5B	595633361	5.08	-0.02	
		M1	bgabw004229	8.37E-06	0.111	5B	595633361	5.08	-0.02	
Pouch	$Theta_{SR2}$	F	cfn0618948	1.01E-06	-	2B	578595970	6.00	0.16	34
		F	cfn1597800	8.11E-06	-	2B	714492038	5.09	0.12	35
		B	cfn1868786	4.77E-11	-	3A	728419195	10.32	-	
		M2	cfn1868786	3.64E-08	-	3A	728419195	7.44	-	
		E	cfn1868786	5.61E-08	0.229	3A	728419195	7.25	-	
		S	cfn1868786	9.60E-07	-	3A	728419195	6.02	-	36
		M1	cfn1868786	1.20E-06	0.249	3A	728419195	5.92	-0.37	
		C	cfn1868786	2.54E-06	0.247	3A	728419195	5.60	-0.39	
		F	cfn1868786	5.42E-06	-	3A	728419195	5.27	-0.19	
		S	cfn2946025	9.96E-07	-	6A	83503884	6.00	-	
		S	cfn2856817	1.57E-06	-	6A	519601594	5.80	-	
		S	cfn0831735	1.57E-06	-	6A	523944965	5.80	-	37
		S	cfn0833934	1.57E-06	-	6A	499207507	5.80	-	
		S	cfn0845239	3.29E-06	-	6A	77780916	5.48	-	
		S	cfn2953784	3.75E-06	-	6A	67497758	5.43	-	
		F	cfn0835914	5.05E-06	-	6A	605360165	5.30	-0.06	38
4PMI	*Width*	B	cfn0152077	3.96E-06	-	3B	666789528	5.40	-	39
		F	cfn0152077	3.96E-06	-	3B	666789528	5.40	1.66	
		E	cfn0152077	4.04E-06	0.103	3B	666789528	5.39	-	
		M2	cfn0152077	4.04E-06	-	3B	666789528	5.39	-	

6. CO-LOCALISATIONS VISUALISATION

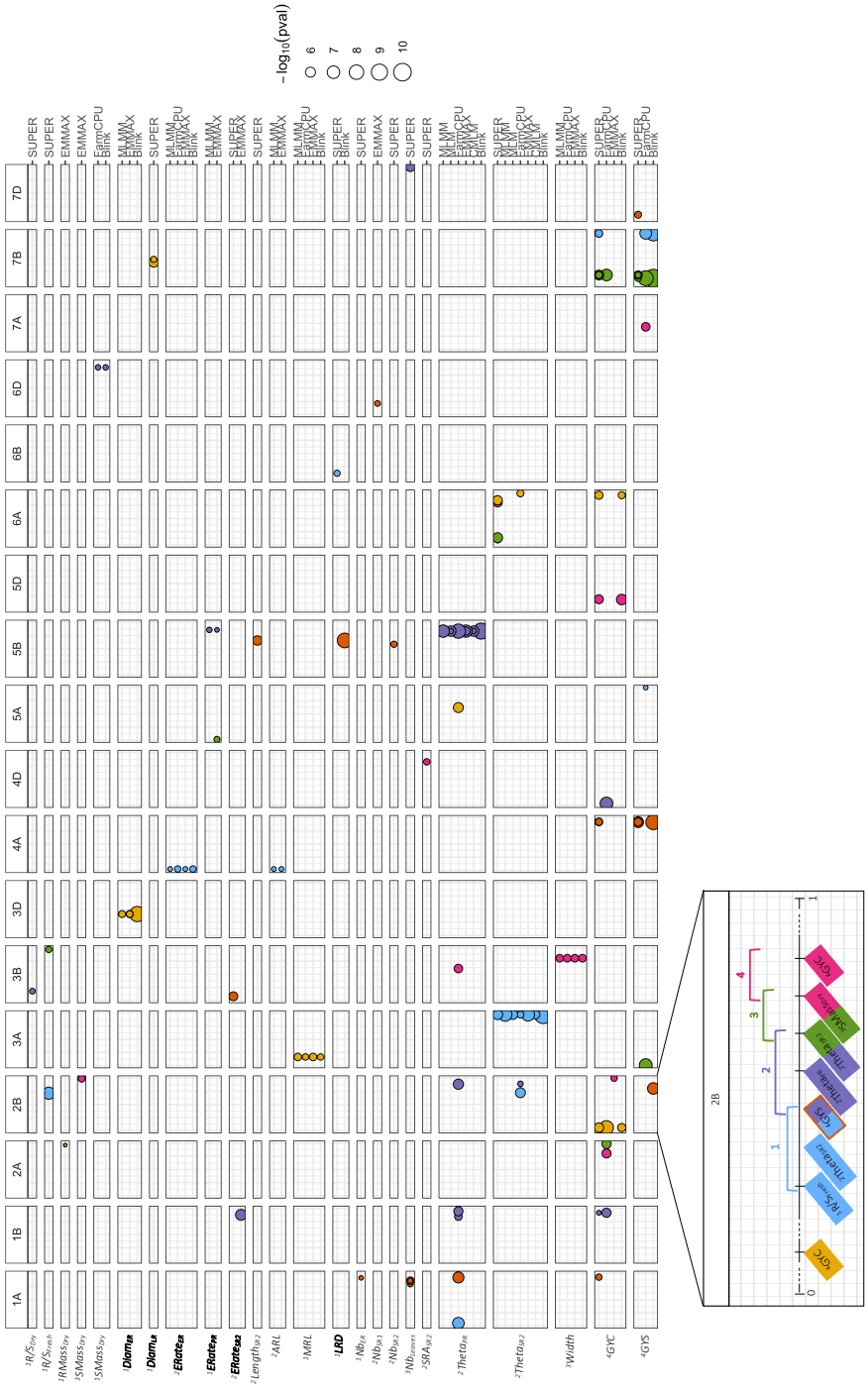


Figure 22 (previous page). This representation corresponds to a Manhattan plot viewed from top with the set of all significant SNPs detected. Traits (and models) for which no QTLs were detected are not represented. In bold, all traits considered to be closely linked to root growth dynamic. Each dot corresponds to one SNP, the diameter being proportional to the -log_{10}(pval). All SNPs co-localising have the same colour. Six colours have been alternated to facilitate the visualisation of co-localising regions succession. The inserted frame represents a zoom on CHR 2B, for which the colocalising situation was more complex to illustrate with colours since several SNPs belonged to several co-location regions. All SNP positions are relative since the widths of each chromosome have been scales from 0 to 1. One unknown positioned SNP for Nb_{Leaves} was omitted ([1] = RootPhAir, [2] = Pouch, [3] = 4PMI, [4] = Field, ARL = average root length, Diam = diameter, ER = embryonic roots, ERate = elongation rate, GYC = grain yield under controlled conditions, GYS = grain yield under stressed conditions, Length = root length, LR = lateral root, LRD = lateral root density, MRL = maximum root length, Nb = number, PR = primary root, R/S = root to shoot ratio, RMass = root biomass, SMass = shoot biomass, SR1 = first pair of seminal roots, SR2 = second pair of seminal roots , SRA = seminal root angle, Theta = root angle from vertical).

7. SIGNIFICANT SNPS DETECTED WITH FDR METHOD



Figure 23 (previous page). This representation corresponds to a Manhattan plot viewed from top with the set of all significant SNPs detected with the FDR method (pval < 0,3). Traits (and models) for which no QTLs were detected are not represented. In bold, all traits considered to be closely linked to root growth dynamic. Each dot corresponds to one SNP, the diameter being proportional to the -log$_{10}$(pval). All SNPs belonging to the same QTL have the same colour. Five colours have been alternated to facilitate the visualisation of QTL successions (white has been assigned to SNPs for which limits have not been set). All SNP positions are relative since the widths of each chromosome have been scales from 0 to 1. One hundred and thirteen unknown positioned SNPs were omitted for R/S$_{Fresh}$ (15), ERate$_{PR}$ (1), ERate$_{SR2}$ (1), Nb$_{Leaves}$ (4), SRA$_{SR1}$ (1), Theta$_{SR2}$ (1), GYC (88), GYS (2) ([1] = RootPhAir, [2] = Pouch, [3] = 4PMI, [4] = Field, ARL = average root length, Diam = diameter, ER = embryonic roots, ERate = elongation rate, GYC = grain yield under controlled conditions, GYS = grain yield under stressed conditions, Length = root length, LR = lateral root, LRD = lateral root density, MRL = maximum root length, Nb = number, PR = primary root, R/S = root to shoot ratio, RMass = root biomass, SMass = shoot biomass, SR1 = first pair of seminal roots, SR2 = second pair of seminal roots , SRA = seminal root angle, Theta = root angle from vertical).